AD_____

Award Number: DAMD17-98-1-8254

TITLE: Targeted Chemotherapy of Tumors and Metastases with Hyaluronic Acid-Anti-Tumor Bioconjugates

PRINCIPAL INVESTIGATOR: Glenn Prestwich, Ph.D.

CONTRACTING ORGANIZATION: University of Utah
Salt Lake City, Utah 84102

REPORT DATE: August 2000

TYPE OF REPORT: Annual

PREPARED FOR: U.S. Army Medical Research and Materiel Command
Fort Detrick, Maryland 21702-5012

REPORT DOCUMENTATION PAGE

OMB No. 0704-0188

1. AGENCY USE ONLY (Leave blank)	2. REPORT DATE	3. REPORT TYPE AND DATES COVERED
	August 2000	Annual (15 Jul 99 - 14 Jul 00)

4. TITLE AND SUBTITLE
Targeted Chemotherapy of Tumors and Metastases with Hyaluronic Acid-Anti-Tumor Bioconjugates

5. FUNDING NUMBERS
DAMD17-98-1-8254

6. AUTHOR(S)
Glenn Prestwich, Ph.D.

7. PERFORMING ORGANIZATION NAME(S) AND ADDRESS(ES)
University of Utah
Salt Lake City, Utah 84102

E-MAIL:
GPRESTWICH@DEANS.PHARM.UTAH.EDU

8. PERFORMING ORGANIZATION REPORT NUMBER

9. SPONSORING / MONITORING AGENCY NAME(S) AND ADDRESS(ES)
U.S. Army Medical Research and Materiel Command
Fort Detrick, Maryland 21702-5012

10. SPONSORING / MONITORING AGENCY REPORT NUMBER

11. SUPPLEMENTARY NOTES

12a. DISTRIBUTION / AVAILABILITY STATEMENT
Approved for public release; distribution unlimited

12b. DISTRIBUTION CODE

13. ABSTRACT ***(Maximum 200 Words)***

Metastatic cancer cells over-express characteristic variants of the hyaluronic acid (HA) receptors CD44 and RHAMM that mediate cell adhesion, cell motility, and cell proliferation. Rapid uptake and catabolism of HA is common in several breast cancer cell-lines. We have developed a targeted delivery system for controlled release of chemotherapeutic drugs, and we prepared HA-Taxol to test our hypothesis that HA-anti-tumor prodrugs will be more effective therapeutic agents than the unconjugated drugs. Fluorescently-labeled HA shows selective uptake, and HA-Taxol shows selective cytotoxicity to breast, colon, and ovarian cancer cells in culture; it also shows release of free drug from the HA-prodrug form that is consistent with improved selectivity. Studies are in progress to (**i**) prepare an HA-brefeldin A prodrug, and (**ii**) evaluate the HA-Taxol in nude mice bearing xenografted human tumors. Chondroitin sulfate will saturate HA uptake by non-target tissues. Animal data are being obtained to support use of radiolabeled HA and HA-Taxol in Phase I clinical trials in terminal diagnosis patients. A second line of research revealed the molecular basis of the RHAMM-HA interaction, and has provided unexpected molecular leads that disrupt the oncogenic transformation of RHAMM-overexpressing cells.

14. SUBJECT TERMS
Breast Cancer
Taxol, receptor-mediated uptake, selective toxicity, peptide library

15. NUMBER OF PAGES
179

16. PRICE CODE

17. SECURITY CLASSIFICATION OF REPORT	18. SECURITY CLASSIFICATION OF THIS PAGE	19. SECURITY CLASSIFICATION OF ABSTRACT	20. LIMITATION OF ABSTRACT
Unclassified	Unclassified	Unclassified	Unlimited

Table of Contents

A. Introduction

In this project, we are developing an innovative approach to the use of a natural polysaccharide biopolymer, hyaluronic acid (HA), to solubilize, stabilize, and achieve targeted intracellular delivery of anti-cancer agents to tumors and metastases. The coupling of an anti-tumor agent to HA gives a soluble, tumor-targeted drug conjugate. HA receptors are over-expressed on a variety of aggressively growing cancers, and in many cell-types, correlate with increased metastatic potential and with rate of HA uptake and degradation. The use of HA receptor-mediated uptake of a cytotoxic agent to cancerous and invasive cells represents a significant advance in cell-specific drug targeting, as all commonly-used anti-cancer drugs (e.g., anti-metabolites and DNA-targeted agents) and adjuvant techniques (e.g., radiation therapy) have inadequate specificity for cancerous lesions. Our efforts in the second year have continued to focus on synthesis and cell-based assays with the hydrophobic anti-tumor drug Taxol. Our HA-Taxol adduct is water-soluble, shows enhanced target specificity for transformed and metastatic cells; and shows increased uptake and liberation of drug in the target tumor cells. Two papers describing the selective cytotoxicity and selective uptake of HA-Taxol and HA-FITC-Taxol were published. Current efforts include four new collaborations for use of HA-Taxol : (**i**) effects in diabetes using PDGF stimulated NIH-3T3 L1 cells (with E.A. Turley, Hospital for Sick Children, Toronto, Canada), (**ii**) specific cellular effects on CD44 clustering of HA-Taxol (with L. Bourguignon, University of Miami Medical Center, Florida), (**iii**) *in vivo* human tumor xenograft studies with nude mice (with L. Zhang and C. Underhill, Georgetown University, Washington), and (**iv**) examination of the ability of HA-Taxol to overcome *p*-glycoprotein-mediated resistance in breast cancer cell lines (with S. Horwitz, Albert Einstein Medical Center, New York). In addition, we have initiated the synthesis of new HA-drug derivatives (brefeldin A and geldanomycin) and we are mid-way through a very encouraging application of HA fragments for improving the targeting and selective toxicity of HPMA-ADR, a polymer-bound derivative of adriamycin (with J. Kopecek, UUtah).

B. Body

This section describes research accomplishments associated with the specific tasks outlined in the original IDEA award application.

Task 1. Synthesize HA-anti-tumor drug bioconjugates with four anti-cancer drugs (Brefeldin A, Taxol, geldanomycin, and camptothecin)

We synthesized and chemically characterized hemisuccinate active-ester forms of brefeldin A and Taxol. HA-adipic dihyrdazide (HA-ADH) conjugates of Taxol hemisuccinate were prepared and evaluated in cell-based toxicity assays. The purity and molecular size of drug bioconjugates was established by GPC and drug loading was evaluated by UV. The final published version (from *Bioconjugate Chemistry*) is provided as an appendix. In addition, we synthesized and purified fluorescently-labeled HA with three fluorophores at each of three molecular sizes (12 , 200, and 1,200 kDa), as well as a doubly-labeled HA-Taxol-FITC molecule for simultaneous monitoring of selective cellular uptake and toxicity. This work has also been published in *Biomacromolecules* and appears as an Appendix. Geldanomycin, was obtained from the NCI and coupled to simple hydrazides in preparation for conjugation with low molecular weight HA (HA-ADH).

Task 2. Establish analytical methods to monitor enzymatic release of drugs from bioconjugates and quantify metabolites in cell cultures

We conducted *in vitro* tests with commercial esterase and hyaluronidase (HAse) and developed a robust HPLC assay for the quantification of Taxol release. No other Taxol-containing materials (except free Taxol drug) were released from the HA-Taxol bioconjugates. We also investigated the release rates of Taxol from the optimal HA-Taxol preparation using cell culture media (with and without cells) and human serum. This has now been published in the *Biomacromolecules* paper.

Task 3. Determine efficacy of HA-AT (*vs.* free AT drugs) in cultured breast cancer and other cell-lines *in vitro*

We obtained and cultured a number of cell-lines: MDA-MB-231, MCF-7, and HBL-100 human breast epithelial cells; HL-60 human leukemia cells,; SK-OV-3 human ovarian cancer cells; HCT-116 human colon cancer cells, and NIH 3T3 mouse fibroblast cells. Optimal HA modification levels and drug loading were established. Extensive studies of dose-response and selective cytotoxicity were completed with HA-Taxol, and uptake studies were performed with HA-BODIPY. The uptake of HA-Taxol or HA-BODIPY into cells was blocked by pre-incubation of cells with HA, but not with chondroitin sulfate. A similar result was obtained by flow cytometry using HA-Taxol-FITC. These data were published in the two papers, *Bioconjugate Chemistry* and *Biomacromolecules*, as indicated above.

Task 4. Measure efficacy of bioconjugates (vs. free drugs) using human breast cancer epithelial cell tumor xenografts in nude mice

Protocols to accomplish this task using our optimized HA-Taxol preparation have been implemented in experiments underway in two laboratories: UUtah and with collaborators L. Zhang and C. Underhill, Georgetown University. We have established dosing protocols and levels, and we have established which tumor cell-lines will be optimal for observing efficacy of the new models.

Task 5. Initiate planning for Phase I safety testing of one or two optimal HA bioconjugates in terminal diagnosis human patients with drug- and radiation-refractory metastasis

We are working with Dr. Richard Wheeler, Director of Clinical Trials of the Huntsman Cancer Institute (UUtah) to develop protocols for Phase I safety tests of HA-ADH and HA-Taxol. Scale-up sterile synthesis of selected HA bioconjugates for larger scale preclinical animal studies and for human trials will be necessary to accomplish these post-award safety trials. Mechanisms for funding the GLP synthesis and preclinical evaluation are being explored.

C. Key Research Accomplishments

This section provides a bulleted list of key accomplishments, both those within the initial objectives and tasks and those that arose as promising leads during the pursuit of the originally outlined tasks.

1. Accomplishments based on original tasks

   - HA-Taxol preparations were evaluated for selective cytotoxicity in six cell-lines.
   - Fluorescently-labeled HA and fluorescenly-labeled HA-Taxol were prepared and characterized.
   - Cell binding and uptake of fluorescent HA and HA-Taxol was measured by confocal microscopy and flow cytometry.
   - Release of Taxol from HA-Taxol in cell cultures was determined by HPLC.
   - *In vivo* testing of HA-Taxol in nude mice with xenografted human tumors was initiated (internal results plus collaboration)
   - Brefeldin A was chemically modified as a prodrug for chemical attachment to HA.
   - Geldanomycin was chemically modified with hydrazides
   - Toxicity of HA-Taxol to wild-type and MDR breast cancer cell-lines was evaluated (collaboration)
   - Use of HA for targeting of HPMA-ADR was established (collaboration)
   - Cell biology of HA-FITC-Taxol in CD44 wild-type and mutant cell lines was measured (collaboration)

2. Accomplishments ancillary to original tasks but leading to a greater understanding of the mechanism of uptake and to novel drug leads

   - The transforming HA receptor RHAMM was expressed in recombinant form and with ^{13}C, ^{15}N labels for structural biological studies whose solution structure was determined using high resolution 2-D and 3-D NMR methods.
   - Rapid and novel HA-binding assays were established.
   - Peptide libraries (phage-display and beads) were screened and peptides were identified that bind to RHAMM and are taken up by cells.
   - Peptide leads were synthesized, fluorescently-tagged or biotinylated, and biophysical and functional studies of these peptides were initiated.

D. Reportable Outcomes

1. Publications

Y. Luo and G.D. Prestwich, "Synthesis and Cytotoxicity of Hyaluronan-Taxol Antitumor Bioconjugates," *Bioconjugate Chem.*, **10**, 755-763 (1999).

G.D. Prestwich, Y. Luo, M.R. Ziebell, K.P. Vercruysse, K.R. Kirker, and J.S. MacMaster, "Chemically-Modified Hyaluronan: New Biomaterials and Probes for Cell Biology," in *New Frontiers in Medical Sciences: Redefining Hyaluronan* Padua, Italy (G. Abatangelo and P.H. Weigel, eds.) Elsevier Science, pp. 181-194 (2000).

Y. Luo, M.R. Ziebell, and G.D. Prestwich, "A Hyaluronic Acid -Taxol Anti-tumor Bioconjugate Targeted to Cancer Cells," *Biomacromolecules,* 1, 208-218 (2000).

Y. Luo, K.R. Kirker, and G.D. Prestwich, "Chemical Modification of Hyaluronic Acid," *Methods of Tissue Engineering* (A. Atala and R. Lanza, eds.), Academic Press, Orlando, Florida, in press (2000).

M.R. Ziebell, Z.G. Zhao, B. Luo, Y. Luo, E.A. Turley, and G.D. Prestwich, "Peptides that Mimic Carbohydrates: High Affinity Ligands for A Hyaluronic Acid Binding Domain," *J. Biol. Chem.* submitted (2000).

S. Zhang, W.F. Cheung, J. Lu, M.R. Ziebell, S.A. Turley, R. Harrison, D. Zylka, N. Ahn, D. Litchfield, G.D. Prestwich, T. Cruz, and E.A. Turley, "Intracellular RHAMM Isoforms Bind Directly to erk1 and These Interactions are Required for Transformation and for Podosome Formation via the erk Kinase Pathway," *Molec. Cell. Biol.*, in press (2000).

2. Patents, licenses and disclosures

G.D. Prestwich, Y. Luo, K.P. Vercruysse, "Method for Preparing and Isolating High-Purity Bioconjugates of Hyaluronic Acid," UUtah disclosure filed March 10, 1998.

G.D. Prestwich, "Discovery of Peptides That Mimic Hyaluronic Acid," US Provisional Patent Application No. 60/091,758 filed July 6, 1998. Full filing, July 3, 1999. Full patent filed 2000

3. Degrees

Michael R. Ziebell, Physiology & Biophysics, The University at Stony Brook, Stony Brook, New York, PhD, January 2000.

4. Leveraged funding

The chemical modification technology developed was employed in several on-campus applications which were supported. These include preparation of HA hydrogel films for drug release and wound healing and the development of HA-modified particles for binding cancer cells. A manuscript is in press describing the new hydrogel films, and a grant application has been submitted to the NIH to support development of this material for wound healing.

On-campus support was obtained to search for inhibitors of HAse, and to examine other glycosaminoglycan-based films

Our chemically-modified HA was a prominent part of an application for an NIH consortium project to prepare tissue for developing HA substitutes to treat vocal insufficiency. This project was recently funded (Steven Gray, MD, Principal Investigator, UUtah) and we are developing HA materials for prosthetic HA replacement uses, anti-scarring applications, and for preparing tissue scaffolds for tissue regeneration.

An ovarian cancer grant is in preparation to exploit the novel finding that HA fragments increase the selective targeting and selective toxicity of HPMA-ADR by over twenty-fold.

5. Invited presentations

Seven seminars have been presented at universities or companies, a poster was presented at the DOD Era of Hope meeting, and invited talks were presented at three major meetings listed below.

Gordon Research Conference, Signal Transduction by Engineered Extracellular Matrices, Tilton, New Hampshire, June 25 - June 29, 2000

Gordon Research Conference, Frontiers of Science, Proteoglycans, New Hampshire, July 9 - July 14, 2000

International Hyaluronan 2000, Wrexham, Wales, UK, September 4 - September 9, 2000

E. Conclusions

Our results to-date provide an exciting and promising method for the development of a new drug delivery system, and in basic research to identify new drug targets and mechanisms. First, we have successfully demonstrated that HA-Taxol prodrugs are selective and soluble cytotoxic agents against cancer cells, and that their mode of action requires HA receptor-mediated uptake by target cells. We expect that *in vivo* experiments in the next year will demonstrate safety and selective toxicity. Second, we have obtained important new knowledge about the structure of RHAMM-HA complexes, and we have identified two kinds of polypeptides that selectively interfere with HA-RHAMM interactions and also affect the ability of RHAMM to cause cell transformation.

F. References

Literature references may be found in the preprints included as appendix materials.

G. Appendices

Biosketches of PI and research scientists

Glenn D. Prestwich

Koen P. Vercruysse

Yi Luo

Michael R. Ziebell

Publications

Y. Luo and G.D. Prestwich, "Synthesis and Cytotoxicity of Hyaluronan-Taxol Antitumor Bioconjugates," *Bioconjugate Chem.*, **10**, 755-763 (1999).

G.D. Prestwich, Y. Luo, M.R. Ziebell, K.P. Vercruysse, K.R. Kirker, and J.S. MacMaster, "Chemically-Modified Hyaluronan: New Biomaterials and Probes for Cell Biology," in *New Frontiers in Medical Sciences: Redefining Hyaluronan* Padua, Italy (G. Abatangelo and P.H. Weigel, eds.) Elsevier Science, pp. 181-194 (2000).

Y. Luo, M.R. Ziebell, and G.D. Prestwich, "A Hyaluronic Acid -Taxol Anti-tumor Bioconjugate Targeted to Cancer Cells," *Biomacromolecules,* 1, 208-218 (2000).

Y. Luo, K.R. Kirker, and G.D. Prestwich, "Chemical Modification of Hyaluronic Acid," *Methods of Tissue Engineering* (A. Atala and R. Lanza, eds.), Academic Press, Orlando, Florida, in press (2000).

M.R. Ziebell, Z.G. Zhao, B. Luo, Y. Luo, E.A. Turley, and G.D. Prestwich, "Peptides that Mimic Carbohydrates: High Affinity Ligands for A Hyaluronic Acid Binding Domain," *J. Biol. Chem.* submitted (2000).

S. Zhang, W.F. Cheung, J. Lu, M.R. Ziebell, S.A. Turley, R. Harrison, D. Zylka, N. Ahn, D. Litchfield, G.D. Prestwich, T. Cruz, and E.A. Turley, " Intracellular RHAMM Isoforms Bind Directly to erk1 and These Interactions are Required for Transformation and for Podosome Formation via the erk Kinase Pathway," *Molec. Cell. Biol.*, in press (2000).

BIOGRAPHICAL SKETCH

NAME	POSITION TITLE
PRESTWICH, GLENN D.	Presidential Professor and Chair of Medicinal Chemistry

EDUCATION/TRAINING (*Begin with baccalaureate or other initial professional education, such as nursing, and include postdoctoral training.*)

INSTITUTION AND LOCATION	DEGREE	YEAR(s)	FIELD OF STUDY
California Institute of Technology, Pasadena, California	1970	1970 (Honors)	Chemistry
Stanford University, Palo Alto, California	Ph.D.	1974	Organic Chemistry

Research and Professional Experience

1974, 1977: Cornell University, NIH postdoctoral fellowship, Department of Chemistry (Prof. J. Meinwald)
1974 - 1976: ICIPE, P.O. Box 30772, Nairobi, Kenya; Research Scientist in Chemistry Unit
1977 - 1982: Assistant Professor of Chemistry, SUNY, Stony Brook, New York
1982 - 1984: Associate Professor of Chemistry, SUNY, Stony Brook, New York
1984 - 1996: Professor of Chemistry, SUNY, Stony Brook, New York
1991 - 1992: Visiting Professor, Departments of Chemistry at Harvard University and The University of Utah
1992 - 1996: Professor of Biochemistry and Cellular Biology, SUNY, Stony Brook, New York
1992 - 1996: Director, Center for Biotechnology, SUNY, Stony Brook, New York
1996 - current: Presidential Professor and Chair, Medicinal Chemistry, The University of Utah
1996 - current: Research Professor of Biochemistry; Adjunct Professor of Chemistry and of Bioengineering; Program Leader, Molecular Pharmacology Program, Huntsman Cancer Institute; Director, Center for Cell Signaling, The University of Utah

Research interests: Structures of protein-ligand complexes; phosphoinositide affinity probes; cell signaling; isoprenoid chemical biology; hyaluronic acid biomaterials; molecular olfaction.

Honors: NIH Postdoctoral Fellow, January 1976-June 1977; Fellow of the Alfred P. Sloan Foundation, 1981-1985; Camille and Henry Dreyfus Teacher-Scholar, 1981-1986; Distinguished Research Fellow, Bodega Marine Laboratory, 1989; H.C. Brown Lecturer, Purdue University, 1990; National Institutes of Health Senior Fellowship, 1992; Paul Dawson Biotechnology Award, American Association of Colleges of Pharmacy, 1998; 1999 Tibbetts Award for Utah [to Echelon Research Laboratories, Inc.]; *ChemTracts* (Organic Chemistry), Invited Expert Analyst (1989-current); *Bioconjugate Chemistry* (1992-current); *Current Opinion in Chemical Biology* (1997-current); *Journal of Biological Chemistry* (2000-current); *M.D. Anderson Cancer Center Advisory Board, University of Texas (2001 - current.*

Publications: G.D. Prestwich is author of over 360 journal research articles and book chapters since 1974. Selected relevant publications on HA and other topics from the last six years are included.

T. Pouyani and G.D. Prestwich, "Functionalized Derivative of Hyaluronic Acid as Drug Carriers and as Novel Biomaterials," *Bioconjugate Chem.*, **5**, 339-347 (1994).

T. Pouyani, G.S. Harbison, and G.D. Prestwich, "Novel Hydrogels of Hyaluronic Acid: Synthesis, Surface Structure and Solid-State NMR," *J. Am. Chem. Soc.*, **116**, 7515-7522 (1994).

G.D. Prestwich, G. Dormán, J.T. Elliott, D.M. Marecak, and A. Chaudhary, "Benzophenone Photoprobes for Phosphoinositides, Peptides, and Drugs," *Photochem. Photobiol.*, **65**, 222-234 (1997).

G.D. Prestwich "Touching all the Bases: Inositol Polyphosphate and Phosphoinositide Affinity Probes from Glucose," *Acc. Chem. Res.*, **29**, 503-513 (1996).

J. Chen, A.A. Profit, and G.D. Prestwich, "Synthesis of Photoactivatable 1,2-*O*-Diacyl-*sn*-glycerol Derivatives of 1-L-Phosphatidyl-D-*myo*-inositol 4,5-Bisphosphate (PtdInsP$_2$) and 3,4,5-Trisphosphate (PtdInsP$_3$)," *J. Org. Chem.*, **61**, 6305-6312 (1996).

T. Pouyani and G.D. Prestwich, "Functionalized Derivatives of Hyaluronic Acid," U.S. Patent No. 5,616,568 (April, 1, 1997).

Q.-M.Gu and G.D. Prestwich, "Synthesis of Phosphotriester Analogues of the Phosphoinositides PtdIns(4,5)P$_2$ and PtdIns(3,4,5)P$_3$," *J. Org. Chem.*, **61**, 8642-8647 (1996).

O. Thum, J. Chen, and G.D. Prestwich, "Synthesis of a Photoaffinity Analogue of Phosphatidylinositol 3,4-Bisphosphate, an Effector in the Phosphoinositide 3-Kinase Signaling Pathway," *Tetrahedron Lett.*, **37**, 9017-9020 (1996).

B. Mehrotra, J.T. Elliott, J. Chen, J.D. Olszewski, A.A. Profit, A.Chaudhary, M. Fukuda, K. Mikoshiba, and G.D. Prestwich, "Selective Photoaffinity Labeling of the Inositol Polyphosphate Binding C2B Domains of Synaptotagmins," *J. Biol. Chem.*, **272**, 4237-4244 (1997).

Q.-M. Gu and G. D. Prestwich, "Efficient Peptide Ladder sequencing by MALDI-TOF Mass Spectrometry Using Allyl Isothiocyanate," *Int. J. Peptide Protein Res.*, **49**, 484-491 (1997).

G.D. Prestwich, D.M. Marecak, J.F. Marecek, K.P. Vercruysse, and M.R. Ziebell, "Controlled Chemical Modification of Hyaluronic Acid:Synthesis, Applications, and Biodegradation of Hydrazide Derivatives," *J. Controlled Rel.* **53**, 93-103 (1998).

L. Feng and G.D. Prestwich, "Expression and Characterization of a Lepidopteran General Odorant Binding Protein," *Insect Biochem. & Molec. Biol.,* **27**, 405-412 (1997).

A. Chaudhary and G.D. Prestwich, "Photoaffinity Analogue for the Anti-inflammatory Drug α-Trinositol: Synthesis and Identification of Putative Molecular Targets," *Bioconjugate Chem.* **8**, 680-685 (1997).

G.D. Prestwich, D.M. Marecak, J.F. Marecek, K.P. Vercruysse, and M.R. Ziebell, "Chemical Modification of Hyaluronic Acid for Drug Delivery, Biomaterials, and Biochemical Probes," in *The Chemistry, Biology, and Medical Applications of Hyaluronan and its Derivatives* (T. C. Laurent, ed.), pp. 43-65 (1998).

K.P. Vercruysse, D.M. Marecak, J.F. Marecek, and G.D. Prestwich, "Synthesis and *In vitro* Degradation of New Polyvalent Hydrazide Cross-Linked Hydrogels of Hyaluronic Acid," *Bioconugate Chem.*,**8**,686-694(1997).

D.M. Marecak, Y. Horiuchi, H. Arai, M. Shimonaga, Y. Maki, T. Koyama, K. Ogura, and G.D. Prestwich," Benzoylphenoxy Analogs of Isoprenoid Diphosphates as Photoactivatable Substrates For Bacterial Prenyltransferases," *BioMed. Chem. Lett.*, **7**, 1973-1978 (1997).J.T. Elliott, R.A. Jurenka, G.D. Prestwich, and W.L. Roelofs, "Identification of Soluble Binding Proteins for an Insect Neuropeptide, " *Biochem. Biophys. Res. Commun.,* **238**, 925-930 (1997)

I. Abe, T. Dang, Y.F. Zheng, B.A. Madden, C. Feil, K. Poralla, and G. D. Prestwich, "Cyclization of (3*S*)29-Methylidene-2,3-oxidosqualene by Bacterial Squalene:Hopene Cyclase: Irreversible Enzyme Inactivation and Isolation of an Unnatural Dammarenoid," *J. Am. Chem. Soc.,* **119**, 11333-11334 (1997).A. Chaudhary, J. Chen, Q.-M. Gu, W. Witke, D.J. Kwiatkowski, and G.D. Prestwich, "Probing the Phosphoinositide 4,5-*bis*phosphate Binding Site of Human Profilin I," *Chem. & Biol.* **5**, 273-281 (1998).

A. Chaudhary, Q.-M.Gu, O. Thum, A.A. Profit, Y. Qing, L. Jeyakumar, S. Fleischer, and G.D. Prestwich, "Specific Interaction of Golgi Coatomer α-COP with Phosphatidylinositol 3,4,5-Trisphosphate," *J. Biol. Chem.*, **273**, 8344-8350 (1998).

Y.F. Zheng, I. Abe, and G.D. Prestwich, "Inhibition Kinetics and Affinity Labeling of Bacterial Squalene:Hopene Cyclase by Thia-Substituted Analogs of 2,3-Oxidosqualene," *Biochemistry,* **37**, 5981-5987 (1998).

K.P. Vercruysse and G.D. Prestwich, "Hyaluronate Derivatives in Drug Delivery," *Crit.Rev. Ther. Drug Carrier Syst,* **15**, 513-555 (1998).

I.Abe, Y.F. Zheng, and G. D. Prestwich, "Photoaffinity Labeling of Oxidosqualene Cyclase and Squalene Cyclase by a Benzophenone-Containing Inhibitor," *Biochemistry*, **37**, 5779-5784 (1998).

G.D. Prestwich and K.P. Vercruysse, "Therapeutic Applications of Hyaluronic Acid and Hyaluronan Derivatives," *Pharmaceut. Sci. & Technol. Today,* **1**, 42-43 (1998).

L. Collis, C. Hall, L. Lange, M.R. Ziebell, G.D. Prestwich, and E.A. Turley, "Rapid Hyaluronan Uptake is Associated with Enhanced Motility: Implications for an Intracellular Mode of Action," *FEBS Lett.,* **440**, 444-449 (1998).

M. Mason, K.P. Vercruysse, K.R. Kirker, R. Frisch, D.M. Marecak, G.D. Prestwich, and W. Pitt, "Hyaluronic Acid-Modified Polypropylene, Polysterene, and Polytetrafluoroethylene," *Biomaterials,* in press (1999).

K.P. Vercruysse, M.R. Ziebell, and G.D. Prestwich, "Control of Enzymatic Degradation of Hyaluronan by Divalent Cations," *Carbohydr. Res.*, **318**, 26-37 (1999).

Y. Luo and G.D. Prestwich, "Synthesis and Cytotoxicity of a Hyaluronic Antitumor Bioconjugate," *Bioconjugate Chem.*, 10, 755-763 (1999).

G.D. Prestwich, Y. Luo, M.R. Ziebell, K.P. Vercruysse, K.R. Kirker, and J.S. MacMaster, "Chemically-Modified Hyaluronan: New Biomaterials and Probes for Cell Biology," in *New Frontiers in Medical Sciences: Redefining Hyaluronan* Padua, Italy (G. Abatangelo, ed.) Elsevier, pp. 181-194 (2000).

J.T. Elliott, W.J. Hoekstra, B.E. Maryanoff, and G.D. Prestwich, "Photoactivatable Peptides Based on BMS-197525, A Potent Antagonist of the Human Thrombin Receptor (PAR-1)," *Bioorg. Med. Chem. Lett.,* **9**, 279-284 (1999).

Q. Yan, G.D. Prestwich, and W.J. Lennarz, "The Ost1p Subunit of Yeast Oligosaccharyl Transferase Recognizes the Peptide Glycosylation Site Sequence, -Asn-*X*-Ser/Thr-," *J. Biol. Chem.* **274**, 5021-5025 (1999).

S.M. Jones, R. Klinghoffer, G.D. Prestwich, A. Toker, and A. Kazlauskas, "PDGF Induces an Early and a Late Wave of PI 3-Kinase Activity, and Only the Late Wave is Required for Progression Through G1," *Curr. Biol.*, **9**, 512-521 (1999).

S. Zhang, W.F. Cheung, J. Lu, M.R. Ziebell, S.A. Turley, R. Harrison, D. Zylka, N. Ahn, D. Litchfield, G.D. Prestwich, T. Cruz, and E.A. Turley, " Intracellular RHAMM Isoforms Bind Directly to erk1 and These Interactions are Required for Transformation and for Podosome Formation via the erk Kinase Pathway," *Molec. Cell. Biol.*, in press (2000).

M. Mason, K.P. Vercruysse, K.R. Kirker, R. Frisch, D.M. Marecak, G.D. Prestwich, and W.G. Pitt, "Hyaluronic Acid-Modified Polypropylene, Polystyrene, and Polytetrafluoroethylene," *Biomaterials,* **21**, 31-36 (2000).

Y. Luo, M.R. Ziebell, and G.D. Prestwich, "A Hyaluronic Acid - Taxol® Anti-tumor Bioconjugate Targeted to Cancer Cells," *Biomacromolecules,* **1**, 208-218 (2000).

Y. Luo, K.R. Kirker, and G.D. Prestwich, "Cross-Linked Hyaluronic Acid Hydrogel Films: New Biomaterials for Drug Delivery," *J. Controlled Release,* in press (2000).

BIOGRAPHICAL SKETCH

NAME	POSITION TITLE
KOEN P. VERCRUYSSE	Research Assistant Professor

EDUCATION/TRAINING

INSTITUTION AND LOCATION	DEGREE *(if applicable)*	YEAR(s)	FIELD OF STUDY
University of Ghent, Belgium	B.Sc.	1990	Pharmaceutical Sciences
University of Ghent, Belgium	Ph.D.	1995	Pharmaceutical Sciences

Research and Professional Experience

1991 Lab of Galenic Development, Lilly Services S.A., Mont-Saint-Guibert, Belgium
1991 - 1995 Lab of General Biochemistry and Physical Pharmacy, University of Ghent, Belgium
1995 - 1996 Postdoctoral Research Associate, Department of Chemistry, SUNY at Stony Brook, NY
1996 - 1998 Postdoctoral Research Associate, Department of Medicinal Chemistry, University of Utah, Salt Lake City, Utah.
1998 - 2000 Research Assistant Professor, Department of Medicinal Chemistry, University of Utah
2000 - current Assistant Professor, Tennessee State University, Nashville, Tennessee

Publications

Dekeyser, P.M; De Smedt, S.; Vercruysse, K.; Demeester, J.; Lauwers, A. "High-performance size-exclusion chromatography of proteoglycans extracted from bovine articular cartilage" Anal. Chim. Acta, 1993, 279, 123-127.

Vercruysse, K.P.; Lauwers, A.R.; Demeester, J.M. "Kinetic investigation of the degradation of hyaluronan by hyaluronidase using gelpermeation chromatography" J. Chrom. B: Biomed. Appl., 1994, 656, 179-190.

Vercruysse, K.P.; Lauwers, A.R.; Demeester, J.M. "Absolute and empirical determination of the enzymatic activity and kinetic investigation of the action of hyaluronidase on hyaluronan using viscosimetry" Biochem. J., 1995, 306, 153-160.

Vercruysse, K.P.; Lauwers, A.R.; Demeester, J.M. "Kinetic investigation of the action of hyaluronidase on hyaluronan using the Morgan-Elson and neocuproine assay" Biochem. J., 1995, 310, 55-59.

Demeester, J.; Vercruysse, K.P.; "Hyaluronidase" in "Pharmaceutical Enzymes" (Lauwers, A.; Scharpe, S.; editors), 1997, pp 155-186, Marcel Dekker, Inc., New York.

Vercruysse, K.P.; Marecak, D.M.; Marecek, J.F.; Prestwich, G.D. "Synthesis and in vitro degradation of new polyvalent hydrazide cross-linked hydrogels of hyaluronic acid" Bioconjugate Chem. , 1997, 8, 686-694.

Van Eeckhout, N., Vercruysse, K., Lauwers, A., and Demeester, "Investigation of the activation of hyaluronidase by $CaCl_2$ using viscosimetry and gel-permeation chromatography", Archives of Physiology and Biochemistry, 1997, 105, p133.

Prestwich, G.D.; Marecak, D.M.; Marecek, J.F.; Vercruysse, K.P.; Ziebell, M.R. "Chemical modification of hyaluronic acid for drug delivery, biomaterials, and biochemical probes" Wenner-Gren Foundation International Symposium : The chemistry, biology, and medical applications of hyaluronan and its derivatives, 1998, 72, pp 43-65.

Prestwich, G.D.; Marecak, D.M.; Marecek, J.F.; Vercruysse, K.P.; Ziebell, M.R. "Controlled chemical modification of hyaluronic acid: synthesis, applications, and biodegradation of hydrazide derivatives" J. Controlled Rel , 1998, 53, 93-103.

Prestwich, G.D. and Vercruysse, K.P. "Therapeutic applications of hyaluronic acid and hyaluronan derivatives", Pharm. Sci. & Tech. Today, 1998, 1,42-43.

Vercruysse, K.P. and Prestwich, G.D.; "Hyaluronate derivatives in drug delivery"; Crit. Rev.Therap. Drug Car. Syst.; 1998, 15, pp.513-555.

Mitchell, M.; Vercruysse, K.; Kirker, K.; Frish, R.; Marecak, D.; Prestwich, G.; Pitt, W. "Hyaluronic acid-modified polypropylene, polystyrene, and polytetrafluoroethylene"; Biomaterials, 1999 (in press).

K.P. Vercruysse, M.R. Ziebell, and G.D. Prestwich, "Control of Enzymatic Degradation of Hyaluronan by Divalent Cations," *Carbohydr. Res.*, **318**, 26-37 (1999).

G.D. Prestwich, Y. Luo, M.R. Ziebell, K.P. Vercruysse, K.R. Kirker, and J.S. MacMaster, "Chemically-Modified Hyaluronan: New Biomaterials and Probes for Cell Biology," in *New Frontiers in Medical Sciences: Redefining Hyaluronan* Padua, Italy (G. Abatangelo and P.H. Weigel, eds.) Elsevier Science, pp. 181-194 (2000).

Grants awarded

May 1998	University of Utah Faculty Research and Creative Grant for "Hyaluronan-fluorescent probe conjugate with quenched fluorescence as substrate for hyaluronidase"
September 1998	University of Utah Research Foundation Funding Incentive Seed Grant Program for "Development of New, Selective Inhibitors of Hyaluronidase" with Glenn D. Prestwich

BIOGRAPHICAL SKETCH

Provide the following information for the key personnel in the order listed on Form Page 2.

NAME	POSITION TITLE
LUO, YI	Research Assistant Professor

EDUCATION/TRAINING (*Begin with baccalaureate or other initial professional education, such as nursing, and include postdoctoral training.*)

INSTITUTION AND LOCATION	DEGREE (*if applicable*)	YEAR(s)	FIELD OF STUDY
Nanjing University, Nanjing, PR China	BSc	1989	Organic Synthesis
Wuhan University, Wuhan, PR China	MSc	1991	Organic Synthesis
Wuhan University, Wuhan, PR China	PhD	1994	Bioactive Polymers

RESEARCH AND PROFESSIONAL EXPERIENCE: Concluding with present position, list, in chronological order, previous employment, experience, and honors. Include present membership on any Federal Government public advisory committee. List, in chronological order, the titles, all authors, and complete references to all publications during the past three years and to representative earlier publications pertinent to this application. If the list of publications in the last three years exceeds two pages, select the most pertinent publications. **DO NOT EXCEED TWO PAGES.**

Research and Professional Experience:

1994 - 1996 Postdoctoral Researcher, Department of Chemistry, Beijing University, Beijing, PR China
1996 - 1997 Researcher, National Institute of Health Sciences, Tokyo, Japan
1997 - 2000 Postdoctoral Research Associate, Medicinal Chemistry, The University of Utah
2000 - current Research Assistant Professor, Medicinal Chemistry, The University of Utah

Publications

Y.Luo, "Study on Reaction Mechanism with Basic Principles of Organic Chemistry," *DAXUE HUAXUE (University Chemistry),* 1991, 6(4), 42.

Y.Luo, X.J.Wu, Z.P.Chen, Z.X.Jiang, "Synthesis and Structure of Langmuir-Blodgett Films of A Novel Amphiphilic Porphyrin," *Chin. Chem. Lett.,* 1992, 3(5), 377.

Y.Luo, X.J.Wu, Z.P.Chen, Z.X.Jiang, "Synthesis of A Novel Amphiphilic Porphyrin and Properties of Langmuir-Blodgett Films," *Chem. J. Chin. Universities,* 1992, 13(8), 1092.

X.J.Wu, Y.Luo, Z.P.Chen, Z.X.Jiang, G.G.Xiong, "Structure of L-B Flim of A Novel Amphiphilic Porphyrin," *Thin Film Sci. and Tech.,* 1993, 6(4), 314.

Y.Luo, R.X.Zhuo, C.L.Fan, "Synthesis and Antitumor Activity of Peptidyl-N^1-hydroxymethyl-5-Fluorouracil," *Chin. Chem. Lett.,* 1993, 4(7), 581.

Y.Luo, R.X.Zhuo, C.L.Fan, "Synthesis and Antitumor Activity of Peptidyl-N^1-hydroxymethyl-5-Fluorouracil," *Chem. J. Chin. Universities,* 1994,15(4), 545.

Y.Luo, R.X.Zhuo, C.L.Fan, "Synthesis and Antitumor Activity of Biodegradable Polyphosphamides Containing 5-Fluorouracil," *Chem. J. Chin. Universities,* 1994, 15(5), 767.

Y.Luo, R.X.Zhuo, C.L.Fan, "Synthesis and Drug Release Properties of Biodegradable Polyphosphate Esters," *Chem. J. Chin. Universities,* 1994, 15(6), 932.

Y.Luo, R.X.Zhuo, C.L.Fan, "Biodegradable Polyphosphate Esters and Drug Release," *Chem. J. Pharmaceuticals,* 1994, 25(6), 265.

Y.Luo, R.X.Zhuo, C.L.Fan, "Synthesis and Antitumor Activity of Polyphosphate Polymeric Drugs Containing Hexestrol," *Chem. J. Chin. Universities,* 1994, 15(7), 1090.

R.X.Zhuo, Y.Luo, G.L.Tao, "Immobilized Enzymes"(Review), *Ionic Exchange and Absorption,* 1994, (5), 447.

Y.Luo, R.X.Zhuo, C.L.Fan, "Sustained Release of Levonorgestrel Using Polyphosphate as Drug Carrier," *Chin. Chem. Lett.,* 1995, 6(4), 333.

Y.Luo, R.X.Zhuo, C.L.Fan, "Studies on The Magnetic Resonance Contrast Agents: Synthesis and Spin-lattice Relaxivity of Amino Acids and Oligopeptidyl Derivatives of Gd-DTPA," *Chin. Chem. Lett.* 1995, 6(5), 377.

Y.Luo, R.X.Zhuo, C.L.Fan, "Study on Synthesis of Crosslinking Polyphosphate and Sustained Release of Levonorgestrel," *Chin. J. Synth. Chem.,* 1995, 3(3), 271.

Y.Luo, R.X.Zhuo, C.L.Fan, "Studies on the Synthesis and Relaxivity of Amino Acids and Oligopeptides of Gd-DTPA Derivatives," *Chemical Journal of Chinese Universities,* 1995, 16(9), 1476.

Y.Luo, R.X.Zhuo, C.L.Fan, "Studies on Water-soluble Metalloporphyrins as Tumor Targeting Magnetic Resonance Imaging Contrast Agents," *Chemical Journal of Chinese Universities,* 1995, 16(10), 1629.

Y.Luo, R.X.Zhuo, C.L.Fan, "Synthesis of Crosslinked Polyphosphates and Drug Release," *Chemical Journal of Chinese Universities,* 1995, 16(10), 1633.

Y.Luo, R.X.Zhuo, "Polymeric Drugs"(Review), *YAOXUE JINZHAN (Progress in Pharmaceutical Sciences),* 1995, 19(3), 135.

Y.Luo, R.X.Zhuo, "Magnetic Resonance Imaging Contrast Agents"(Review), *GUOWAI YIYAO (World Pharmacy),* 1995, 16(4), 200.

A.S. Hoffman (Translated by Y.Luo), "Intelligent Polymers: Synthesis and Applications in Medicine and Biotechnology" (Review), *GAO FEN ZI TONG BAO (Polymer Bulletin),* 1995, (4), 245.

Y.Luo, R.X.Zhuo, C.L.Fan, "Synthesis and Drug Release of Crosslinking Polyphosphates," *Chinese Journal of Reactive Polymers,* 1995, 4(1~2), 127-133.

Y.Luo, R.X.Zhuo, C.L.Fan, "Sustained Release of Methotrexate with Crosslinking Polyphosphate as Drug Carrier," *Chinese Journal of Pharmaceuticals,* 1996, 27(1), 6.

Y.Luo, "Controlled Release Methods" (Review), *GAO FEN ZI TONG BAO (Polymer Bulletin),* 1996, (1), 18.

Y.Luo, S.Yoshioka, Y.Aso, "Swelling Behavior and Drug Release of Amphiphilic N-Isopropylacrylamide Terpolymer Xerogels Depending on Polymerization Methods: γ-Irradiation Polymerization and Redox Initiated Polymerization," *Chem. Pharm. Bull.*, 1999, 47(4), 579-581.

Y. Luo, G. D. Prestwich, "Synthesis and Selective Cytotoxicity of a Hyaluronic Acid-Antitumor Bioconjugate," *Bioconjugate Chem.*, 1999, 10(5), 755-763.

G. D. Prestwich, Y. Luo, M.R. Ziebell, K.P. Vercruysse, K.R. Kirker and J.S. MacMaster, "Chemically-Modified Hyaluronan: New Biomaterials and Probes for Cell Biology," *New Frontiers in Medial Sciences: Redifining Hyaluronan (G. Abatangelo and P.H. Weigel, Ed),* 2000 Elsevier Science, 2000, 181-194.

Y. Luo, M. R. Ziebell, G. D. Prestwich, "A Hyaluronic Acid-Taxol Antitumor Bioconjugate Targeted to Cancer Cells," *Biomacromolecules*, 2000, 1(2), 208-218.

Y. Luo, K.R. Kirker, G. D. Prestwich, "A Novel Hyaluronic Acid Hydrogel Film for Drug Delivery," *J. Controlled Rel.*, in press.

Y. Luo, K.R. Kirker, G.D. Prestwich, "Chemical Modification of Hyaluronic Acid," *Methods of Tissue Engineering* (Anthony Atala and Robert Lanza Ed.), Academic Press, in press.

B.L. Oliver, Y. Luo, J.Liang, G.D. Prestwich, P.W. Noble, "Low Molecular Weight Hyaluronan Fragments Induce Chemokine Expression by An Extracellular Regulated Kinase-Dependent Pathway in Mouse Macrophage," *J. Exp. Medicine*, in press.

M.R. Ziebell, B. Luo, Z.G. Zhao, Y. Luo, E.A. Turley, G.D. Prestwich, "The Convergence of Peptide Libraries in the Search of Artificial Ligands to the Hyaluronic Acid Binding Domains of RHAMM and TSG-6," *J. Biol. Chem.*, submitted.

BIOGRAPHICAL SKETCH

NAME	POSITION TITLE
MICHAEL R. ZIEBELL	Graduate Research Assistant, The University of Utah

EDUCATION/TRAINING (*Begin with baccalaureate or other initial professional education, such as nursing, and include postdoctoral training.*)

INSTITUTION AND LOCATION	DEGREE	YEAR(s)	FIELD OF STUDY
Earlham College, Richmond, Indiana	BA	1991	Physics
Indiana University, Bloomington		1992-93	Coursework in Chemistry and Biology
The University at Stony Brook, Stony Brook, New York	PhD	2000	Physiology & Biophysics

March 2000 - current Postdoctoral Associate, Harvard Medical School

Publications

G.D. Prestwich, D.M. Marecak, J.F. Marecek, K.P. Vercruysse, and M.R. Ziebell, "Controlled Chemical Modification of Hyaluronic Acid:Synthesis, Applications, and Biodegradation of Hydrazide Derivatives,"*J. Controlled Rel.*, **53**, 93-103 (1998).

G.D. Prestwich, D.M. Marecak, J.F. Marecek, K.P. Vercruysse, and M.R. Ziebell, "Chemical Modification of Hyaluronic Acid for Drug Delivery, Biomaterials, and Biochemical Probes," in *The Chemistry, Biology, and Medical Applications of Hyaluronan and its Derivatives* (T. C. Laurent, ed.), Portland Press, London, pp. 43-65 (1998).

G.D. Prestwich, Y. Luo, M.R. Ziebell, K.P. Vercruysse, K.R. Kirker, and J.S. MacMaster, "Chemically-Modified Hyaluronan: New Biomaterials and Probes for Cell Biology," in *New Frontiers in Medical Sciences: Redefining Hyaluronan* Padua, Italy (G. Abatangelo and P.H. Weigel, eds.) Elsevier Science, pp. 181-194 (2000).

Y. Luo, M.R. Ziebell, and G.D. Prestwich, "A Hyaluronic Acid -Taxol Anti-tumor Bioconjugate Targeted to Cancer Cells," *Biomacromolecules,* 1, 208-218 (2000).

S. Zhang, W.F. Cheung, J. Lu, M.R. Ziebell, S.A. Turley, R. Harrison, D. Zylka, N. Ahn, D. Litchfield, G.D. Prestwich, T. Cruz, and E.A. Turley, "Intracellular RHAMM Isoforms Bind Directly to erk1 and These Interactions are Required for Transformation and for Podosome Formation via the erk Kinase Pathway," *Molec. Cell. Biol.*, in press (2000).

M.R. Ziebell, Z.G. Zhao, B. Luo, Y. Luo, E.A. Turley, and G.D. Prestwich, "Peptides that Mimic Carbohydrates: High Affinity Ligands for A Hyaluronic Acid Binding Domain," *J. Biol. Chem.* submitted (2000).

Synthesis and Selective Cytotoxicity of a Hyaluronic Acid–Antitumor Bioconjugate

Yi Luo and Glenn D. Prestwich*

Department of Medicinal Chemistry, The University of Utah, 30 South 2000 East, Room 201, Salt Lake City, Utah 84112-5820. Received March 18, 1999; Revised Manuscript Received May 21, 1999

A cell-targeted prodrug was developed for the anti-cancer drug Taxol, using hyaluronic acid (HA) as the drug carrier. HA–Taxol bioconjugates were synthesized by linking the Taxol 2′-OH via a succinate ester to adipic dihydrazide-modified HA (HA-ADH). The coupling of Taxol-NHS ester and HA-ADH provided several HA bioconjugates with different levels of ADH modification and different Taxol loadings. A fluorescent BODIPY–HA was also synthesized to illustrate cell targeting and uptake of chemically modified HA using confocal microscopy. HA–Taxol conjugates showed selective toxicity toward the human cancer cell lines (breast, colon, and ovarian) that are known to overexpress HA receptors, while no toxicity was observed toward a mouse fibroblast cell line at the same concentrations used with the cancer cells. The drug carrier HA-ADH was completely nontoxic. The selective cytotoxicity is consistent with the results from confocal microscopy, which demonstrated that BODIPY–HA only entered the cancer cell lines.

INTRODUCTION

Hyaluronic acid (HA)[1] (Figure 1), a linear polysaccharide of alternating D-glucuronic acid (GlcUA) and *N*-acetyl-D-glucosamine (GlcNAc) units, adopts a three-dimensional structure in solution that shows extensive intramolecular hydrogen bonding. This restricts the conformational flexibility of the polymer chains and induces distinctive secondary (helical) and tertiary (coiled coil) interactions (*1*). HA is one of several glycosaminoglycan components of the extracellular matrix (ECM), the synovial fluid of joints, and the scaffolding comprising cartilage (*2*). The remarkable viscoelastic properties of HA and commercial cross-linked derivatives (*3*) account for their usefulness in joint lubrication. HA–protein interactions play crucial roles in cell adhesion, growth, and migration (*4–6*), and HA acts as a signaling molecule in cell motility, in inflammation, wound healing, and cancer metastasis (*7*). The immunoneutrality of HA makes it an excellent building block for the development of novel biocompatible and biodegradable biomaterials used in tissue engineering and drug delivery systems (*8–10*). For example, HA has been employed as both a vehicle and angiostatic agent in cancer therapy (*11–13*).

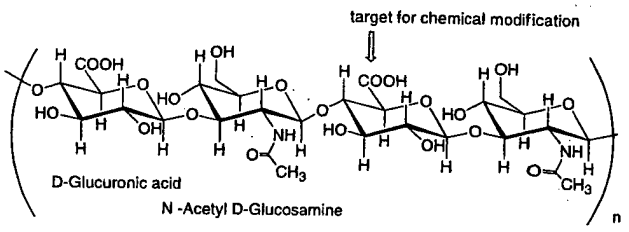

Figure 1. Tetrasaccharide fragment of HA showing the disaccharide repeat units.

The use of biocompatible polymers in the treatment of various ailments has expanded rapidly in the last two decades (*14*). Moreover, derivatization of such polymers with reporter groups (*15*) and drugs (*16, 17*) has emerged as a powerful method for controlling delivery and release of a variety of compounds. Small drug molecules can be linked to the polymer that allows controlled release of the free bioactive group. In general, coupling of antitumor agents to biopolymers provides advantages in drug solubilization, stabilization, localization, and controlled release (*18*). For example, the linking of a cytotoxic small molecule such as adriamycin to poly(hydroxymethyl)-acrylamide (HPMA) gives a new material with improved in vitro tumor retention, a higher therapeutic ratio, avoidance of multidrug resistance (*19*), and encouraging clinical results. In work with a naturally occurring biocompatible polymer, mitomycin C and epirubicin were coupled to HA by carbodiimide chemistry; the former adduct was selectively taken up by, and toxic to, a lung carcinoma xenograft (*20*).

HA is overexpressed at sites of tumor attachment (*21*) to the mesentery and provides a matrix that facilitates invasion (*22*). HA is an important signal for activating kinase pathways (*23, 24*) and regulating angiogenesis in tumors (*25*). Moreover, several types of cellular HA receptors respond to HA as a signal. These include CD44, a family of glycoproteins originally associated with lymphocyte activation; RHAMM, the receptors for HA-mediated cell motility (*26, 27*); and HARLEC, responsible

* To whom correspondence should be addressed. Phone: (801) 585-9051. Fax: (801) 585-9053. E-mail: gprestwich@deans.pharm.utah.edu.

[1] Abbreviations: α-MEM, Minimal Essential Medium, Eagle; ADH, adipic dihydrazide; BODIPY-FL, 4,4-difluoro-5,7-dimethyl-4-bora-3a, 4a-diaza-*s*-indacene-3-propionic acid; D-MEM, Dulbecco's Modified Eagle Medium; DPPC, diphenylphosphoryl chloride; ECM, extracellular matrix; EDCI, 1-ethyl-3-[3-(dimethylamino)-propyl]carbodiimide; FBS, fetal bovine serum; GlcNAc, *N*-acetyl-D-glucosamine; GlcUA, D-glucuronic acid; GPC, gel permeation chromatography; HA, hyaluronic acid; HA-ADH, adipic dihydrazide-modified HA; HAse, hyaluronidase; HMPA, poly(hydroxymethyl)acrylamide; LMW, low molecular weight; MTT, thiazoyl blue; SDPP, *N*-hydroxysuccinimido diphenyl phosphate.

10.1021/bc9900338 CCC: $18.00
Published on Web 07/27/1999

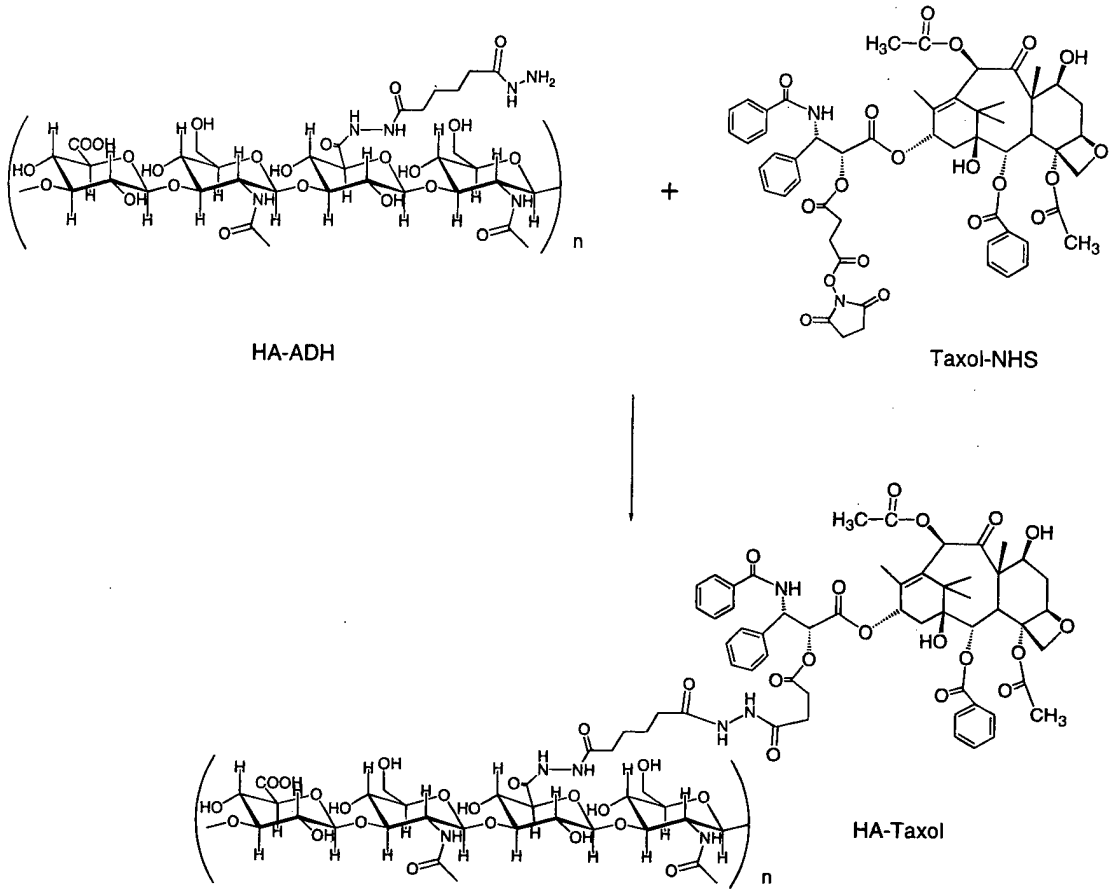

Figure 2. Synthesis of HA–Taxol.

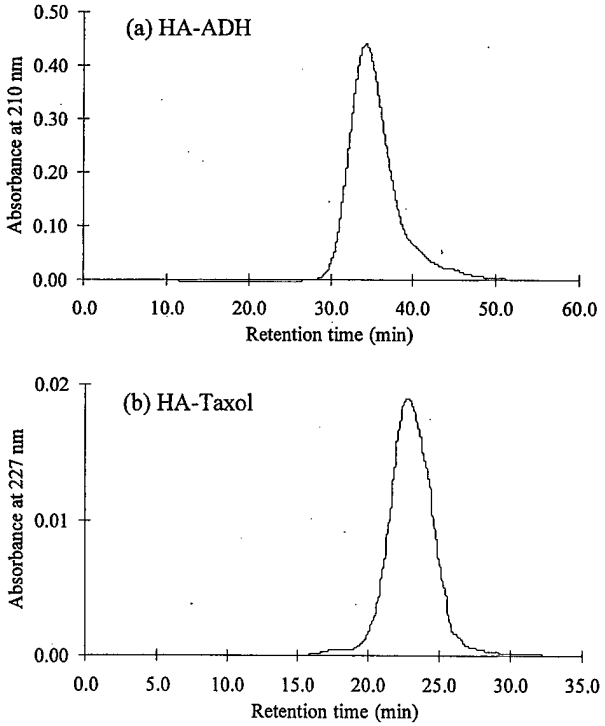

Figure 3. GPC profile. (a) Purified HA-ADH detection at λ = 210 nm. Waters Ultrahydrogel 250, 2000 columns (7.8 mm ID × 30 cm) were used in the analysis. (b) Purified HA–Taxol conjugate detection at λ = 227 nm. Only the Ultrahydrogel 250 column was employed. Eluent was 150 mM, pH 6.5, phosphate buffer/MeOH = 80:20 (v/v); the flow rate was 0.5 mL/min.

for receptor-mediated uptake of HA in liver. Using radiolabeled HA analogues and HA-coupled prodrugs, it

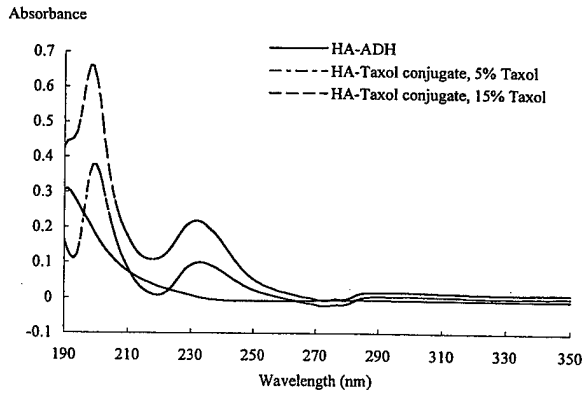

Figure 4. UV spectra of HA–Taxol conjugates.

was possible to selectively target tumor cells and tumor metastases through the use of chondroitin sulfate to block "housekeeping" receptors in the liver without affecting specific HA receptors of tumor cells (*28–31*). Targeting of anti-cancer agents to tumor cells and tumor metastases can be accomplished by receptor-mediated uptake of bioconjugates of these agents to HA (*20*). Since HA receptors (CD44, RHAMM) are overexpressed in transformed human breast epithelial cells and other cancers (*32*), selectivity for cancerous cells is markedly enhanced and overall dosages may be reduced. Moreover, coupling of antitumor agents to biopolymers can provide advantages in drug solubilization, stabilization, localization, and controlled release (*18*). Our methodology (*33*) for coupling antitumor agents to HA adds further value by specifically targeting the bioconjugate to aggressively growing cancers that overexpress HA receptors.

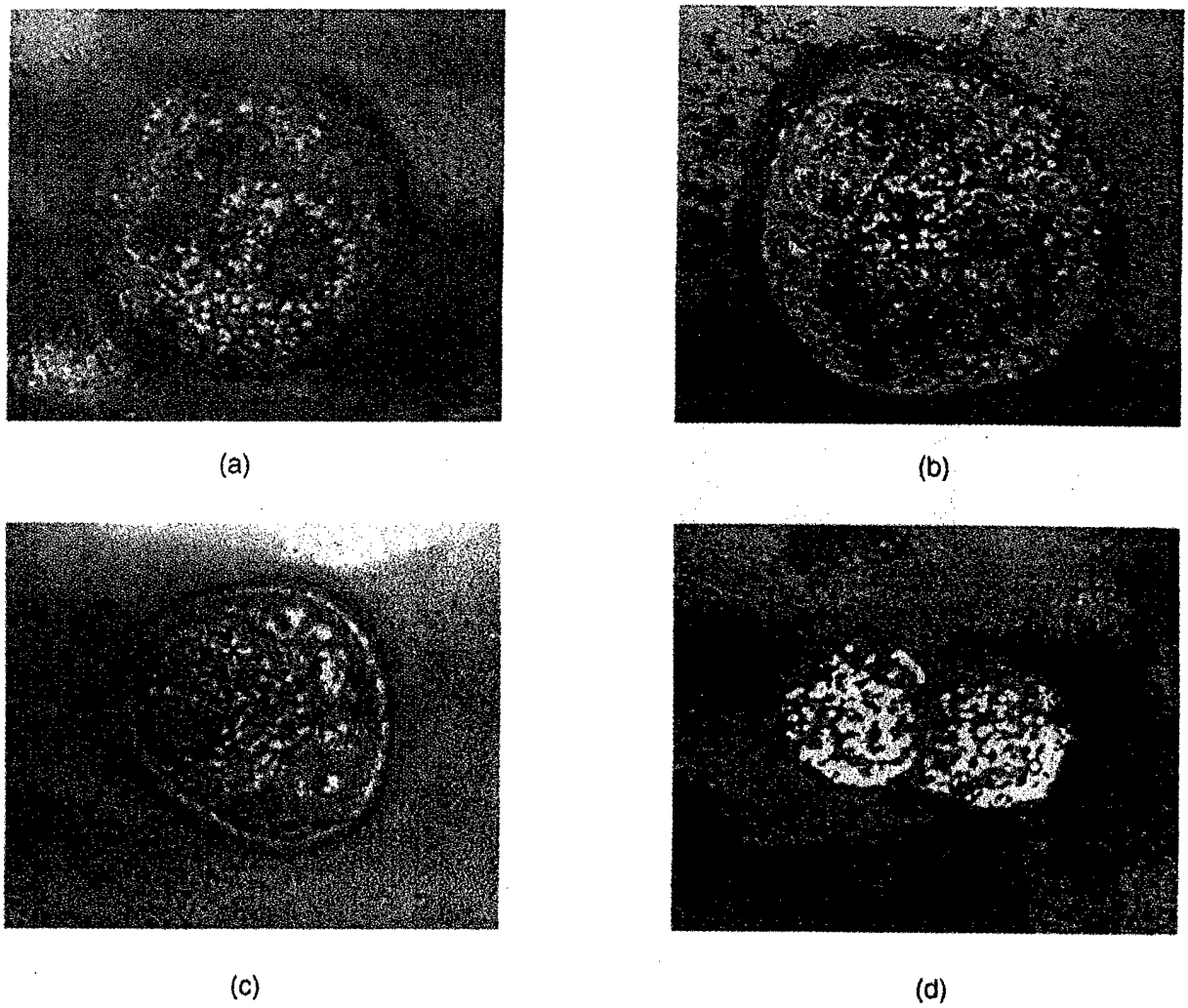

Figure 5. Targeting human breast cancer HBL-100 cells with HA-BODIPY. Panel a fluorescence image shows HA binding to cell surfaces in 3 min. Panels b and c show HA accumulation in the nucleus after 6 and 9 min. In panel d, after 20 min HA, has been completely taken up and fluorescence is dispersed throughout the cells.

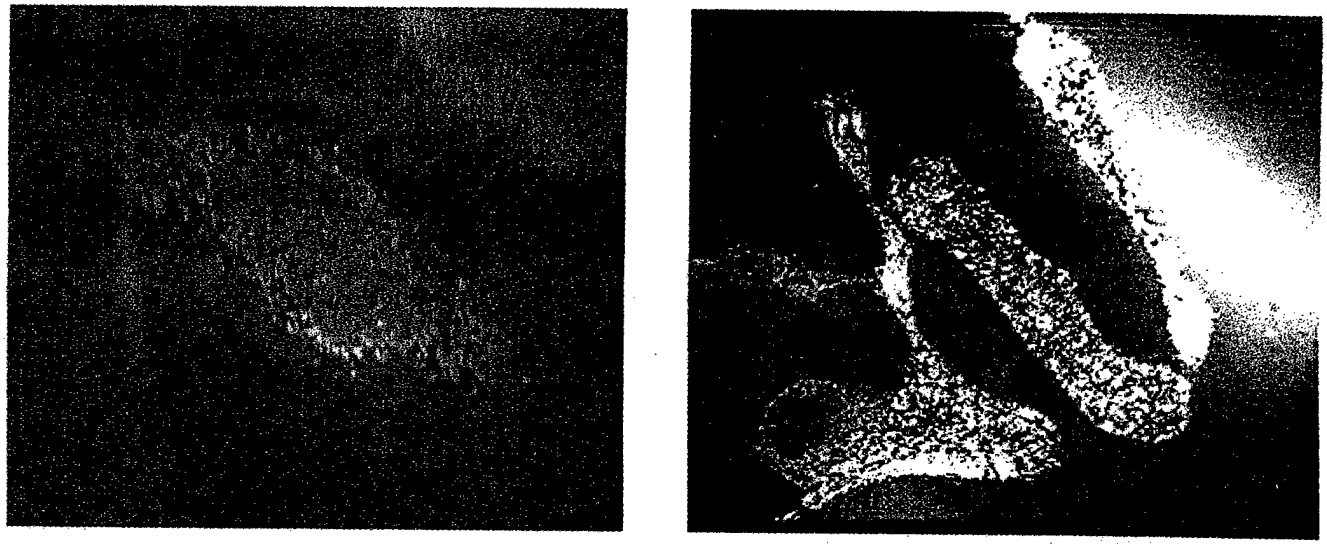

Figure 6. Targeting ovarian cancer SK-OV-3 cells with HA-BODIPY. Panel a shows HA uptake by cells in 15 min. Panel b shows HA uptake by cells in 60 min.

Paclitaxel (Taxol) (*34*), a diterpenoid originally isolated from the bark of the Pacific yew, *Taxus brevifolia*, is a powerful anti-mitotic agent that acts by promoting tubulin assembly into stable aggregated structures. It binds to microtubules and inhibits their depolymerization into tubulin. Although Taxol has shown tremendous potential as an anti-cancer compound, its use as an anti-cancer drug is compromised by its poor aqueous solubility. One attempt to address this involved preparation of 2′-OH linked water-soluble poly(ethylene glycol) derivatives

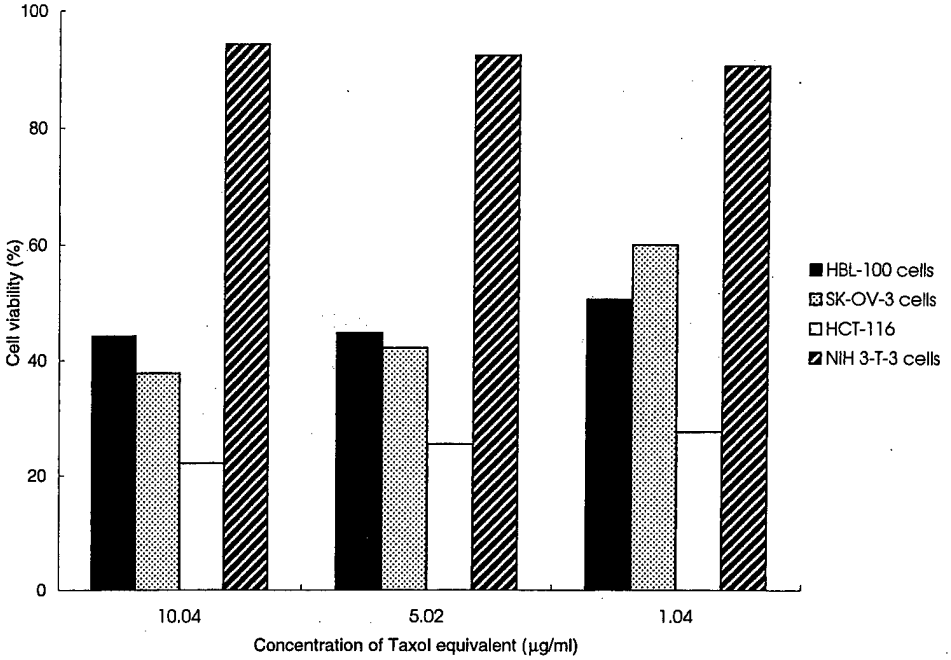

Figure 7. Cytotoxicity of HA–Taxol conjugate with 5% Taxol loading against HBL-100, SK-OV-3, HCT-116, and NIH 3-T-3 cells.

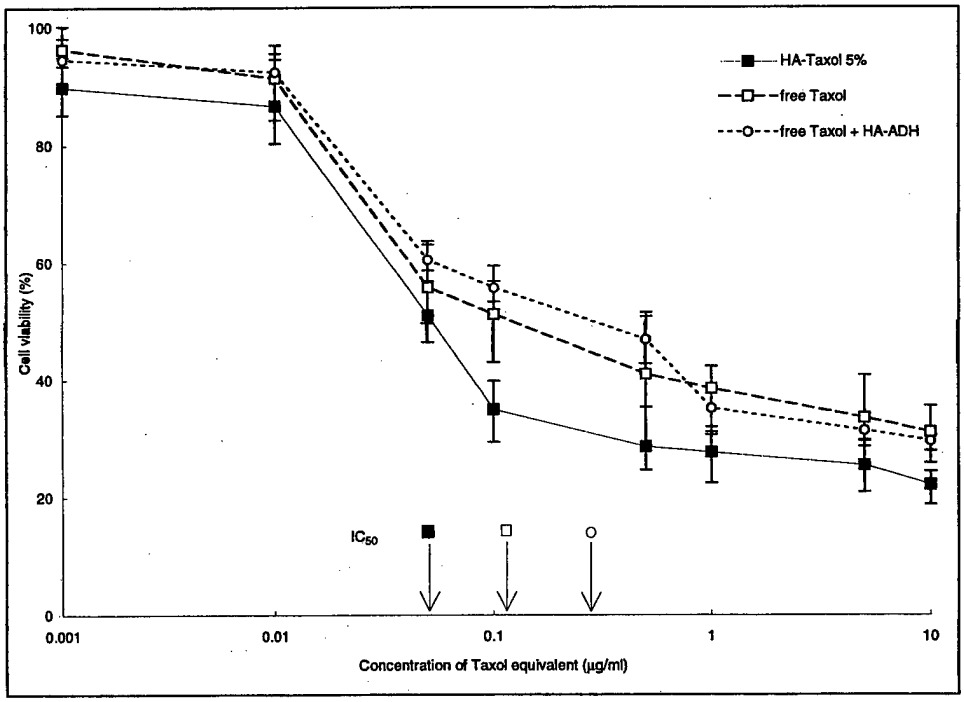

Figure 8. In vitro cytotoxicity of HA–Taxol conjugate with 5% Taxol loading against colon tumor HCT-116 cells.

(*35*). In this paper, we have taken a different approach that uses a prodrug strategy to both increase water solubility and provide cellular targeting. Thus, we selected Taxol as a model anti-cancer drug for covalent attachment to HA that had been modified with adipic dihydrazide (ADH) (*36–38*). The coupling of Taxol-2′-hemisuccinate NHS ester to HA-ADH was optimized to give HA–Taxol conjugates with a variety of ADH and Taxol loadings (Figure 2). Selective in vitro cell cytotoxicity was studied with an untransformed mouse fibroblast cell line (NIH 3-T-3) and with three human cell lines: HCT-116 colon tumor cells, HBL-100 breast cancer cells, and SK-OV-3 ovarian cancer cells. In addition, a fluorescent (BODIPY)-labeled HA bioconjugate was prepared and employed to visualize selective uptake of HA by confocal microscopy.

MATERIALS AND METHODS

General. Fermentation-derived HA (sodium salt, M_w 1.5 MDa) was provided by Clear Solutions Biotechnology, Inc. (Stony Brook, NY). 1-Ethyl-3-[3-(dimethylamino)-propyl]carbodiimide (EDCI), ADH, succinic anhydride, diphenylphosphoryl chloride (DPPC), *N*-hydroxysuccinimide, and triethylamine were purchased from Aldrich Chemical Co. (Milwaukee, WI). Bovine testicular hyaluronidase (HAse, 880 units/mg) was obtained from Sigma Chemical Co. (St. Louis, MO). Paclitaxel (Taxol) was purchased from CBI Tech, Inc. (Cambridge, MA). 4,4-

Difluoro-5,7-dimethyl-4-bora-3a,4a-diaza-*s*-indacene-3-propionic acid, hydrazide (BODIPY-FL hydrazide) was obtained from Molecular Probes, Inc. (Portland, OR). All solvents were of reagent grade or HPLC grade (Fisher Scientific Co., Santa Clara, CA). CH_2Cl_2 and acetonitrile were distilled from CaH_2.

Analytical Instrumentation. All ^1H NMR spectral data were obtained using an NR-200 FT-NMR spectrometer at 200 MHz (IBM Instruments Inc.). UV–Vis spectra were recorded on a Hewlett-Packard 8453 UV–Vis diode array spectrophotometer (Palo Alto, CA). Gel permeation chromatography (GPC) analysis was carried out on the following system: Waters 515 HPLC pump, Waters 410 differential refractometer, Waters 486 tunable absorbance detector, Waters Ultrahydrogel 250 and 2000 columns (7.8 mm ID × 30 cm) (Milford, MA). The GPC eluent was 150 mM phosphate buffer, pH 6.5:MeOH = 80:20 (v/v), and the flow rate was 0.5 mL/min. The system was calibrated with HA standards supplied by Dr. S. Gustafson (University of Uppsala, Sweden), and thus the molecular sizes of each HA oligosaccharide and the corresponding bioconjugates were calculated from the standard samples. Confocal fluorescence images of HA-BODIPY binding and uptake by cells were recorded using a Zeiss Microscope (Carl Zeiss, Inc., Germany). Coulter Counter was from Coulter Electronics, Inc. (Hialeah, FL). Cell viability was determined by thiazoyl blue (MTT) dye uptake protocols at 540 nm, which was recorded on a Bio-Rad M-450 microplate reader (Hercules, CA).

Synthesis of Taxol-NHS Ester. To a stirred solution of 270 mg of Taxol and 38 mg (1.2 equiv) of succinic anhydride in 13 mL of CH_2Cl_2 at room temperature was added 36 μL (10-fold molar excess) of dry pyridine. The reaction mixture was stirred for 3 days at room temperature and then concentrated in vacuo. The residue was dissolved in 5 mL of CH_2Cl_2, and Taxol-2′-hemisuccinate was purified on silica gel (wash with hexane; elute with ethyl acetate) to give 258 mg of product (86%). FAB-MS calcd for $C_{51}H_{55}NO_{17}$: 953.99. Found: 954.4 (MH^+).

Next, *N*-hydroxysuccinimido diphenyl phosphate (SDPP) was prepared from 10 mmol of diphenylphosphoryl chloride, 10 mmol of *N*-hydroxysuccinimide, and 10 mmol of triethylamine in 6 mL of CH_2Cl_2 as previously described (*39*). Crude SDPP was triturated with ether, dissolved in ethyl acetate, washed (2 × 10 mL H_2O), dried ($MgSO_4$), and concentrated in vacuo to give SDPP with mp 89–90 °C (85%). To a solution of 150 mg of Taxol-hemisuccinate and 82 mg (1.5 equiv) of SDPP in 5 mL of acetonitrile was added with 88 μL (4 equiv) of triethylamine. The reaction was stirred for 6 h at room temperature, and then concentrated in vacuo. The residue was dissolved in 5 mL of ethyl acetate and 2 mL of hexane and purified on silica gel. SDPP gave superior yields in less time and under milder conditions than did any carbodiimide coupling reagent. The purified Taxol-NHS ester was dried for 24 h in vacuo at room temperature to give 134 mg (80%). FAB-MS calcd for $C_{55}H_{58}N_2O_{19}$: 1051.07. Found: 1051.5 (MH^+).

Preparation of Low Molecular Weight (LMW) HA. To a solution of 2.0 g of high molecular mass HA (1.5 MDa) in pH 6.5 PBS buffer (4 mg/mL) was added hyaluronidase (HAse) (10 units/mg of HA). The degradation was carried out at 37 °C, 190 rpm stirring for 1 h, then 95 °C for 20 min. Dialysis tubing (M_w cutoff 3 500 Da) was prepared by soaking the membrane in water at room temperature for 3–4 h and subsequently rinsing it with water. The solution was dialyzed against water for 4 days using this washed membrane tubing. The retained material was filtered through a 0.2 μm cellulose acetate membrane (Corning) and lyophilized to give 1.12 g of LMW HA (56%).

Adipic Dihydrazido-Functionalized HA (HA-ADH). HA-ADH was prepared as described previously (*37*, *38*, *40*). In a representative example, LMW HA (50 mg) was dissolved in water to give a concentration of 4 mg/mL, and then a 5-fold excess of ADH was added into the solution. The pH of the reaction mixture was adjusted to 4.75 by addition of 0.1 N HCl. Next, 1 equiv of EDCI was added in solid form. The pH of the reaction mixture was maintained at 4.75 by addition of 0.1 N HCl. The reaction was quenched by addition of 0.1 N NaOH to adjust the pH of reaction mixture to 7.0. The reaction mixture was then transferred to pretreated dialysis tubing (Mw cutoff 3 500) and dialyzed exhaustively against 100 mM NaCl, then 25% EtOH/H_2O and finally H_2O. The solution was then filtered through 0.2 μm cellulose acetate membrane, flash frozen, and lyophilized. The purity of HA-ADH was measured by GPC. The substitution degree of ADH was determined by the ratio of methylene hydrogens to acetyl methyl protons as measured by ^1H NMR. In this example, 37 mg of HA-ADH was obtained with an 18% loading based on available carboxylates modified.

HA–Taxol. Several loadings were prepared following a general protocol (Figure 2). In a representative example, HA-ADH with 18% ADH loading (10 mg, 4.4 μmole hydrazide) was dissolved in 3 mM, pH 6.5, phosphate buffer to give a concentration of 1 mg/mL. To this mixture was added Taxol-NHS ester dissolved in sufficient DMF (DMF:H_2O = 2:1, v/v) to give a homogeneous solution, and the reaction mixture was stirred at room temperature for 24 h. The reaction mixture was dialyzed successively against 50% acetone/H_2O and water (membrane tubing, Mw cutoff 3 500). The solution was then filtered through a 0.2 μm membrane and then lyophilized. The purity of HA–Taxol conjugate was measured by GPC analysis. Taxol loading was determined by UV absorbance (λ_{max} = 227 nm, $\epsilon = 2.8 \times 10^4$) in 80:20 CH_3CN:H_2O.

BODIPY-FL-Labeled HA. In a representative reaction, 100 mg of LMW HA was dissolved in 10 mL of H_2O, and 10 mL of an acetone solution (0.8 mg/mL) of BODIPY–FL hydrazide was added. The pH was adjusted to 4.75 with 0.1 N HCl, and then 51.5 mg (3 molar equiv) of EDCI was added in solid form into the mixture. The reaction was stirred overnight at room temperature at pH 4.75. The HA-BODIPY was purified by dialysis against H_2O, and its purity was characterized by GPC with detection at 210 nm (HA) and 502 nm (BODIPY).

In Vitro Cell Culture Cytotoxicity. The cytotoxicity of HA–Taxol conjugates was determined using a 96-well plate format in quadruplicate with increasing doses: 0.001, 0.01, 0.1, 0.5, 1, 5, 10, 50, and 100 μg/mL. Each well contained approximately 20 000 cells in 200 μL of cell culture media. Cells were cultured in the following media: HBL-100 cells, high glucose D-MEM (Dulbecco's Modified Eagle Medium) + 10% FBS (fetal bovine serum) + 1% sodium pyruvate; SK-OV-3 cells, D-MEM/F12 + 10% FBS; HCT-116 cells, α-MEM (Minimal Essential Medium, Eagle) + 10% FBS; NIH 3-T-3 cells, high glucose D-MEM + 10% FBS.

HA–Taxol conjugates and HA-ADH control were added as stock solutions in DMSO:H_2O = 1:1 (v/v); free Taxol was added as a DMSO stock solution. A 2 μL aliquot of the stock solution was added to each well of the cell culture plate. Cells were incubated at 37 °C for 3 days with the test material, and cell viability was determined using MTT dye uptake by reading plates at 540 nm.

Table 1. Optimization of ADH Modification of HA and the Reaction Condition

molar ratio of HA:ADH:EDCI	reaction time (min)	ADH loading (%)
1:40:4	5	28.3
	10	31.2
	15	31.4
	30	32.2
	60	38.6
	120	45.7
	240[a]	44.0
1:5:0.5	15	9.0
1:5:1	15	17.5
1:10:1	15	18.0
1:20:1	15	19.0
1:10:0.2	180	19.3

[a] No 0.1 N HCl was used to maintain the pH of the reaction mixture.

Response was graded as percent live cells compared to untreated controls (*41*).

RESULTS

Degradation and Modification of HA. LMW HA was generated by degradation of high molecular mass HA (1.5 MDa) with testicular HAse. This enzyme degrades HA to generate a series of even-numbered HA oligosaccharides with the *N*-acetylglucosamine moiety at the reducing terminus (*42*). Thus, incubation of a solution of high molecular mass HA in pH 6.5 PBS buffer with testicular HAse at 37 °C provided partially degraded HA. Small fragments, HA oligosaccharides, and buffer salts were removed by dialysis against H_2O (four changes per day). The final LMW HA product was lyophilized, and an aliquot was analyzed by GPC analysis: $M_n = 3883$, $M_w = 11\,199$, and molecular dispersity (DP) = 2.88. This corresponds to an average of 28 disaccharide repeats/LMW HA molecule. This preparation is quite reproducible as time, temperature, and concentrations of HA and HAse are controlled.

The use of the mild and versatile hydrazide method for preparation of chemically modified HA derivatives (*36*, *37*) allows attachment of reporter molecules, drugs, cross-linkers, and any combination of the above moieties to HA (*10*, *33*, *40*). Covalent attachment of ADH to the carboxylic acid groups of HA provides a controlled loading of pendant hydrazide functionalities arrayed along the hyaluronate backbone, used herein for the attachment of an antitumor agent. We selected LMW HA for modification in this study for four main reasons. First, it was possible to perform reproducible chemical modifications and to monitor the extent of modification by simple proton NMR methods. Second, LMW HA can be cleared from the body via ultrafiltration by the kidney. Third, the LMW HA bioconjugates were expected to provide a readily injectable nonviscous solution at concentrations up to 10 mg/mL, and the LMW materials should suffer minimal further degradation in plasma and would be rapidly taken up by cells. Finally, with LMW HA bioconjugates, we were confident that future efforts to cross-link the material into a hydrogel could also be easily controlled.

Thus, LMW HA (4 mg/mL) was mixed with ADH at several concentrations (Table 1). The pH of the reaction mixture was adjusted to 4.75, and then different quantities of solid EDCI were added in solid form to initiate the reaction. An increase in pH was observed immediately corresponding to proton uptake in the coupling reaction. The pH of the reaction mixture was maintained at 4.75 by addition of 0.1 N HCl. Preliminary studies had provided guidelines as to ratios of HA:ADH:EDCI suitable to achieve a given percentage modification of the glucuronate functions of HA. The reaction was stopped by addition of 0.1 N NaOH to adjust the pH of reaction mixture to 7.0. The HA-ADH was purified by sequential dialysis against 100 mM NaCl, 25% EtOH/H_2O, and H_2O. The dialyzed solutions were filtered through a 0.2 μm membrane, and then lyophilized to give HA-ADH in yields ranging 50–70%.

Table 2. Optimization of Taxol Loading. Both the Total ADH Modification of HA and the Molar Ratio of ADH to Taxol-NHS Ester during the Conjugation Reaction Were Varied

$(HA)_x(HA\text{-}ADH)_y(HA\text{-}ADH\text{-}Taxol)_z$

preparation	composition of HA–Taxol conjugates: HA (x) (%)	HA-ADH (y) (%)	HA-ADH-Taxol (z) (%)	solubility in H_2O	ADH%: Taxol-NHS[a]
	A. ADH loading = 9%[b]				
1	91	7.8	1.2	yes	9:5
2	91	7.7	1.3	yes	9:9
3	91	3.8	5.2	yes	9:18
	B. ADH loading = 18%				
4	82	16.4	1.6	yes	18:5
5	82	16.1	1.9	yes	18:10
6	82	15.8	2.2	yes	18:15
7	82	3.1	14.9	partially[c]	18:36
	C. ADH loading = 45%				
8	55	30	15	no	45:90

[a] The molar ratio used in the grafting reaction of HA-ADH and Taxol-NHS that resulted in the composition of the HA–Taxol conjugates. [b] Total ADH loading for modified HA = $y + z$. [c] Limited solubility; only soluble below 0.1 mg/mL due to high loading of Taxol.

The purity and molecular size distribution of the HA-ADH was measured by GPC. The narrow single-peak GPC profile detected by UV (210 nm) (Figure 3a) and RI indicated that both large and small impurities had been completely removed. It is essential to establish this fact rigorously to ensure that all subsequent molecules added also become covalently attached, rather than remaining noncovalently associated. In addition, the GPC results showed that there was virtually no molecular weight decrease due to further HA degradation or increase due to bifunctional cross-linking during the modification reaction. The loading of ADH on the polymer backbone was determined by ^1H NMR spectroscopy studies with D_2O as a solvent. The degree of substitution could be calculated by integration of the ADH methylene signals using the methyl resonance ($\delta = 1.95–2.00$ ppm) of the acetamido moiety of the GlcNAc residues of HA as an internal standard (*37*). Thus, ^1H NMR integration confirmed that different ADH loadings occurred with different ratios of reactants and for different reaction times. The relationship between the degree of substitution of ADH and the reaction conditions, i.e., molar ratio of HA:ADH:EDCI, and reaction time was optimized. The results are shown in Table 1. Importantly, the degree of ADH substitution on HA was influenced primarily by the HA:EDCI ratio, with the amount of excess ADH varying from 5 to 25-fold having little effect. The carbodiimide quantity is thus the controlling factor for determining ADH loading on HA.

Taxol (paclitaxel) is a taxane natural product that promotes polymerization of tubulin and stabilizes the structure of intracellular microtubules. This process has the effect of inhibiting the normal dynamics reorganization of the microtubules, which is necessary for inter-

Table 3. In Vitro Cytotoxcity of HA–Taxol Conjugates against Different Cell Lines

HA–Taxol preparations	IC_{50} (μg/mL)[d] HBL-100[e] conjugate[b]	HBL-100[e] Taxol equivalents[c]	SK-OV-3[e] conjugate	SK-OV-3[e] Taxol equivalent	HCT-116[e] conjugate	HCT-116[e] Taxol equivalent
1	48.0 (118 μM)	1.21 (1.42 nM)	21.5 (53 μM)	0.54 (0.64 nM)	7.20 (17.8 μM)	0.18 (0.21 nM)
3	16.4 (37 μM)	1.65 (1.93 nM)	8.0 (18.2 μM)	0.80 (0.94 nM)	0.52 (1.2 μM)	0.052 (0.061 nM)
7	6.8 (12.4 μM)	1.58 (1.85 nM)	0.37 (0.68 μM)	0.086 (0.10 nM)	0.11 (0.20 μM)	0.026 (0.030 nM)
8[a]	68.0 (115 μM)	1.48 (17.3 nM)	7.2 (17.3 nM)	1.56 (1.83 nM)	2.15 (3.65 μM)	0.47 (0.55 nM)

[a] Dissolved in 3:1 DMSO/H_2O. [b] The data in these columns show the IC_{50} of HA–Taxol conjugates against the tumor cell line. [c] The data in these columns are calculated as the Taxol equivalents present in the HA–Taxol bioconjugate using the molar ratios in Table 2. This calculation allows comparison of conjugated and free Taxol. [d] The IC_{50} value is the molarity at which 50% of tumor cell death was observed after 72 h under standard tissue culture conditions. [e] Cell type.

phase and mitotic functions. Because of the problems in administering emulsified forms of this water-insoluble drug, Taxol was selected as the model anti-cancer drug in our study. Taxol was first converted to its 2′-hemisuccinate derivative by standard methods (*43*), and its structure was confirmed spectroscopically. Second, the activated Taxol-NHS ester was prepared by coupling with SDPP. Taxol-NHS was then coupled to HA-ADH in 3 mM phosphate buffer at pH 6.50 using DMF as a cosolvent to maintain a homogeneous solution. The purification of HA–Taxol bioconjugate was carried out by dialysis of the reaction mixture against 50% acetone/H_2O. The purity of the HA–Taxol conjugate was determined by GPC analysis, monitoring absorbance at 227 nm (Figure 3b) and RI. The single symmetrical GPC peak showed that no free Taxol or other small molecular impurities remained in this preparation. The Taxol was quantified by UV absorbance at 227 nm (Figure 4) in 80% acetonitrile: H_2O. To obtain the optimal modification on HA for anti-cancer ability, HA–Taxol conjugates with different Taxol loading were synthesized. Table 2 shows the optimization of Taxol loading and the molar ratio of HA-ADH to Taxol-NHS during the conjugation reaction. These data demonstrate that the molar ratio of ADH to Taxol-NHS during the grafting reaction is critical in determining the Taxol loading of the bioconjugate.

Fluorescently labeled HA has been prepared with several chemistries and used in other studies of receptor-mediated uptake. Most recently, RHAMM-mediated uptake and trafficking of HA by transformed fibroblasts (*44*) was observed with Texas Red-HA. Previously, fluorescein-HA was employed to study HA uptake in a variety of systems, e.g., cells expressing CD44 variants (*21*, *45–48*), uptake by tumor cells for correlation with metastatic potential (*49*, *50*), internalization by chondrocytes (*51*), and as a measure of liver endothelial cell function (*52*). In this study and in the Texas Red study, hydrazide derivatives of the dyes were used to form covalent bishydrazide linkages to the HA carboxylic acid functions under the mild all-aqueous conditions employed for other hydrazide modifications of HA (*33*).

To study the binding ability of HA to tumor cells and uptake by cells, a variety of fluorescently labeled HA derivatives were prepared. Of those evaluated for use with cancer cells, we obtained the best results with the BODIPY fluorophore (Y. Luo, M. R. Ziebell, unpublished results). Thus, BODIPY–FL hydrazide was coupled to LMW HA using EDCI as the condensing agent to give HA-BODIPY, which was purified by dialysis against H_2O; the loading of GPC-homogeneous HA-BODIPY was determined spectrophotometrically to be 1.8% (based on available glucuronates).

Cell-Based Assays for Uptake and Toxicity. An aliquot (2 μL) of a 1.5 mg/mL aqueous stock solution HA-BODIPY was added to 100 μL cell culture media with tumor cells cultured on cover slips. Confocal images of HA-BODIPY uptake by HBL-100 cells can be seen in Figure 5. Initially, the HA-BODIPY can be seen on cell membrane; over the course of several minutes, it is taken up into the cell and then gradually begins to accumulate in the nucleus. After 20 min, cells showed HA-BODIPY in most compartments. Uptake of HA-BODIPY into SK-OV-3 cells occurred with a similar appearance and time course (Figure 6). These data suggest that HA binds readily to tumor cell surface and is rapidly taken up via HA receptor-mediated pathways. This supports the notion that HA should be a good targeting polymer for selective delivery of anti-cancer drugs to tumor cells. Similar results were observed independently with HA–Texas Red uptake by transformed fibroblasts (*44*). Importantly, nontransformed cells, such as the NIH 3-T-3 fibroblasts, did not show this binding and rapid uptake of HA-BODIPY.

Next, the cytotoxicity of HA–Taxol conjugates was measured using a 96-well plate format in quadruplicate with increasing doses from 0.001 to 100 μg/mL. The cytotoxicity of HA–Taxol conjugates was studied by using the MTT assay to identify cells still active in respiration (*41*). HA–Taxol conjugates showed effective cytotoxicity against SK-OV-3, HBL-100, and HCT-116 cell lines, while no cytotoxicity against NIH 3-T-3 cells was observed at concentrations up to 10 μg/mL of Taxol equivalents (Figure 7). These results confirm the selective toxicity of HA–Taxol toward different cells lines, and the known overexpression of CD44 by HBL-100 (*53*) and SK-OV-3 cells (*54*) suggests that this selective toxicity is due to receptor-mediated binding and uptake of the HA–Taxol bioconjugate.

The HA-BODIPY binding and uptake results support the hypothesis that selective toxicity of HA–Taxol is due to receptor-mediated events. This was further explored by investigating the relative toxicity of polymer-bound and free Taxol, as well as examining the effect of the polymeric carrier itself on the toxicity of the drug. Thus, Figure 8 summarizes the cytotoxicity data for HA–Taxol (5% Taxol loading) with HCT-116 colon cancer cells. The bioconjugate showed increased cytotoxicity, e.g., lower IC_{50}, relative to free Taxol or free Taxol mixed with the HA-ADH carrier. In a further control experiment, we had established that HA-ADH alone elicited no detectable change in cell viability at a concentration 10 times higher than the maximal concentration of HA–Taxol conjugate used. These data support the notion that the increased cytotoxicity of HA–Taxol conjugates requires cellular uptake of the complex followed by hydrolytic release of the active Taxol by cleavage of the labile 2′ ester linkage.

The in vitro cytotoxicity results of HA–Taxol conjugates with different modifications against different cell lines are shown in Table 3. For the least-modified HA (9% ADH modification), higher cytotoxicity was observed

as Taxol loading increased. However, the cytotoxicity of highly modified HA actually decreased at the highest Taxol loading. Apparently, high loading of Taxol decreased the solubility of HA–Taxol conjugate, masked the HA receptor recognition elements of HA, caused aggregation of the polymeric conjugate, and thus limited the toxicity of the conjugate relative to that of free drug. Clearly, the cytotoxicity of HA–Taxol conjugates depends on a balance between minimal HA modification and maximal Taxol loading.

ACKNOWLEDGMENT

Financial support for this work was provided by Department of Army (DAMD 17-9A-1-8254) and by the Huntsman Cancer Foundation at The University of Utah. Initial studies of HA modification and degradation were performed with M.R. Ziebell (UUtah) and we thank Drs. D.M. Marecak and C.M. Amann (UUtah) for assistance with Taxol modification. We are grateful to D. Schmehl and Dr. L. R. Barrows (UUtah) for assistance with cell cytotoxicity experiments and Mr. Ziebell and Dr. W. G. Pitt (Brigham Young University, Provo, UT) for assistance with confocal microscopy. We thank Dr. L. Y.-W. Bourguignon (University of Miami Medical School, Miami, FL) for providing HBL-100 and SK-OV-3 cells. We are grateful to Clear Solutions Biotech, Inc. (Stony Brook, NY) for providing HA and the Center for Cell Signaling (UUtah) for equipment and facilities.

LITERATURE CITED

(1) Scott, J. E., Secondary structures in hyaluronan solutions: chemical and biological implications; In *The Biology of Hyaluronan*; C. Foundation, Ed.; J. Wiley & Sons, Ltd.: Chichester, UK, 1989; pp 6–20.

(2) Laurent, T. C., Laurent, U. B. G., and Fraser, J. R. E. (1995) Functions of hyaluronan. *Ann. Rheum. Dis. 54*, 429–432.

(3) Larsen, N. E., Leshchiner, E., and Balazs, E. A. (1995) Biocompatibility of Hylan polymers in various tissue compartments. *Mater. Res. Soc. Symp. Proc. 394*, 149–153.

(4) Knudson, C. B., and Knudson, W. (1993) Hyaluronan-Binding proteins in development, tissue homeostasis, and disease. *FASEB J. 7*, 1233–1241.

(5) Turley, E. A., The role of a cell-associated hyaluronan binding protein in fibroblast behavior; In *The Biology of Hyaluronan*; C. Foundation, Ed.; J. Wiley & Sons, Ltd.: Chichester, UK, 1989; pp 121–137.

(6) Underhill, C. B., The interaction of hyaluronate with the cell surface: the hyaluronate receptor and the core protein; In *The Biology of Hyaluronan*; C. Foundation, Ed.; J. Wiley & Sons, Ltd.: Chichester, UK, 1989; pp 87–106.

(7) Entwistle, J., Hall, C. L., and Turley, E. A. (1996) Hyaluronan receptors: regulators of signaling to the cytoskeleton. *J. Cell Biochem. 61*, 569–577.

(8) Vercruysse, K. P., and Prestwich, G. D. (1998) Hyaluronate derivatives in drug delivery. *Crit. Rev. Ther. Drug Carr. Syst. 15*, 513–555.

(9) Freed, L. E., Vunjak-Novakovic, G., Biron, R. J., Eagles, D. B., Lesnoy, D. C., Barlow, S. K., and Langer, R. (1994) Biodegradable polymer scaffolds for tissue engineering. *Bio/Technology 12*, 689–693.

(10) Prestwich, G. D., Marecak, D. M., Marecek, J. F., Vercruysse, K. P., and Ziebell, M. R., Chemical modification of hyaluronic acid for drug delivery, biomaterials, and biochemical probes; In *The Chemistry, Biology, and Medical Applications of Hyaluronan and its Derivatives*; T. C. Laurent, Ed.; Portland Press: London, 1998; pp 43–65.

(11) Alam, C. A. S., Seed, M. P., and Willoughby, D. A. (1995) Angiostasis and vascular regression in chronic granulomatous inflammation induced by diclofenac in combination with hyaluronan in mice. *J. Pharm. Pharmacol. 47*, 407–411.

(12) Ziegler, J. (1996) Hyaluronan seeps into cancer treatment trials. *J. Nat. Cancer Inst. 88*, 397–399.

(13) Falk, R. E. In *PCT Int. Appl. WO 9740841*; 1997.

(14) Duncan, R., Dimitrijevic, S., and Evagorou, E. G. (1996) The role of polymer conjugates in the diagnosis and treatment of cancer. *J. Therap. Polymers Pharmaceut. Sci. 6*, 237–263.

(15) Brinkley, M. (1992) A brief survey of methods for preparing protein conjugates with dyes, haptens, and cross-linking agents. *Bioconjugate Chem. 3*, 2–13.

(16) Puttnam, D., and Kopecek, J. (1995) Polymer conjugates with anticancer activity. *Adv. Polym. Sci. 122*, 55–123.

(17) Krinick, N. L., and Kopecek, J., Soluble polymers as targetable drug carriers; In *Targeted Drug Delivery. Handbook of Experimental Pharmacology*; R. L. Juliano, Ed.; Springer-Verlag: Berlin, 1991; pp 105–179.

(18) Maeda, H., Seymour, L., and Miyamoto, Y. (1992) Conjugates of anticancer agents and polymers: advantages of macromolecular therapeutics in vivo. *Bioconjugate Chem. 3*, 351–362.

(19) Minko, T., Kopeckova, P., Pozharov, V., and Kopecek, J. (1998) HPMA copolymer bound adriamycin overcomes MDR1 gene encoded resistance in a human ovarian carcinoma cell line. *J. Controlled Release 54*, 223–233.

(20) Akima, K., Ito, H., Iwata, Y., Matsuo, K., Watari, N., Yanagi, M., Hagi, H., Oshima, K., Yagita, A., Atomi, Y., and Tatekawa, I. (1996) Evaluation of antitumor activities of hyaluronate binding antitumor drugs: synthesis, characterization and antitumor activity. *J. Drug Targeting 4*, 1.

(21) Yeo, T. K., Nagy, J. A., Yeo, K. T., Dvorak, H. F., and Toole, B. P. (1996) Increased hyaluronan at sites of attachment to mesentery by CD44-positive mouse ovarian and breast tumor cells. *Am. J. Pathol. 148*, 1733–1740.

(22) Knudson, W. (1996) Tumor-associated hyaluronan: providing an extracellular matrix that facilitates invasion. *Am. J. Pathol. 148*, 1721–1726.

(23) Nelson, R. M., Venot, A., Bevilacqua, M. P., Linhardt, R. J., and Stamenkovic, I. (1995) Carbohydrate-protein interactions in vascular biology. *Annu. Rev. Cell Dev. Biol. 11*, 601–631.

(24) Hall, C. L., Yang, B. H., Yang, X. W., Zhang, S. W., Turley, M., Samuel, S., Lange, L. A., Wang, C., Curpen, G. D., Savani, R. C., Greenberg, A. H., and Turley, E. A. (1995) Overexpression of the hyaluronan receptor RHAMM is transforming and is also required for h-ras transformation. *Cell 82*, 19–28.

(25) Rooney, P., Kumar, S., Ponting, J., and Wang, M. (1995) The role of hyaluronan in tumour neovascularization (review). *Int. J. Cancer 60*, 632–636.

(26) Hoare, K., Savani, R. C., Wang, C., Yang, B., and Turley, E. A. (1993) Identification of hyaluronan binding proteins using a biotinylated hyaluronan probe. *Connect. Tissue Res. 30*, 117–126.

(27) Turley, E. A., Belch, A. J., Poppema, S., and Pilarski, L. M. (1993) Expression and function of a receptor for hyaluronan-mediated motility on normal and malignant lymphocytes-B. *Blood 81*, 446–453.

(28) Gustafson, S., Bjorkman, T., and Westlin, J. E. (1994) Labeling of high molecular weight hyaluronan with I-125-tyrosine: studies in vitro and in vivo in the rat. *Glycoconjugate J. 11*, 608–613.

(29) Gustafson, S., Hyaluronan in drug delivery; In *The Chemistry, Biology, and Medical Applications of Hyaluronan and its Derivatives*; T. C. Laurent and E. A. Balazs, Ed.; Portland Press: UK, 1997.

(30) Gustafson, S., and Bjorkman, T. (1997) Circulating hyaluronan, chondroitin sulphate and dextran sulphate bind to a liver receptor that does not recognize heparin. *Glycoconjugate J. 14*, 561–568.

(31) Samuelsson, C., and Gustafson, S. (1998) Studies on the interaction between hyaluronan and a rat colon cancer cell line. *Glycoconjugate J. 15*, 169–175.

(32) Culty, M., Nguyen, H. A., and Underhill, C. B. (1992) The hyaluronan receptor (CD44) participates in the uptake and degradation of hyaluronan. *J. Cell Biol. 116*, 1055–1062.

(33) Prestwich, G. D., D. M., M., Marecek, J. F., Vercruysse, K. P., and Ziebell, M. R. (1998) Controlled chemical modification of hyaluronic acid: synthesis, applications and biodegradation of hydrazide derivatives. *J. Controlled Release* 93–103.

(34) Teicher, B. A. *Cancer Therapeutics: Experimental and Clinical Agents*; Humana Press: Totowa, New Jersey, 1997; p 451.

(35) Greenwald, R. B., Gilbert, C. W., Pendri, A., Conover, C. D., Xia, J., and Martinez, A. (1996) Drug delivery systems: water soluble taxol 2′-poly(ethylene glycol) ester prodrugs - - design and in vivo effectiveness. *J. Med. Chem. 39*, 424–431.

(36) Pouyani, T., and Prestwich, G. D. In *US Patent 5,616, 568*; Research Foundation of SUNY: USA, 1997.

(37) Pouyani, T., and Prestwich, G. D. (1994) Functionalized derivatives of hyaluronic acid oligosaccharides – drug carriers and novel biomaterials. *Bioconjugate Chem. 5*, 339–347.

(38) Pouyani, T., Harbison, G. S., and Prestwich, G. D. (1994) Novel hydrogels of hyaluronic acid: synthesis, surface morphology, and solid-state NMR. *J. Am. Chem. Soc. 116*, 7515–7522.

(39) Ogura, H., Nagai, S., and Takeda, K. (1980) A novel reagent (N-succinimidyl diphenyl phosphate) for synthesis of active ester and peptide. *Tetrahedron Lett. 21*, 1467–1468.

(40) Vercruysse, K. P., Marecak, D. M., Marecek, J. F., and Prestwich, G. D. (1997) Synthesis and in vitro degradation of new polyvalent hydrazide cross-linked hydrogels of hyaluronic acid. *Bioconjugate Chem. 8*, 686–694.

(41) Kokoshka, J. M., Ireland, C. M., and Barrows, L. R. (1996) Cell-based screen for identification of inhibitors of tubulin polymerization. *J. Nat. Prod. 59*, 1179–1182.

(42) Kreil, G. (1995) Hyaluronidases – a group of neglected enzymes. *Protein Sci. 4*, 1666–1669.

(43) Nicolaou, K. C., Riemer, C., Kerr, M. A., Rideout, D., and Wrasidlo, W. (1993) Design, synthesis and biological activity of protaxols. *Nature 364*, 464–466.

(44) Collis, L., Hall, C., Lange, L., Ziebell, M., Prestwich, G., and Turley, E. (1998) Rapid hyaluronan uptake is associated with enhanced motility: implications for an intracellular mode of action. *FEBS Lett. 440*, 444–449.

(45) Chow, G., Knudson, C. B., Homandberg, G., and Knudson, W. (1995) Increased expression of CD44 in bovine articular chondrocytes by catabolic cellular mediators. *J. Biol. Chem. 270*, 27734–27741.

(46) Lesley, J., and Hyman, R. (1992) CD44 Can be activated to function as an hyaluronic acid receptor in normal murine T-cells. *Eur. J. Immunol. 22*, 2719–2723.

(47) Lesley, J., English, N., Perschl, A., Gregoroff, J., and Hyman, R. (1995) Variant cell lines selected for alterations in the function of the hyaluronan receptor CD44 show differences in glycosylation. *J. Exp. Med. 182*, 431–437.

(48) Perschl, A., Lesley, J., English, N., Trowbridge, I., and Hyman, R. (1995) Role of CD44 cytoplasmic domain in hyaluronan binding. *Eur. J. Immunol. 25*, 495–501.

(49) Asplund, T., and Heldin, P. (1994) Hyaluronan receptors are expressed on human malignant mesothelioma cells but not on normal mesothelial cells. *Cancer Res. 54*, 4516–4523.

(50) Culty, M., Shizari, M., Thompson, E. W., and Underhill, C. B. (1994) Binding and degradation of hyaluronan by human breast cancer cell lines expressing different forms of CD44: correlation with invasive potential. *J. Cell. Physiol. 160*, 275–286.

(51) Hua, Q., Knudson, C. B., and Knudson, W. (1993) Internalization of hyaluronan by chondrocytes occurs via Receptor-Mediated endocytosis. *J. Cell Sci. 106*, 365–375.

(52) Nakabayashi, H., Tsujii, H., Okamoto, Y., and Nakano, H. (1996) Fluorescence-labeled-hyaluronan loading test as an index of hepatic sinusoidal endothelial cell function in the rat. *Int. Hepatol. Commun. 5*, 345–353.

(53) Iida, N., and Bourguignon, L. Y. W. (1997) Coexpression of CD44 variant (v10/ex14) and CD44S in human mammary epithelial cells promotes tumorigenesis. *J. Cell. Physiol. 171*, 152–160.

(54) Bourguignon, L. Y.-W., Zhu, H. B., Chu, A., Iida, N., Zhang, L., and Hung, M. C. (1997) Interaction between the adhesion receptor, CD44, and the oncogene product, p185(HER2), promotes human ovarian tumor cell activation. *J. Biol. Chem. 272*, 27913–27918.

BC9900338

New Frontiers in Medical Sciences: Redefining Hyaluronan.
G. Abatangelo and P.H. Weigel, editors.

Chemically modified hyaluronan: new biomaterials and probes for cell biology

Glenn D. Prestwich, Yi Luo, Michael R. Ziebell, Koen P. Vercruysse, Kelly R. Kirker and John S. MacMaster
Department of Medicinal Chemistry, The University of Utah, Salt Lake City, Utah, USA

Abstract. A mild, controllable modification of hyaluronic acid (HA) has been developed in which monovalent, divalent, or polyvalent hydrazides can be covalently attached to HA to give functionalized derivatives with a high degree of synthetic versatility. Firstly, HA can be covalently modified to produce drug delivery systems and novel hydrogel biomaterials with a variety of desired physical and chemical properties. Specific applications include localizable hydrogels for release of anti-inflammatory agents, materials for tissue engineering and prevention of postsurgical adhesions, novel grafted copolymers for drug delivery, tumor targeted anticancer drugs, and techniques for coating surfaces of polymeric and metal medical devices. Secondly, basic cell biological research on the changes in the location of HA and HA binding proteins (e.g., CD44 and RHAMM) can be demonstrated using cellular probes. Our laboratories have developed versatile routes to synthesize HA-fluors (fluorescein, Texas Red, BODIPY), HA-nanogold, and HA-biotin with controllable levels of modification on the carboxylate groups. Thirdly, HA can be modified to provide biochemical probes for developing new hyaluronidase (HAse) assays and for the discovery of new HA-binding proteins. Examples of each of these three current research areas are presented.

Keywords: binding proteins, drug delivery, hyaluronidase, hydrazide.

Introduction

We have developed a versatile method for chemical modification of HA in which monovalent, divalent, or polyvalent hydrazides can be covalently attached to HA to give functionalized derivatives with many subsequent uses [1—3]. Covalent modifications can alter the chemical and biomechanical properties of HA in ways that permit production of drug delivery systems and novel hydrogel biomaterials [4]. Specific applications described herein include tumor targeted anticancer drugs, hydrogels for localized release of anti-inflammatory or other therapeutic agents, scaffold materials for tissue engineering and slowly bioresorbable films for prevention of postsurgical adhesions. In addition, HA fragments can be incorporated either pre- or postpolymerization to provide novel receptor targeted grafted copolymers for drug delivery. Several techniques for covalently attaching HA onto the surfaces of polymeric or metal medical devices have also been developed [5,6].

Address for correspondence: Prof. Glenn D. Prestwich, The University of Utah, Department of Medicinal Chemistry, 30 South 2000 East, Room 201, Salt Lake City, UT 84112-5820, USA. Tel.: +1-801-585-9051. Fax: +1-801-585-9053. E-mail: gprestwich@deans.pharm.utah.edu

HA can be modified to provide biochemical probes for developing new hyaluronidase (HAse) assays and for the discovery of new HA-binding proteins (HABPs) [6]. These probes can be used to understand the effects of HA on cell physiology, and the uptake, transport, and signaling functions of HA in cells [7]. For example, changes in the location and abundance of both HA and HABPs such as CD44 and RHAMM can be demonstrated using cellular probes.

Current research areas

Five areas of current research at The University of Utah are summarized in this overview: 1. Tumor targeted drug delivery of Taxol®; 2. Swellable HA hydrogel biomaterial for wound healing, adhesion management, and drug delivery; 3. Biophysical and biochemical studies of HA-receptor interactions, including novel binding assays and ligands; 4. Surface modification chemistry; and 5. Assays for HAse that permit screening for new inhibitors.

Tumor targeted drug delivery

The uses of chemically modified HA for drug delivery have been recently reviewed [5,8]. A fluorescent BODIPY-HA was synthesized to illustrate cell targeting and uptake of chemically modified HA using confocal microscopy [9]. Next, a cell targeted prodrug was developed for the anticancer drug Taxol®, using HA as the drug carrier [9]. HA-Taxol® conjugates were synthesized by linking the Taxol® 2′-OH via a succinate ester to adipic dihydrazide modified HA (HA-ADH) (Fig. 1A). The coupling of Taxol®-NHS ester and HA-ADH provided several HA conjugates with different levels of ADH modification and different Taxol® loadings. HA-Taxol® conjugates showed selective toxicity towards the human cancer cell lines (breast, colon, and ovarian) that are known to overexpress HA receptors, while no toxicity was observed towards a mouse fibroblast cell line at the same concentrations used with the human tumor cells. The drug carrier HA-ADH was completely nontoxic. The selective cytotoxicity is consistent with the results from confocal microscopy, which demonstrated that BODIPY-HA entered only the tumor cells.

Selective HA-BODIPYuptake by tumor cells

HA-BODIPY was used to probe the selectivity of HA targeting to tumor cells [9]. HA-BODIPY binding and uptake by tumor cells such as human breast cancer cells HBL-100, ovarian cancer cells SK-OV-3 and colon tumor cells HCT-116, were studied by laser confocal microscopy. The fluorescence images indicated that HA bound readily to tumor cell surfaces and was rapidly taken up via HA receptor mediated pathways. This supports the notion that HA should be a good targeting polymer for selective delivery of anticancer drugs to tumor cells. Similar results were observed independently with HA-Texas Red uptake by transformed fibroblasts [10]. Importantly, nontransformed cells, such as the NIH 3T3

mouse fibroblasts, did not show this binding and rapid uptake of HA-BODIPY. The HA-BODIPY binding and uptake results support the hypothesis that selective toxicity of HA-Taxol® is due to receptor mediated events.

Selective toxicity of HA-Taxol®

The in vitro cytotoxicity of HA-Taxol® conjugates was studied by using the MTT assay to identify cells still active in respiration [11]. HA-Taxol® conjugates showed toxicity to SK-OV-3, HBL-100 and HCT-116 cell lines, while no toxicity was observed towards a mouse fibroblast cell line NIH 3T3 at the same concentrations used with the cancer cells (Fig. 1). The selective cytotoxicity is consistent with the results from confocal microscopy, which demonstrated that BODIPY-HA only entered the cancer cells. In addition, the efficacy of HA-Taxol® conjugates could be blocked by preincubation of the cells with a 20-fold excess of HA. Together with the known overexpression of CD44 by HBL-100 [12] and SK-OV-3 cells [13], these data suggest that the selective cytotoxicity is due to receptor mediated binding and uptake of the HA-Taxol® conjugate. The conjugate showed higher potency, e.g., lower IC_{50}, relative to free Taxol® or free Taxol® mixed with the HA-ADH carrier [9]. In a further control experiment we established that the drug carrier HA-ADH alone was completely nontoxic.

Studies on the release of Taxol® from HA-Taxol® were carried out in cell cul-

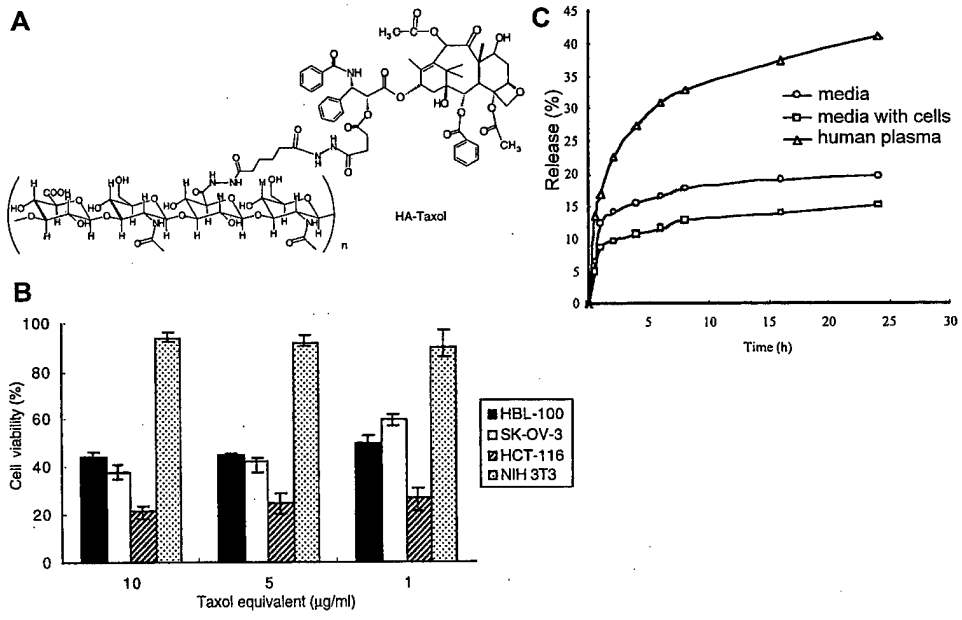

Fig. 1. Tumor-targeting of Taxol® with HA. **A:** structure of HA-Taxol®; **B:** selective toxicity of HA-Taxol® to three human cancer cell lines and nontoxicity to mouse fibroblasts; **C:** time course of Taxol® release from HA-Taxol®.

ture medium with and without cells, and with either HAse, esterase, or human plasma. Figure 1C shows the data for the effects of medium and human plasma. HPLC analysis suggested that only active Taxol® was released, corresponding to cleavage of the labile 2′ ester linkage; no Taxol® hemisuccinate was detected. The conjugate was stable in cell culture media, and the presence of HAse did not affect the Taxol® release rate. Taxol® release rate is significantly faster in the presence of added esterase. These data support the notion that the increased cytotoxicity of HA-Taxol® requires cellular uptake of the complex followed by hydrolytic release of the active Taxol® by cleavage of the labile 2′ ester linkage.

Fluorescence-activated cell sorting (FACS) with FITC-HA-Taxol®

Laser flow cytometry was used to investigate the interaction of the HA-Taxol® conjugate with tumor cells using fluorescein-labeled HA-Taxol® as the fluorescent probe. It was found that FITC-HA-Taxol® bound to the cell surface and was taken up rapidly by tumor cells (HBL-100, SK-OV-3, HCT-116). Binding and uptake of this dual modified HA could be blocked by preincubation with excess of HA, while no binding and uptake was detected in fibroblasts. In addition, the binding and uptake of FITC-HA-Taxol® by different cell lines was also evaluated by confocal microscopy, giving results analogous to those obtained with HA-BODIPY. The selective cytotoxicity of HA-Taxol® is thus, clearly due to receptor mediated uptake followed by hydrolytic release of the active Taxol® via cleavage of the labile 2′ ester linkage.

Swellable HA hydrogels

Hydrogels have received significant attention as delivery vehicles. These materials can be engineered to be tissue compatible and to be permeable to different solutes [14]. HA hydrogels can, in principle, be completely bioresorbable materials and have been studied for over two decades [15,16]. Mirroring the new sol gel injectable drug delivery system [17], a novel fast gelling and fast swelling HA hydrogel film was developed as a potential drug delivery system. The new HA film is biocompatible and biodegradable and is produced from HA-ADH and a bioinert cross-linker. An in vitro drug release device was evaluated and drug release was initially studied by using dyes (i.e., acridine orange, amaranth, and fast green FCF), followed by examination of release rates of several therapeutic agents (i.e., hydrocortisone, dexamethasone, indomethacin, gentamicin, pilocarpine, and diclofenac). It was found that the new HA film could maintain a slow release rate for certain drugs, such as acridine orange, dexamethasone and gentamicin. Differential scanning calorimetric analysis suggested that a polymer-drug interaction exists within the HA hydrogel that could account for the slow release. In particular, prolonged delivery of anti-inflammatory or anti-infective drugs suggested the utility of this novel HA film as a wound dressing material.

The functionalized HA-ADH derivative was cross-linked by a macromolecular cross-linker to give an interpenetrating network hydrogel. The hydrogel could be prepared under extremely mild conditions e.g., in water, phosphate-buffered sa-

line (PBS), or in cell culture medium at room temperature. The gelling process began immediately and was essentially complete in minutes. A solvent casting method was used to obtain HA hydrogel films, which were then dried in air at 37°C for 24 h.

The extent of swelling of HA hydrogel films was investigated using both kinetic and equilibrium swelling studies (Fig. 2). For the kinetic studies HA films were cut into small disks and dyed with acridine orange to facilitate visualization. Next, the diameters of dried disks were measured using a microscope. Then, a buffer solution was added to the film and the diameter was measured at various times. A similar procedure was followed for the equilibrium studies; however, the diameter of the film was measured only after 24 h of equilibration in a buffer solution at 37°C. The swelling ratio, Q, was calculated as indicated below.

$$\left(\frac{\text{Diameter}_{t=x}}{\text{Diameter}_{t=0}}\right)^3 = Q$$

where: $\text{Diameter}_{t=x}$ = Diameter of disk at time interval x

$\text{Diameter}_{t=0}$ = Diameter of dry disk

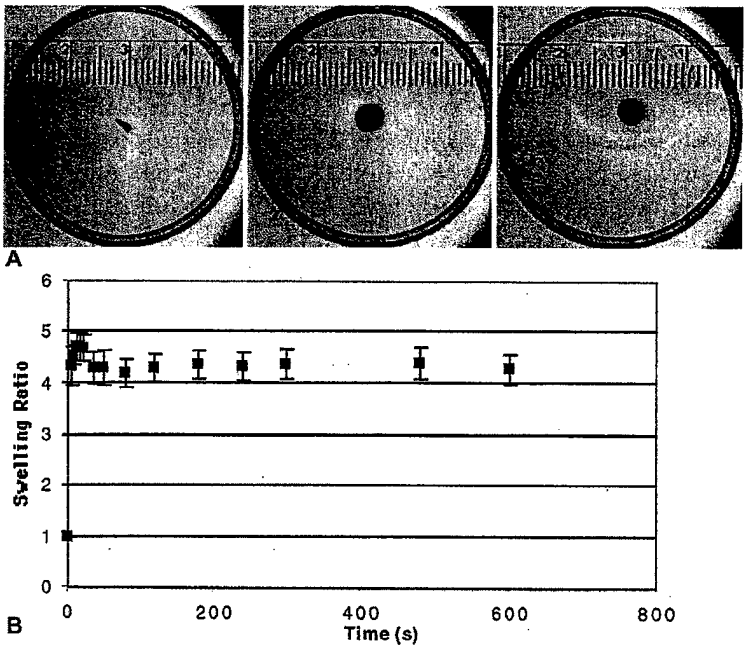

Fig. 2. Swellable HA hydrogel films. **A:** photographs of an acridine orange stained HA hydrogel film swelling in PBS. From left to right: dry HA film, film after 4 s in PBS, film after 600 s in PBS; **B:** swelling kinetics of an HA hydrogel film in PBS.

Figure 2B shows the results of kinetic studies; Fig. 2A shows the actual films as seen under the microscope at times 0, 4, and 600 s. These data indicate that the films swell quickly and reach an equilibrium size in less than a minute. The rapid swelling of these proprietary films will be exploited for a variety of in vivo applications in human medicine.

Surface modification chemistry

Plasma etching

Surfaces of polypropylene (PP), polystyrene (PS), and polytetrafluroethylene (PTFE) were activated with Ar and NH_3 plasmas to aminate the polymer surface [18]. Aminated surfaces were then reacted with HA using three modification conditions. Results showed that ammonia plasma-treated polymers were more reactive toward HA attachment. Of the three chemistries tried, condensation of the aminated surface with succinic anhydride followed by coupling of the newly formed carboxylic acid group with HA-ADH gave the most effective and reproducible HA attachment. HA coatings were evaluated by spectroscopic and physicochemical methods. HA-modified plastic surfaces were quite hydrophilic, as determined by measuring the water contact angle, and should exhibit selectivity in cell attachment and growth.

Controlled chemical modifications of particles

Three types of HA-modified particulate materials (HAMPs) have been produced: 1. affinity resins based on cross-linked agarose; 2. superparamagnetic polystyrene (PS) beads, and 3. controlled pore glass (CPG). In each case, ADH-modified HA was covalently coupled to chemically activated residues on the surface. The affinity resins were prepared by coupling HA-ADH to NHS ester activated Affigel. This affinity matrix has been employed for purification of native and recombinant HABPs. The HA modified magnetic beads and CPG were prepared by oxidative cleavage of glycol modified surfaces to give surface aldehydes. Coupling of HA-ADH to the particle surface resulted in hydrazone linkages, and the extent and location of coupling was monitored in two ways (Fig. 3). Firstly, fluorescence microscopy was employed to detect coupling of fluoresceinylated HA-ADH (rather than nonfluorescent HA-ADH). In addition, the presence of HA on these HAMPs was also checked functionally by testing their ability to bind to the HA-binding domain (HABD) of the receptor for HA mediated motility (RHAMM), described in more detail in Section 4 below. For this detection strategy, Texas Red was conjugated to a GST fusion protein of the 61 amino acid recombinant RHAMM-P1 peptide to give a novel nonimmunological reagent for the detection of HA on surfaces. HAMPs will be employed to isolate HABPs in automated high throughput screens, and in an in vitro process to remove selectively cells expressing high affinity cell surface HABPs.

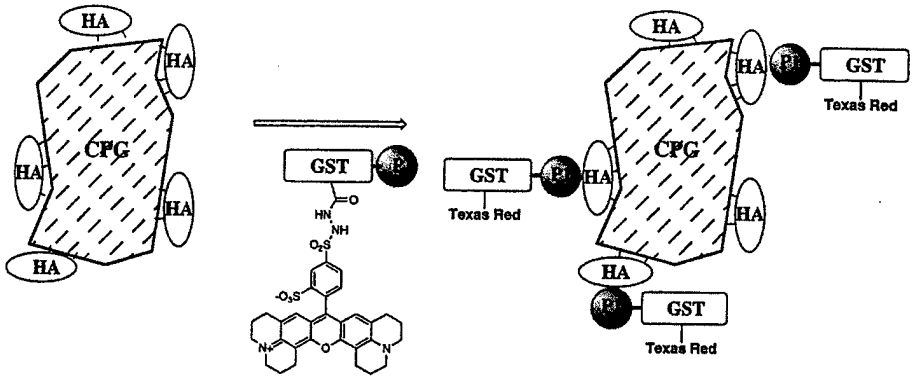

Fig. 3. Surface modification chemistry. The detection of HA covalently coupled through hydrazone linkages to controlled pore glass (CPG) can be accomplished by direct fluorescent detection of the binding of a Texas Red-labeled recombinant GST-RHAMM-P1 polypeptide.

Biophysical and biochemical studies

Biochemical probes and surfaces

Versatile routes to synthesize HA-fluors (including fluorescein, Texas Red, and BODIPY), HA-nanogold, and HA-biotin with controllable levels of modification on the carboxylate groups [10,19] have been developed. In addition, the preparation of HAMPs, such as HA affinity resins on cross-linked dextran (> 300 μm), CPG (100 μm), and superparamagnetic beads (4 μm) was summarized above.

Structural studies of RHAMM

The RHAMM is a cell surface HA receptor, found on fibroblasts and certain tumor cell lines, that modulates cell function through binding extracellular matrix components [20]. Certain isoforms of this receptor have been identified as important in intracellular signaling and extracellular binding [21]. High resolution multidimensional NMR is being used to solve the structure of the HABD of RHAMM; this is the first predominately helical HABD to be studied this way. A solution structure of the mostly beta-sheet containing TGS-6 link module was previously determined by NMR [22,23]. A RHAMM polypeptide that contains the two basic amino acid-rich HABDs was expressed and purified. Based on circular dichroism and NMR experiments, it appeared that the domain was alpha-helical. A complete structure may provide a model for how the two domains selectively bind HA and which amino acid side chains account for the high binding affinity. Based on molecular modeling we hypothesize that a long narrow groove is formed by a helix-loop-helix structure, in which the substrate (e.g., an HA octasaccharide) would be flanked on each side by one of the two HABDs.

Peptide mimics of HA

HABPs control cell function and are implicated in cancer, arthritis, adhesion, and wound healing [7,24] One medicinal chemistry approach to developing new antagonists and agonists that mimic HA in binding to HABPs involves the use of combinatorial libraries of peptides, either synthetic or from phage display. The first library tested was a random set of 15 amino acid polypeptides encoded in the fUSE-5 phage [25]. The next libraries were eight amino acid, "one-bead, one-peptide" libraries synthesized on 100 μm PS beads [26]. Each of these libraries was screened against our RHAMM construct expressed as a GST fusion protein (GST-RHAMM-P1). To detect peptides that bound solely to the HABD, we included a competition step in each of our screens, in which HA was first incubated with GST-RHAMM-P1; this preincubation was followed by addition of peptides. In this negative selection step, the peptides that did not bind in this final step were selected as those molecules that exhibited exclusive interaction with the HABD. Phage-displayed peptides are summarized in Table 1, and the affinity of independently synthesized peptides for RHAMM-P1 has been assessed using the assay described below. Interestingly, these peptides interfere with the interaction of RHAMM with erk1 [27]. Although not shown, the bead-derived peptides include an abundance of aromatic and acidic residues. Several recognizable motifs repeat in the twenty peptides sequenced, and the inclusion of unnatural amino acids resulted in novel peptides with nanomolar affinity.

We conclude that a series of hydrophobic amino acids are important in binding, and that the amino acid motif may have quite different characteristics from HA itself. Current efforts focus on identification of peptides that bind uniquely to either RHAMM or to TSG-6 link module.

Rapid binding assays in microtiter plates

In order to verify the binding selectivity and affinity of these above peptides, we developed a series of binding assays that allows us to monitor their binding and determine binding constants to describe their interactions. One such method utilizes a 96 well plate format in which the target protein, GST-RHAMM-P1, is immobilized and biotin-labeled peptides are incubated in the wells. Streptavidin conjugated to horseradish peroxidase is then added followed by a chromogenic substrate. Figure 4A illustrates the basic method, and Fig. 4B shows the determination of a 21 nM binding constant for the binding of the HA2 peptide to

Table 1. Phage-displayed peptides that interact with RHAMM.

HA1	WPVSLTVCSAVWCPL
HA2	GVCNADFCWLPAVVV
HA3	SASPSASKLSLMSTV
HA4	IPPILPAYTLLGHPR
HA5	YSVYLSVAHNFVLPS
HA6	HWCLPLLACDTFARA

RHAMM-P1. Figure 4C illustrates the relative binding affinity and relative ability to displace HA binding for four of the phage-derived peptides.

Fluorescence polarization (FP) assays

To compare the above solid phase assay to solution phase binding we used FP, which measures the degree of anisotropic change of a fluorescent probe [28]. As the binding complex forms, the anisotropy increases, which in turn is a marker for peptide binding. In these experiments, fluorescently labeled peptides were titrated with increasing amounts of the recombinant RHAMM-P1. Preliminary data (not shown) allow estimation of the K_d values, which are consistent with the data obtained from microplate assays.

Hyaluronidase assays

Effects of metals on HAse

The enzymatic degradation of HA by testicular HAse, hyaluronate 4-glucanohydrolase, has an absolute requirement for the inclusion of mono or divalent cations in the reaction mixture. We tested the effects of metal salts on the enzy-

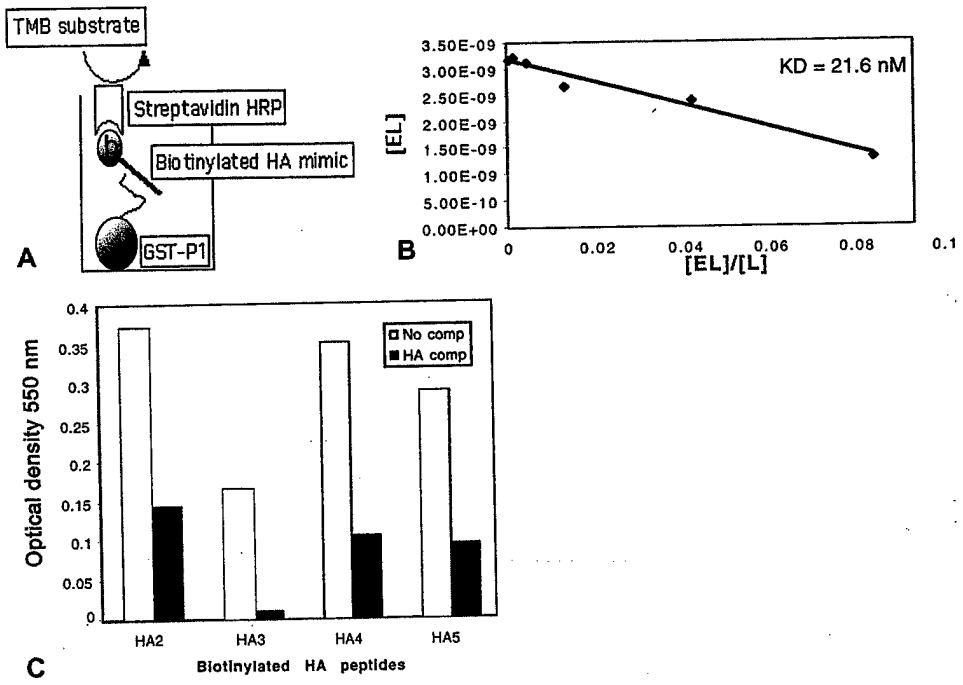

Fig. 4. Binding of HA mimetic peptides to GST-RHAMM-P1-coated microtiter plates. **A:** schematic of assay; **B:** Eadie-Hofstee plot of data for binding of biotinylated HA2, where E is the RHAMM-PI fusion and L is the HA2 peptide; **C:** relative affinity of binding of four biotinylated phage-derived synthetic peptides showing competition by excess HA. The y-axis is optical density at 550 nm.

matic degradation of HA by HAse by preincubating the metal salts with either HA or with the HAse prior to the enzymatic reaction [29]. The digestion occurred more slowly in the presence of monovalent cations compared to the divalent cations. Most divalent cations activated HAse with equal potency, except for Cu^{2+}. Compared to the digestion in the presence of the other divalent salts, Cu^{2+} suppressed the degradation of HA; however, compared to the digestion in the absence of any salt, Cu^{2+} still activated the digestion of HA by HAse. When HA was preincubated with NaCl or when HAse was incubated with salts like $CaCl_2$, $CoCl_2$, $ZnCl_2$ or $CuCl_2$, surprisingly no effects on the enzymatic activity could be observed (except for $CuCl_2$). The combined results suggested that the activating effect of the cations occurs through an activation of HA rather than an activation of HAse. That is, the addition of the cations to HA may change its conformation such that more endoglucanase sites are exposed, thus, facilitating the hydrolysis by the enzyme.

These experiments suggested that any metal-chelating compound might inhibit the degradation of HA by HAse. As predicted, preincubation of EGTA-Na_4 with HA/$CaCl_2$ inhibited the degradation of HA by HAse. No inhibition was observed when EGTA-Na_4 was preincubated with HAse prior to the digestion. Thus, judicious selection of HAse assay parameters is critical for the discovery of novel, selective HAse inhibitors and not mere metal-chelating compounds. Total enzymatic digestion of HA in the presence of varying concentrations of Ca^{2+} showed a concentration-dependent regulation of the size of the oligosaccharide end products. These oligosaccharides were fractionated to monodisperse species using anion exchange perfusion chromatography and their size and purity were confirmed using MALDI-TOF analysis.

Fluorescence-based assays for HAse

In most mammals, HAse is found on the acrosomal membrane of spermatozoa and plays a major role in the passage of the spermatozoa towards the oocyte [30]. The enzyme is also present in most animal venoms and several bacterial species produce HAse, enhancing their virulence. Tumors are often enriched in HAse activity compared to normal tissues. This production of HAse can affect the further development of the tumor, e.g., by generating small, angiogenic oligosaccharide fragments from HA polymers present in the extracellular matrix [31]. Thus, inhibitors of the enzyme could have potential as nonhormonal contraceptive agents or as novel anti-angiogenic compounds. In view of the importance of HAse and its inhibitors, there is a need for a simple, rapid, and sensitive assay to evaluate the HAse activity present in any sample or to search for inhibitors of this enzyme.

Methods currently employed often lack the necessary sensitivity, selectivity, or versatility to perform all these tasks. We are developing a fluorescence-dequenching assay using a fluorescently labeled HA conjugate as a substrate for HAse (Fig. 5A). Using the hydrazide methodology, HA was modified with FITC and with Texas Red. This gave a doubly labeled HA substrate in which the fluores-

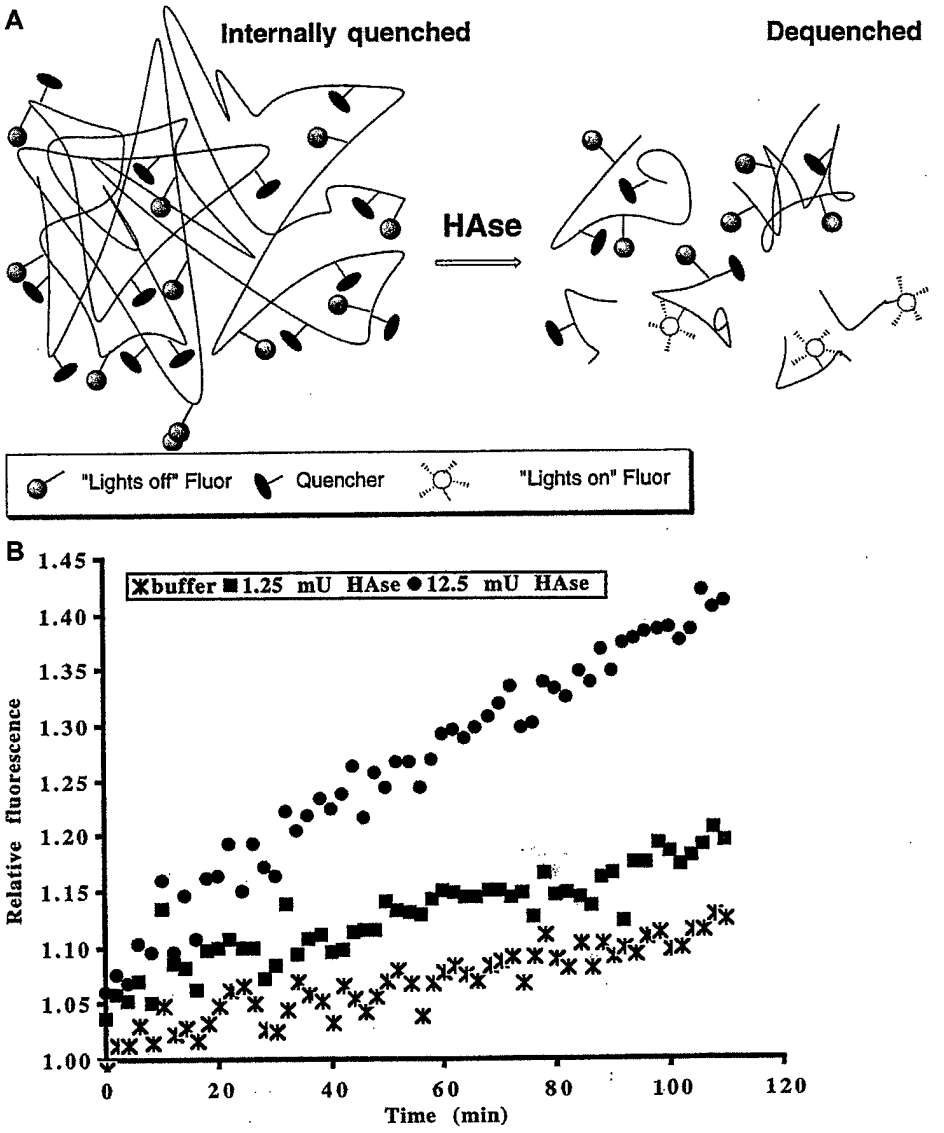

Fig. 5. Fluorescence-dequenching assay for HAse. **A:** schematic of assay; **B:** data from digestion of HA, labeled with FITC and Texas Red, by HAse (0, 1.25 or 12.5 mUnits) in phosphate buffer (pH = 6.4) containing 150 mM NaCl in wells of a 96 well microplate. The fluorescence of FITC (excitation 490 nm, emission 535 nm) was monitored as a function of the reaction time; each data point is the average of three measurements.

cence of FITC was partially quenched by the presence of nearby Texas Red fluorophores. Digestion of this substrate by HAse separates FITC from the Texas Red-containing regions, resulting in an increased fluorescence that can be moni-

tored as a function of the reaction time. Figure 5B illustrates such an increase in FITC fluorescence when HA conjugated with FITC and Texas Red is incubated with two different amounts of HAse compared to the incubation with buffer alone. This proprietary assay can be performed in a 96 well format yielding a high through-put screening assay for HAse activity and/or inhibition.

Conclusions

Modification of HA using adipic dihydrazide (ADH) permits preparation of a wide variety of biomaterials and biochemical probes. In this overview we showed five examples. Firstly, selective toxicity of anticancer drugs coupled to HA to tumor cells illustrated an important method for solubilization and cell targeted intracellular delivery of known antitumor drugs. This method can significantly improve the therapeutic ratio. Secondly, swellable HA hydrogel films with slow release properties for both small molecules and macromolecular drugs allow penetration of a combined wound dressing; drug delivery system that is bioresorbable. Thirdly, attachment of HA to surfaces provides materials for cell sorting and protein panning to identify new HABPs. Fourthly, interactions of HABPs with HA and HA-mimetic peptides offer insight into cell biology and structural biology of HABP-HA complexes. Finally, doubly labeled HA (using two different covalently attached fluors) creates a novel assay for detection of HAse activity and thus, for discovery of new HAse inhibitors.

Acknowledgements

We thank the Center for Biopolymers at Interfaces, The University of Utah, the National Institutes of Health Chemical Biology Training Grant, and the US Department of the Army (Breast Cancer IDEA award) for current financial support. We thank Clear Solutions Biotech, Inc. (Stony Brook, NY) for providing HA for these studies and for cooperating in the development of practical uses for the hydrazide technology. New technologies described herein in Sections 1 through 5 may be licensed from The University of Utah and from Clear Solutions.

References

1. Pouyani T, Prestwich GD. Functionalized derivatives of hyaluronic acid oligosaccharides; drug carriers and novel biomaterials. Bioconjugate Chem 1994;5(4):339–347.
2. Pouyani T, Prestwich GD. Functionalized derivatives of hyaluronic acid. US Patent No. 5, 616, 568. Research Foundation of SUNY, 1997.
3. Vercruysse KP, Marecak DM, Marecek JF, Prestwich GD. Synthesis and in vitro degradation of new polyvalent hydrazide cross-linked hydrogels of hyaluronic acid. Bioconjugate Chem 1997; 8(5):686–694.
4. Pouyani T, Harbison GS, Prestwich GD. Novel hydrogels of hyaluronic acid: synthesis, surface morphology, and solid-state NMR. J Am Chem Soc 1994;116(17):7515–7522.
5. Vercruysse KP, Prestwich GD. Hyaluronate derivatives in drug delivery. Crit Rev Ther Drug

Carr Syst 1998;15(5):513–555.
6. Prestwich GD, Marecak DM, Marecek JF, Vercruysse KP, Ziebell MR. Chemical modification of hyaluronic acid for drug delivery, biomaterials, and biochemical probes. In: Laurent TC, Balazs EA (eds) The Chemistry, Biology, and Medical Applications of HA and its Derivatives. London: Portland Press, 1998;43–65.
7. Entwistle J, Hall CL, Turley EA. HA receptors: regulators of signalling to the cytoskeleton. J Cell Biochem 1996;61(4):569–577.
8. Gustafson S. HA in drug delivery. In: Laurent TC, Balazs EA (eds) The Chemistry, Biology, and Medical Applications of HA and its Derivatives. UK: Portland Press, 1998;291–304.
9. Luo Y, Prestwich GD. Synthesis and selective cytotoxicity of a hyaluronic acid-anti-tumor bioconjugate. Bioconjugate Chem 1999 (In press).
10. Collis L, Hall C, Lange L, Ziebell MR, Prestwich GD, Turley EA. Rapid HA uptake is associated with enhanced motility: implications for an intracellular mode of action. FEBS Lett 1998;440:444–449.
11. Kokoshka JM, Ireland CM, Barrows LR. Cell-based screen for identification of inhibitors of tubulin polymerization. J Nat Prod 1996;59(12):1179–1182.
12. Iida N, Bourguignon LY-W. Coexpression of CD44 variant (v10/ex14) and CD44S in human mammary epithelial cells promotes tumorigenesis. J Cell Physiol 1997;171:152–160.
13. Bourguignon LY-W, Zhu HB, Chu A, Iida N, Zhang L, Hung MC. Interaction between the adhesion receptor, CD44, and the oncogene product, p185(HER2), promotes human ovarian tumor cell activation. J Biol Chem 1997;272(44):27913–27918.
14. Kim SW, Bae YH, Okano T. Hydrogel: swelling, drug loading and release. Pharmacol Res 1992; 9:283–290.
15. Tomihata K, Ikada Y. Preparation of cross-linked hyaluronic acid films of low water content. Biomaterials 1997;18:189–195.
16. Yui N, Okano T, Sakurai Y. Inflammation responsive degradation of cross-linked hyaluronic acid gels. J Contr Rel 1992;22:105–116.
17. Jeong B, Bae YH, Lee DS, Kim SW. Biodegradable block copolymers as injectable drug-delivery systems. Nature 1997;388:860–862.
18. Mason M, Vercruysse KP, Kirker KR, Frisch R, Marecak DM, Prestwich GD, Pitt W. Hyaluronic acid modified polypropylene, polystyrene, and polytetrafluoroethylene. Biomaterials 1999(In press).
19. Prestwich GD, Marecak DM, Marecek JF, Vercruysse KP, Ziebell MR. Controlled chemical modification of hyaluronic acid: synthesis, applications, and biodegradation of hydrazide derivatives. J Contr Rel 1998(53):93–103.
20. Wang C, Thor AD, Moore DH II, Zhao Y, Kerschmann R, Stern R, Watson PH, Turley EA. The overexpression of RHAMM, a HA-binding protein that regulates ras signaling, correlates with overexpression of mitogen activated protein kinase and is a significant parameter in breast cancer progression. Clin Cancer Res 1998;4(3):567–576.
21. Zhang S, Chang MC, Zylka D, Turley S, Harrison R, Turley EA. The HA receptor RHAMM regulates extracellular regulated kinase. J Biol Chem 1998;273(18):11342–11348.
22. Kohda D, Morton CJ, Parkar AA, Hatanaka H, Inagaki FM, Campbell ID, Day AJ. Solution structure of the link module: an HA-binding domain involved in extracellular matrix stability and cell migration. Cell 1996;86(5):767–775.
23. Day AJ. The structure and regulation of HA-binding proteins. Biochem Soc Trans 1999;27(2): 115–121.
24. Laurent TC, Laurent UBG, Fraser JRE. Functions of HA. Ann Rheum Dis 1995;54(5):429–432.
25. Smith GP, Patel SU, Windass JD, Thornton JM, Winter G, Griffiths AD. Small binding proteins selected from a combinatorial repertoire of knottins displayed on phage. J Molec Biol 1998; 277(2):317–332.
26. Lam KS, Sroka T, Chen ML, Zhao Y, Lou Q, Wu J, Zhao Z-G. Application of "One-bead One-

compound" combinatorial library methods in signal transduction research. Life Sci 1998;62 (17–18):1577–1583.

27. Zhang S, Cheung W, Lu J, Ziebell MR, Turley SA, Harrison, R, Zylka D, Ahn, N, Litchfield D, Prestwich GD, Cruz T, Turley EA. Intracellular RHAMM isoforms bind directly to erk1 and these interactions are required for transformation and for podosome formation via the erk kinase pathway. J Biol Chem 1999, submitted.
28. Wu P, Brasseur M, Schindler U. A high through-put STAT binding assay using fluorescence polarization. Anal Biochem 1997;249(1):29–36.
29. Vercruysse KP, Ziebell MR, Prestwich GD. Control of enzymatic degradation of HA by divalent cations. Carbohydr Res 1999, In press.
30. Li M-W, Yudin AI, VandeVoort CA, Sabeur K, Primakoff P, Overstreet JW. Inhibition of monkey sperm hyaluronidase activity and heterologous cumulus penetration by flavanoids. Biol Reprod 1997;56:1383–1389.
31. Lokeshwar VB, Lokeshwar BL, Pham HT, Block NL. Association of elevated levels of hyaluronidase, a matrix-degrading enzyme, with prostate cancer progression. Cancer Res 1996;56(3): 651–657.

A Hyaluronic Acid−Taxol Antitumor Bioconjugate Targeted to Cancer Cells

Yi Luo,† Michael R. Ziebell,†,‡ and Glenn D. Prestwich*,†

Department of Medicinal Chemistry, The University of Utah, Salt Lake City, Utah 84112-5820, and Department of Physiology and Biophysics, The University at Stony Brook, Stony Brook, New York 11794-8661

Received January 10, 2000

A cell-targeted polymeric prodrug prepared from Taxol and chemically modified hyaluronic acid (HA) was evaluated in vitro. Herein we report four results in support of the selective uptake and targeted toxicity of the HA−Taxol prodrug. First, a fluorescently labeled HA−Taxol (FITC−HA−Taxol) was synthesized and used to demonstrate cell-specific binding and uptake using flow cytometry and confocal microscopy. Second, the selective cytotoxicity of FITC−HA−Taxol allowed direct correlation of uptake with selective cytotoxicity. Third, the rapid uptake and selective cytotoxicity of HA-Taxol bioconjugates could be blocked by either excess HA or by an anti-CD44 antibody, but not by chondroitin sulfate (CS). Finally, the release of free Taxol from HA−Taxol in human plasma or in cell culture media revealed that the free drug was hydrolytically released from the bioconjugate by cleavage of the labile 2′ ester linkage. Taken together, these data support the notion that the targeted cytotoxicity of HA−Taxol bioconjugates requires receptor-mediated cellular uptake of the bioconjugate followed by hydrolytic release of free Taxol.

Introduction

A major challenge in cancer therapy is to selectively target cytotoxic agents to tumor cells. To decrease undesirable side effects of small molecule anticancer agents, many targeting approaches have been examined. One of the most promising methods involves the combination or covalent attachment of the cytotoxin with a macromolecular carrier.[1] Many kinds of drug carriers, including soluble synthetic and natural polymers,[2] liposomes,[3] microspheres,[4] and nanospheres[5,6] have been employed to increase drug concentration in target cells; by altering the pharmacokinetic distribution of drugs, a sustained therapeutic concentration can be maintained at tolerable doses. Soluble polymers seem to offer great potential because they can traverse compartmental barriers in the body[7] and therefore gain access to a greater number of cell types. A variety of water-soluble polymers, such as human serum albumin (HSA),[2] dextran,[8] lectins,[9] poly(ethylene glycol) (PEG),[10] poly(styrene-*co*-maleic anhydride) (SMA),[11] poly(*N*-hydroxylpropylmethacrylamide) (HPMA),[12] and poly(divinyl ether-*co*-maleic anhydride) (DIVEMA)[13] have been used to prepare polymeric anticancer prodrugs. Such drug−polymer conjugates have demonstrated good solubility in water, increased half-life in the body, and high antitumor effects. For example, the linking of adriamycin to HPMA gives a new prodrug with improved in vitro tumor retention, a higher therapeutic ratio, and avoidance of multidrug resistance.[12] This system is currently in phase II trials against ovarian cancer.

Anticancer polymeric prodrugs can be divided into two targeting modalities: passive and active. The biological activity of the passive targeting drug delivery systems is based on the anatomical characteristics of tumor tissue and allows polymeric prodrugs to more easily permeate tumor tissues and accumulate over time. This is often referred to as the enhanced permeability and retention (EPR) effect. In contrast, active targeting drug delivery systems can be developed using specific interactions between receptors on the cell surface and targeting moieties conjugated to the polymer backbone. In this way, active therapeutic agents conjugated to polymers can be selectively transported to tumor tissues. The active approach therefore takes advantage of the EPR effect but further increases selectivity through receptor-mediated uptake by target cancer cells.

Hyaluronic acid (HA), a linear polysaccharide of alternating D-glucuronic acid (GlcUA) and *N*-acetyl-D-glucosamine (GlcNAc) units, is the only non-sulfated glycosaminoglycan and occurs primarily in vivo as sodium hyaluronate. The term hyaluronan refers to both forms. HA is present in the extracellular matrix, the synovial fluid of joints, and the scaffolding that comprises cartilage.[14] It is an immunoneutral building block for preparing biocompatible and biodegradable biomaterials,[15−18] and has been employed as both a vehicle and an angiostatic agent in cancer therapy.[19−21] Mitomycin C and epirubicin were coupled to HA by carbodiimide chemistry, and the HA-mitomycin adduct was selectively toxic to a lung carcinoma xenograft.[22] Recently, we have described the use of mild hydrazide chemistry to prepare an HA−Taxol bioconjugate,[23] which showed good selectivity

* To whom correspondence may be addressed at The University of Utah, Department of Medicinal Chemistry, 30 South 2000 East, Room 201, Salt Lake City, UT 84112-5820; phone, 801 585-9051; fax, 801 585-9053; e-mail, gprestwich@deans.pharm.utah.edu.

† The University of Utah.

‡ The University at Stony Brook.

10.1021/bm000283n CCC: $19.00
Published on Web 03/25/2000

in preliminary cell culture studies. In this report, we provide evidence that directly correlates uptake with cytotoxicity using a fluorescently labeled HA–Taxol derivative, and we demonstrate that toxicity is due to hydrolytic release of the parent drug.

HA serves a variety of functions within the extracellular matrix, including direct receptor-mediated effects on cell behavior. These effects occur via intracellular signaling pathways in which HA binds to, and is internalized by, cell surface receptors. Several cell-membrane-localized receptors (HA binding proteins) have been identified including: CD44, RHAMM, IVd4, and the liver endothelial cell clearance receptor.[24-27] HA–protein interactions play crucial roles in cell adhesion, growth, and migration,[28-30] and HA acts as a signaling molecule in cell motility, inflammation, wound healing, and cancer metastasis.[31] The structure and regulation of HA receptors[32] are growing areas of structural and cellular biology that are critical to understanding how HA–protein interactions enhance metastasis.

Most malignant solid tumors contain elevated levels of HA,[33] and these high levels of HA production provide a matrix that facilitates invasion.[34] Clinically, high HA levels correlate with poor differentiation and decreased survival rate in some human carcinomas. HA is an important signal for activating kinase pathways[35,36] and regulating angiogenesis in tumors.[37] HA internalization is mediated via matrix receptors, including CD44, which is a transmembrane receptor that can communicate cell–matrix interactions into cells and can alter the matrix in response to intracellular signals. The pathological enrichment of HA in tumor tissues suggests that manipulation of the interactions between HA and its receptors could lead to dramatic inhibition of growth or metastasis of several types of tumors. Antibodies to CD44, soluble forms of CD44 or RHAMM, HAse, and oligomers of HA have all been used effectively to inhibit tumor growth or metastasis in animal models.

In addition to elevated HA in the environment surrounding tumors, most malignant cell types overexpress CD44 and RHAMM. As a result, malignant cells with the highest metastatic potential often show enhanced binding and internalization of HA.[38] Apparently, such cells can effectively breach the tumor-associated HA barrier by binding, internalizing, and degrading this glycosaminoglycan. Cell culture experiments suggest that CD44-HA interactions occur in vivo and are likely to be responsible for retention of HA-enriched matrixes. Thus, HA can bind to the cell surface via interactions with CD44, and a portion subsequently undergoes endocytosis. In addition, internalization of [^{3}H]-labeled HA revealed that intracellular degradation of HA occurs within a low pH environment, such as that of lysosome. Targeting of anticancer agents to tumor cells and tumor metastases can be accomplished by receptor-mediated uptake of bioconjugates of anticancer agents to HA,[22,23] followed by the release of free drugs through the degradation of HA in cell compartments. Since CD44 and RHAMM isoforms are overexpressed in transformed human breast epithelial cells,[39] human ovarian tumor cells,[40] and other cancers,[41,42] the selectivity for drug delivery to cancerous cells should be markedly enhanced and overall dosages may be reduced. Using HA as drug carrier should thus combine the advantages of both the passive and active targeting ability of a polymeric prodrug. Moreover, coupling of antitumor agents to HA can provide advantages in drug solubilization, stabilization, localization, and controlled release.[11] Coupling antitumor agents to hydrazide-modified HA[18,43] adds further selectivity by specifically targeting the polymeric prodrug to aggressively growing cancers that overexpress HA receptors.

Paclitaxel (Taxol) is a powerful antimitotic agent that promotes tubulin assembly into stable aggregated structures.[44] It binds to microtubules and inhibits their depolymerization into tubulin. Expanding the applications of Taxol in cancer therapy is limited by poor aqueous solubility and by drug-associated neuropathies. Previous attempts to address the solubility issue involved preparation of 2′-OH linked water-soluble PEG derivatives[10] or poly(L-glutamic acid) derivatives.[45] In our study, Taxol was covalently attached through a labile ester linkage to HA, which had been modified with adipic dihydrazide (ADH).[46,47] Drug release from the HA–Taxol prodrug was studied in vitro in cell culture media with or without cells and also with exogenously added HAse or esterase. Selective in vitro cell cytotoxicity was studied with an untransformed mouse fibroblast cell line (NIH 3T3) and with three human cell lines (HCT-116 colon tumor, HBL-100 breast cancer, and SK-OV-3 ovarian cancer). In addition, a fluorescently labeled HA bioconjugate (FITC–HA–Taxol) was prepared (Figure 1) and employed to visualize selective uptake of HA using flow cytometry and confocal microscopy. Both the toxicity and FITC–HA–Taxol uptake by cells were prevented by preincubation with HA or an anti-CD44 antibody, but not by chondroitin sulfate (CS), providing compelling evidence for receptor-mediated uptake of the prodrug.

Materials and Methods

Reagents. Fermentation-derived HA (sodium salt, M_r 1.5 MDa) was provided by Clear Solutions Biotechnology, Inc. (Stony Brook, NY). 1-Ethyl-3-[3-(dimethylamino)propyl]-carbodiimide (EDCI), adipic dihydrazide (ADH), succinic anhydride, diphenylphosphoryl chloride (DPPC), *N*-hydroxysuccinimide, and triethylamine were purchased from Aldrich Chemical Co. (Milwaukee, WI). Bovine testicular HAse (880 U/mg), esterase from porcine liver crude (19 U/mg), and CS type C from shark cartilage, cell culture media, and supplements were obtained from Sigma Chemical Co. (St. Louis, MO). Paclitaxel (Taxol) was purchased from CBI Tech, Inc. (Cambridge, MA). Cephalomannine was purchased from Handetech USA, Inc. (Houston, TX). FITC "isomer I" was obtained from Molecular Probes, Inc. (Portland, OR). All chemicals were reagent grade or HPLC grade (Fisher Scientific Co., Santa Clara, CA). CH_2Cl_2 and acetonitrile were distilled from CaH_2. Anti-human CD44 monoclonal antibody (anti-CD mAb) was purchased from Calbiochem-Novabiochem Corp. (La Jolla, CA).

Cell Culture. HBL-100, a human breast cancer cell line, was maintained in culture in high-glucose D-MEM (Dulbecco's Modified Eagle Medium), which was supplemented with 10% γ-irradiated fetal bovine serum (FBS) and 1%

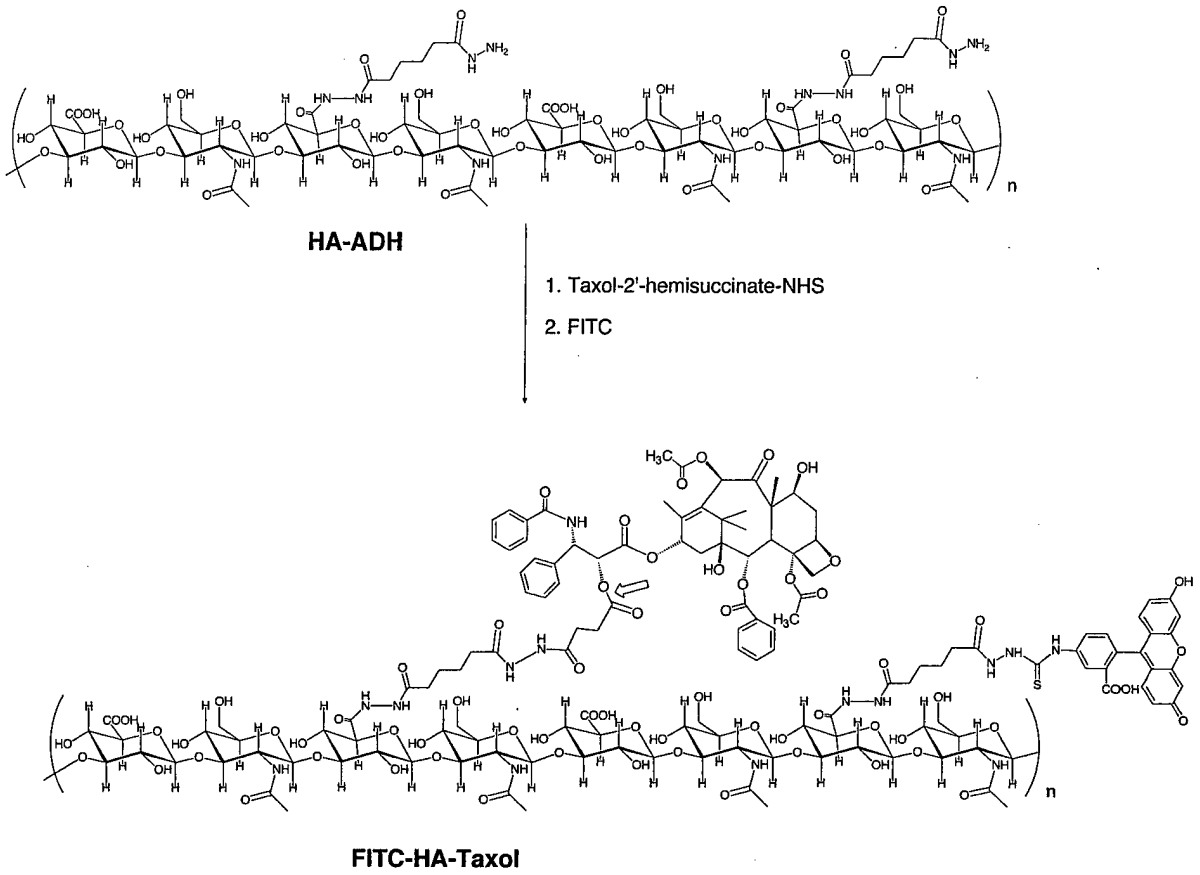

Figure 1. Synthesis of FITC–HA–Taxol.

sodium pyruvate; SK-OV-3, a human ovarian cancer cell line was cultured in D-MEM/F12 + 10% FBS; HCT-116, a colon tumor cell line, was maintained in culture in McCoy's 5A Medium Modified + 10% FBS; NIH 3T3, a mouse fibroblast cell line was cultured in high-glucose D-MEM + 10% FBS.

Analytical Instrumentation. All ^{1}H NMR spectral data were obtained using an NR-200 FT-NMR spectrometer at 200 MHz (IBM Instruments Inc.). UV–vis spectra were recorded on a Hewlett-Packard 8453 UV–Vis diode array spectrophotometer (Palo Alto, CA). Gel permeation chromatography (GPC) and high-performance liquid chromatography (HPLC) were carried out on the following system: Waters 515 HPLC pump, Waters 410 differential refractometer, and Waters 486 tunable absorbance detector. Waters Ultrahydrogel 250 and 2000 columns (7.8 mm i.d. × 30 cm) (Milford, MA) were used for GPC analysis, the eluent was 150 mM pH 6.5 phosphate buffer/MeOH = 80:20 (v/v), and the flow rate was 0.5 mL/min. The system was calibrated with HA standards supplied by Dr. O. Wik (Pharmacia). HPLC analysis of Taxol release from HA–Taxol bioconjugate was performed on Altech HYPERSIL ODS C_{18} 5U 150 mm × 4.6 mm i.d. along with Altech HYPERSIL ODS C_{18} 5U 7.5 mm × 4.6 mm i.d. as guard column at room temperature; the eluent was acetonitrile/H_2O = 45:55 with flow rate of 0.8 mL/min. A 1-mL C_{18} cartridge was obtained from Varian Inc. (Palo Alto, CA). Fluorescence-activated cell sorting (FACS) was performed on a Becton Dickinson FACScan (San José, CA) with an argon-ion laser for cell binding and uptake measurement. Confocal fluorescence images of fluorescently labeled HA binding and uptake by cells were recorded using a Zeiss Microscope (Carl Zeiss, Inc., Germany). Cell viability in cell culture was determined by thiazoyl blue (MTT) dye uptake protocols measured at 540 nm, which was recorded on a BIO-RAD M-450 microplate reader (Hercules, CA). Coulter Counter was from Coulter Electronics, Inc. (Hialeah, FL).

Preparation of Low Molecular Weight (LMW) HA and HA Hydrazide Derivative (HA–ADH). Low molecular weight HA (LMW HA) was obtained by the degradation of high molecular weight HA (1.5 MDa) in pH 6.5 phosphate-buffered saline (PBS) buffer (4 mg/mL) with HAse (10 U/mg HA) as previously described.[23] The size profile was evaluated by GPC analysis. Hydrazide-derivatized HA (HA–ADH) was prepared[46,47] using a modified purification method that gives preparations free of small molecules.[23] In one example, LMW HA (50 mg) was modified with a 5-fold excess of ADH to obtain 37 mg of HA–ADH with an 18% ADH loading based on available carboxylates modified.

Preparation of HA–Taxol Bioconjugates. Taxol 2′-hemisuccinate, which was synthesized from Taxol and succinic anhydride and purified as described,[23] was used as

a standard for release studies. Activation to the *N*-hydroxysuccinimide ester[23] gave the reagent used for coupling to HA–ADH. Several loadings were prepared. In a representative example, HA–ADH with 18% ADH loading (10 mg, 4.4 μmol of hydrazide) was dissolved in 3 mM pH 6.5 phosphate buffer to give 1 mg/mL. To this mixture was added Taxol–NHS ester dissolved in sufficient DMF (DMF:H_2O = 2:1, v/v) to give a homogeneous solution, and the reaction mixture was stirred at room temperature for 24 h. The reaction mixture was dialyzed successively against 50% acetone/H_2O and water (membrane tubing, M_r cutoff 3500). The solution was then filtered through a 0.2 μm membrane and then lyophilized. The purity of HA-Taxol conjugate was measured by GPC analysis. Taxol loading was determined by UV absorbance (λ_{max} = 227 nm, $\epsilon = 2.8 \times 10^4$) in 80:20 CH_3CN:H_2O.

Taxol Release from HA–Taxol Bioconjugate. Solid-phase extraction (SPE) and liquid–liquid extraction (LLE) methods were introduced to recover the liberated Taxol, Taxol 2′-hemisuccinate, or other potential metabolites.

SPE Method. A 1-mL C_{18} cartridge was first conditioned with 5 mL of ethyl acetate, 5 mL of methanol, and 5 mL of Nanopure H_2O. A small amount of H_2O remained above the top frit in the cartridge at the time the crude extract was transferred to the cartridge. Several "crude extract" model solutions were prepared for calibration: 2 μL of Taxol in DMSO (1 mg/mL) + 2 μL of Taxol 2′-hemisuccinate in DMSO (1 mg/mL), 1 μL of Taxol in DMSO (1 mg/mL) + 1 μL of Taxol 2′-hemisuccinate in DMSO (1 mg/mL), and 2 μL of Taxol in DMSO (0.1 mg/mL) + 2 μL of Taxol 2′-hemisuccinate in DMSO (0.1 mg/mL), each mixed with 200 μL of cell culture media (α-MEM + 10% FBS). The final concentrations of Taxol and Taxol 2′-hemisuccinate in cell culture media were 10, 5, and 1 μg/mL (from 1 to 12 nmol/mL). After the crude extract was transferred into the cartridge, the cartridge was washed (four 1-mL portions of H_2O, 3 × 1 mL of 20% methanol/H_2O, 4 × 1 mL of methanol). To the combined methanol fractions was added 1 μg of cephalomannine (internal standard) as a methanol stock solution (100 μL of 10 μg/mL stock solution), and solvents were concentrated in vacuo using a centrifugal concentrator at room temperature. The residue was dissolved in 500 μL of methanol, and a 200-μL aliquot was analyzed by HPLC.

LLE Method. The same model extracts as above were diluted with 300 μL of H_2O. Taxol and Taxol 2′-hemissuccinate were extracted using 4.0 mL of *tert*-butyl methyl ether and vortex-mixing the sample for 1 min. The mixture was centrifuged for 10 min at 500*g* at room temperature, and then 2.0 mL of the organic layer was transferred to a new tube. Internal standard (1 μg of cephalomannine) was added as a methanol stock, the mixture was evaporated to dryness, the residue was dissolved in 500 μL of methanol, and a 200-μL aliquot was analyzed by HPLC.

Each experiment with either the SPE method or the LLE method was performed in triplicate. The recovery of Taxol or Taxol 2′-hemisuccinate was evaluated according to the equation:

$$\text{recovery} = \frac{\text{mean peak area ratio, extract drug}}{\text{mean peak area ratio, direct injection drug}} \times 100\%$$

Taxol release from HA–Taxol prodrug experiments was carried out in five different media: (1) cell culture media, cell culture media with added (2) HAse (1 U/mL, 10 U/mL) or (3) esterase (0.1 U/mL, 1 U/mL), (4) cell culture media with cells, and (5) human plasma. For each system, 2 μL of HA–Taxol bioconjugate stock solution (10 mg/mL in DMSO/H_2O = 1:1, v/v) was added into 200 μL of media solution and then maintained at 5% CO_2, 37 °C. Samples (crude extracts) were taken out at different time intervals, and SPE was used to follow drug release.

Preparation of FITC–HA–Taxol. LMW HA–ADH with 9% ADH loading (20 mg, 3.7 μmol of hydrazide) was dissolved in 5 mL of 3 mM pH 6.5 phosphate buffer, and 10 mL of a DMF solution of Taxol NHS ester (7.8 mg, 7.4 μmol) was added. The reaction mixture was stirred at room temperature overnight. To this mixture, FITC (1 mg, 2.6 μmol) in 2 mL of DMF was added, and the reaction was stirred at room temperature overnight. FITC–HA–Taxol was purified by dialysis against 50% acetone/H_2O, and its purity was determined by GPC with UV detection at 210 nm (HA, Taxol), and 493 nm (FITC).

In Vitro Cell Culture Cytotoxicity. The cytotoxicity of HA–Taxol conjugates was determined using a 96-well plate format in quadruplicate with increasing doses: 0.001, 0.01, 0.1, 0.5, 1, 5, 10, 50, and 100 μg/mL. Each well contained approximately 20 000 cells in 200 μL of cell culture media. HA–Taxol conjugates were added as a stock solution in DMSO:H_2O = 1:1, v/v); free Taxol was added as a DMSO stock solution. Thus, a 2-μL aliquot of the stock solution was added to each well, cells were incubated at 37 °C for 3 days with the test substance, and cell viability was determined using MTT dye uptake at 540 nm. Response was graded as percent live cells compared to untreated controls.[48]

In competition experiments, 100-fold excess of either high molecular weight HA or CS (as compared to HA–Taxol) was employed; either the competitor was added at the same time as the drug or, alternatively, cells were preincubated with competitor for 4 h before the addition of HA–Taxol conjugate or free Taxol. The in vitro cytotoxicity was analyzed as described above.

Binding and Uptake Measurement by FACS. Cells were incubated in a cell culture flask, harvested by trypsinization, and transferred into clean tubes. An aliquot (1 μL) of FITC–HA–Taxol (stock solution 1 mg/mL in PBS buffer) was added into tubes with suspension cells and analyzed by FACS. For competition or blocking studies, a 100-fold excess of either high molecular weight HA or CS (as compared to FITC–HA–Taxol) was preincubated with cells for 4 h, or an anti-CD44 mAb was preincubated with cells for 30 min, prior to addition of FITC–HA–Taxol and FACS analysis.

Uptake Measurement by Confocal Microscopy. An aliquot (2 μL) of FITC–HA–Taxol (stock solution 1 mg/mL in PBS buffer) was added to 100 μL of cell culture media containing cells cultured on cover slips, and confocal images

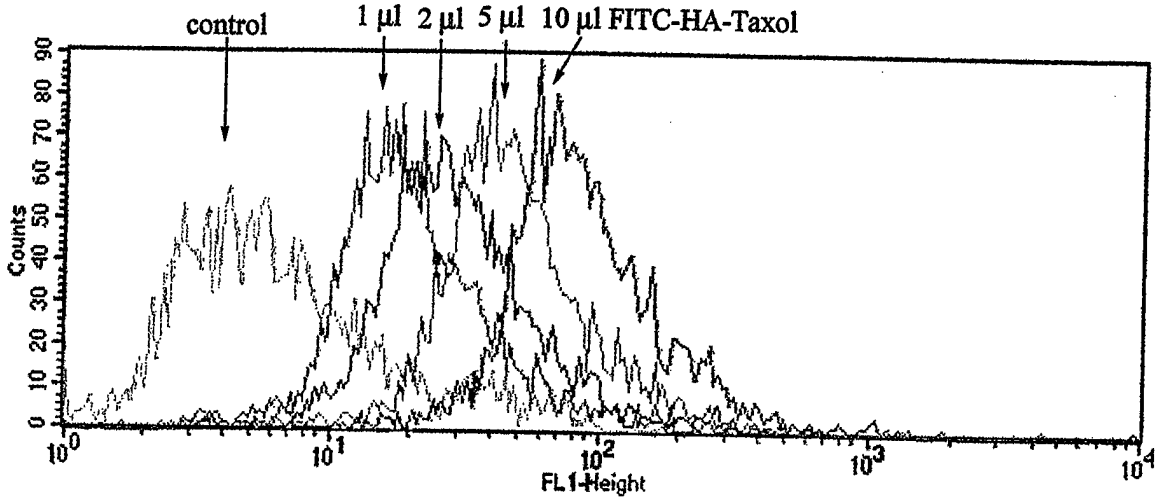

Figure 2. Flow cytometry measurements of FITC–HA–Taxol binding SK-OV-3 cells. Colored peaks show dose-dependent binding of the labeled polymeric prodrug to the CD44-overexpressing cells.

were recorded immediately. Competition experiments used cells preincubated with 100-fold excess HA for 4 h prior to addition of the FITC–HA–Taxol.

Results

Preparation of HA–Taxol. The hydrazide method[46,47] allows attachment of reporter molecules, drugs, cross-linkers, and combinations of these moieties to HA.[16,18,43] LMW HA was modified in this study for three reasons: (i) proton NMR allowed rapid quantification of the modification, (ii) LMW HA and its derivatives give injectable, nonviscous solution at concentrations up to 10 mg/mL, and (iii) LMW HA has a longer plasma half-life and is readily cleared by renal ultrafiltration. The LMW HA was generated by partial degradation of high molecular weight HA (1.5 MDa) with testicular HAse [49] in pH 6.5 PBS buffer at 37 °C. The final LMW HA product was characterized by GPC analysis: M_n = 3883, M_w = 11 199, and molecular dispersity (DP) = 2.88. Next, HA–ADH samples with different ADH loadings were prepared by carbodiimide coupling chemistry,[23] in which the extent of ADH modification was controlled through use of specific molar ratios of hydrazide, carboxylate equivalents, and carbodiimide. The purity and molecular size distribution of the HA–ADH were measured by GPC, and the loading of ADH on the polymer backbone was determined by ^{1}H NMR in D_2O.[46] HA–ADH with ADH loadings of 9% and 18% were obtained and used in preparing the HA–Taxol bioconjugates.

Because of the problems in administering emulsified forms of Taxol,[50] a water-soluble bioconjugate was prepared. The single symmetrical GPC peak showed that no free Taxol or other small molecular impurities remained. The loading of Taxol on polymer backbone was quantified by UV absorbance at 227 nm in 80% acetonitrile:H_2O. HA–Taxol bioconjugates $[(HA)_x(HA–ADH)_y(HA–ADH–Taxol)_z]$ with the compositions of x = 91%, y = 4%, z = 5% and x = 82%, y = 3%, z = 15% were used in the following experiments, based on previous loading optimization studies.[23]

Cell-Based Assays for Binding and Uptake. Several different fluorescently labeled HA derivatives have been prepared in order to study receptor-mediated uptake. Most recently, RHAMM-mediated uptake and trafficking of HA by transformed fibroblasts[51] was observed with Texas Red-HA, and BODIPY-labeled HA was employed to distinguish HA uptake in cancer vs untransformed cell lines.[23] Both of these derivatives were prepared with hydrazide modification chemistry. Previously, fluorescein–HA was employed to study HA uptake in a variety of systems, e.g., cells expressing CD44 variants,[33,52–55] uptake by tumor cells for correlation with metastatic potential,[42,56] internalization by chondrocytes,[38] and as a measure of liver endothelial cell function.[57]

To correlate the binding and uptake by cells with toxicity, fluorescently labeled HA–Taxol (FITC–HA–Taxol) was prepared and purified by dialysis against 50% acetone/H_2O. The fluorescence loading of FITC–HA–Taxol was determined spectrophotometrically to be 0.6% (based on available glucuronates). GPC confirmed that mass, UV absorption, and fluorescence coeluted in the same symmetrical peak.

The interaction of the HA–Taxol bioconjugate with cells was initially investigated by laser flow activated cell sorting using FITC–HA–Taxol as fluorescence probe. To the suspended cells (after trypsin digestion), an aliquot of FITC–HA–Taxol (stock solution 1 mg/mL in PBS buffer) was added to give five different dosages. The measurements were immediately taken by FACS with untreated suspended cells as the control. The conjugate was strongly adsorbed to SK-OV-3 cells (Figure 2); similar results (not shown) were observed for HBL-100 and HCT-116 cells. The shift of the fluorescence peak in FACS was dose-dependent based on the amount of FITC–HA–Taxol added. Moreover, no fluorescence binding or shift was detected with mouse fibroblast NIH 3T3 cells. These results indicated that FITC–

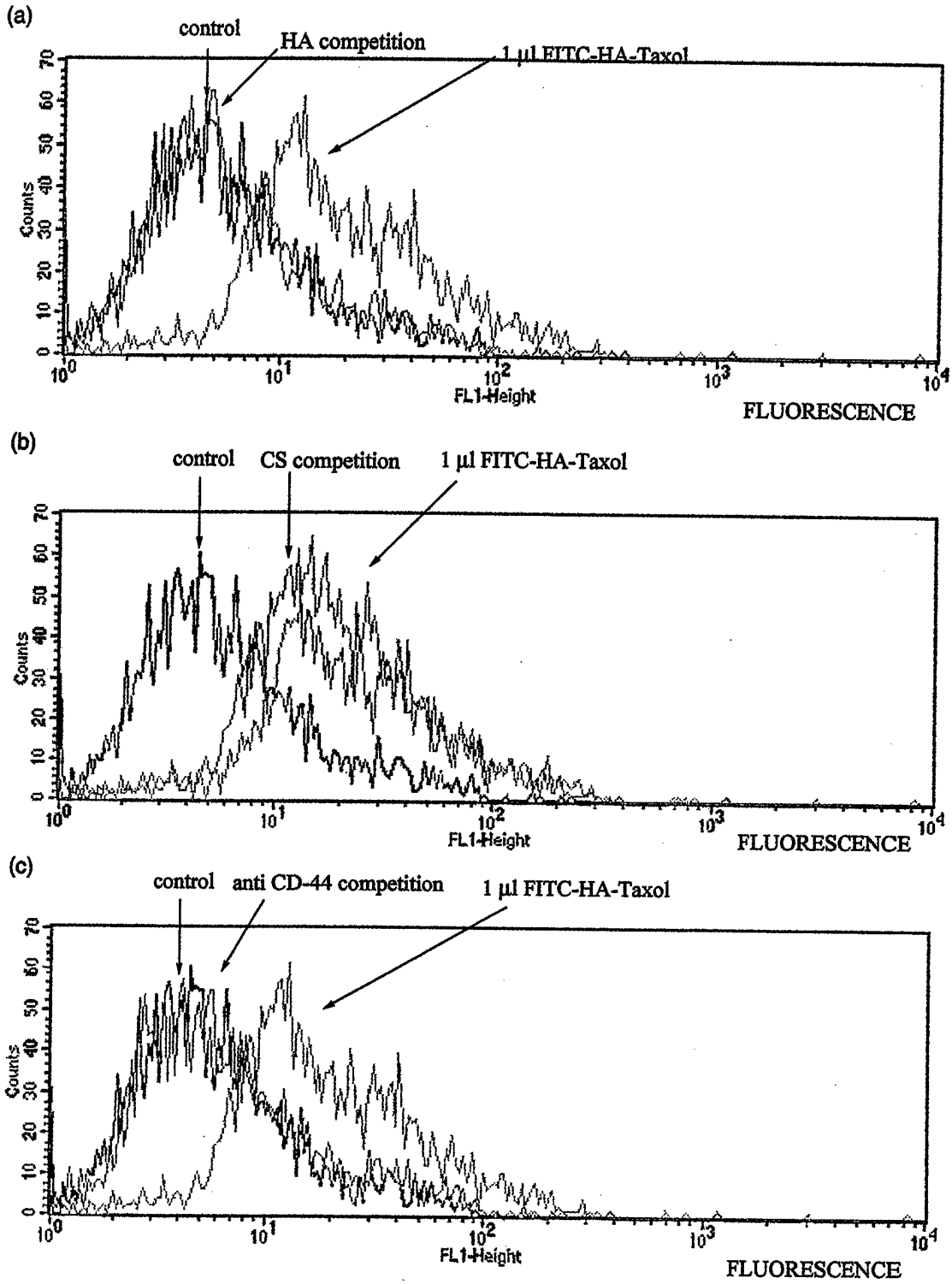

Figure 3. FACS analysis of FITC–HA–Taxol binding (red lines) to SK-OV-3 cells. Panel a shows competition by 100-fold excess HA (green) relative to controls (black) and no competitor (red); panel b shows absence of competition by excess CS (green); panel c shows blocking of uptake by anti-CD 44 mAb (green).

HA–Taxol selectively bound to, and was taken up by, the SK-OV-3, HBL-100, and HCT-116 cells. These results corroborate the previously reported selective cytotoxicity of the HA–Taxol bioconjugate to HBL-100 cells, SK-OV-3 cells, and HCT-116 cells[23] and provide an important linkage between fluorescence-visualized uptake and selective toxicity.

Since binding and uptake by cells determined the cytotoxicity of the HA–Taxol bioconjugate, experiments were

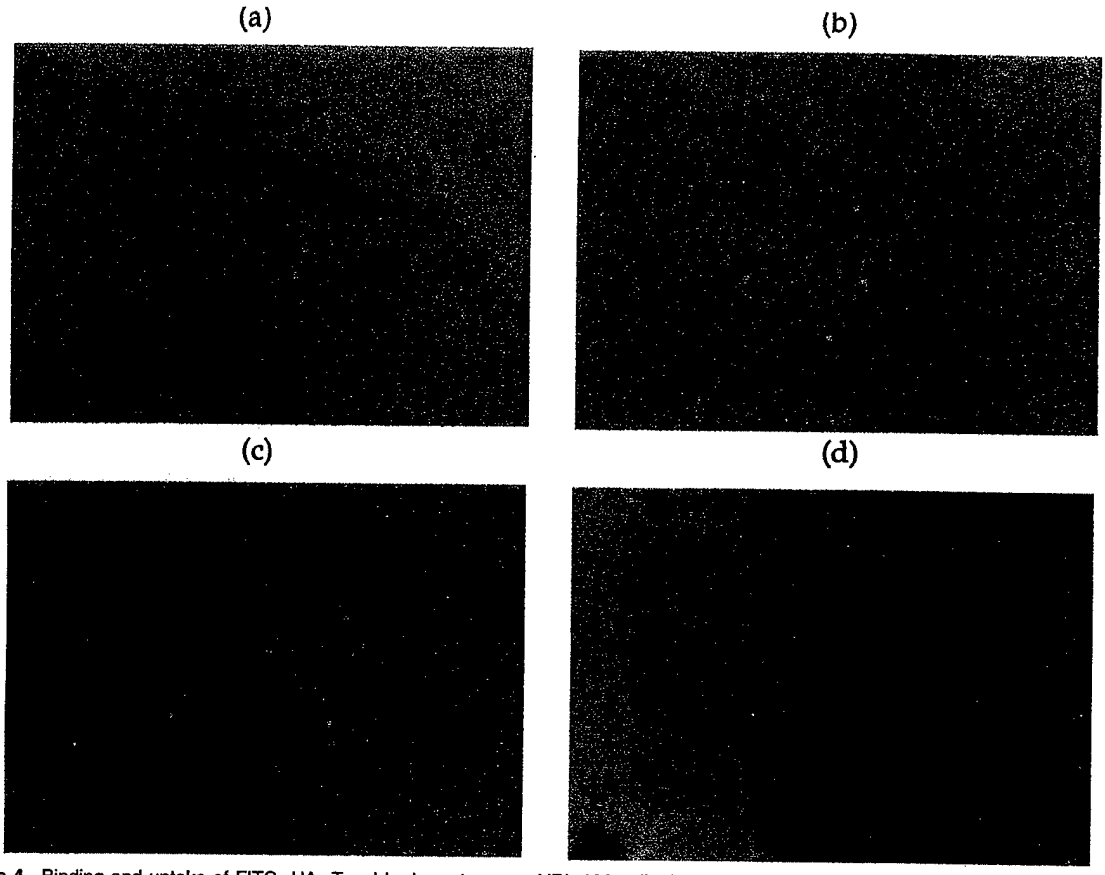

Figure 4. Binding and uptake of FITC−HA−Taxol by breast cancer HBL-100 cells. Panels a−c are confocal images indicating binding and uptake after 4 (a), 10 (b), and 20 min (c) of incubation. Panel d is a 5-fold lower magnification image that shows that preincubation with excess HA blocks the cellular uptake of FITC−HA−Taxol even at 20 min.

performed to block each of these two processes. The HA binding protein CD44 is overexpressed on the surface of HBL-100[39] and SK-OV-3 cells.[40] A series of competition experiments was carried out with SK-OV-3 cells using a 100-fold excess of high molecular weight HA, a 100-fold excess of CS, and an anti-CD44 mAb as potential disrupters of the cellular uptake of the FITC−HA−Taxol bioconjugate. Thus, cells were preincubated for 4 h with either HA or CS, or for 30 min with the anti-CD44 mAb. Next, FITC−HA−Taxol was added and FACS analysis was performed. Figure 3 shows that the binding and uptake of FITC−HA−Taxol into SK-OV-3 cells could be blocked by excess HA (panel a) and by the anti-CD44 mAb (panel c) but not by excess CS (panel b).

Liver endothelial cells display at least two different binding proteins for HA, including a scavenger receptor that binds to both CS and HA, and other glycosaminoglycans.[58] However, at sites in need of treatment, e.g., tumor metastases, only receptors that are HA specific appear to be expressed. We previously showed that the binding of fluorescently labeled HA alone could be blocked by excess HA in cancer cell lines.[23] The data presented herein now provide direct evidence that unambiguously correlates uptake and subsequent cytotoxicity of the bioconjugate. The ability to block uptake and toxicity with excess HA and with anti-CD44 mAb but not with excess CS confirms the receptor-mediated nature of the selective targeting and cytotoxicity. This further substantiates the proposal that radionuclide-modified HA derivatives and HA-coupled prodrugs could be used to selectively target primary tumors and tumor metastases, provided that CS is preadministered to block "housekeeping" receptors in the liver without affecting specific HA receptors of tumor cells.[58−61]

Confocal Microscope Images of Cellular Uptake of HA−Taxol Bioconjugate. An aliquot (1 μL) of a 1 mg/mL aqueous stock solution in PBS buffer FITC−HA−Taxol was added to 100 μL of cell culture media containing tumor cells grown on cover slips. Confocal images of FITC−HA−Taxol uptake by HBL-100 cells are presented in Figure 4. Initially, FITC−HA−Taxol can be seen on the cell membrane; over the course of several minutes, it is taken up into the cell and then gradually begins to accumulate in the nucleus. After 20 min, cells showed FITC−HA−Taxol in most subcellular compartments. The uptake of FITC−HA−Taxol into SK-OV-3 cells (Figure 5) and HCT-116 cells (not shown) occurred with a similar appearance and time course. Figure 5a provides a particularly dramatic illustration of the initial binding of the FITC−HA−Taxol to the cell surface prior to cellular uptake. These data confirm that HA binds readily to tumor cell surfaces and is rapidly endocytosed via HA receptor-mediated pathways. In addition, the data show that HA can act as a targeting polymer for solubilization and selective delivery of anticancer drugs to tumor cells. Importantly, nontransformed cells, such as the NIH 3T3 fibroblasts,

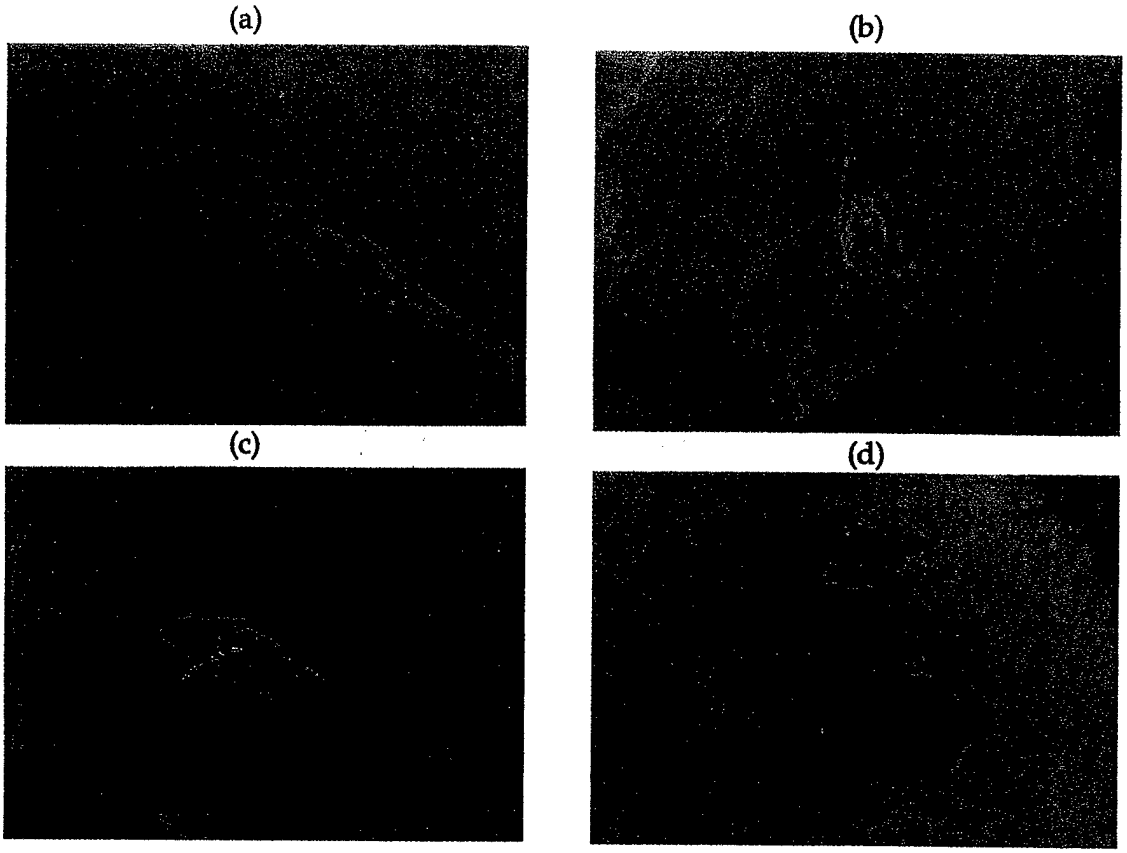

Figure 5. Binding and uptake of FITC–HA–Taxol by ovarian cancer SK-OV-3 cells. Panels a–c are confocal images indicating binding and uptake after 4 (a), 10 (b), and 20 min (c) of incubation. Panel d shows that preincubation with excess HA blocks the cellular uptake of FITC–HA–Taxol even at 20 min.

did not show this binding and rapid uptake of FITC–HA–Taxol in similar experiments (data not shown). Finally, the competition experiments show that the uptake of FITC–HA–Taxol conjugate by HBL-100 cells (Figure 4d) and SK-OV-3 cells (Figure 5d) could be blocked by preincubation of the cells with excess HA; in these images, fluorescence only accumulates outside cells. These results provide further support for the FACS experiments that the binding and cellular uptake of the HA bioconjugates are mediated through an HA-specific, receptor-mediated process.

Taxol Release from HA–Taxol Bioconjugate. Taxol release from HA–Taxol conjugate experiments was carried out in different media: cell culture media with or without cells, cell culture media with HAse (1 U/mL, 10 U/mL), esterase (0.1 U/mL, 1 U/mL), and human plasma. An HA–Taxol conjugate with composition of $(HA)_{0.82}(HA–ADH)_{0.03}$-$(HA–ADH–Taxol)_{0.15}$ was used for the drug release study. There are two possible cleavage sites (see Figure 1) that would result in the release of either free Taxol (ester hydrolysis) or Taxol 2′-hemisuccinate (hydrazide hydrolysis). SPE and LLE methods were introduced to extract Taxol and Taxol 2′-hemisuccinate standards from cell culture media. Table 1 shows that LLE is only suitable for the extraction of Taxol but gives poor recovery of Taxol 2′-hemisuccinate from cell culture media. In contrast, SPE showed reproducible and high recovery for both Taxol and Taxol 2′-hemisuccinate. Thus, SPE was used as the extraction method of choice in the release study.

Table 1. Taxol and Taxol 2′-Hemisuccinate Recovery by Solid Phase Extraction (SPE) and Liquid–Liquid Extraction (LLE)

Taxol concn (μg/mL)	Taxol recovery (%)	Taxol 2′-hemisuccinate concn (μg/mL)	Taxol 2′-hemisuccinate recovery (%)
	Solid-Phase Extraction (SPE) Method		
10	101.4 ± 3.6	10	94.2 ± 4.5
5	95.3 ± 4.5	5	96.8 ± 3.0
1	96.4 ± 6.5	1	95.5 ± 3.2
	Liquid-Liquid Extraction (LLE) Method		
10	90.2 ± 3.2	10	31.7 ± 2.0
5	102.8 ± 4.5	5	36.2 ± 1.3
1	102.0 ± 4.0	1	no detection

A 2-μL aliquot of the HA–Taxol stock solution (10 mg/mL in DMSO/H_2O = 1:1, v/v) was added to 200 μL of media and incubated at 5% CO_2 at 37 °C. Samples (crude extract) were removed at different time intervals and processed by standardized SPE protocols, and the released drug was quantified by HPLC using an internal standard. Figure 6a shows the HPLC separation of Taxol and Taxol 2′-hemisuccinate with cephalomannine as the internal standard. Figure 6b shows a typical analysis of extracted media. Figure 7a shows the time course of drug release from the bioconjugate (without added hydrolytic enzymes) in media and human plasma. HPLC analysis (Figure 6b) clearly demonstrated that

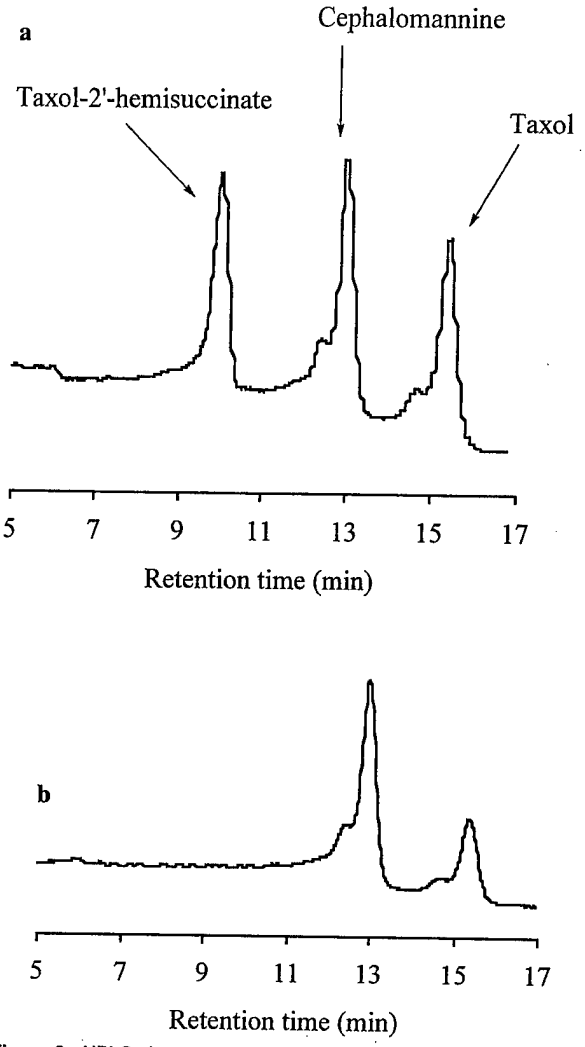

Figure 6. HPLC chromatograms of the separation of Taxol, Taxol 2′-hemisuccinate and cephalomannine. Panel a shows the separation of the standards; panel b illustrates the release of Taxol alone from HA–Taxol incubated with human plasma.

only Taxol was released from the HA–Taxol bioconjugate; no Taxol 2′-hemisuccinate was released under any of experimental conditions. This conforms with the expectation that the hydrazide linkage is much more hydrolytically stable than ester bond linkage. Moreover, the time course shows that HA–Taxol is quite long-lived in a hydrolase-free extracellular environment, with less than 20% of Taxol released from the bioconjugate during 24 h. Importantly, Taxol release rate from cell culture media with cells is similar to, or even lower than, that from cell culture media only. NIH 3T3 cells were employed for these experiments, since they did not internalize the HA–Taxol prodrug. Release from plasma was accordingly more rapid, since plasma contains a variety of endogenous hydrolytic enzymes.

Similar biphasic release rate profiles were obtained with enzyme-catalyzed drug release from HPMA-drug conjugates employing biodegradable oligopeptide spacers.[62] In these cases, the solution behavior of polymer–drug conjugate may differ from that of the polymeric carrier when a hydrophilic

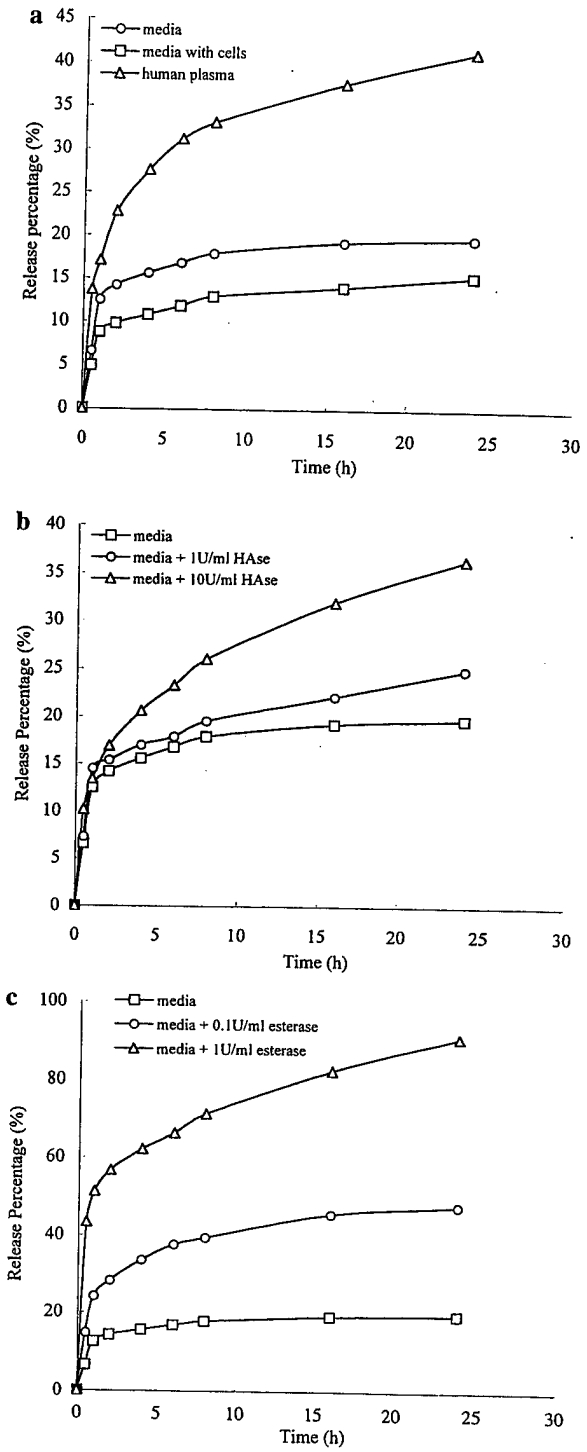

Figure 7. In vitro free Taxol release from HA-Taxol. Panel a shows release in cell culture media under cell-free conditions (○), with NIH 3T3 cells (□), and from incubation with human plasma (△). Panel b shows release from cell culture media in the presence of testicular HAse. Panel c shows release of drug from cell culture media with added porcine esterase.

polymeric carrier contains hydrophobic drug molecules on the side chain. Polymeric drugs containing a hydrophobic active component often aggregate due to intermolecular hydrophobic interactions. The formation of such hydrophobic

aggregates impedes formation of the enzyme–substrate complex and thus becomes an important factor in the drug release rate from the side chain of polymer–drug conjugate. Moreover, the formation of aggregates may in turn affect the accessibility of various compartments in the living organism and also the rate of release of the active drug following the entry of the polymer–drug conjugate into the target cells.

Figure 7b shows the drug release in cell culture media to which HAse (1 and 10 U/mL) was added. At the lower enzyme level, the Taxol release rate is only slightly increased over that in the HAse-free media. In contrast, the Taxol release rate increased sharply in the presence of even very modest amounts of esterase (Figure 7c). Extremely rapid release was observed in the 1 U/mL esterase experiment. Indeed, the Taxol release rate in the presence of esterase was similar to that found in human plasma. In summary, the HA–Taxol prodrug released only free Taxol, and the presence of esterase dramatically accelerated Taxol release from the bioconjugate. We conclude that following receptor-mediated cellular uptake of the HA–Taxol bioconjugate, free Taxol drug is released from the polymeric prodrug by intracellular enzymatic hydrolysis, thereby delivering the toxic agent inside the cell and disrupting mitosis leading to cell death.

In Vitro Selective Cytotoxicity. Further determinations of the cytotoxicity of HA–Taxol were performed using a 96-well plate format in quadruplicate with increasing doses ranging from 0.001 to 100 μg/mL. The cytotoxicity of HA–Taxol conjugates was studied using the MTT assay to identify cells still active in respiration.[48] In our previous experiments,[23] HA–Taxol conjugates were selective cytotoxins, killing HBL-100, SK-OV-3, and HCT-116 cells but sparing NIH 3T3 fibroblast cells at concentrations up to 10 μg/mL of Taxol equivalents. The FITC–HA–Taxol binding and uptake results reported in this study indicate that selective cytotoxicity of HA–Taxol is due to receptor-mediated events. The in vitro cytotoxicity data confirm the selective toxicity of HA–Taxol toward different cell lines, and the known overexpression of CD44 by HBL-100[39] and SK-OV-3 cells[40] suggests that this selective toxicity is due to receptor-mediated binding and uptake of the HA–Taxol.

Competition experiments in which preincubation with HA protected susceptible cancer cells from the cytotoxicity of HA–Taxol strengthened this conclusion. Thus, HA–Taxol (5% loading) was employed over a 10-fold dosage range. Figure 8a summarizes the results obtained using a 100-fold excess of HA as the competitor. Simultaneous addition of HA with either Taxol or with HA–Taxol to the cells produced only modest protection against cytotoxicity of the polymeric prodrug. However, a significant reduction in cytotoxicity of the HA–Taxol was observed when cells were preincubated for 2 h with excess HA prior to the addition of HA–Taxol conjugate. Figure 8b shows that excess CS did not reduce cytotoxicity of prodrug or free Taxol under any of the conditions, thus indicating that there was no reduction in the uptake of the HA–Taxol by the HBL-100 cells. Analogous results were obtained with this prodrug conjugate with SK-OV-3 cells and HCT-116 cells (not shown). Thus,

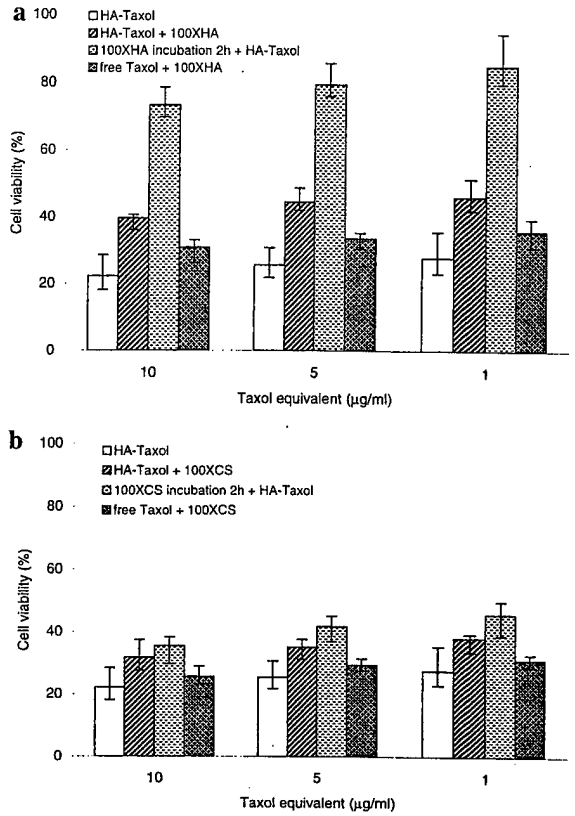

Figure 8. In vitro cytotoxicity of HA–Taxol with 5% Taxol loading against HBL-100 human breast cancer cells with excess HA (panel a) or CS (panel b) as competitors. Key: HA–Taxol only (open bars); HA–Taxol with either 100-fold excess of either HA or CS (diagonal lines); preincubation with 100-fold excess of either HA or CS, for 2 h, then additional HA–Taxol (speckled); free Taxol, plus 100-fold excess of either HA or (crosshatched).

at a 15% Taxol loading for the HA–Taxol prodrug, preincubation with HA, but not with CS, caused competitive displacement.

These data confirm the FACS and confocal microscopy results that HA–Taxol conjugate must enter the tumor cells through an HA-receptor-mediated process. Apparently, binding and uptake are not readily blocked when HA and HA–Taxol are premixed. Our previous experiments[23] showed that uptake of chemically modified HA was very rapid. Thus, effective competition and reduction of HA–Taxol uptake seem to require preincubation of the cells with HA to presaturate the receptor-mediated uptake system. This phenomenon can be rationalized in two ways. First, it is possible that the high molecular weight HA used for the competition experiments may bind with slower kinetics than the LMW HA–Taxol. Conversely, the receptor clustering that occurs in response to multivalent binding of HA to receptors provides a very effective block of the endocytotic pathway. An alternative explanation is that the attachment of multiple hydrophobic Taxol molecules to HA on flexible tethers provides the opportunity for multivalent insertion into the lipid bilayer, with receptor-mediated endocytosis occurring subsequently. In this case, HA would be ineffective in preventing this initial hydrophobic-type association. Once the HA–Taxol was immobilized on the membrane, two-

dimensional migration and receptor-mediated uptake would be entropically favored.

In conclusion, the data reported herein indicate that the cytotoxicity of HA−Taxol requires cellular uptake of the bioconjugate followed by hydrolytic release of the active Taxol by cleavage of the labile 2′ ester linkage. Targeting of a variety of anticancer agents to tumor cells and tumor metastases could be achieved by receptor-mediated uptake of an HA−anticancer agent conjugate, followed by the intracellular release of the active drug and subsequent cell death. The ability to "seek and destroy" micrometastases is one of the most compelling and attractive potential outcomes for the HA−antitumor bioconjugates.

Acknowledgment. Financial support for this work was provided by Department of Army (DAMD 17-9A-1-8254) and by the Huntsman Cancer Foundation at The University of Utah (UUtah). We are grateful to D. Schmehl and Dr. L. R. Barrows (UUtah) for assistance with cell cytotoxicity experiments, Dr. W. G. Pitt (Brigham Young University, Provo, UT) for assistance with confocal microscopy, and D. Augello and Dr. W. F. Green for assistance with FACS experiments (Flow Cytometry Facility, UUtah). We thank Dr. L. Y.-W. Bourguignon (University of Miami Medical School, Miami, FL) for providing HBL-100 and SK-OV-3 cells. We are grateful to Clear Solutions Biotechnology, Inc. (Stony Brook, NY), for providing HA and the Center for Cell Signaling (UUtah) for equipment and facilities.

References and Notes

(1) Kim, K. H.; Hirano, T.; Ohashi, S. In *Polymeric Materials Encyclopedia*; Salamone, J. C., Ed.; CRC Press: Boca Raton, FL, 1996; pp 272−285.
(2) Trouet, A.; Masquelier, M.; Baurain, R.; Campeneere, D. D. *Proc. Natl. Acad. Sci. U.S.A.* **1982**, *79*, 626−629.
(3) Kim, S. *Drugs* **1993**, *46*, 618−638.
(4) Arshady, R. *J. Controlled Release* **1990**, *14*, 111−131.
(5) Kreuter, J. *J. Controlled Release* **1991**, *16*, 169−176.
(6) Waser, P. G.; Kreuter, J.; Berger, S.; Munz, K.; Kaiser, E.; Pfluger, B. *Int. J. Pharm.* **1987**, *39*, 213−227.
(7) Cartlidge, S. A.; Duncan, R.; Lloyd, J. B.; Kopeckova, R. P.; Kopecek, J. *J. Controlled Release* **1987**, *4*, 265−278.
(8) Molteni, L. In *Drugs Carriers in Biology and Medicine*; Gregoriadis, G., Ed.; Academic: London, 1979; p 107.
(9) Molteni, L. In *Drugs Carriers in Biology and Medicine*; Gregoriadis, G., Ed.; Academic Press: London, 1979; p 43.
(10) Greenwald, R. B.; Gilbert, C. W.; Pendri, A.; Conover, C. D.; Xia, J.; Martinez, A. *J. Med. Chem.* **1996**, *39*, 424−431.
(11) Maeda, H.; Seymour, L.; Miyamoto, Y. *Bioconjugate Chem.* **1992**, *3*, 351−362.
(12) Minko, T.; Kopeckova, P.; Pozharov, V.; Kopecek, J. *J. Controlled Release* **1998**, *54*, 223−233.
(13) Hirano, T.; Ohashi, S.; Morimoto, S.; Tsuda, K. *Makromol. Chem.* **1986**, *187*, 2815−2824.
(14) Laurent, T. C.; Laurent, U. B. G.; Fraser, J. R. E. *Ann. Rheum. Dis.* **1995**, *54*, 429−432.
(15) Vercruysse, K. P.; Prestwich, G. D. *Crit. Rev. Ther. Drug Carrier Syst.* **1998**, *15*, 513−555.
(16) Prestwich, G. D.; Marecak, D. M.; Marecek, J. F.; Vercruysse, K. P.; Ziebell, M. R. In *The Chemistry, Biology, and Medical Applications of Hyaluronan and its Derivatives*; Laurent, T. C., Ed.; Portland Press: London, 1998; pp 43−65.
(17) Freed, L. E.; Vunjak-Novakovic, G.; Biron, R. J.; Eagles, D. B.; Lesnoy, D. C.; Barlow, S. K.; Langer, R. *Bio/Technology* **1994**, *12*, 689−693.
(18) Prestwich, G. D.; Luo, Y.; Ziebell, M. R.; Vercruysse, K. P.; Kirker, K. R.; MacMaster, J. S. In *New Frontiers in Medical Sciences: Redefining Hyaluronan*; Abatangelo, G., Ed.; Portland Press: London, in press.
(19) Alam, C. A. S.; Seed, M. P.; Willoughby, D. A. *J. Pharm. Pharmacol.* **1995**, *47*, 407−411.
(20) Falk, R. E. PCT Int. Appl. WO 9740841, 1997.
(21) Ziegler, J. *J. Natl. Cancer Inst.* **1996**, *88*, 397−399.
(22) Akima, K.; Ito, H.; Iwata, Y.; Matsuo, K.; Watari, N.; Yanagi, M.; Hagi, H.; Oshima, K.; Yagita, A.; Atomi, Y.; Tatekawa, I. *J. Drug Targeting* **1996**, *4*, 1.
(23) Luo, Y.; Prestwich, G. D. *Bioconjugate Chem.* **1999**, *10*, 755−763.
(24) Turley, E. A.; Belch, A. J.; Poppema, S.; Pilarski, L. M. *Blood* **1993**, *81*, 446−453.
(25) Toole, B. P. *J. Intern. Med.* **1997**, *242*, 35−40.
(26) Rudzki, Z.; Jothy, S. *J. Clin. Pathol. Mol. Pathol.* **1997**, *50*, 57−71.
(27) Lesley, J.; Hyman, R.; English, N.; Catterall, J. B.; Turner, G. A. *Glycoconjugate J.* **1997**, *14*, 611−622.
(28) Underhill, C. *J. Cell Sci.* **1992**, *103*, 293−298.
(29) Turley, E. A. In *The Biology of Hyaluronan*; CIBA Foundation, Ed.; J. Wiley & Sons: Ltd.: Chichester, U.K., 1989; pp 121−137.
(30) Knudson, C. B.; Knudson, W. *FASEB J.* **1993**, *7*, 1233−1241.
(31) Entwistle, J.; Hall, C. L.; Turley, E. A. *J. Cell Biochem.* **1996**, *61*, 569−577.
(32) Day, A. J. *Biochem. Soc. Trans.* **1999**, *27*, 115−121.
(33) Yeo, T. K.; Nagy, J. A.; Yeo, K. T.; Dvorak, H. F.; Toole, B. P. *Am. J. Pathol.* **1996**, *148*, 1733−1740.
(34) Knudson, W. *Am. J. Pathol.* **1996**, *148*, 1721−1726.
(35) Hall, C. L.; Yang, B. H.; Yang, X. W.; Zhang, S. W.; Turley, M.; Samuel, S.; Lange, L. A.; Wang, C.; Curpen, G. D.; Savani, R. C.; Greenberg, A. H.; Turley, E. A. *Cell* **1995**, *82*, 19−28.
(36) Nelson, R. M.; Venot, A.; Bevilacqua, M. P.; Linhardt, R. J.; Stamenkovic, I. *Annu. Rev. Cell Dev. Biol.* **1995**, *11*, 601−631.
(37) Rooney, P.; Kumar, S.; Ponting, J.; Wang, M. *Int. J. Cancer* **1995**, *60*, 632−636.
(38) Hua, Q.; Knudson, C. B.; Knudson, W. *J. Cell Sci.* **1993**, *106*, 365−375.
(39) Iida, N.; Bourguignon, L. Y.-W. *J. Cell. Physiol.* **1997**, *171*, 152−160.
(40) Bourguignon, L. Y.-W.; Zhu, H. B.; Chu, A.; Iida, N.; Zhang, L.; Hung, M. C. *J. Biol. Chem.* **1997**, *272*, 27913−27918.
(41) Culty, M.; Nguyen, H. A.; Underhill, C. B. *J. Cell Biol.* **1992**, *116*, 1055−1062.
(42) Culty, M.; Shizari, M.; Thompson, E. W.; Underhill, C. B. *J. Cell. Physiol.* **1994**, *160*, 275−286.
(43) Prestwich, G. D.; Marecak, D. M.; Marecek, J. F.; Vercruysse, K. P.; Ziebell, M. R. *J. Controlled Release* **1998**, 93−103.
(44) Lesley, J.; Kincade, P. W.; Hyman, R. *Eur. J. Immunol.* **1993**, *23*, 1902−1909.
(45) Li, C.; Yu, D.; Newman, R. A.; Cabral, F.; Stephens, L. C.; Hunter, N.; Milas, L.; Wallace, S. *Cancer Res.* **1998**, *58*, 2404−2409.
(46) Pouyani, T.; Prestwich, G. D. *Bioconjugate Chem.* **1994**, *5*, 339−347.
(47) Pouyani, T.; Prestwich, G. D. US Patent 5,616,568; Research Foundation of SUNY, USA, 1997.
(48) Kokoshka, J. M.; Ireland, C. M.; Barrows, L. R. *J. Natl. Prod.* **1996**, *59*, 1179−1182.
(49) Kreil, G. *Protein Sci.* **1995**, *4*, 1666−1669.
(50) Li, C.; Newman, R. A.; Wallace, S. *Sci. Med.* **1999**, 38−47.
(51) Collis, L.; Hall, C.; Lange, L.; Ziebell, M.; Prestwich, G.; Turley, E. *FEBS Lett.* **1998**, *440*, 444−449.
(52) Chow, G.; Knudson, C. B.; Homandberg, G.; Knudson, W. *J. Biol. Chem.* **1995**, *270*, 27734−27741.
(53) Lesley, J.; Hyman, R. *Eur. J. Immunol.* **1992**, *22*, 2719−2723.
(54) Lesley, J.; English, N.; Perschl, A.; Gregoroff, J.; Hyman, R. *J. Exp. Med.* **1995**, *182*, 431−437.
(55) Perschl, A.; Lesley, J.; English, N.; Trowbridge, I.; Hyman, R. *Eur. J. Immunol.* **1995**, *25*, 495−501.
(56) Asplund, T.; Heldin, P. *Cancer Res.* **1994**, *54*, 4516−4523.
(57) Nakabayashi, H.; Tsujii, H.; Okamoto, Y.; Nakano, H. *Int. Hepatol. Commun.* **1996**, *5*, 345−353.
(58) Gustafson, S.; Bjorkman, T. *Glycoconjugate J.* **1997**, *14*, 561−568.
(59) Samuelsson, C.; Gustafson, S. *Glycoconjugate J.* **1998**, *15*, 169−175.
(60) Gustafson, S.; Bjorkman, T.; Westlin, J. E. *Glycoconjugate J.* **1994**, *11*, 608−613.
(61) Gustafson, S. In *The Chemistry, Biology, and Medical Applications of Hyaluronan and its Derivatives*; Laurent, T. C., Balazs, E. A. Eds.; Portland Press: London, U.K., 1997.
(62) Ulbrich, K.; Konak, C.; Tuzar, Z.; Kopecek, J. *Makromol. Chem.* **1987**, *188*, 1261−1272.

BM000283N

Methods of Tissue Engineering
in press (2000).

Running title: Chemical Modification of Hyaluronic Acid

Chemical Modification of Hyaluronic Acid

Yi Luo*, Kelly R. Kirker†, Glenn D. Prestwich*

*Department of Medicinal Chemistry
30 South 2000 East, Room 201
and †Department of Bioengineering
20 South 2030 East, Room 506
The University of Utah
Salt Lake City, Utah 84112

Abstract

Hyaluronic acid (HA) is an abundant non-sulfated glycosaminoglycan component of synovial fluid and the extracellular matrix. A combination of unique physicochemical properties and biological functions suggest HA as an attractive building block for new biocompatible and biointeractive materials with applications in drug delivery, tissue engineering, and viscosupplementation. This chapter highlights the chemical modification of HA and medical applications of these HA-based biomaterials. Important new products have already reached the marketplace, the approval and introduction of an increasing number of medical devices and new drugs using HA-derived biomaterials can be anticipated in the next decade.

I. Introduction

Hyaluronic acid (hyaluronan, HA) is a naturally-occurring polysaccharide consisting of 200 to 10,000 repeating disaccharide units. It is composed of (β-1,4)-linked D-glucuronic acid and (β-1,3) *N*-acetyl-D-glucosamine (Figure 1), and has a molecular weight ranging from 1×10^5 to 5×10^6. HA is an abundant glycosaminoglycan (GAG) found in the extracellular matrix (ECM)

of all higher animals, and it is the only non-sulfated GAG. HA forms highly viscous aqueous solutions, and takes on an expanded random coil structure due to strong hydrogen bonding. The coiled structure of HA can trap approximately 1,000 times its weight in water. These characteristics give it unique physiochemical properties as well as distinctive biological functions [1]. HA has been implicated in the water homeostasis of tissues, in the regulation of permeability of other substances by steric exclusion phenomena, and in the lubrication of joints [2]. HA plays an important role in the structure and organization of the ECM, including the maintenance of extracellular space, the transport of ion solutes and nutrients, and the preservation of tissue hydration. HA concentrations increase whenever rapid tissue proliferation regeneration and repair occur.

HA also binds specifically to proteins in the ECM, on cell-surface receptors, and within the cell cytosol. These protein-ligand interactions are important in stabilizing the cartilage ECM [2,3], regulating cell adhesion and motility [4,5], mediating proliferation and differentiation [6] and the action of growth factors [7]. HA has also been implicated in morphogenesis and embryonic development [8], in cancer [9-15], in modulating inflammation [13], in stimulating angiogenesis and healing [16], and as a protective coating [17]. In most situations, HA signaling occurs *via* cell-surface receptors, such as CD44 and RHAMM, but cytosolic and nuclear proteins are also implicated in signaling.

The actions of HA appear to be related to molecular size. For example, high molecular weight HA inhibits angiogenesis, while low molecular weight HA stimulates angiogenesis [18]. At a molecular level, HA can act as a scavenger molecule for oxygen-derived toxic free radical species [18]. This unique suite of properties make HA an attractive building block for new biocompatible and biointeractive materials that have medical applications in drug delivery, tissue

engineering, and viscosupplementation [19]. This chapter highlights the chemistry and medical applications of these HA-based biomaterials.

In the past decade, approved uses for highly-purified HA have greatly increased in surgery, drug delivery, and cosmetics [20]. The unique rheological properties of high molecular weight HA ($> 1 \times 10^6$ Da) are exploited in clinical treatment of osteoarthritis [21,22] and in ophthalmic surgery. HA has shown beneficial properties in corneal transplantation, intraocular lens implantation, and the treatment of cataracts, vitro-retinal diseases, and tympanic membrane perforations. In addition, HA solutions have been investigated as space filling substances in laryngeal augmentation such as vocal fold injection, and are in clinical use for urinary incontinence in woman and in pediatric urology for the treatment of vesico-urethral reflux [23]. HA injections also facilitate nerve growth [24], and topical HA can improve wound healing. High levels of high molecular weight HA or of an HA/sucrose formulation can enhance the healing of wounds in collagen-containing tissues, including skin, bone, and mucosa with limited scarring [16,25]. In addition, HA is also used as an adjuvant for ophthalmic drug delivery [26], and can enhance the absorption of drugs and proteins *via* mucosal tissues [27-29]. The rapid skin permeability and epidermal retention of HA prolongs the pharmacokinetic half-life of topically-delivered drugs and growth factors [30].

However, the poor biomechanical properties of this soluble, natural polymer currently precludes many direct applications in medicine. Thus, to obtain more mechanically and chemically robust materials, it has become necessary to chemically modify natural HA. The resulting HA derivatives have physicochemical properties that are significantly different from the native polymer, but maintain the biocompatibility and biodegradability, as well as the potential pharmacological and therapeutic properties of HA itself. This chapter will explore the

chemical modification of HA (several architectures are shown in Figure 2) and the potential uses of these biomaterials in tissue engineering and drug delivery.

II. Chemical Modifications

A. Modification of the HA carboxyl group

1. Modification of HA by esterification

Fidia Advanced Biopolymers (Abano Terme, Padova, Italy) manufactures a number of HA-derivatized materials collectively called HYAFF® (R = alkyl group, Figure 1). The HYAFF® materials [31] are prepared by alkylation of the tetrabutylammonium salt of HA with an alkyl halide in DMF solution. At higher percentages of esterification, solubility in water is reduced. HYAFF® materials can be extruded to produce membranes and fibers, lyophilized to obtain sponges, or treated by spray-drying, extraction, and evaporation to produce microspheres. These polymers show good mechanical strength when dry, but the hydrated materials are less robust [32].

The biocompatibility and biodegradability of the HYAFF® materials have been studied extensively. The degree of esterification influences the size of hydrophobic patches, which produces a polymer chain network that is more rigid and stable, and less susceptible to enzymatic degradation [33,34]. Drug release from HYAFF®-based devices was examined for entrapped or covalently attached molecules. For example, release of the steroids hydrocortisone and α-methylpredisolone from microspheres fabricated from different HYAFF® materials was examined with the drug either dispersed or bound to the polymer. While the hydrocortisone diffused out of the microspheres in 10 min, the release rate of the covalently bound drug was found to show zero-order release requiring more than 100 h, consistent with ester-bond

hydrolysis [31,35]. Preclinical *in vivo* evaluations in a rabbit animal model demonstrated that an α-methylpredisolone carried by a HYAFF® 11 formulation could maintain its anti-inflammatory and chondroprotective properties [36] and increase the residence time of the drug in the tear fluid [37,38]. Microspheres and thin films of HYAFF® 11 have been found to be the most suitable physical forms for drug delivery systems.

Studies of macromolecule diffusion and release suggested a possible use of HYAFF® 11 microspheres for peptide delivery. Furthermore, the mucoadhesive properties of HYAFF® materials make realistic drug delivery *via* nasal, oral and vaginal mucosal routes, e.g., intranasal delivery of insulin in sheep [39], vaginal delivery of calcitonin in rats [40,41], and flu vaccine in rodents [42]. Microspheres could also deliver recombinant human granulocyte macrophage-colony stimulating factor (huGM-CSF) [43].

HA plays fundamental roles during embryonic development [44-46] and wound healing [47,48], suggesting a use for HA derivatives to create a suitable environment for the growth of cells derived from organ biopsies. In particular, stem elements or adults cells can be stimulated to divide and differentiate in this embryo-like environment [49,50]. HYAFF® products also have water and vapor transport properties similar to those of commercial products for wound coverage, such as Bioprocess®, Biobrane II® (a composite of polydimethylsiloxane on nylon fabric), and OpSite® (polyurethane dressing with an adhesive layer of vinyl ether applied to one side).

The cultivation of fibroblasts in ECM-like structures is receiving widespread attention not only because of the need to provide a dermal substitute to epithelial sheets, but also because these living constructs may be applied in other pathologies such as ligament/tendon repair, vascular prosthesis, and dermal augmentation. As expected, cultured human fibroblasts actively

proliferated in 30 days until the degradation of HYAFF® 11 non-woven mesh commenced, and morphological on paraffin-embedded specimens demonstrated that cells migrated through the non-woven mesh and populated both sides of the biomaterial. Furthermore, immunohistochemical analysis revealed the presence of collagen I, III, and fibronectin fibers which were evident after only 15 days of culture in the HYAFF® 11 scaffold, and allowed preparation of a living dermal equivalent [51]. *In vitro* studies of Laserskin® membranes, which are produced with regular laser-made microperforations from HYAFF® 11, showed that keratinocytes grew on these membranes and expressed a proliferative phenotype within the microperforations. The epithelial cells cultured on the membranes were able to differentiate, and after 15 days of standard culture, the formation of several distinct layers -- starting from a basal proliferative through an upper keratinized zone -- was observed [52-54]. A three-dimensional (3-D) artificial skin [55] was developed for the treatment of second- and third-degree burns, chronic wounds such as larger phlebopathic ulcers [52,56], and diabetic foot ulcers [57]. In clinical trials on extensive burns of humans, the underlying wound bed of this 3-D scaffold-treated area showed evidence of new collagen synthesis and organization into dermis-like structure. The wounds were completely healed seven weeks after burn excision with no unusual scarring [58].

In vitro culture of chondrocytes on a HYAFF® 11 non-woven was investigated in tissue-engineering procedures for cartilage reconstruction. One month after subcutaneous implantation of the scaffold seeded with human chondrocytes in an athymic nude mouse model, the development of tissue similar to hyaline cartilage was observed [59]. Moreover, pluripotent mesenchymal stem cells, which are capable of giving rise to several kinds of differentiated elements (myoblasts, chondroblasts, osteoblasts, adipocytes, fibroblasts), could be cultured

within a HYAFF® scaffold. The mesenchymal cells within the scaffold could be induced towards a chondrocyte phenotype with the addition of basic fibroblast growth factor (bFGF) [60-62]. Similarly, culture-expanded bone marrow-derived mesenchymal progenitor cells differentiate into chondrocytes or osteoblasts implanted subcutaneously *in vivo* in combination with a HYAFF® 11 sponge as well as when porous calcium phosphate ceramic is used as delivery vehicle. When coated with fibronectin, HYAFF® 11 sponge bound 130% more cells than coated ceramics, which indicates the HA-based delivery vehicles are superior to porous calcium ceramic. Additionally, the HA-based vehicles have the advantage of degradation/resorption characteristics that allow complete replacement of the implant with newly formed tissue [63].

2. Modification of HA with hydrazides, amines, and carbodiimides

The chemical modification of HA using its carboxylic functions, hydrazides, and carbodiimide compounds has been studied in great detail [64,65]. The modification of HA with hydrazides is performed in water at pH 4.75, with continuous addition of aqueous HCl to maintain the mild acidic pH. Although the carbodiimide reaction fails to give efficient coupling to amines, the high levels of *O*- to *N*-acyl migration gave *N*-acylureas with potentially important medical uses, as discussed below [66-68]. Alternatively, carbodiimide-mediated coupling to dihydrazide compounds such as adipic dihydrazide (ADH) provided an efficient and mild route to introduce multiple pendant hydrazide groups for further derivatization with drugs [69], for making biochemical probes [70], or for crosslinking [67,71]. For example, HA-Taxol® bioconjugates were synthesized by the conjugation of HA-ADH and ester activated Taxol®. The conjugate showed selective binding and uptake by human breast cancer cells, human ovarian cancer cells, and human colon tumor cells. Increased cytotoxicity required cellular uptake of the conjugate followed by hydrolytic release of the active free Taxol® [72,73]. Targeting can be

accomplished by receptor-mediated uptake of the HA-drug bioconjugate releasing the drug only inside the target cell, thereby enhancing selectivity for cancerous cells [72].

As indicated above, attempted carbodiimide-mediated coupling of primary amines to HA, to generate polymeric amides, resulted in negligible coupling due to the protonation of the required nucleophilic nitrogen at the reaction pH. Recently, a modified method for carbodiimide/active ester-mediated coupling of polyfunctional amines to HA was developed [74]. HA (Mw > 1 MDa) was reacted with 30-fold excess of the amine component at pH 6.8 in the presence of a soluble carbodiimide and 1-hydroxybenzotriazole (HOBt) with DMSO/H_2O (1:1) as solvent.

Many HA-drug bioconjugates have been prepared using the method of carbodiimide activation. HA-mitomycin C and HA-epirubicin conjugates were synthesized and found to enhance the selective delivery of the parent anti-tumor drugs into regional lymph nodes and cancerous tissues through HA receptor CD44 [75]. Mitomycin C was coupled to HA (1,200 kDa) through an amide bond in a DMF-water co-solvent with a water-soluble carbodiimide EDCI as the coupling agent. The HA-mitomycin C conjugate exhibited potent anti-metastatic effects against Lewis lung carcinoma xenograft at an extremely low dose (0.01 mg/kg) whereas free mitomycin C had no effect. Similarly, adriamycin was reported to couple to HA through an amide bond linkage [76]. Epirubicin was coupled to HA after the synthesis of acetylated HA in order to increase its solubility in organic solvents. Similarly, daunomycin, 5-fluorouracil and cytosine arabinoside have been coupled to HA. The same carbodiimide technology was applied to prepare HA-superoxide dismutase (HA-SOD) conjugate, which was synthesized by a water-soluble carbodiimide coupling of HA and bovine Cu/Zn-SOD or bacterial Mn-SOD at pH 4.8, 4 °C for 20 h. Some 20% of the amino groups on SOD were

conjugated to HA, and the HA-SOD conjugate exhibited a more pronounced anti-inflammatory effect than SOD or HA alone [77].

B. Modification of the HA hydroxyl groups

1. Modification of HA by sulfation

HA is an ideal hydrophilic coating for a variety of medical devices, including catheters, guide wires, and sensors. Various *in vitro* and *in vivo* tests have been conducted over the years by Biocoat Inc. (Fort Washington, PA) to demonstrate biocompatibility of the HA coating, Hydak™. However, in order to obtain the optimum blood compatible material when used in the body, approaches involving sulfating the OH group present in the HA molecule were devised.

The sulfation of HA (Mw 150-200 kDa) with sulfur trioxide pyridine complex in DMF produced different degrees of sulfation, HyalSx, x = 1 - 4 [78]. The sulfated hyaluronic acid $HyalS_{3.5}$ was then immobilized onto plasma-processed polyethylene (PE) using a diamine polyethylene glycol derivative and a water-soluble carbodiimide. The thrombin time test and platelet adhesion behavior indicated that this procedure was promising for the preparation of blood-compatible, anti-thrombotic PE surface [79,80]. In addition, the anti-coagulant polysaccharides was photoimmobilized on a poly (ethylene terephthalate) (PET) film [81]. Sulfated HA (HyalSx) was conjugated with azidoaniline in the presence of a water-soluble carbodiimide to prepare azidophenylamino-derivatized HyalSx. The derivative was dried on PET surface before UV irradiation. Micropatterning profile of the anti-coagulant polysaccharides was achieved using photolithography, and platelet adhesion was reduced on the sulfated hyaluronic acid areas. Surfaces coated with sulfated HA exhibited a marked reduction of cellular attachment, fouling, and bacterial growth compared with uncoated surfaces [82]. The coating

was stable to degradation by chondroitinase and hyaluronidase and acquired new anti-thrombogenic properties [83].

2. Other chemistries

Several other modifications have been accomplished using the hydroxyl groups in the HA molecule. Butyric acid, which is known to induce cell differentiation and to inhibit the growth of a variety of human tumors, was conjugated to HA [84] *via* the reaction between butyric anhydride and HA (Mw 85 kDa) *sym*-collidinium salt, in the presence of pyridine or dimethylamino pyridine with DMF as solvent at room temperature for 24 h. The results of cell culture on a human breast cancer cell-line (MCF-7) suggested that the conjugation of butyrate residue to HA led to an increased half-life of the active component. In addition, HA butyrate offered a novel drug-delivery system targeted specifically to tumor cells.

The anthracycline antibiotics adriamycin and daunomycin were coupled to HA *via* cyanogen bromide (CNBr) activation [76]. This reaction scheme is purported to lead to the attachment of the drug *via* a urethane bond to one of the hydroxylic functions of the polysaccharide, but no spectroscopic verification was provided.

A wider utilization of HA biomaterials can be envisaged if two obstacles can be overcome: enzymatic degradation and the poor mechanical properties. Approaches to solve the first problem are based on the formation of chemically-modified HA sols and hydrogels. Approaches to solve the second problem include the preparation of HA composite materials by grafting of other polymers or by formation of interpenetrating networks.

C. Modification of HA by hydrogel formation

HA can be readily degraded by tissue hyaluronidases and free radicals, which commonly occur during inflammation. A small number of breaks in the molecular structure can result in a profound decrease in its molecular size resulting in drastic alterations in viscosity. Currently, several crosslinking chemistries are being investigated to improve the stability of HA towards biodegradation.

1. Autocrosslinked polymer

Autocrosslinked polymer (ACP™, Fidia) consists of inter- and intra- molecularly esterified HA (200 kDa) in which both the carboxyl groups and hydroxyl groups belong to HA molecules. ACP is a white powder and upon hydration with water gives rise to a transparent gel [85]. This novel biomaterial has shown promising results for several applications. For example, it can be used as a barrier between organs to reduce postoperative adhesions after abdominal and gynecological surgery [86-88]. In addition, the biocompatible, biodegradable, porous ACP behaves as a scaffolding for reparative cells to regenerate and to integrate when it is placed in natural reparative tissue defects, such as osteochondral defects in a rabbit knee model [89]. Subcutaneous implantation of ACP porous sponges seeded with chondrocytes or osteoblasts were found to regenerate bone and cartilage [63,90].

2. HA crosslinked with diepoxide crosslinkers

Laurent and colleagues [91] crosslinked high concentration HA (average molecular mass 1.5 MDa, 50-175 mg/ml) in an alkaline environment with 1,2,3,4-diepoxybutane and sodium borohydride (50 °C, 2 h). Using similar chemistry, HA (average molecular mass 870 kDa) at high concentration was allowed to react with either ethyleneglycol diglycidylether

[92] or polyglycerol polyglycidylether [93] in 0.1 N NaOH at 60 °C with ethanol as a co-solvent. The gels obtained had a high water content (95%) despite the fact that high concentrations of crosslinker were used. This HA gel was specifically degraded *in vitro* and *in vivo* by hydroxyl radicals, and the inflammatory responsive degradation proceeded *via* surface erosion [94,95]. This HA gel has been investigated for use as inflammation (stimulus)-responsive degradable matrices and as an electrically-responsive and pulsatile release system [92] for implantable drug delivery. Hydrogels prepared by reaction of HA with 1,4-butanediol diglycidyl ether in the presence of 0.5% NaOH gave a porous material that was activated with periodate [96] and then modified with an 18-amino acid peptide containing a cell attachment domain, Arg-Gly-Asp (RGD) sequence. The presence of this peptide markedly enhanced cell attachment to the HA gels. Following cell attachment (MG63 cells (human osteosarcoma)), cells actively proliferated and colonized the pores of the matrix. This material may prove useful for the maintenance of cells as a scaffold for enhancing tissue repair, and could have clinical implications for wound healing therapies [97].

3. Photocrosslinking of HA

A methacrylate anhydride-modified HA (14% modification) was synthesized by the reaction between HA and excess methacrylate anhydride; this derivative was photocrosslinked to form a stable hydrogel using ethyl eosin 0.5% w/v in 1-vinyl-2-pyrrolidone and triethanolamine as an initiator under argon ion laser with wavelength of 514 nm. The use of *in situ* photopolymerization of an HA derivative resulting in the formation of a cohesive gel enveloping the injured tissue may provide isolation from surrounding organs and thus prevent the formation of adhesions [98]. A preliminary cell encapsulation study was also successfully performed with islet of Langerhans.

4. HA crosslinked by glutaraldehyde

HA strands fabricated from the cation-exchanged sodium hyaluronate (Mw 1.6 MDa) were crosslinked in glutaraldehyde aqueous solution [99]. Afterwards, the strand surfaces were remodeled by the absorption of poly-D-lysine and poly-L-lysine. The polypeptide-resurfaced HA strands have good biocompatibility and positive advantages for cellular adhesion.

5. HA crosslinked by trivalent iron

Intergel® (FeHA, formerly Lubricoat) is a formulation of HA electrostatically crosslinked with trivalent iron. This gel is intended for post-surgical applications to prevent adhesions [100].

6. HA crosslinked with carbodiimide chemistry

Incert®, under development by Anika Therapeutics, Inc. (Woburn, MA), is a bioresorbable sponge derived from crosslinked HA with a biscarbodiimide-coupling agent in the presence of isopropanol/H_2O as co-solvent [19]. It adheres to tissues without the need for sutures and retains its efficacy even in the presence of blood. Recently, it was found to be effective at preventing postoperative adhesions in a rabbit cecal abrasion study. In addition, Ossigel®, which incorporates with bFGF, was examined for acceleration of fracture healing.

Building on the hydrazide modification described above, hydrogels have been prepared using bishydrazide, trishydrazide, or polyvalent hydrazide compounds as crosslinkers [71]. HA (average molecular weight 1.5-2.0 MDa) would react with the hydrazide crosslinkers in the presence of a water-soluble carbodiimide at pH 3.5 - 4.7. Depending on the reaction conditions and the molar ratios of the reagents involved, gels with physicochemical properties ranging from soft-pourable gels to more mechanically-rigid and brittle gels could be obtained. Applications of this chemistry are in development by Clear Solutions Biotech, Inc. (Stony Brook, NY).

HA-ADH can be crosslinked using commercially-available homobifunctional crosslinkers [67]. HA-ADH was dissolved in 0.1 M $NaHCO_3$ to give a concentration of 15 mg/ml and the crosslinker was added in solid form. Gelation was observed within 30 - 90 sec. After washing with water, the gels appeared clear and colorless.

Recently, an *in situ* polymerization technique was developed by crosslinking HA-ADH with a macromolecular crosslinker, PEG-dialdehyde under physiological conditions (Y. Luo, K.R. Kirker and G.D. Prestwich, unpublished results). Biocompatible and biodegradable HA hydrogel films with well-defined mechanical strength were obtained after the evaporation of solvent. Drug release from these HA hydrogel films was investigated, and preliminary data with the HA films showed accelerated re-epithelialization during wound healing.

A low-water content HA hydrogel film [101] was made by crosslinking HA (1.6 MDa) film with a water-soluble carbodiimide as a coupling agent in H_2O containing a water-miscible non-solvent of HA, e.g., ethanol or acetone. The highest degree of crosslinking that gave a low-water content hydrogel was achieved in 80% ethanol. This film, having 60% water content, remained stable for two weeks after immersion in buffered solution. The crosslinking of HA films with a water-soluble carbodiimide in the presence of L-lysine methyl ester prolonged the *in vivo* degradation of HA film. The higher resistance to hydrolytic degradation might be attributable to amide bonds in contrast to those crosslinked through ester bonds.

7. Hylans

Hylan is a hydrogel formed by crosslinking HA containing residual protein with formaldehyde (soluble gel) or divinyl sulfone [102]. In an alkaline environment at 20 °C (10 – 15 min), the divinyl sulfone reagent is believed to react with hydroxyl groups of HA, forming crosslinks. Similar crosslinking was obtained by using dimethylolurea, ethylene oxide,

and polyisocyanate reagents. Soluble hylan is a high Mw form (8 - 23 MDa) of HA (5 - 6 MDa) that exhibits enhanced rheological properties compared to HA. Hylan gel is an insoluble form that has greater elasticity (at all frequencies) and viscosity (at low shear rates) than soluble hylan and retains the high biocompatibility of the native macromolecule (non-immunogenic, non-inflammatory, and non-toxic). The hylans are produced by Biomatrix, now owned by Genzyme (Cambridge, MA).

Hylan exhibits biocompatibility identical to that of native HA and has been investigated in a number of medical applications. In the treatment of degenerative joint disease and rheumatoid arthritis, hylan was found to protect cartilage and prevent further chondrocyte injury. However, the effect was found to be reversible and viscosity-dependent [103]. The hylan product Synvisc® has been developed specifically as a device for viscosupplementation therapy in osteroarthritis of the knee. It can increase the viscoelastic properties of the synovial fluid and the intercellular matrix of the synovial tissue and capsule [104] [105].

Results from the clinical trials of hylan B gel slurry injections (Hylaform® gel) suggested that it provides a safe, effective alternative for soft tissue augmentation [106-108]. Additionally, the injection of viscoelastic hylan B gel gave a durable augmentation of the soft tissues in the vocal fold in a rabbit model [109]. The gel can remain in place for 12 months, allowing the in-growth of newly formed connective tissue after only one month. The new soft tissue contained collagen, HA, fibroblasts, and a few new vessels, without causing inflammation and adverse reactions. Finally, hylan has been used in plastic surgery for intradermal implantations and cosmetic injection [110]. Similarly, Restylane (Q-Med Inc., Sweden), a partially-crosslinked HA derivative, has been available for soft tissue augmentation in Europe for more than four years [108]. However, neither Restylane nor hylan gel are currently approved by the FDA.

Hylagel is an engineered hylan gel being investigated as an adjuvant to prevent post-surgical adhesions. Finally, hylans can be used as drug carriers by the incorporation of therapeutic agents. For example, the *in vitro* biological activity of cytokine α-interferon was enhanced by approximately 40% as a result of its covalent attachment to hylan matrix [111].

8. Multiple component crosslinking of HA

Another way to prepare hyaluronan-based networks is based on Passerini reaction and Ugi reaction [112]. In the Passerini reaction, an aqueous solution of hyaluronan is mixed with aqueous glutaraldehyde (or other water-soluble dialdehyde) and added to a known amount of cyclohexylisocyanide. In the Ugi four-component reactions, the mixture above also contains a diamine. The degree of crosslinking is controlled by the amount of dialdehyde and diamine. Passerini reactions are kinetically faster and give good yields of a single condensation product. The ensuing hydrogels are transparent, mechanically stable, swell in aqueous salt solutions depending on ion strength, and exhibit values of the compression modulus markedly dependent on the degree of crosslinking.

D. Composites

Synthetic polymers have been prepared as biomedical devices, and different physicochemical and mechanical properties are required for a given application. Synthetic polymers often have optimized mechanical properties but suffer from insufficient biocompatibility. In contrast, biocompatible biopolymers often have suboptimal mechanical properties. Blending synthetic polymers with biological macromolecules can yield composite materials that feature the desired properties of the individual polymers. Specifically, HA has been blended with other materials in order to produce novel biomaterials with the desired

physicochemical, mechanical, and biocompatible properties. Two different synthetic polymers, poly(vinyl alcohol) (PVA) and poly(acrylic acid) (PAA) were blended with either collagen or HA [113]. HA/PAA sponges were prepared by dissolving both polymers in water at different ratios, lyophilizing, and crosslinking them by thermal treatment at 130 °C under vacuum for 24 h. HA/PVA hydrogels were prepared by dissolving both polymers in water at different ratios and subjecting these mixtures to eight cycles of freeze-thawing.

1. HA/liposome composites

HA has been incorporated into liposomes. For example, HA was combined with cyclosporin A and encapsulated within phospholipid liposomes [114]. HA (Mw 10 kDa and 1,000 kDa) powder was added into and hydrated with CsA/liposomes to provide a final solution concentration of 2.5 wt% HA. The solution was developed as a topically administered pharmaceutical agent, and was found to effectively treat skin disorders while minimizing systemic circulation. These compositions can also be administered orally, parenterally, and intrarectally.

Bioadhesive liposomes, in which HA is the surface-anchored bioadhesive ligand on a liposome surface, were prepared by the preactivation of HA with a carbodiimide and then added to a suspension of multi-lamellar liposomes consisting of phosphatidylcholine, phosphatidylethanolamine, and cholesterol [115]. In principle, an HA-coated liposome functionally resembles the PEG-coated "stealth" liposomes. These were investigated for their ability to act as site-adherent and sustained-release carriers of epidermal growth factor for the topical therapy of wounds and burns [116].

2. HA-gelatin composites

A porous matrix composed of gelatin and HA was prepared by dipping a gelatin-HA water-soluble sponge into 90% (w/v) acetone/water mixture with a small amount of a carbodiimide (EDCI) as crosslinking agent [117]. This sponge-type biomaterial was constructed for either wound dressings or scaffolds for tissue engineering. The silver sulfadiazine-impregnated sponge was found to facilitate the epidermal healing rate in a rat model.

3. HA-alginate composites

The association of alginate with another polysaccharide has been proposed in order to combine alginate's gel-forming effects with the properties of the partner macromolecule. Alginate-HA gels were prepared through the diffusion of calcium into alginate-HA mixtures. The resulting gels with an alginate: HA weight ratio up to 0.50 had satisfactory mechanical properties. This composite matrix might be suitable as a biopolymeric carrier, or for articular surgery applications, due to its stability in synovial fluid [118,119].

4. HA-collagen composite

Composite materials consisting of HA and collagen have been prepared by complexing both components into a coagulate followed by crosslinking using either glyoxal or starch dialdehyde as the crosslinking agents [120]. Atelocollagen was suspended in 0.5 M acetic acid and the addition of an HA solution resulted in formation of coagulated material. The fabricated membrane was then chemically crosslinked with starch dialdehyde and glyoxal by immersing the membrane into a solution of this crosslinker. This was quite resistant to collagenase and permitted fibroblast growth. Other composite materials consisting of HA and collagen were

prepared by crosslinking the dried HA/collagen coagulates with polyethylene oxide and hexamethylene diisocyanate [121].

In addition, a hydroxyapatite-collagen-HA composite material was prepared by adding hydroxyapatite particles to an HA solution followed by blending with an aqueous dispersion of collagen fibers [122]. The final material consisted of 90% hydroxyapatite, 9.2% collagen, and 0.8% HA (w/w), was biocompatible, mechanically robust, and can be used as a bone defect filler. Recently, a porous collagen-HA matrix was prepared by crosslinking collagen with HA-aldehyde made from the periodate oxidation of HA [123]. The presence of HA within collagen matrix supported new bone formation, and this collagen-HA matrix has potential uses for the delivery of growth factors or as an implantable cell-seeded matrix.

High concentrations of HA (1 mg/ml) in cell culture medium not only inhibits fibroblast contraction of a floating collagen fibrillar matrix (CFM), but also stimulates fibroblast migration on the CFM [52]. HA incorporation in to an artificial skin material (collagen-gelatin sponge) accelerates the ingrowth of granulation tissue, thus providing a more suitable graft bed to support a skin graft [124]. Further investigation of HA covalently-bound to a collagen matrix found significantly reduced collagen contraction in fibroblast cultures. Such results warrant consideration of HA as an alternative biomaterial for building a dermal substitute and tissue engineering scaffold [125].

5. HA-carboxymethylcellulose composites

A bioabsorbable membrane, Seprafilm®, has been developed as a physical barrier for prevention of post-surgical adhesions. Genzyme scientists prepared this material by blending two anionic polymers, HA and carboxymethylcellulose (CMC) [126], followed by carbodiimide-mediated modification. An anionic-cationic crosslinked network produces a rather

fragile biomaterial. Seprafilm® was approved in 1996 and is FDA-approved for use in patients undergoing abdominal or pelvic laparotomy in order to reduce the incidence, extent and severity of postoperative adhesion [127]. The use of Seprafilm® is limited to accessible areas that can be fully covered. Since the location of many adhesions are unpredictable or inaccessible, the general clinical utility of Seprafilm® is compromised. In addition, Seprafilm® is reported to suffer from handling difficulties, hampering its acceptance by surgeons. The same technology has been expanded to reduce the development of adhesions to synthetic non-absorbable mesh, such as hernia repair products. Sepramesh is a composite of polypropylene mesh and a foam form of the Seprafilm® membrane. This composite reduces the development of adhesions to the surface of the hernia repair mesh without compromising the long-term abdominal wall incorporation into the mesh [128]. Similar technology has also been used in pre-surgical coating, which would theoretically limit tissue trauma and prevent desiccation during surgery. However, a Genzyme-conducted clinical trial of Sepracoat®, an HA/CMC solution applied pre-surgical manipulation, failed to meet efficacy endpoints.

6. HA-grafted copolymers

A variety of HA-grafted copolymers have been prepared in recent years. In one example, several polyampholyte comb-type copolymers consisting of poly(L-lysine) (PLL) main chains, a DNA binding site, and an HA side-chain with cell-specific ligands were prepared to target sinusoidal endothelial cells of liver [129]. The reducing end of HA and ε–amino groups of PLL were covalently coupled by reductive amination using sodium cyanoborohydride to obtain the resulting comb-type copolymers (PLL-*graft*-HA). The PLL backbone selectively formed the polyion complex with DNA even in the presence of the HA side-chain. In addition, the PLL-*graft*-HA-DNA complex may form a multiphase structure in which the hydrophobic

PLL-DNA complex was surrounded by a hydrated shell of free HA. Complex formation with free HA chains was considered to be essential for directing the complex to target cells.

A PEG-grafted-HA copolymer was prepared by coupling HA with methoxy-PEG-hydrazide in the presence of EDCI as a coupling agent at acidic pH [130]. The copolymer is expected to be used for the delivery of water-soluble peptides. For example, when loaded with insulin, the loaded insulin appeared to partition into PEG moieties and intermolecular interactions preventing the conformational changes of insulin. This appears to be a reasonable method to prevent drug leakage and to achieve degradation-controlled insulin release. Moreover, such a heterogeneous-structured polymeric solution may be useful as an injectable therapeutic formulation for ophthalmic or arthritis treatment with a suitable drug.

III. Conclusion

HA is an important starting material for preparation of new biocompatible and biodegradable polymers that have applications in drug delivery, tissue engineering, and visocosupplementation. HA derivatives containing a variety of versatile functional groups can be produced with varying chemical structures and morphology. In this way, the rate of degradation, the degree of hydration, the cellular responses, and the overall tissue response can be manipulated. Approval and introduction of an increasing number of medical devices and new drugs using HA-derived biomaterials can be anticipated in the next decade.

IV. Acknowledgement

We thank The University of Utah (UUtah), Clear Solutions Biotech, Inc. (Stony Brook, NY), the Department of Defense, and the Center for Biopolymers at Interfaces (UUtah) for financial support of research developed in our laboratories.

Figure Legends

Figure 1. Tetrasaccharide fragment of HA showing the disaccharide repeat units (R = H)

Figure 2. Schematic structure of HA derivatives. (**a**) HA-liposome composite; (**b**) HA-grafted copolymer; (**c**) HA-drug bioconjugate; (d) crosslinked HA

References

1. Laurent, T. C., Laurent, U. B. G., & Fraser, J. R. E. (1995). Functions of hyaluronan. *Ann. Rheum. Dis.* ***54***, 429-432.

2. Fraser, J. R. E., Laurent, T. C., & Laurent, U. B. G. (1997). Hyaluronan: Its nature, distribution, functions and turnover. *J. Intern. Med.* ***242***, 27-33.

3. Dowthwaite, G. P., Edwards, J. C. W., & Pitsillides, A. A. (1998). An essential role for the interaction between hyaluronan and hyaluronan binding proteins during joint development. *J. Histochem. Cytochem.* ***46***, 641-651.

4. Hardwick, C., Hoare, K., Owens, R., Hohn, H. P., Hook, M., Moore, D., Cripps, V., Austen, L., Nance, D. M., & Turley, E. A. (1992). Molecular cloning of a novel hyaluronan receptor that mediates tumor cell motility. *J. Cell Biol.* ***117***, 1343-1350.

5. Collis, L., Hall, C., Lange, L., Ziebell, M. R., Prestwich, G. D., & Turley, E. A. (1998). Rapid hyaluronan uptake is associated with enhanced motility: implications for an intracellular mode of action. *FEBS Lett.* ***440***, 444-449.

6. Entwistle, J., Hall, C. L., & Turley, E. A. (1996). Receptors: regulators of signalling to the cytoskeleton. *J. Cell Biochem.* ***61***, 569-577.

7. Cheung, W. F., Cruz, T. F., & Turley, E. A. (1999). Receptor for hyaluronan-mediated motility (RHAMM), a hyaladherin that regulates cell responses to growth factors. *Biochem. Soc. Trans.* ***27***, 135-142.

8. Toole, B. P. (1997). Hyaluronan in morphogenesis. *J. Intern. Med.* ***242***, 35-40.

9. Gotoda, T., Matsumura, Y., Kondo, H., Saitoh, D., Shimada, Y., Kosuge, T., Kanai, Y., & Kakizoe, T. (1998). Expression of CD44 variants and its association with survival in pancreatic cancer. *Jpn. J. Cancer Res.* ***89***, 1033-1040.

10. Herrlich, P., Sleeman, J., Wainwright, D., Konig, H., Sharman, L., Hilberg, F., & Ponta, H. (1998). How tumor cells make use of CD44. *Cell Adhes. Commun.* ***6***, 141-147.

11. Baumgartner, G., Boltzman, L., & Hamilton, G. (1998). The impact of extracellular matrix on chemoresistance of solid tumors - experimental and clinical results of hyaluronidase as additive to cytostatic chemotherapy - Symposium on novel aspects in chemoresistance, Vienna, 20th March 1998 - Editorial. *Cancer Lett.* ***131***, 1-2.

12. Baumgartner, G., Gomar-Hoss, C., Sakr, L., Ulsperger, E., & Wogritsch, C. (1998). The impact of extracellular matrix on the chemoresistance of solid tumors - experimental and clinical results of hyaluronidase as additive to cytostatic chemotherapy. *Cancer Lett.* ***131***, 85-99.

13. Gerdin, B., & Hallgren, R. (1997). Dynamic role of hyaluronan (HYA) in connective tissue activation and inflammation. *J. Intern. Med.* ***242***, 49-55.

14. Delpech, B., Girard, N., Bertrand, P., Courel, M. N., Chauzy, C., & Delpech, A. (1997). Hyaluronan: Fundamental principles and applications in cancer. *J. Intern. Med.* ***242***, 41-48.

15. Hall, C. L., Yang, B. H., Yang, X. W., Zhang, S. W., Turley, M., Samuel, S., Lange, L. A., Wang, C., Curpen, G. D., Savani, R. C., Greenberg, A. H., & Turley, E. A. (1995). Overexpression of the hyaluronan receptor RHAMM is transforming and is also required for H-ras transformation. *Cell* ***82***, 19-28.

16. Boyce, D. E., Thomas, J. H., Moore, K., & Harding, K. (1997). Hyaluronic acid induces tumour necrosis factor-α production by human macrophages *in vitro*. *British J. Plastic Surgery* ***50***, 362-368.

17. Partsch, G., Ch., S., Neumuller, J., Dunky, A., Petera, P., Broll, H., Ittner, G., & Jantsch, S. (1989). Modulation of the migration and chemotaxis of PMN cells by hyaluronic acid. *Zeitsch. Rheum.* ***48***, 123-8.

18. Chen, W. Y. J., & Abatangelo, G. (1999). Functions of hyaluronan in wound repair. *Wound Rep. Regen.* ***7***, 79-89.

19. Vercruysse, K. P., & Prestwich, G. D. (1998). Hyaluronate derivatives in drug delivery. *Crit. Rev. Therapeut. Carrier Syst.* ***15***, 513-555.

20. Sutherland, I. W. (1998). Novel established applications of microbial polysaccharides,. *Trends Biotechnol.* ***16***, 41-46.

21. Pasquali, R. I., Guerra, D., Taparelli, F., Georgountoz, A., & Frizziero, L. In *New Frontiers in Medical Sciences: Redefining Hyaluronan*; Abbazia di Praglia, Padua, Italy, 1999; pp N28.

22. Punzi, L., Pianon, M., Schiavon, F., & Todesco, S. In *New Frontiers in Medical Sciences: Redefining Hyaluronan*; Abbazia di Praglia, Padua, Italy, 1999; pp N32.

23. Hallen, L., Johansson, C., Dahlqvist, A., & Laurent, C. In *New Frontiers in Medical Sciences: Redefining Hyaluronan*; Abbazia di Praglia, Padua, Italy, 1999; pp N22.

24. Seckel, B. R., Jones, D., Hekimian, K. J., Wang, K. K., Chakalis, D. P., & Costas, P. D. (1995). Hyaluronic acid through a new injectable nerve guide delivery system enhances peripheral nerve regeneration in the rat. *J. Neurosci. Res.* ***40***, 318-324.

25. Jorgensen, T., Moss, J., Nicolajsen, H. V., & L.S., N. In *PCT Int Appl WO 9822114A1*; 1998; pp .

26. Saettone, M. F., Monti, D., Torracca, M. T., & Chetoni, P. (1994). Mucoadhesive ophthalmic vehicles: Evaluation of polymeric low-viscosity formulations. *J. Ocular Pharm.* ***10***, 83-92.

27. Morimoto, K., Yamaguchi, H., Iwakura, Y., Morisaka, K., Ohashi, Y., & Nakai, Y. (1991). Effects of viscous hyaluronate-sodium solutions on the nasal absorption of vasopressin and an analogue. *Pharm. Res.* ***8***, 471-474.

28. Miller, J. A., Ferguson, R. L., Powers, D. L., Burns, J. W., & Shalaby, S. W. (1997). Efficacy of hyaluronic acid/nonsteroidal anti-inflammatory drug systems in preventing postsurgical tendon adhesions. *J. Biomed. Mater. Res. (Appl. Biomater.)* ***38***, 25-33.

29. Gowland, G., Moore, A. R., Willis, D., & Willoughby, D. A. (1996). Marked enhanced efficacy of cyclosporin when combined with hyaluronic acid. Evidence from two T cell-mediated models. *Clin. Drug Invest.* ***11***, 245-250.

30. Brown, T. J., Alcorn, D., & Fraser, J. R. E. (1999). Absorption of hyaluronan applied to the surface of intact skin. *J. Invest. Dermatol.* ***113***, 740-746.

31. Benedetti, L. M., Topp, E. M., & Stella, V. J. (1990). Microspheres of hyaluronic acid esters -- fabrication methods and *in vitro* hydrocortisone release. *J. Controlled Rel.* ***13***, 33-41.

32. Iannace, S., Ambrosio, L., Nicolais, L., Rastrelli, A., & Pastorello, A. (1992). Thermomechanical properties of hyaluronic acid-derived products. *J Mater. Sci.: Mater. Med.* ***3***, 59-64.

33. Campoccia, D., Hunt, J. A., Doherty, P. J., Zhong, S. P., Oregan, M., Benedetti, L., & Williams, D. F. (1996). Quantitative assessment of the tissue response to films of hyaluronan derivatives. *Biomaterials* ***17***, 963-975.

34. Benedetti, L., Cortivo, R., Berti, T., Berti, A., Pea, F., Mazzo, M., Moras, M., & Abatangelo, G. (1993). Biocompatibility and biodegradation of different hyaluronan derivatives (HYAFF) implanted in rats. *Biomaterials* ***14***, 1154-1160.

35. Benedetti, L. M., Joshi, H. N., Goei, L., Hunt, J. A., Callegaro, L., Stella, V. J., & Topp, E. M. (1991). Dosage forms from polymeric prodrugs: hydrocortisone esters of hyaluronic acid. *New Polymeric Mater.* ***3***, 41-48.

36. Drobnik, J. (1991). Hyaluronan in drug delivery. *Adv. Drug Delivery Res.* ***7***, 295-308.

37. Hume, L. R., Lee, H. K., Benedetti, L., Sanzgiri, Y. D., Topp, E. M., & Stella, V. J. (1994). Ocular sustained delivery of prednisolone using hyaluronic acid benzyl ester films. *Int. J. Pharm.* ***111***, 295-298.

38. Kyyronen, K., Hume, L., Benedetti, L., Urtti, A., Topp, E., & Stella, V. (1992). Methyl-prednisolone esters of hyaluronic acid in opthalmic drug delivery. *Int. J Pharm.* ***80***, 161-169.

39. Illum, L., Farraj, N. F., Fisher, A. N., Gill, I., Miglietta, M., & Benedetti, L. M. (1994). Hyaluronic acid ester microspheres as a nasal delivery system for insulin. *J. Controlled Rel.* ***29***, 133-141.

40. Richardson, J. L., Ramires, P. A., Miglietta, M. R., Rochira, M., Bacelle, L., Callegaro, L., & Benedetti, L. (1995). Novel vaginal delivery systems for calcitonin .1. evaluation of HYAFF calcitonin microspheres in rats. *Int. J. Pharm.* ***115***, 9-15.

41. Bonucci, E., Ballanti, P., Ramires, P. A., Richardson, J., & L., B. (1995). Prevention of ovariectomy osteopenia to rats after vaginal administration of HYAFF 11 microspheres containing calcitonin. *Calcif. Tissue Int.* ***56***, 274-279.

42. Singh, M., Briones, M., & O'Hagan, D. In *New Frontiers in Medical Sciences: Redefining Hyaluronan*; Abbazia di Praglia, Padua, Italy, 1999; pp N34.

43. Nightlinger, N. S., Benedetti, L., Soranzo, C., Pettit, D. K., Pankey, S. C., & Gombotz, W. R. In *Proceed. Intern. Symp. Control. Rel. Bioact. Mater.*; Controlled Release Society Inc., Deerfield, USA: Seattle, Washington, USA, 1995; pp 738-739.

44. Rooney, P., & Kumar, S. (1993). Inverse relationship between hyaluronan and collagens in development and angiogenesis. *Differentiation **54***, 1-9.

45. Wheatley, S. C., Isacke, C. M., & Crossley, P. H. (1993). Restricted expression of the hyaluronan receptor, CD44, during postimplantation mouse embryogenesis suggests key roles in tissue formation and patterning. *Development **119***, 295-306.

46. Peterson, P. E., Pow, C. S. T., Wilson, D. B., & Hendrickx, A. G. (1993). Distribution of extracellular matrix components during early embryonic development in the macaque. *Acta Anat. **146***, 3-13.

47. Knudson, C. B., & Knudson, W. (1993). Hyaluronan-Binding proteins in development, tissue homeostasis, and disease. *FASEB J. **7***, 1233-1241.

48. Siebert, J. W., Burd, A. R., MaCarthy, J. G., Weinzweig, J., & Ehrlich, H. P. (1990). Fetal wound healing: a biochemical study of scarless healing. *Plast. Reconstr. Surg. **85***, 495-502.

49. Cortivo, R., De Galateo, A., Castellani, I., Brun, P., Giro, M. G., & Abatangelo, G. (1990). Hyaluronic acid promotes chick embryo fibroblast and chondroblast expression. *Cell Biol. Int. Rep. **14***, 111-122.

50. Shepard, S., Becker, H., & Hartmann, J. X. (1996). Using hyaluronic acid to create a fetal-like environment *in vitro*. *Ann. Plast. Surg. **36***, 65-69.

51. Denizot, F., & Lang, R. (1986). Rapid colorimetric assay for cell growth and survival. *J. Immunol. Meth.* ***89***, 271-277.

52. Pianigiani, E., Andreassi, A., Taddeucci, P., Alessandrini, C., Fimiani, M., & Andreassi, L. (1999). A new model for studying differentiation and growth of epidermal cultures on hyaluronan-based carrier. *Biomaterials* ***20***, 1689-1694.

53. Burn, P., Cortivo, R., Zavan, B., Vecchiato, N., & Abatangelo, G. (1999). In vitro reconstructed tissues on hyaluronan-based temporary scaffolding. *J. Mater.Sci., Mater. Med.* ***10***, 683-688.

54. Andreassi, L., Casini, L., Trabucchi, E., Diamantini, S., Rastrelli, A., & Donati., L. (1991). Human keratinocytes cultured on membranes composed of benzyl ester of hyaluronic acid suitable for grafting. *Wounds* ***3***, 116-126.

55. Soranzo, C., Abaatangelo, G., & Callegaro, L. In *PCT Int Appl WO 9633750*; 1996; pp .

56. Zacchi, V., Soranzo, C., Cortivo, R., Radice, M., Brun, P., & Abatangelo, G. (1998). *In vitro* engineering of human skin-like tissue. *J. Biomed. Mater. Res.* ***40***, 187-194.

57. Caravaggi, C., Faglia, E., L.D., P., De Giglio, R., Cavaiani, P., Mantero, M., Gino, M., Quarantiello, A., Sommariva, E., & Pritelli, C. In *New Frontiers in Medical Sciences: Redefining Hyaluronan*; Abbazia di Praglia, Padua, Italy, 1999; pp N9.

58. Harris, P. A., Francesco, F., Barisono, D., Leigh, I. M., & Navsaria, H. A. (1999). Use of hyaluronic acid and cultured autologous keratinocytes and fibroblasts in extensive burns. *The Lancets* ***353***, 35-36.

59. Aigner, J., Tegeler, J. A., Hutzler, P., Campoccia, D., Pavesio, A., C., H., E., K., & Naumann, A. (1998). Cartilage tissue engineering with novel nonwoven structured biomaterial based on hyaluronic acid benzyl ester. *J. Biomed. Mater. Res.* ***42***, 172-181.

60. Radice, M., Burn, P., Cortivo, R., Scapinelli, R., Battaliard, C., & Abatangelo, G. (2000). Hyaluronan-based biopolymers as delivery vehicles for bone-marrow-derived mesenchymal progenitors. *J. Biomed. Mater. Res.* ***50***, 101-109.

61. Wakitani, S., Goto, T., Pineda, S. J., Young, R. G., Mansour, J. M., Caplan, A. I., & Goldeberg, V. M. (1994). Mesenchymal cell-based repair of large, full-thickness defects of articular cartilage. *J. Bone Jt. Surg.* ***76-A(4)***, 579-592.

62. Butnariu-Ephrat, M., Robinson, D., Mendes, D. G., Halperin, N., & Nevo, Z. (1996). Resurfacing of goat articular cartilage by chondrocytes derived from bone marrow. *Clin. Orthop. Relat. Res.* ***330***, 234-243.

63. Solchaga, L. A., Goldberg, V. M., & Caplan, A. I. In *New Frontiers in Medical Sciences: Redefining Hyaluronan*; Abbazia di Praglia, Padua, Italy, 1999; pp N55.

64. Prestwich, G. D., D.M., M., Marecek, J. F., Vercruysse, K. P., & Ziebell, M. R. (1997). Controlled chemical modification of hyaluronic acid: synthesis, applications and biodegradation of hydrazide derivatives. *J. Controlled Release* ***53***, 99.

65. Kuo, J.-w., Swann, D. A., & Prestwich, G. D. In U.S. Patent 5,356,883, 1994; pp .

66. Kuo, J.-w., Swann, D. A., & Prestwich, G. D. (1991). Chemical Modification of Hyaluronic Acid by Carbodiimides. *Bioconjugate Chem.* ***2***, 232-241.

67. Pouyani, T., Harbison, G. S., & Prestwich, G. D. (1994). Novel hydrogels of hyaluronic acid: Synthesis, surface morphology, and solid-state NMR. *J. Am. Chem. Soc.* ***116***, 7515-7522.

68. Pouyani, T., Kuo, J.-w., Harbison, G. S., & Prestwich, G. D. (1992). Solid-state NMR of *N*-acylureas derived from the reaction of hyaluronic acid with isotopically-labeled carbodiimides. *J. Am. Chem. Soc.* ***114***, 5972-5976.

69. Pouyani, T., & Prestwich, G. D. (1994). Functionalized derivatives of hyaluronic acid oligosaccharides: drug carriers and novel biomaterials. *Bioconjugate Chem.* ***5***, 339-347.

70. Pouyani, T., & Prestwich, G. D. (1994). Biotinylated hyaluronic acid: A new tool for probing hyaluronate-receptor interactions. *Bioconjugate Chemistry* ***5***, 370-372.

71. Vercruysse, K. P., Marecak, D. M., Marecek, J. F., & Prestwich, G. D. (1997). Synthesis and *in vitro* degradation of new polyvalent hydrazide cross-linked hydrogels of hyaluronic acid. *Bioconjugate Chemistry* ***8***, 686-694.

72. Luo, Y., & Prestwich, G. D. (1999). Synthesis and selective cytotoxicity of a hyaluronic acid-antitumor bioconjugate. *Bioconjugate Chem.* ***10***, 755-763.

73. Luo, Y., Ziebell, M. R., & Prestwich, G. D. A hyaluronic acid-Taxol antitumor bioconjugate targeted to cancer cells. *Biomacromolecules* ***in press***,

74. Bulpitt, P., & Aeschlimann, D. (1999). New strategy for chemical modification of hyaluronic acid: preparation of functionalized derivatives and their use in the formation of bovel biocompatible hydrogels. *J. Biomed. Mater. Res.* ***47***, 152-169.

75. Akima, K., Ito, H., Iwata, Y., Matsuo, K., Watari, N., Yanagi, M., Hagi, H., Oshima, K., Yagita, A., Atomi, Y., & Tatekawa, I. (1996). Evaluation of antitumor activities of hyaluronate binding antitumor drugs: synthesis, characterization and antitumor activity. *J. Drug Targeting* ***4***, 1.

76. Cera, C., Terbojevich, M., Cosani, A., & Palumbo, M. (1988). Anthracycline antibiotics supported on water-soluble polysaccharides: synthesis and physicochemical chracterization. *Int. J. Biol. Macromol.* ***10***, 66-74.

77. Sakurai, K., Miyazaki, K., Kodera, Y., Nishimura, H., Shingu, M., & Inada, Y. (1997). Anti-inflammatory activity of superoxide dismutase conjugated with sodium hyaluronate. *Glycoconjugate J.* ***14***, 723-728.

78. Magnani, A., Albanese, A., Lamponi, S., & Barbucci, R. (1996). Blood-interaction performance of different sulphated hyaluronic acids. *Thrombosis Res.* ***81***, 383-395.

79. Favia, P., Palumbo, F., & D'Agostino, R. (1997). Grafting of functional groups onto polyethylene by means of RE glow discharges as first step to the immobilization of biomolecules. *Polym. Prepr.* ***38***, 1039-1040.

80. Favia, P., Palumbo, F., D'Agostino, R., Lamponi, S., Magnani, A., & Barbucci, R. (1998). Immobilization of heparin and highly-sulfated hyaluronic acid onto plasma-treated polyethylene. *Plasma Polym.* ***3***, 77-96.

81. Chen, G. P., Ito, Y., Imanishi, Y., Magnani, A., Lamponi, S., & Barbucci, R. (1997). Photoimmobilization of sulfated hyaluronic acid for antithrombogenicity. *Bioconjugate Chem.* ***8***, 730-734.

82. Hoekstra, D. (1999). Hyaluronan-modified surfaces for medical devices. *Med. Device & Diag. Ind.* 48-58.

83. Barbucci, R. In *New Frontiers in Medical Sciences: Redefining Hyaluronan*; Abbazia di Praglia, Padua, Italy, 1999; pp N4.

84. Coradini, D., Pellizzaro, C., Miglierini, G., Daidone, M. G., & Perbellini, A. (1999). Hyaluronic acid as drug delivery for sodium butyrate: improvement of the anti-proliferative activity on a breast-cancer cell line. *Int. J. Cancer* ***81***, 411-416.

85. Mensitieri, M., Ambrosio, L., & Nicolais, L. (1996). Viscoelastic properties modulation of a novel autocrosslinked hyaluronic acid polymer. *J. Mater. Sci.: Mater. Med.* 7, 695-698.

86. De Iaco, P. A., Stefanetti, M., Pressato, D., Piana, S., Dona, M., Pavesio, A., & Bovicelli, L. (1998). A novel hyaluronan-based gel in laparoscopic adhesion prevention: preclinical evaluation in an animal model. *Fertil. and Steril.* ***69***, 318-323.

87. De Iaco, P. In *New Frontiers in Medical Sciences: Redefining Hyaluronan*; Abbazia di Praglia, Padua, Italy, 1999; pp N12.

88. Lise, M. In *New Frontiers in Medical Sciences: Redefining Hyaluronan*; Abbazia di Praglia, Padua, Italy, 1999; pp N24.

89. Caplan, A. I., Solchaga, A. I., & Goldberg, V. M. In *New Frontiers in Medical Sciences: Redefining Hyaluronan*; Abbazia di Praglia, Padua, Italy, 1999; pp N8.

90. Solchaga, L. A., Dennis, J. E., Goldberg, V. M., & Caplan, A. I. (1999). Hyaluronic acid-based polymers as cell carriers for tissue-engineered repair of bone and cartilage. *J. Orthopaedic Res.* ***17***, 205-213.

91. Laurent, T. C., Hellsing, K., & Gelotte, B. (1964). Cross-linked gels of hyaluronic acid. *Acta Chem. Scand.* ***18***, 274-275.

92. Tomer, R., Dimitrijevic, D., & Florence, A. T. (1995). Electrically controlled release of macromolecules from cross-linked hyaluronic acid hydrogels. *J. Controlled Rel.* ***33***, 405-413.

93. Yui, N., Okano, T., & Sakurai, Y. (1993). Photo-Responsive degradation of heterogeneous hydrogels comprising crosslinked hyaluronic acid and lipid microspheres for temporal drug delivery. *J. Controlled Rel.* ***26***, 141-145.

94. Yui, N., Okano, T., & Sakurai, Y. (1992). Inflammation Responsive Degradation of Crosslinked Hyaluronic Acid Gels. *J. Controlled Rel.* ***22***, 105-116.

95. Yui, N., Nihira, J., Okano, T., & Sakurai, Y. (1993). Regulated release of drug microspheres from inflammation responsive degradable matrices of crosslinked hyaluronic acid. *J. Controlled Rel.* ***25***, 133-143.

96. Glass, J. R., Dickerson, K. T., Stecker, K., & Polarek, J. W. (1996). Characterization of a hyaluronic acid-Arg-Gly-Asp peptide cell attachment matrix. *Biomaterials* ***17***, 1101-1108.

97. Cooper, M. L., Hansbrough, J. F., & Polarek, J. W. (1996). The effect of an arginine-glycine-aspartic acid peptide and hyaluronate synthetic matrix on epithelialization of meshed skin graft interstices. *J. Burn Care Rehabil.* ***17***, 108-116.

98. Burns, J. M., Skinner, K., Colt, J., Sheidlin, A., Bronson, R., Yaacobi, Y., & Goldberg, E. P. (1995). Prevention of tissue injury and postsurgical adhesions by precoating tissues with hyaluronic acid solutions. *J. Surg. Res.* ***59***, 644-652.

99. Hu, M., Sabelman, E. E., Lai, S., Timek, E. K., Zhang, F., Hentz, V. R., & Lineaweaver, W. C. (1999). Polypeptide resurfacing method improves fibroblast's adhesion to hyaluronan strands. *J. Biomed. Mater. Res.* ***47***, 79-84.

100. diZerega, G. S. In *New Frontiers in Medical Sciences: Redefining Hyaluronan*; Abbazia di Praglia, Padua, Italy, 1999; pp N13.

101. Tomihata, K., & Ikada, Y. (1997). Crosslinking of hyaluronic acid with water-soluble carbodiimide. *J. Biomed. Mater. Res.* ***37***, 243-251.

102. Larsen, N. E., & Balazs, E. A. (1991). Drug delivery systems using hyaluronan and its derivatives. *Adv. Drug Delivery Rev.* ***7***, 279-293.

103. Larsen, N. E., Lombard, K. M., Parent, E. G., & Balazs, E. A. (1992). Effects of hylan on cartilage and chondrocyte cultures. *J. Orthopaedic Res.* ***10***, 23-32.

104. Pozo, M. A., Balazs, E. A., & Belmonte, C. (1997). Reduction of sensory responses to passive movements of inflamed knee joints by hylan, a hyaluronan derivative. *Exp. Brain Res.* ***116***, 3-9.

105. Adams, M. E. (1993). An analysis of clinical studies of the use of crosslinked hyaluronan, hylan, in the treatment of osteoarthritis. *J. Rheumatol.* ***20***, 16-18.

106. Larsen, N. E., Pollak, C. T., Reiner, K., Leshchiner, E., & Balazs, E. A. (1993). Hylan gel biomaterial: dermal and immunologic compatibility. *J. Biomed. Mater. Res.* ***27***, 1129-1134.

107. Larsen, N. E., Pollak, C. T., Reiner, K., Leschiner, E., & Balazs, E. A. (1994). Hylan gel for soft tissue augmentation. In *Biotechnology and Bioactive Polymers*; (Gebelein, C. & Carrahar, C., Ed.), pp 25-33 Plenum Press, New York.

108. Krauss, M. C. (1999). Recent advances in soft tissue augmentation. *Seminars in Cutaneous Medicine and Surgery* ***18***, 119-128.

109. Hallen, L., Johansson, C., & Laurent, C. (1999). Cross-linked hyaluronan (hylan B gel): a new injectable remedy for treatment of vocal folds insufficiency-an animal study. *Acta Otolaryngol. (Stockholm)* ***119***, 107-111.

110. Piaquadio, D., Jarcho, M., & Glotz, R. (1997). Evaluation of hylan B gels as a soft tissue augmentation implant material. *J. Am. Acad. Dermatol.* ***36***, 544-549.

111. Larsen, N. E., Parent, E., & Balazs, E. In *New Frontiers in Medical Sciences: Redefining Hyaluronan*; Abbazia di Praglia, Padua, Italy, 1999; pp N21.

112. Crescenzi, V., Tomasi, M., & Francescangeli, A. In *New Frontiers in Medical Sciences: Redefining Hyaluronan*; Abbazia di Praglia, Padua, Italy, 1999; pp N11.

113. Cascone, M. G., Sim, B., & Downes, S. (1995). Blends of synthetic and natural polymers as drug delivery systems for growth hormone. *Biomaterials **16***, 569-574.

114. Marriott, C., Martin, G. P., & Brown, M. B. In *PCT Int Appl WO 9813024*; 1998; pp .

115. Yerushalmi, N., & Margalit, R. (1998). Hyaluronic acid-modified bioadhesive liposomes as local drug depots: effects of cellular and fluid dynamics on liposome retention at target sites. *Arch. Biochem. Biophys. **349***, 21-26.

116. Yerushalmi, N., Arad, A., & Margalit, R. (1994). Molecular and cellular studies of hyaluronic acid-modified liposomes as bioadhesive carriers for topical drug delivery in wound healing. *Arch. Biochem. Biophys. **313***, 267-273.

117. Chio, Y. S., Hong, S. R., Lee, Y. M., Song, K. W., Park, M. H., & Nam, Y. S. (1999). Studies on gelatin-containing artificial skin: II. Preparation and characterization of cross-linked gelatin-hyaluronate sponge. *J. Biomed. Mater. Res. **48***, 631-639.

118. Oerther, S., Gall, H. L., Payan, E., Lapicque, F., Presle, N., Hubert, P., Dexheimer, J., Netter, P., & Lapicque, F. (1999). Hyaluronate-alginate gel as a novel biomaterial: mechanical properties and formation mechanism. *Biotech. and Bioeng. **63***, 206-215.

119. Oerther, S., Payan, E., Lapicque, F., Presle, N., Hubert, P., Muller, S., Netter, P., & Lapicque, F. (1999). Hyaluronate-alginate combination for the preparation of new biomaterials: investigation of the behavior in aqueous solutions. *Biochim. Biophys. Acta **1426***, 185-194.

120. Rehakova, M., Bakos, D., Vizarova, K., Soldan, M., & Jurickova, M. (1996). Properties of collagen and hyaluronic acid composite materials and their modification by chemical crosslinking. *J. Biomed. Mater. Res. **30***, 369-372.

121. Soldan, M., & Bakos, D. In *Advances in Medical Physics, Biophysics and Biomaterials*; Stara Lesna, Slovak Republic, 1997; pp 58-61.

122. Bakos, D., Soldan, M., & Vanis, M. In *Adv. Med. Phys., Biophys. and Biomat.*; Stara Lesna, Slovak Republic, 1997; pp 54-56.

123. Liu, L., Thompson, A. Y., Heidaran, M. A., Poser, J. W., & Spiro, R. C. (1999). An osteoconductive collagen/hyaluronate matrix for bone regeneration. *Biomaterials **20***, 1097-1108.

124. Murashit, T., Nakayama, Y., Hirano, T., & Ohashi, S. (1996). Acceleration of granulation tissue ingrowth by hyaluyronic acid in artificial skin. *Brit. J. Plast. Surg. **49***, 58-63.

125. Huang-Lee, L. L. H., & Nimni, M. E. (1994). Crosslinked CNBr-activated hyaluronan-collagen matrices: effects on fibroblast contraction. *Matrix Biol. **14***, 147-157.

126. Burns, J. W., Burgess, L., Skinner, K., Rose, R., Colt, M. J., & Diamond, M. P. (1996). A hyaluronate based gel for the prevention of postsurgical adhesions: Evaluation in two animal species. *Fertil. Steril.® **66***, 814-821.

127. Bowers, D., Raybon, B., & Wheeless, C. R. (1999). Hyaluronic acid - carboxymethyl-cellulose film and perianastomotic adheisons in previously irradiated rats. *Am. J. Obstet. Gynecol. **181***, 1335-1338.

128. Hooker, G. D., Taylor, B. M., & Driman, D. K. (1999). Prevention of adhesion formation with use of sodium hyaluronate-based bioresorbable membrane in a rat model of ventral hernia repair with polypropylene mesh-A randomized, controlled study. *Surgery **125***, 211-216.

129. Asayama, S., Nogawa, M., Takei, Y., Akaike, T., & Maruyama, A. (1998). Synthesis of novel polyampholyte comb-type copolymers consisting of a poly(L-lysine) backbone and hyaluronic acid side chains for a DNA carrier. *Bioconjugate Chem.* ***9***, 476-481.

130. Moriyama, K., Ooya, T., & Yui, N. (1999). Hyaluronic acid grafted poly (ethylene glycol) as a novel peptide formulation. *J. Controlled Rel.* ***59***, 77-86.

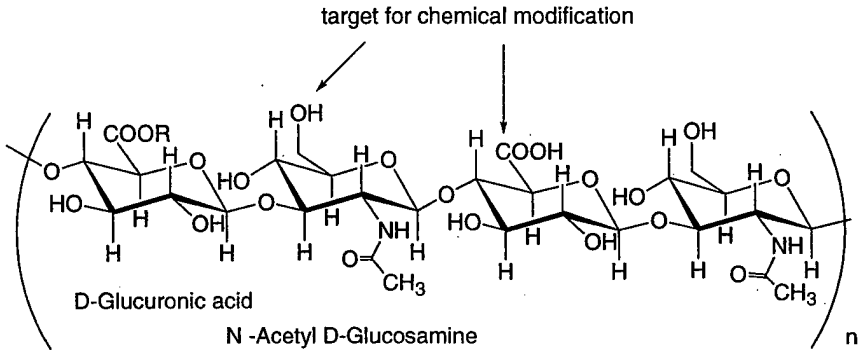
target for chemical modification
D-Glucuronic acid
N -Acetyl D-Glucosamine
n

Figure 1

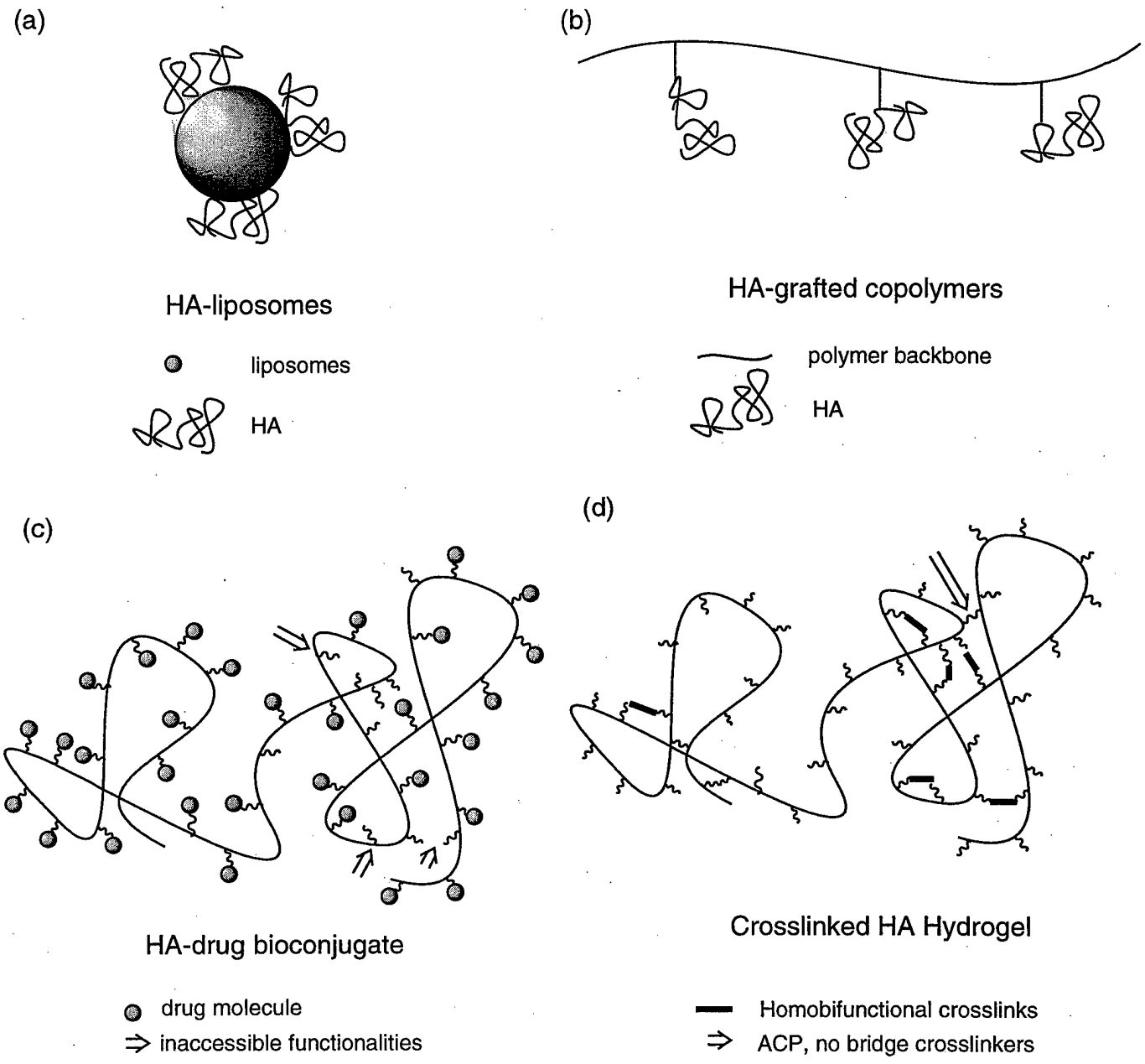
(a)
HA-liposomes
liposomes
HA
(b)
HA-grafted copolymers
polymer backbone
HA
(c)
HA-drug bioconjugate
drug molecule
inaccessible functionalities
(d)
Crosslinked HA Hydrogel
Homobifunctional crosslinks
ACP, no bridge crosslinkers

Figure 2

Manuscript for: *Journal of Biological Chemistry*
Submitted: June 8, 2000

Peptides that Mimic Glycosaminoglycans:

High Affinity Ligands for A Hyaluronic Acid Binding Domain*

Michael R. Ziebell[‡,†,^], Zhan-Gong Zhao[‡], Bai Luo[∞], Yi Luo[‡], Eva A. Turley[§],

and Glenn D. Prestwich[‡,@,¶]

[†]Department of Physiology and Biophysics, The University of Stony Brook,
Stony Brook, New York 11794-8661

[‡]Department of Medicinal Chemistry, The University of Utah,
30 South 2000 East, Room 201, Salt Lake City, Utah 84112-5820

[§]Division of Cardiovascular Research Hospital for Sick Children,
55 University Avenue, Toronto, Ontario, M5G 1X8 Canada

[∞]Huntsman Cancer Institute, 2000 Circle of Hope, Room LL376,
The University of Utah, Salt Lake City, Utah 84112-5550

[@]Center for Cell Signaling, 421 Wakara Way, Suite 360,
Salt Lake City, Utah 84108

Running Title: Peptide Mimics of Hyaluronic Acid

*This work was supported by grants to G.D.P. from the Department of Defense, the State of Utah Centers of Excellence Program, and The University of Utah and by a grant to E.A.T. from the National Cancer Institute of Canada. This article must therefore be hereby marked "*advertisement*" in accordance with 18 U.S.C. Section 1734 solely to indicate this fact.

^Current address: Department of Neurobiology, Harvard Medical School, 220 Longwood Avenue, Boston, Massachusetts 02115

¶To whom all correspondence should be addressed:
Department of Medicinal Chemistry
The University of Utah
30 South 2000 East, Room 201
Salt Lake City, Utah 84112-5820
Phone: 801 585 9051; **fax:** 801 585-9053
E-mail: gprestwich@deans.pharm.utah.edu

[1]The abbreviations used are:

bHA, biotinylated hyaluronic acid; **BCIP**, 5-bromo-4-chloro-3-indolyl phosphate; **BD**, binding domain; **CS**, chondroitin sulfate; **EDCI**, 1-[3-(dimethylamino)propyl]-3-ethylcarbodiimide hydrochloride; **Erk1**, extracellular signal-regulated protein kinase; **FACS**, fluoresence-activated cell sorting; **FAK**, focal adhesion kinase; **Fmoc**, 9-fluorenylmethoxycarbonyl; **FP**, fluorescence polarization; **GAG**, glycosaminoglycan; **GnHCl**, guanidinium hydrochloride; **GPI**, glycosyl phosphatidyl inositol; **GST**, glutathione-S transferase; **HA**, hyaluronic acid or hyaluronan; **HABD**, hyaluronic acid binding domain; **HAse**, hyaluronidase; **HBTU**, (*o*-benzotriazol-1-yl-*N,N,N',N'*-tetramethyluronium hexafluorophosphate); **HOBt**, 1-hydroxybenzotriazole; **PBS**, phosphate-buffered saline; **PEG**, polyethylene glycol; **mP**, millipolarization units; **PVP-40**, polyvinyl pyrolidone; **RHAMM**, receptor for hyaluronan mediated motility; **SA-HRP**, streptavidin-horseradish peroxidase; **TBS**, Tris-buffered saline; **TMB**, 3,3',5',5-tetramethylbenzidene.

SUMMARY

Peptide ligands that bind specifically to hyaluronic acid (HA) binding domains (BDs) of the HA receptor RHAMM were obtained from three peptide libraries: (**i**) phage displayed 15-mers, (**ii**) random 8-mers, and (**iii**) biased 8-mers with alternating acidic side chains, i.e., XZXZXZXZ (X = all L-amino acids except Cys, Lys, or Arg; Z = D-Asp, L-Asp, D-Glu, or L-Glu). Dipeptide and tripeptide motifs could be recognized in both random phage and biased bead-based libraries. Selectivity of the peptide ligands for the HABDs was established by (**i**) detection of binding of biotin- or fluorescein-labeled peptides to immobilized proteins, and (**ii**) fluorescence polarization of FITC-labeled peptides with HABDs in solution. High-affinity peptides bound only the HABD employed as the bait for screening. HA competitively displaced peptide-HABD binding, while other glycosaminoglycans were less effective competitors. The absolute stereochemistry of the three highest affinity-biased octapeptides was established by synthesis and binding assays with the 16 stereoisomers of each peptide. A strong preference for alternating D and L configurations for the acidic residues was observed, consistent with the predicted orientation of glucuronic acid moieties of HA. Finally, MDA-MB-231 breast cancer cells that overexpress RHAMM bind and internalize fluorescent peptides, and this uptake was prevented by pre-incubation with HA. This suggests that non-glycosaminoglycan ligands specific for a given HA receptor could be designed to permit targeted drug delivery to a chosen cell population.

INTRODUCTION

The extracellular matrix polysaccharide hyaluronic acid [β-1,4-GlcUA-β-1,3-GlcNAc-]$_n$ (HA[1]) is a non-sulfated glycosaminoglycan (GAG) that promotes cell motility, adhesion, and proliferation in mammalian cells (1), thereby playing roles in morphogenesis (2), wound healing (3) and metastasis (4). These functions are mediated by cell-surface HA receptors, which initiate key cell signaling cascades when activated by HA, leading to physiological changes (4). Non-carbohydrate ligands that would bind to and activate cell-surface HA receptors could have important therapeutic uses in cancer, wound healing, and arthritis, since they would be resistant to degradation by hyaluronidase (HAse). To this end, three peptide libraries were prepared and screened to identify high-affinity ligands for the HA receptor RHAMM (**R**eceptor for **H**y**A**luronan **M**ediated **M**otility).

RHAMM mediates cell migration and proliferation in many normal cells and in tumor cell lines (5). Isoforms of RHAMM are functionally active both in the cytoplasm and on the cell surface (4). The extracellular forms of RHAMM appear to act as co-receptors, which modulate the signaling through integral receptors, such as the PDGF receptor (6-8). RHAMM requires the small GTPase p21 ras and pp60 src to promote motility (8, 9). A target of src regulated phosphorylation is focal adhesion kinase (FAK) (pp125^{FAK}) which is an important integrin binding protein. Phosphorylation of FAK leads to focal adhesion turnover, a critical step in cell locomotion (10).

RHAMM is overexpressed as several isoforms in human tumors and tumor cell lines including colorectal (11), breast (12, 13), pancreas (14), and multiple myeloma (15). A dominant negative mutant of RHAMM, mutated in its HA binding domains (BDs), blocks cell transformation by mutant active ras. Furthermore, overexpression of one RHAMM isoform constitutively activates erk kinase (7) and is transforming in fibroblasts (10). RHAMM occurs as an intracellular protein but can be expressed on the cell surface, a condition observed most often in single cells such as white cells (16, 17) and in subconfluent fibroblasts (7). Cell-surface RHAMM binds to

extracellular HA and the HA-RHAMM complex undergoes receptor-mediated endocytosis (18). Intracellular RHAMM binds to cytoskeletal proteins (19) and associates with erk kinase (7).

Mutation studies of RHAMM identified two regions near the C-terminus that are required for full HA binding (20). These regions have clusters of basic residues and have a characteristic BX_7B motif (B = basic residue, X = any non-acidic residue) present on many HA binding proteins (21). Synthetic peptides representing the RHAMM domains inhibited HA binding to full length RHAMM, while peptides representing other parts of the primary sequence failed to inhibit binding (20). CD44 and other link module-containing proteins may have this linear basic motif, but they are architecturally and possibly functionally distinct (22). Although RHAMM is known to bind heparin at the same binding site as HA, no other GAGs are reported to bind to RHAMM with high affinity.

The secondary structure of RHAMM is predicted to be predominantly helical. The structure of the HA binding domain (HABD) was recently studied using multi-dimensional NMR and was observed at 3 Å resolution to be a helix-loop-helix with a coiled-coil tertiary structure (23). This contrasts with the link module of the protein TSG-6 (24, 25), which has mostly beta sheet elements. Using RHAMM numbering (26), the N-terminal of the HABD is completely contained within a loop (residues 531-539), while the second half of the domain (residues 553-562) spans a loop and a helical region. The interaction of HA with HA binding proteins requires both electrostatic interactions between the glucuronate carboxylates and HABD basic residues, as well as hydrophobic interactions involving C-H rich patches on HA (25).

Two synthetic peptide libraries, one composed of random octapeptides and one containing alternating acidic and non-acidic residues, were examined for potential non-GAG ligands for the HABD. These one-bead, one-peptide libraries (27) and a library of phage-displayed 15-mers were screened with the a RHAMM-HABD to identify high-affinity peptides for the HABD. The biased acidic library was designed to mimic the natural pattern of alternating glucuronic acid carboxylates present in HA; this represents the first rational approach to identification of a non-GAG ligand for an HA binding site. Importantly, this library included both natural and unnatural configurations of

the acidic residues to further explore possible oligosaccharide conformations that could be important in ligand recognition.

This paper presents four major results. First, recurring peptide motifs that bind to HABDs were identified in both biased and random libraries. Second, a solid-phase binding assay and a fluorescent polarization (FP) assay were developed to quantify the relative affinity and selectivity of peptide-RHAMM interactions. Third, the importance of including acidic amino acids with unnatural configurations was demonstrated. The data supported a molecular interpretation for the structural similarity between these peptides and HA. Fourth, fluorescently-labeled high-affinity peptide ligands were recognized by cell-surface HA receptors, leading to ligand-selective receptor-mediated uptake. These results suggest important new uses of HA-mimicking peptides in basic cell biology and in the development of new therapeutic drugs.

EXPERIMENTAL PROCEDURES

Sub-cloning of RHAMM(518-580) into PGEX-2T -- The RHAMMv4 cDNA in a pCRII vector (10) was used as a template for PCR production of the RHAMM constructs. Sequence-specific primers encoded restriction sites to permit ligation of PCR products into the appropriate vectors. Thus, the RHAMM(518-580) PCR product was digested, purified, and ligated directly into PGEX-2T (Pharmacia) using unique *Eco*R1 and *Bam*H1 restriction sites. Initial ligation of PCR products into a PGEM-T vector (Novagen) improved the ligation efficiency. Plasmid and PCR insert purification followed standard protocols, and DNA was purified by either phenol chloroform extraction (28) or with Qiagen columns.

Purification of Glutathione-S Transferase (GST) Fusion Protein -- GST-RHAMM(518-580) (R D S Y A Q L L G H Q N L K Q K I K H V V K L K D E N S Q L K S E V S K L R S Q L V K R K Q N E L R L Q G E L D K A L G I R) (29, 26), with BX_7B motifs underlined, was expressed in BL21 *E. coli* cells in ampicillin-containing media by induction with IPTG (2 mM). Cells were harvested by centrifugation at 2,000 × g for 30 min, resuspended in phosphate-buffered saline (PBS) with 30 μg/ml leupeptin and 1 mM PMSF, and lysed using a French press at 20,000 psi. TX-100 (1% final concentration) was added to the lysate, incubated on ice for 30 min, and centrifuged at 12,000 × g for 30 min. The brown supernatant was applied to a 10-ml bed volume of glutathione Sepharose equilibrated in PBS at 4 °C. The supernatant was passed through the resin by gravity, the column was washed with 15-20 bed volumes of PBS at 1 ml/min, and the GST-RHAMM(518-580) was eluted with 50 mM glutathione, 10 mM Tris, pH 8.0. Glycerol was added to 10% final concentration, and 1.5-ml aliquots of purified protein were flash frozen on dry ice and stored at -30°C until use. Then, a sample was thawed in ice water and diluted in Tris-buffered saline (TBS) to the required concentration. Unused protein from a thawed aliquot was discarded; no loss of activity was noted for a single freeze-thaw cycle.

Expression and Purification of Thioredoxin-RHAMM(523-580) -- The PCR product for RHAMM(523-580) was first ligated into pGEM-T, followed by restriction digestion and ligation

into pET-32b+ (Novagen). This plasmid encoded an N-terminal thioredoxin fusion protein and a C-terminal poly-histidine tag, and contained thrombin and enterokinase cleavage sites. Cells were grown at 37 °C, and at OD_{600} = 1.2, protein synthesis was induced for 4 h with 1 mM IPTG. Cells were harvested, resuspended in 50 ml binding buffer (5 mM imidazole, 500 mM NaCl, 20 mM Tris-HCl, pH 7.9) with 30 μg/ml leupeptin and 1 mM PMSF, and lysed using a French press at 20,000 psi. TX-100 (1% final concentration) was added to the lysate, the solution was incubated on ice for 30 min, centrifuged at 12,000 × g for 30 min, and the brown supernatant was applied to a nickel-chelating resin (His-bind Resin, Novagen). The column was washed (60 mM imidazole, 500 mM NaCl, 20 mM Tris-HCl, pH 7.9) followed by elution with 800 mM imidazole. The protein was collected in 5-ml aliquots and frozen as described above. After elution the column was stripped and recharged with 50 mM $NiSO_4$.

For phage screening experiments the protein was stored in elution buffer. For other uses, the protein was dialyzed in MW 3,500 cutoff-membranes against 2,000 volumes of PBS. Amicon units (Millipore) with MW 3,000 cutoff-membranes were used to concentrate the protein.

Synthesis of Biotinylated Hyaluronic Acid --Biotinylated HA (bHA) was prepared using the hydrazide method as described (30, 31). Bacterially-expressed HA (100 mg, 0.25 mmol disaccharide equivalents, MW 700,000) (Clear Solutions Biotech, Inc., Stony Brook, NY) was dissolved in 20 ml of water by stirring vigorously overnight. To obtain ca. 5% modification of carboxyl groups (0.0125 mmol), 18.6 mg of biotin-LC-hydrazide (Pierce, Rockford, IL) dissolved in 180 μl DMSO was added, followed by 24 mg (0.125 mmol) of 1-[3-(dimethylamino)propyl]-3-ethylcarbodiimide hydrochloride (EDCI). The bHA was purified by extensive dialysis over several days, alternating between 500 mM NaCl and water (32).

Biotinylated-HA Blot Method -- PVDF membranes (BioRad) were pre-wetted in MeOH and then 3-5 μl of the protein was added dropwise as the MeOH evaporated. After the membrane absorbed the protein solution, it was immediately immersed in blocking buffer (TBS + 1% polyvinyl pyrolidone (PVP-40) and 1% casein) for 2 h. The membrane was then incubated with 10 μg/ml of bHA in blocking solution for 2 h, washed three times with TBS-T,

incubated with 1:4,000 dilution of streptavidin-horseradish peroxidase (SA-HRP) for 40 min, washed, and visualized using BM chemiluminescent enzyme linked immunosorbent assay (ELISA) substrate (Boehringer Mannheim) (60 sec incubation). The membrane was wrapped in plastic wrap and immediately exposed to X-ray film (X-Omat-AR film, Kodak). The signal was quantified with a computer-controlled scanner (UMAX 1200S), and the digitized signal was analyzed using NIH Image.

Phage Screening -- A solution of purified GST-RHAMM(518-580) (0.5 mg/ml) in 50 mM Tris-HCl, pH 8.0 was either nonspecifically adsorbed onto a 30 mM polystyrene dish (Fisher), or immobilized on 20 µl of glutathione Sepharose (Pharmacia) in a 1.5-ml microfuge tube. An M13 filamentous phage library with random 15-amino acid peptides presented as fusion proteins of gene product III (pIII) was obtained from Dr. George Smith (University of Missouri) (33). A starting titer of 10^{11} colony forming units (cfu) of phage was diluted 1:1,000 in TBS (20 mM Tris, 130 mM NaCl, pH 7.5) with 0.1% w/v PVP-40 and 0.05% Tween 20. The phage library (Library **P**) was applied to the immobilized GST-RHAMM(518-580) and incubated at rt for 1 h. Non-binding phage were removed with ten washes, and specifically-bound phage were eluted by cleavage of the GST-RHAMM construct using one unit of thrombin incubated at 37°C for 40 min. RHAMM(518-580) and specifically-bound phage were eluted, while GST (and GST-bound phage) should remain immobilized. For the construct thioredoxin-RHAMM(523-580), protein was immobilized on a petri dish. The experiment was otherwise equivalent to that of screens using GST-RHAMM(518-580).

Library **P** was titered by infecting K91-Kan cells and adding serial dilutions dropwise onto LB plates with kanamycin and tetracycline antibiotics (Kan/Tet). The phage bound to GST-RHAMM(518-580) was propagated in 20 ml K91-Kan cultures overnight, and the phage precipitated using polyethylene glycol (PEG) from the broth supernatant after removal of cells. This procedure was repeated a total of four times, retaining fewer phage after each iteration. In the final screen, phage binding to the HABD were eluted with 1 mg/ml digested HA (MW average 60,000 Da) instead of the thrombin cleavage method. Positive colonies from LB Kan/Tet plates

were propagated, the plasmid purified using the phenol/chloroform, and DNA was sequenced by the The University of Utah (UUtah) DNA Sequencing Facility. The insert was identified by finding the known sequences flanking the random insert. The 45 bases between the recognized sequences represent the random insert and are translated to provide a 15-amino acid peptide. Two sample Library **P** sequences are shown.

SADGA GVCNADFCWLPAVVV GAAGA

SADGA SASPSASKLSLMSTV GAAGA

Construction of the Peptide Libraries -- Two eight-amino acid one-bead, one-peptide libraries were constructed (34). Library **R** was a completely random library in which only cysteine was omitted during synthesis. Library **B** had an alternating acidic pattern, XZXZXZXZ, with X = any residue except Cys, Arg, or Lys, and Z = D-Asp, L-Asp, D-Glu, and L-Glu. Thus, Tentagel S NH_2 beads from (Rappe Polymere GmbH, Tübingen, Germany) are 80-100 μm beads with 0.3 mmol reactive amine/dry gram beads (34, 35). A typical starting sample size was six million beads, which were incubated with 9-fluorenylmethoxycarbonyl (Fmoc)-protected amino acids whose free carboxyls were activated with HOBt (1-hydroxybenzotriazole) and HBTU (*o*-benzotriazol-1-yl-*N*,*N*,*N*',*N*'-tetramethyluronium hexafluorophosphate) (Advanced Chemtech, Louisville, KY). The reaction proceeded in dimethylformamide (DMF) and the beads were purified by sequential DMF washes. The Fmoc-protected amine was deprotected using 20% piperidine in DMF and quantitative analysis determined the amount of available amine. To ensure a completely random library for Library **R**, the following strategy was used. The entire batch of beads was split into 19 equal pools each in a separate plastic column. Each batch was allowed to react with a single variety of Fmoc amino acid followed by a DMF wash. All beads were then combined, mixed, and then separated again into 19 new pools, and the process was repeated eight times. This method ensures the presence of a random population of peptides, while only one species is attached per bead. An analogous split-pool-split procedure was performed for Library **B**, alternating between a four-pool split and a 17-pool split.

Bead Screening -- Beads (2-ml, approximately 2×10^5 beads) from Library **B** or Library **R** were placed in a 5-ml plastic column (Biorad) and pretreated by washing with decreasing concentrations of DMF in TBS and finally with TBS containing 0.1% PVP-40. Next, 1 ng/ml of GST-RHAMM(518-580) was incubated with the beads for 1 h at rt on an orbital shaker. The beads were washed with 20 column volumes of buffer, and incubated with a 1:5,000 dilution of anti-GST. This washing was repeated, followed by incubation with a 1:10,000 dilution anti-goat IgG-alkaline phosphatase. After extensive washing, the beads were then incubated with 0.27 mM BCIP (5-bromo-4-chloro-3-indolyl phosphate) in detection buffer (TBS + 2 mM $MgCl_2$). The positive beads turned blue during 10-30 min, and were then sorted under 100 × magnification using a syringe fitted with a 10-µl pipette tip. The beads were stripped of bound protein and color by washing with 6 M guanidinium hydrochloride (GnHCl), pH 2.5, followed by three washes with DMF. This screening process was repeated three times, with the total number of beads decreasing after each successive screen. The final screen included a pre-incubation step with 1 mg/ml digested HA as competitor, such that beads that did not turn blue in the final screen were candidates for binding to the HABD of RHAMM.

Peptides on beads were sequenced by placing a single bead on a filter in the same manner that a polypeptide in solution would be immobilized on such a filter disk. Sequencing was accomplished using Edman degradation chemistry on an Applied Biosystems gas phase peptide sequencer model 477A.

Pepspots® Analysis of Biased Library Results to Determine Chirality of Peptides -- Each of the sixteen possible diastereomers for four positive Library **B** peptides were synthesized in spots immobilized on cellulose (Pepspots®, Jerini Biotools, Wilmington, NC). Four diastereomers of the negative control peptide **NB** (IDSDWEGE) were also synthesized. The amount of immobilized peptide is reported to be 3-5 nmol on the membrane as a 2-mm dot.

Binding to the Pepspots® was detected by incubation of the blocked (TBS + 0.1% casein) membrane with 50 µg/ml GST-RHAMM(518-580) in blocking buffer. After washing, the bound protein was semi-dry electrotransferred from the cellulose membrane onto a PVDF membrane

using the Phast (Pharmacia) system. A system of three buffers recommended by Jerini Biotools was used in this transfer: cathode buffer (25 mM Tris, 40 mM 6-aminohexanoic acid, 0.01% SDS and 20% methanol); anode buffer I (30 mM Tris base, 20% methanol); and anode buffer II (300 mM Tris base, 20% methanol). Filter paper squares were soaked in these buffers, three sets for each membrane to be transferred. First, the anode buffer I-soaked filter papers are placed on the anode, followed by the anode buffer II-soaked membranes; the two membranes are arranged with the PVDF membrane on the anode side of the cellulose membrane. The sandwich is completed with the cathode buffer-soaked filter papers. The cathode is placed on top of the sandwich and the transfer was performed at 0.8 mA/cm^2 of membrane for 40 min at 4 °C.

The PVDF membrane with the blotted GST-RHAMM(518-580) was blocked and incubated with a 1:5,000 dilution of anti-GST, followed by a 1:10,000 dilution of anti-goat antibody-HRP. To detect bound material, a chemiluminescence detection kit (Boehringer Manheim) was used followed by exposure to film. The developed film was scanned and quantified as above. Each experiment was repeated several times with different GST-RHAMM(518-580) concentrations; increased GST-RHAMM(518-580) concentrations resulted in increased background and non-specific binding.

Synthesis of Labeled Peptides for Binding Assays -- Peptides were synthesized using conventional Fmoc chemistry on an Applied Biosystems Model 431A Peptide synthesizer. The synthesized peptides were split into two batches. The first batch remained unlabeled, while a second batch was carried through an additional synthetic cycle to add an N-terminal Cys. All cleaved peptides were characterized by MALDI-TOF and purified on high performance liquid chromatography (HPLC) prior to use.

Either *N*α-(3-maleimidylpropionyl)biocytin or fluorescein-5-maleimide (Molecular Probes, Eugene, OR) was linked to the free thiol of the N-terminal Cys, using a 3 × molar excess of maleimide and ca. 1 mg of peptide. The maleimide probe was dissolved in DMSO to 10 mg/ml and the peptide was dissolved in 20 mM Tris, pH 7.0 to 1 mg/ml concentration in a microfuge tube. The Cys-containing peptides were handled in degassed reaction buffers and lyophilized from

trifluoroacetic acid solutions to maintain the free thiol. After mixing the peptide and maleimide reagents, precipitation can occur. In these cases, the reaction was centrifuged at 16,000 × g for 2 min, and the reaction supernatant was removed and recombined with DMSO-redissolved precipitate. After shaking for 12 h at rt, the conjugated peptides were purified by HPLC.

Preparation of Low Molecular Weight HA -- Bacterially-expressed HA (700 -1,200 kDa) was dissolved overnight in 50 mM sodium acetate buffer, pH 6.0 to give a 4 mg/ml solution. Ten units of testicular HAse (Sigma) per mg HA were added to the solution and the reaction was incubated for 12 h at 37 °C with shaking. An additional aliquot of HAse was added and the solution was again incubated at 37 °C for 12 h. This material was boiled for 5 min to inactivate any remaining HAse, and particulate matter was removed by centrifugation. The molecular weight was analyzed using gel permeation chromatography (Waters), which showed a distribution of molecular sizes from 4 - 40 kDa. This material was employed in the binding assays.

Solid-Phase Binding Assay -- GST-RHAMM(518-580) was immobilized in the wells of a 96-well plate (Greiner GmbH) and bHA or biotinylated peptides were added. Bound probes were detected using SA-HRP and the colorimetric HRP substrate 3,3',5',5-tetramethylbenzidene (TMB). Thus, 50 µl 0.5 mg/ml GST-RHAMM(518-580) in 50 mM Tris, pH 8.0 was incubated in each well of a 96-well plate for 1 h at 4°C with shaking. The wells were washed with TBS-T (20 mM Tris, 130 mM NaCl, pH 7.6, 0.1% Tween) three times, and then blocked with TBS-T-PVP-40 (TBS-T + 0.1% PVP-40) for 2 h at 4 °C. Dilutions of biotinylated probe (either HA or peptide) were added to each well in 50 µl TBS-T-PVP-40. After incubation for 45 min, wells were washed with TBS-T and bound biotinylated probes were detected using 50 µl 0.5 µg/ml SA-HRP (40 min, rt). After three washes, 50 µl TMB was added and color was detected after 10 min using an HTS-7000 microplate reader (Perkin Elmer) with the absorbance filter set at 360 nm. Experiments were performed in triplicate, and background was measured using a biotinylated probe added to blocked wells without GST-RHAMM(518-580). Control experiments included measuring binding with the peptide **NB** (IDSDWEGE).

Alternatively, this experiment was performed using fluorescein-labeled peptides rather than biotinylated peptides. In this case, after the incubation step with fluorescein-labeled probes, the plate was washed three times with TBS-T and 50 µl TBS was added to each well. The plate was then read on the HTS 7000 microplate reader using 485 nm excitation and 535 nm emission filters. The gain was set to optimal and 50 flashes were used to improve sensitivity.

Fluorescence Polarization (FP) Binding Assay -- Purified GST-RHAMM(518-580) was prepared at a stock concentration of 1.3 mg/ml (40 µM), and the initial concentration of fluorescent peptide was 0.1 µM. Thus, 200 µl of each dilution of GST-RHAMM(518-580) was added to the wells of a low-bind 96-well plate with black sides and a clear bottom (Corning Costar). For each set of experiments, the fluorescein-labeled probe concentration was kept constant, while the concentration of protein was increased. Data was collected on a Polarion (Tecan Inc.) microplate spectrofluorimeter equipped with a 485 nm excitation filter and a 585 nm emission filter. Fifty flashes were used to achieve optimal sensitivity, and free fluorescein was used as a standard at a value of 20 mP (millipolarization units). To generate a binding isotherm, a plate was prepared with triplicates of each concentration, serial dilutions of GST-RHAMM(518-580) optimally covering the range from 20-fold below the K_d to approximately 100-fold above the K_d. Identical aliquots of fluorescein-peptide were added to each well, mixed, and the plate was incubated until equilibration was reached and then measured. The binding data, mP values, and receptor concentrations were used to calculate the binding constants. This assay is most useful for probes that bind $K_d < 1$ µM since this constitutes a practical limit of protein concentrations needed to generate the isotherm.

FP data was analyzed as described previously (36, 37) to measure the amount of ligand bound by measurement of the anisotropy of the complex. The total change in polarization is calculated as $\Delta mP = mP_{max} - mP_{min}$. The bound ligand at each concentration is calculated as $B_T = [(mP-mP_{min})(\text{Total tracer concentration})]/\Delta mP$. Assuming 1:1 stoichiometry, $B_T = R_{bound}$, and free [HABD] can be calculated as $R_{free} = R_{tot} - R_{bound}$. Scatchard analysis by plotting R_{bound}/R_{free} *vs.* R_{bound} led to a best fit line with a slope equal to the negative reciprocal of the K_D (37).

Competition Experiments Using a Fluorescence-Based Solid-Phase Binding Assay -- Competition experiments were performed as outlined above except the blocking buffer includes 1 mg/ml competitor. The wells were pre-incubated with competitor, and the biotinylated or fluorescein-labeled probe was added together with competitor. Digested HA was used for competition. Heparin, chondroitin sulfate A (CS-A) and CS-C were dissolved in H_2O to 10 mg/ml, and were diluted to 1 mg/ml in TBS-T-PVP-40 in the competition experiments.

Cell Binding and Uptake Assays -- MDA-MB-231 breast cancer cells were grown to confluence in DMEM 10% fetal bovine serum and antibiotics in 25 mL culture flasks. Competitive displacement was demonstrated by pre-incubation of cells with 1 mg/mL of MW 700,000 HA for 2 h in DMEM prior to the experiment. Then, 1 μg/mL of fluorescent probe was applied concurrently with a second aliquot of competitor. After 15 min of incubation at 37°C with the probe, the cells were washed, treated with trypsin to release from the flask and dissociate, and the reaction was quenched by addition of 5% formaldehyde, 2.5% methanol in PBS. The cells were counted and uptake of fluorescence was measured by fluoresence-activated cell sorting (FACS).

Cell binding was observed using both fluorescence microscopy and FACS analysis. Fluorescence microscopy experiments were performed on a Zeiss Confocal laser microscope (20 scans/min; 60 to 90 × magnification). FACS analysis was accomplished using a FACScan cytofluorometer (Becton Dickinson, Grenoble, France) with a single 15 mW argon (488 nm) laser light source and the detector set at 585 nm; 20,000 events were gathered per sample. Viable cells were carefully gated by light scattering (FSC/SSC). Data analysis was performed using Cyquest software.

RESULTS

Initial Library Screening

A solid-phase method was employed to confirm that RHAMM HABD-containing proteins would bind to bHA, based on earlier methods for bHA-HABD studies (38, 39). To this end, a dot blot of purified GST-RHAMM(518-580), GST and RHAMM(518-580) on PVDF membrane was employed, since the highly-basic, small RHAMM(518-580) polypeptide itself failed to electrotransfer to PVDF. GST-RHAMM(518-580) and RHAMM(518-580) bind bHA, but neither GST alone nor BSA bind bHA (data not shown). Comparison of electrotransferred proteins on PVDF from electrophoretically separated GST-RHAMM(518-580) and thrombin-cleaved GST-RHAMM(518-580) (only GST remained) showed that only the fusion protein could be detected with bHA (data not shown). Similarly, thrombin cleavage of GST-RHAMM(518-580) in a 96-well plate released the HABD, which was detected using a dot blot. These control experiments validated the use of thrombin digestion for the early rounds of phage screening in which positive phage bound to RHAMM(518-580) were eluted by cleavage of the linker to the immobilized GST domain.

The phage library (Library **P**) of random 15-mers was screened using purified GST-RHAMM(518-580) and purified thioredoxin-RHAMM(523-580) to identify peptides binding to these constructs. In the experiments described herein, the use of two different fusion constructs reduced the likelihood of false positives arising from phage binding to the fusion partner, either GST or thioredoxin. Analysis of sequenced cDNAs indicated that motifs in the peptides in Library **P** were common to peptides for both screening protocols. The deduced peptide sequences are summarized in Table 1.

Two eight-amino acid libraries were synthesized on 100-μm Tentagel beads and screened using GST-RHAMM(518-580) as the HABD. Library **R** contained completely random sequences of 19 L-amino acids (excluding Cys), while Library **B** consisted of alternating acidic residues in an XZXZXZXZ pattern. For Library **B,** the acidic (Z) residues were allowed to have either the natural

L or unnatural D absolute configuration. The synthesis generated three million beads for each library; typically, an aliquot of ca. 100,000 beads was used for each screen. The number of beads was selected by the practical limits of the experimental approach, and by the calculation that this number should adequately represent the dipeptide or tripeptide motifs that were anticipated in an octapeptide population. Thus, starting with 100,000 beads, approximately 30 positive "blue" beads were identified after three rounds of screening. The final round of screening included a competition step with HA to block peptide binding to the HABD; positive beads in this step were "white." Table 1 also summarizes the peptides directly sequenced following screening of Libraries **R** and **B** with GST-RHAMM(518-580). Approximately half of the positive beads were sequenced, and of these, 20% of the sequencing attempts failed for technical reasons.

Deconvolution of Library B hits

Since Library **B** was synthesized with either the D- or L-isomers at the alternating acidic residues, it was necessary to deconvolve the particular combination of natural and unnatural amino acids in each positive hit. Solid-phase synthesis on each bead created one of sixteen possible diastereoisomers of a given "letter" sequence, corresponding to a total of two enantiomers at each of four positions. Using automated Edman degradation for peptide sequencing, the chirality of the PTH amino acid sequenced at any given cycle could be determined. Before micromole-scale synthesis of peptides for determination of binding affinities, the diastereomer ambiguity was therefore resolved by construction of a mini-library of the 16 individual diastereomers of the Library **B** peptides. This peptide mini-library was constructed as an array of spots on cellulose membrane (Pepspots®), in which each spot contained a single diastereomer of the Library **B** peptide letter-sequence (3-5 nmol/spot). The custom membrane mini-library commercially produced for this assay contained an array of 72 spots, representing the 16 diastereomers of peptides **B-1**, **B-2**, **B-3**, and **B-4**, four negative control spots (using the sequence of a non-binding negative control, IDSDWEGE), and four spaces between each set of 16 diastereomers, which contained no peptide.

GST-RHAMM(518-580) binding to the Pepspots® mini-library was carried out by semi-dry transfer in order to permit uses of the original membrane for multiple protein-stripping and reprobing experiments. Thus, GST-RHAMM(518-580) was incubated with the blocked Pepspots® membrane and specifically-bound protein was transferred to a PVDF membrane. Bound GST-RHAMM(518-580) was detected using goat anti-GST, followed by anti-goat-IgG HRP conjugated antibodies. Binding was visualized and quantified (Figure 1) with a chemiluminescent HRP substrate. These data allowed selection of specific diastereomers of Library **B** peptides to analyze binding of a single homogeneous species rather than a diastereomeric mixture. Four pairs of diastereomers with ca. 100-fold binding differences were synthesized and used as described below to measure binding affinities for the RHAMM HABD (see Table 2).

The data in Figure 1 illustrate that peptides containing only D-Glu and D-Asp are never the diastereomers with the highest affinity. This most likely reflects the importance of the orientation of the carboxylate-containing side chains. With a combination of D- and L-amino acids in a single peptide, the structures with carboxylates on alternating "sides" of the peptide more closely imitated the orientation of the glucuronate carboxylates in HA.

Affinities of Peptides for RHAMM HABD

Three microplate binding assays were employed to measure the affinity of synthetic peptides for RHAMM(518-580): ELISA, a fluorescence-based analog of the ELISA, and FP. The ELISA required a biotinylated peptide, while both the fluorescence-based solid-phase and the FP assays required a fluorophore-modified peptide. Thus, two thiol-reactive maleimide reporter groups were used, requiring an N-terminal cysteine for probe attachment. For competition assays with probe-modified peptides or bHA, peptides lacking the Cys residue were also required, and were conveniently made by removal of half the synthetic peptide from the synthesizer prior to addition of the final Cys residue. Synthetic peptides from each sub-group of similar peptides were prepared, e.g., both the phage peptide **P-2** containing the WLPA motif, and the **P-3** with the SAS motif were

evaluated. Sequences from Library **R** were similarly selected. For Library **B**, each of the four positive peptides identified by the Pepspots® deconvolution experiment were synthesized.

The binding affinities of the synthetic peptides were measured with the ELISA, and K_D values were determined mathematically (40). In a typical experiment, the K_D for a given biotinylated peptide was determined using successive fivefold dilutions of probe having a fixed amount of immobilized protein. Experiments were performed in triplicate with background (no protein) subtraction prior to calculations. The stoichiometry of binding was determined using a standard curve of SA-HRP serial dilutions. For example, **P-2**, one of the highest affinity phage peptides, had a K_d of 11 nM with a 1:1 binding ratio. The binding affinities are summarized in Table 2.

Domain Selectivity and Competitive Displacement of Peptide Binding by GAGs

The ELISA was modified to address selectivity of binding. Thus, a domain selectivity and a GAG competition assay were both conducted using a modification of the solid-phase ELISA that allowed use of fluorescein-labeled peptides. Although the data from this modification are less accurate for absolute quantitation, a lower background could be achieved than with the SA-HRP ELISA method. First, we demonstrated that RHAMM HABD, not the GST fusion partner, was responsible for peptide binding. Twelve peptides from each of the three libraries were evaluated. Figure 2 illustrates that the majority of peptides show negligible binding to the GST domain. It is possible that the fluorophore modifications may increase the nonspecific binding beyond that detected in the original library screening protocols.

Second, we evaluated the effectiveness of several GAGs to inhibit binding of synthetic peptides to the HABD of RHAMM. HA was used as a competitor for all synthetic peptides, and other GAGs were evaluated with a subset of peptides. Seven fluoroescein-labeled peptides representing each of the libraries were added to ELISA plates containing immobilized GST-RHAMM(518-580) that had been pre-incubated with 4-40 kDa HA, and washed to remove excess ligand. Figure 3 illustrates the competitive displacement of peptide binding to

GST-RHAMM(518-580) by a variety of sulfated GAGs and by HA, a non-sulfated GAG. In all but one instance, 0.1 mg/ml of the 4-40 kDaHA provided optimal competition of the peptide. For the highest-affinity peptide **B-2B,** 1 mg/ml of 4 40 kDa HA was necessary to compete for peptide binding. The data in Figure 3 corroborate the known interactions of the HABD of RHAMM with GAGs. RHAMM shows a tenfold lower affinity for heparin relative to HA but neither CS-A (chondroitin 4-sulfate), CS-C (chondroitin 6-sulfate), nor dextran shows significant binding (41).

FP Assays to Verify Solid-Phase Binding Results

The data from the solid-phase binding assays were supplemented by a second methodology. FP measures the change in anisotropy of a fluorescent probe in free and bound states (42, 37, 43). An increase in anisotropy is proportional to the ligand-protein complex formation; this assay is independent of fluorescence intensity. Using a fixed concentration of each fluorescein-labeled peptide, increasing concentrations of the RHAMM-HABD were added to the wells of a 96-well plate optimized for low-background fluorescence measurements. The concentrations were chosen so that the measurements span the range from $0.01 \times K_D$ to $100 \times K_D$. Figure 4 illustrates the primary data for peptides **P-5** (1200 ± 200 nM), **B-1A** (17 ± 5 nM), and **B-4B** (220 ± 58 nM), which showed affinities of 2300 nM, 49 nM, and 499 nM, respectively, in the ELISA assay. This correlation validated the FP assay for use in measuring peptide-protein interactions for GAG-mimicking peptides.

Uptake of Fluorescent Peptides by Cells

Cellular uptake of fluorescein-labeled peptides was evaluated to address two questions: **(i)** Will RHAMM-binding peptides be recognized in the context of the complex membrane environment of a living cell that is known to overexpress cell-surface RHAMM? **(ii)** Will the fluorescent peptides also be taken up by receptor-mediated endocytosis, as already documented for fluorescent HA (18)? FACS was used to measure the binding and uptake of fluorescein-labeled HA to cells (32). While fluorescein-dextran (77 kD) was not internalized by MDA-MB-231

human mammary epithelial cells, fluorescein-labeled HA was readily internalized and uptake could be inhibited by pre-incubation with MW 700 kDa HA (data not shown). Second, the FACS analysis with these same RHAMM-expressing cells was conducted with fluorescein-labeled peptide **B-2** (Figure 5). In the absence of HA, labeled-peptide **B-2** was rapidly internalized by MDA-MB-231 cells, indeed even more effectively than fluorescein-labeled HA. Addition of 700 kDa HA demonstrates partial competition for the cellular binding and uptake. In these experiments, the competition and binding employed live cells in petri dishes, which were washed and fixed after the incubation and prior to FACS analysis.

Complete competition was not observed for the peptide uptake experiments, suggesting that the peptidic probes could be taken up by cells through more than one mechanism. Many small molecules, including many octapeptides, can diffuse across cell membranes (44, 45).

DISCUSSION

The importance of RHAMM in cell motility and metastatic progression (12, 11) provided the impetus to identify potential non-GAG ligands that could serve as HAse-resistant HA surrogates in basic research and as leads for drug design. We sought ligands that could specifically target the HABD of RHAMM but that would not be recognized by other hyaladerins such as CD44 and link protein. We propose that peptide mimics can explore conformations and chemical functionalities unavailable to natural GAG ligands. Consequently, peptide mimics may achieve novel selectivities for binding to and activation of different HA receptors. To this end, three peptide libraries were screened using the HABD of RHAMM as bait for pentadecapeptides or octapeptides with high affinity and selectivity. All three afforded high affinity binders that acted as HA surrogates, as determined by three *in vitro* binding assays and by cellular uptake experiments. The starting point for the design of Library **B**, a biased library of octamers, which contained alternating acidic residues, was inspired by the alternating pattern of glucuronic acid and N-acetylglucosamine that characterizes the linear HA structure. Moreover, we anticipated that nucleophile-rich residues would be commonly found in the HA-mimetic peptides identified by this screen. Interestingly, we identified common motifs that were rich in hydrophobic amino acids in the random Library **P**, featuring random phage-displayed 15-mers, and Library **R**, a bead-based library of random octamers. This unexpected result is nonetheless consistent with the hypothesis that HA has "hydrophobic patches" created by methine residues on one "face" of the linear HA molecule (46). Thus, by using three different peptide libraries, we approached this project using both semi-rational and unbiased approaches.

A Motif is Present in the Phage Library

The results from screening the random phage library against RHAMM revealed two consensus motifs, each of two to four residues in length. One consensus sequence was an LP motif that occurs in seven of the peptides. This hydrophobic, kinked motif was often flanked by a

hydrophobic residue and either Ala or Ser. The second motif was SAS or SPS, which was present in three of the peptides. These motifs were found using both the GST-RHAMM(518-580) and thioredoxin-RHAMM(523-580) (Table 3A) for screening. The data showed that RHAMM, not the fusion partner, was crucial to the similarity in motif recognition.

The binding affinities of four synthetically prepared phage peptides were evaluated. The Library **P** peptide with the highest affinity for RHAMM-HABD was GVCNADFCW**LP**AVVV (**P-2**) with a K_D value of 10 nM. Other peptides with the W**LP**A or I**LP**A motif, such as P-4 IPPI**LP**AYTLLGHPR (**P-4**), had affinities in the micromolar range. One can speculate as to what causes twofold difference in binding affinities. Disulfide bond formation could occur in **P-2**, thereby providing a structural constraint that presents the motif to the HABD more efficiently than other peptides. Alternatively, the flanking hydrophobic groups appear to be important in augmenting binding affinity. Thus, the lowest affinity peptide **SASPSAS**KLSLMSTV (**P-3**) with a K_D value of 10 mM may rely solely on the hydroxymethyl group recognition by the GlcNAc binding region of the HABD. Both the LP and SAS motifs appear in PHARPVV**SASSILPV** (**P-11**) but the affinity of this extremely hydrophobic and poorly soluble peptide was not determined.

Although these peptides were identified as HA mimetics, the sequence APWLYGPA, which contains the pattern APWLY, was found to be important for binding to an anti-Lewis Y antibody (47). An anagrammed sequence with four of five residues is found in GVCNADFC**WLPA**VVV (**P-2**), the highest-affinity phage-derived peptide. Related work seeking peptides as mimics of covalently-linked carbohydrates included mimics of the sialic acid residues on the envelope protein gp160 (48). In another example, peptides were identified specifically to elicit an immune response. Thus, the tripeptide sequence YRY was found to mimic the meningococcal group C capsular polysaccharide (49). This tripeptide was sufficient to elicit an immune response in mice when it was incorporated into a larger polypeptide.

Despite our preconceived notions, the random 15-mers in Library **P** were hydrophobic and serine-rich, but with the exception of a single Asp in **P-2**, lacked acidic residues. This phenomenon can be rationalized by the absence of D-configured acidic amino acids; the steric constraints on all

L-amino acid peptides limit the orientation of anionic side chains, such that carboxyl groups cannot be 124° to one another as found in HA (Figure 6). As a result, in all L-amino acid peptides, hydrophobic, and in some cases hydrogen-bonding hydroxyl, residues dominate binding and recognition. A corollary of this hypothesis is that the Library **P** peptides interact in a unique fashion with the HABD, but perhaps not precisely in the putative binding site occupied by HA. Since binding can be inhibited by excess HA and some other GAGs, the binding sites for the hydrophobic peptides and GAGs share part of a common binding region, but the sites may be congruent.

The Random Bead Library Has a Phage Motif

Superficially, Libraries **P** and **R** have little in common, since they differ in peptide length, presentation (C-terminal attachment to beads in contrast to N-terminal attachment to pili proteins), and size. The number of unique sequences in the phage Library **P** is in principle 7^{20} larger than that in the octamer beads of Library **R**. The phage peptides thus identified may represent local, but not global, minima since sampling was incomplete.

Nonetheless, a motif common to many random bead peptides was that of Pro followed by a hydrophobic residue, often Val (PX motif). The PX (X = V, Y, L, F) motif was present in five of the eleven peptides, and the PV motif occurred several times in the Library **P** (Table 3B), and was similar to the LP motif present in most of the phage peptides. In both the Libraries **P** and **R**, these motifs are in reverse form; in some cases, both forward and reverse motifs occur on the same peptide. For example, the peptide **PF**LMK**FPI** has a forward and backward PF motif, and the peptide IYI**YP**QPQ has a reverse PY motif. Three peptides were evaluated from the Library **R**: EGE**WPV**YP (**R-3**), QAMNKFTF (**R-5**), and IYIYPQPQ (**R-12**). Of these, the strongest binding peptide is **R-3** with an apparent K_D value of 48 nM. This peptide has a WPV motif similar to that of the phage peptide **WPV**SLTVCSAVWCPL (**P-1**).

The PV, PI, PL, and PF motifs also occurred in peptides screened with the link-module containing HA-binding protein TSG-6 (24). TSG-6 is a 275-amino acid secretory protein involved

in cell-cell and cell-matrix interactions during inflammation (50), and a three-dimensional solution structure of the HABD has been determined by NMR (24). None of the peptides obtained with this structurally different "bait" protein bound to GST-RHAMM(518-580), and these data will be presented in due course (M.R. Ziebell, A.J. Day, and G.D. Prestwich, unpublished results).

Precedent for Alternating Charged D- and L-Amino Acids in the Biased Library

The rationale for synthesizing Library **B** with alternating acidic amino acids was to mimic the alternation of glucuronic acids of HA, in both the linear and three-dimensional distribution of charge. The glucuronic acid moieties of HA are separated by approximately 10 Å (51), with a dihedral angle between -110° and -167°, indicating that they protrude from opposite faces of a plane that approximates the linear sequence of sugars. Since these charge repeats appear to be important in HA - protein interactions, Library **B** was designed to find peptides with alternating carboxylates with high affinity for RHAMM-HABD. To this end, Library **B** was prepared with either D- or L-enantiomers of Glu or Asp in the acidic residue position.

A non-optimized model of a random coil peptide suggested that alternating acidic residues should give a pattern of negative charges separated by approximately 10 Å. A model was thus constructed based on diastereomers discovered from the library screen. The peptides **B-2** (YDSEYESE) and **B-2B** (YDSEYeSE) were modeled using InsightII (Molecular Simulations, Inc.). From a family of ten conformers, each minimized and subjected to a routine molecular dynamics protocol, a marked difference in the orientation of the acidic side chains was apparent (Figure 6). The average distance between Glu4 HE2 and Glu6 OE1 for **B-2** was 6.11 ± 1.72 Å, while this distance for **B-2B** was 12.56 ± 1.47 Å. The averages of the absolute value of the dihedral angles between Glu4 and Glu6 side chains was 41.9 ± 29.6° for **B-2** and 129.5 ± 44.2° for **B-2B**. These parameters suggest that a peptide with alternating acidic residues, one with D configuration and one with L configuration, should most closely mimic HA. The results of this series of minimizations is graphically represented in Figure 6 in which each point is the minimized distance between the two protons, while Figure 7 illustrates three structures obtained from the molecular modeling

experiments. Coordinates for HA (Figure 7, top) were obtained from the Protein Databank (accession no. 4HYA) (51) with the glucuronic acid sugar residues highlighted. The calculated structures for the all L-configuration octapeptide **B-2** (center) and the peptide with a single D-configuration side chain **B-2B** (bottom) show the distance and angular relationships between acidic side chains. In the minimum energy conformer for **B-2**, these constants poorly imitate HA; in contrast, the minimum energy conformer for **B-2B** more adequately approximates the spatial and angular measurements of an HA oligosaccharide.

The Biased Library Favors Unnatural Acidic Residues

A number of high-affinity "hits" were sequenced from beads in Library **B**. However, even though each hit was a unique molecular species, the Edman degradation could not provide information on the absolute configuration of the particular linear sequence obtained. Thus, each sequence represented sixteen possible molecular structures. Deconvolution was accomplished by synthesis of each of the sixteen diastereomers of three Library **B** peptides using the commercial Pepspots® technology. The strongest binding peptides from the biased library were specific diastereomers of peptide **B-1** (MdYEPeQe) and **B-2** (YDSeYeSe); D-amino acids are indicated with lower case letters. Peptides with alternating D- and L-acidic residues showed the highest affinity. The "anti" relationship appeared to most closely reflect the angular orientation of carboxylates on HA, consistent with the model used to design these HA mimetic peptides. In Library **B**, we deliberately created a pattern of charges within each octapeptide. While many octapeptides bound with high affinity to the RHAMM HABD, charge distribution was not the only factor dictating binding affinity, as previously observed for Library **P** and Library **R** peptides.

Small aromatic residues (Tyr or Phe) and Ser were abundant in Library **B**, e.g., **B-2** (YDSEYESE) and **B-3** (FDFDSEYE). These aromatic residues may mimic the hydrophobic face of HA. With alternation of D- and L-acidic side chains with small aromatics or Ser, e.g., the **B-3** diastereomer FDFdSEYe, random coil conformation would have the polar and nonpolar side chains oriented 180° from each other. The formation of a hydrophobic plane

made up of two phenyl rings could reflect the conformation of HA in which the eight methines on the hydrophobic face span three sugar residues. Modeling of these peptides into a three-dimensional model of RHAMM is in progress (23).

In summary, two fusion proteins were generated that contain a 62-amino acid polypeptide comprising the HABD of RHAMM (29). The two RHAMM constructs were shown to have HA binding activity and the purified proteins had defined secondary and tertiary structure (23). Using this HABD as "bait," three peptide libraries were screened for molecules that specifically target the HABD of RHAMM. Several of the peptide hits that were identified and sequenced, were then synthesized and evaluated to determine their affinity and specificity in binding to RHAMM. Most of these peptides bound to RHAMM with high affinity, and competition by HA or other GAGs suggested that the peptides were directed to the HABD.

Potential Applications of HA-mimetic Peptides

Can these peptides act as antagonists, or molecular leads for antagonists, that could block the transforming potential of RHAMM? The cellular and *in vivo* activity of these novel HA-mimetic peptides can now be examined to investigate whether the binding to RHAMM-HABD can occur without the activation that normally occurs when HA binds. The downstream effects of RHAMM activity, in particular the ability to activate Erk1 (7), continues to be an active research area (52). Cells expressing RHAMM could be refractory to changes in extracellular matrix ligands, which could in turn alter their growth, movement, and proliferation. Phage-derived peptides that bound the CTLA4 receptor were found to vary in potency for activation of T cells (53).

Alternatively, peptidic ligands for HA receptors could be valuable for drug targeting. The problem of directing anti-cancer agents to tumors remains one of the technological barriers to developing effective therapies for cancer treatment (54). The overexpression of RHAMM on cancer cells relative to normal epithelial cells provides an opportunity for tumor-specific drug

targeting. HA-conjugated anti-tumor agents (55) and other drugs (56) often lack specificity for a particular class of HA receptors.

Either as therapeutics or targeting moieties, HA-mimetic peptides may offer several pharmacologically unique properties relative to HA. First, the peptides are resistant to HAse degradation. Second, peptides can act as antagonists rather than agonists. Third, peptides can be selected that would not be recognized by liver endothelial cell receptors involved in HA clearance from circulation (57). Fourth, peptides could be selected to be specific for RHAMM isoforms or CD44 isoforms that are present in pathological situations.

ACKNOWLEDGMENTS

We thank Dr. J.T. Elliott (The Univesity at Stony Brook, USB) and Professor R. El Magrahbi (USB) for biophysical advice, Mr. C. Pond and Dr. P. Cassidy for expertise in phage display, Mr. R. Gerhart for bead-picking, and Dr. R.W. Schackmann for peptide sequencing and synthesis.

FIGURE LEGENDS

Figure 1. Deconvolution of Library **B** diastereoisomers. Peptides were synthesized as 5 nmol "Pepspots®" and transferred to PVDF as described in the text. A chemiluminescence assay with an HRP-labeled secondary-antibody was used to detect GST-RHAMM(518-580) bound to each peptide spot. The intensity of each spot was quantified with NIH Image software. Data shown is from a single film, but the results were validated from three blots.

Figure 2. Solid-phase fluorescence binding assay to compare binding of fluorescein-labeled peptides to GST-RHAMM(518-580) and GST alone.

Figure 3. Comparison of the ability of GAGs to inhibit binding of peptides to GST-RHAMM(518-580) using the solid-phase colorimetric binding assay. **Key**: HA, hyaluronic acid; HEP, heparin; DEX SUL, dextran sulfate; CS-A, chondroitin 4-sulfate; CS-C, chondroitin 6-sulfate.

Figure 4. Binding curves and Scatchard analyses of FP measurements of GST-RHAMM(518-580) binding peptides **B-1A**, **B-4B**, and **P-5**.

Figure 5. FACS analysis of **B-2** binding and uptake by MDA-MB-231 cells. **Panel A**, cells with no probe as control; **Panel B**, cells pre-incubated with HA to compete uptake, followed by fluorescein-**B-2**; **Panel C**, cells with fluorescein-HA as a positive control; **Panel D**, cells with fluorescein-**B-2** with no competitor present.

Figure 6. Summary of ten molecular dynamics and minimization routines on peptides **B-2** and **B-2B**. The distance is measured between Glu4 HE2 and Glu6 OE1 on either peptide. The modeling was performed in Discover and included 1,000 iterations of minimization runs using an Amber force field. The dynamics routine had 10,000 steps including charge and Morse terms.

Figure 7. Molecular model showing calculated minimum energy structures for HA (top), peptide **B-2**, YDSEYESE (middle, all L-amino acids), and peptide **B-2B**, YDSEYeSE (bottom) containing a single D-Glu residue. The carboxylate-to-carboxylate distances are indicated by double-headed arrows in each energy-minimized structure.

REFERENCES

1. Fraser, J. R., Laurent, T. C. and Laurent, U. B. (1997) *J. Intern. Med.* **242**, 23-24.

2. Toole, B. P. (1997) *J. Intern. Med.* **242**, 35-40.

3. Oksala, O., Salo, T., Tammi, R., Hakkinen, L., Jalkanen, M., Inki, P. and Larjava, H. (1995) *J. Histochem. Cytochem.* **43**, 125-135.

4. Entwistle, J., Hall, C. L. and Turley, E. A. (1996) *J. Cell. Biochem.* **61**, 569-577.

5. Sherman, L., Sleeman, J., Herrlich, P. and Ponta, H. (1994) *Curr. Opin. Cell. Biol.* **6**, 726-733.

6. Turley, E. A.and Harrison, R. (1999) RHAMM, a member of the hyaladherins. www.glycoforum.gr.jp.

7. Zhang, S., Chang, M. C., Zylka, D., Turley, S., Harrison, R. and Turley, E. A. (1998) *J. Biol. Chem.* **273**, 11342-11348.

8. Hall, C. L., Wang, C., Lange, L. A. and Turley, E. A. (1994) *J. Cell Biol.* **126**, 575-588.

9. Hall, C. L., Lange, L. A., Prober, D. A., Zhang, S. and Turley, E. A. (1996) *Oncogene.* **13**, 2213-2224.

10. Hall, C. L., Yang, B., Yang, X., Zhang, S., Turley, M., Samuel, S., Lange, L. A., Wang, C., Curpen, G. D., Savani, R. C. and Turley, E. (1995) *Cell.* **82**, 19-26.

11. Yamada, Y., Itano, N., Narimatsu, H., Kudo, T., Hirohashi, S., Ochiai, A., Niimi, A., Ueda, M. and Kimata, K. (1999) *Jpn. J. Cancer Res.* **90**, 987-992.

12. Wang, C., Thor, A. D., Moore, D. H., 2nd, Zhao, Y., Kerschmann, R., Stern, R., Watson, P. H. and Turley, E. A. (1998) *Clin. Cancer Res.* **4**, 567-576.

13. Assmann, V., Marshall, J. F., Fieber, C., Hofmann, M. and Hart, I. R. (1998) *J. Cell. Sci.* **111**, 1685-1694.

14. Abetamann, V., Kern, H. F. and Elsasser, H. P. (1996) *Clin. Cancer Res.* **2**, 1607-1618.

15. Crainie, M., Belch, A. R., Mant, M. J. and Pilarski, L. M. (1999) *Blood* **93**, 1684-1696.

16. Till, K. J., Zuzel, M. and Cawley, J. C. (1999) *Cancer Res.* **59**, 4419-4426.

17. Pilarski, L. M., Pruski, E., Wizniak, J., Paine, D., Seeberger, K., Mant, M. J., Brown, C. B. and Belch, A. R. (1999) *Blood* **93**, 2918-2927.

18. Collis, L., Hall, C., Lange, L., Ziebell, M. R., Prestwich, G. D. and Turley, E. A. (1998) *FEBS Lett.* **440**, 444-449.

19. Assmann, V., Jenkinson, D., Marshall, J. F. and Hart, I. R. (1999) *J. Cell. Sci.* **112**, 3943-3954.

20. Yang, B., Zhang, L. and Turley, E. A. (1993) *J. Biol. Chem.* **268**, 8617-8623.

21. Yang, B. H., Yang, B. L., Savani, R. C. and Turley, E. A. (1994) *EMBO J.* **13**, 286-296.

22. Day, A. J. (1999) *Biochem. Soc. Trans.* **27**, 115-121.

23. Ziebell, M. R. (2000) Ph. D. Dissertation, The University at Stony Brook.

24. Kohda, D., Morton, C. J., Parkar, A. A., Hatanaka, H., Inagaki, F. M., Campbell, I. D. and Day, A. J. (1996) *Cell.* **86**, 767-775.

25. Bajorath, J., Greenfield, B., Munro, S. B., Day, A. J. and Aruffo, A. (1998) *J. Biol. Chem.* **273**, 338-343.

26. Entwistle, J., Zhang, S. W., Yang, B. H., Wong, C., Li, Q., Hall, C. L., JA, Mowat, M., Greenberg, A. H. and Turley, E. A. (1995) *Gene.* **163**, 233-238.

27. Lam, K. S. (1997) *Anticancer Drug Dis.* **12**, 145-167.

28. Sambrook, J., Fritsch, E. F. and Maniatis, T. (1989) Molecular Cloning, A Laboratory Manual. Plainview, NY, Cold Spring Harbor Laboratory Press.

29. Wang, C., Entwistle, J., Hou, G. P., Li, Q. A. and Turley, E. A. (1996) *Gene.* **174**, 299-306.

30. Pouyani, T.and Prestwich, G. D. (1994) *Bioconjugate Chem.* **5**, 370-372.

31. Yu, Q.and Toole, B. P. (1995) *Biotechniques* **19**, 122-125.

32. Luo, Y.and Prestwich, G. (1999) *Bioconjugate Chem.* **10**, 755-763.

33. Scott, J. K.and Smith, G. P. (1990) *Science.* **249**, 386-390.

34. Lam, K. S.and Lebl, M. (1994) *Methods: A Companion to Meth. Enz.* **6**, 372-380.

35. Wu, J., Ma, Q. N. and Lam, K. S. (1994) *Biochemistry.* **33**, 14825-14833.

36. Dandliker, W., Hsu, M., Levin, J. and Rao, B. (1981) *Methods Enzymol.* **74**, 3-28.

37. Lynch, B. A., Loiacono, K. A., Tiong, C. L., Adams, S. E. and MacNeil, I. A. (1997) *Analyt. Biochem.* **247**, 77-82.

38. Yang, B. H., Yang, B. L. and Goetinck, P. F. (1995) *Analyt. Biochem.* **228**, 299-306.

39. Hoare, K., Savani, R. C., Wang, C., Yang, B. and Turley, E. A. (1993) *Connect. Tissue Res.* **30**, 117-126.

40. Friguet, B., Chaffotte, A. F., Djavadi-Ohaniance, L. and Goldberg, M. E. (1985) *J. Immun. Meth.* **77**, 305-319.

41. Yang, B., Hall, C. L., Yang, B. L., Savani, R. C. and Turley, E. A. (1994) *J. Cell. Biochem.* **56**, 455-468.

42. Checovich, W., Bolger, R. and Burke, T. (1995) *Nature* **375**, 254-256.

43. Wei, A.and Herron, J. (1993) *Analyt. Chem.* **65**, 3372-3377.

44. Kastin, A. J., Pan, W., Maness, L. M. and Banks, W. A. (1999) *Brain Res.* **848**, 96-100.

45. Oehlke, J., Beyermann, M., Wiesner, B., Melzig, M., Berger, H., Krause, E. and Bienert, M. (1997) *Biochim. Biophys. Acta* **1330**, 50-60.

46. Day, A. J.and Parkar, A. A. (1999) *In*, The Chemistry, Biology and Medical Applications of Hyaluronan and its Derivatives. London, Portland Press.

47. Murali, R.and Kieber-Emmons, T. (1997) *J. Mol. Recognit.* **10**, 269-276.

48. Agadjanyan, M., Luo, P., Westerink, M. A., Carey, L. A., Hutchins, W., Steplewski, Z., Weiner, D. B. and Kieber-Emmons, T. (1997) *Nature Biotechnol.* **15**, 547-51.

49. Westerink, M. A., Giardina, P. C., Apicella, M. A. and Kieber-Emmons, T. (1995) *Proc. Natl. Acad. Sci. USA.* **92**, 4021-5.

50. Lee, T. H., Wisniewski, H. G. and Vilcek, J. (1992) *J. Cell Biol.* **116**, 545-57.

51. Winter, W. T.and Arnott, S. (1977) *J. Molec. Biol.* **117**, 761-84.

52. Zhang, S., Ziebell, M., Cheung, W.-F., Lu, J., Haddad, A., Litchfield, D., Ahn, N., Cruz, T., Prestwich, G. and Turley, E. (2000) *Molec. Biol. Cell* in revision.

53. Fukumoto, T., Torigoe, N., Kawabata, S., Murakami, M., Uede, T., Nishi, T., Ito, Y. and Sugimura, K. (1998) *Nature Biotechnol.* **16**, 267-270.

54. Dubowchik, G. M.and Walker, M. A. (1999) *Pharmacol. Ther.* **83**, 67-123.

55. Luo, Y., Ziebell, M. R. and Prestwich, G. D. (2000) *Biomacromolecules* in press.

56. Vercruysse, K. P.and Prestwich, G. D. (1998) *Crit. Rev. Therap. Drug Carr. Syst.* **15**, 513-555.

57. McCourt, P. A. G. (1999) *Matrix Biology* **18**, 427-432.

Table 1. Sequences of HA-mimetic peptides. Peptides encoded by cDNA from phage Library **P** and obtained from direct Edman degradation on beads are presented below. Phage screening was performed using both GST-RHAMM(518-580) (Target A) and thioredoxin-RHAMM(523-580) (Target B). One-peptide one-bead Libraries **R** and **B** were screened with GST-RHAMM(518-580) only. Peptide **NB** is a negative control bead selected from the first round of screening of Library **B**.

Target		Phage		Random		Biased	
P-1	B	WPVSLTVCSAVWCPL		**R-1**	SGRPYKPP	**B-1**	MDYEPEQE
P-2	B	GVCNADFCWLPAVVV		**R-2**	YXSSNKPG	**B-2**	YDSEYESE
P-3	B	SASPSASKLSLMSTV		**R-3**	EGEWPVYP	**B-3**	FDFDSEYE
P-4	A	IPPILPAYTLLGHPR		**R-4**	WNYTEAKG	**B-4**	EDAENDEE
P-5	A	YSVYLSVAHNFVLPS		**R-5**	QAMNKFTF		
P-6	A	YRVYLSVVHNSVLPS		**R-6**	NTDSNKNM	**NB**	IDSDWEGE
P-7	A	RVGXSATWDQFDVPG		**R-7**	NPVFNDGY		
P-8	A	QWARCNGCSWTALGI		**R-9**	FLRWFIMI		
P-9	A	FFAGGLMYRIGFSSD		**R-10**	EMAQMLLE		
P-10	A	SPSLDCSWPLVKFSS		**R-11**	PFLMKFPI		
P-11	A	PHARPVVSASSILPV		**R-12**	IYIYPQPQ		
P-12	B	GRFGSGNCSSTFCWF					
P-13	A	HWCLPLLACDTFARA					

Table 2. Binding affinities for synthetic HA-mimetic peptides. The data below were obtained using the solid-phase ELISA using N-terminally biotinylated peptides as described in the text. In the amino acid sequences, uppercase letters represent the natural L-configuration and lowercase letters represent the D-configurations of Glu (E, e) and Asp (D, d). **Key**: y = binding competitively displaced by preincubation of RHAMM-HABD with HA; n = binding not displaced; nd = not determined.

Name	Sequence	Competition with HA	K_d from Plate Assay (nM)	K_d from FP(nM)
Library **P**				
P-2	CGVCNADFCWLPAVVV	y	14 ± 2	
P-3	CSASPSASKLSLMSTV	y	130000 ± 150	
P-4	CIPPILPAYTLLGHPR	y	14000 ± 100	
P-5	CYSVYLSVAHNFVLPS	y	2300 ± 50	1200 ± 200
P-6	CHWCLPLLACDTFARA	nd	nd	
Library **B**				
B-1	CMDYEPEQE	nd	nd	
B-1A	CMdYEPeQe	y	49 ± 3	17 ± 5
B-1B	CMDYePEQe	y	73 ± 5	
B-2	CYDSEYESE	y	nd	
B-2A	CYDSeYeSe	y	8 ± 1	
B-2B	CYDSEYeSE	y	74 ± 8	
B-3	CFDFDSEYE	nd	nd	
B-3A	CFDFdSEYe	y	730 ± 25	
B-3B	CFdFdSEYE	y	1400 ± 200	
B-4A	CEDAeNdEe	y	110 ± 13	
B-4B	CEdAENdEe	y	499 ± 75	220 ± 58
Library **R**				
R-3	CEGEWPVYP	y	48 ± 2	
R-5	CQAMNKFTF	y	270 ± 45	
R-12	CIYIYPQPQ	y	5300 ± 85	

Table 3. Motif recognition in HA mimetic peptides. **Panel A**. Alignment of Library **P** sequences showing the XLPX and SAS/SPS consensus motifs. **Panel B**. Alignment of Library **R** sequences showing the PX motif, and one phage sequence included for comparison.

A

Library P Consensus Motif
WPVSLTVCSAV**WCPL**
H**WCLP**LLACDTFARA
PHXRPVVSASS**ILPV**
YSVYLSVAHNF**VLPS**
YRVYLSVVHNS**VLPS**
GVCNAD**F**C**WLPA**VVV
IPP**ILPA**YTLLGHPR
SPSLDCSWPLVKFSS
SA**SPS**ASKLSLMSTV

B

Library R Consensus Motif
PHAR**PV**VSASSIL**PV**
W**PV**SLTVCSAVWCPL
EGEW**PV**YP
N**PV**FNDGY
PFLMKFPI
SGR**PY**KPP
IYIY**PQ**PQ
YXSSNK**PG**

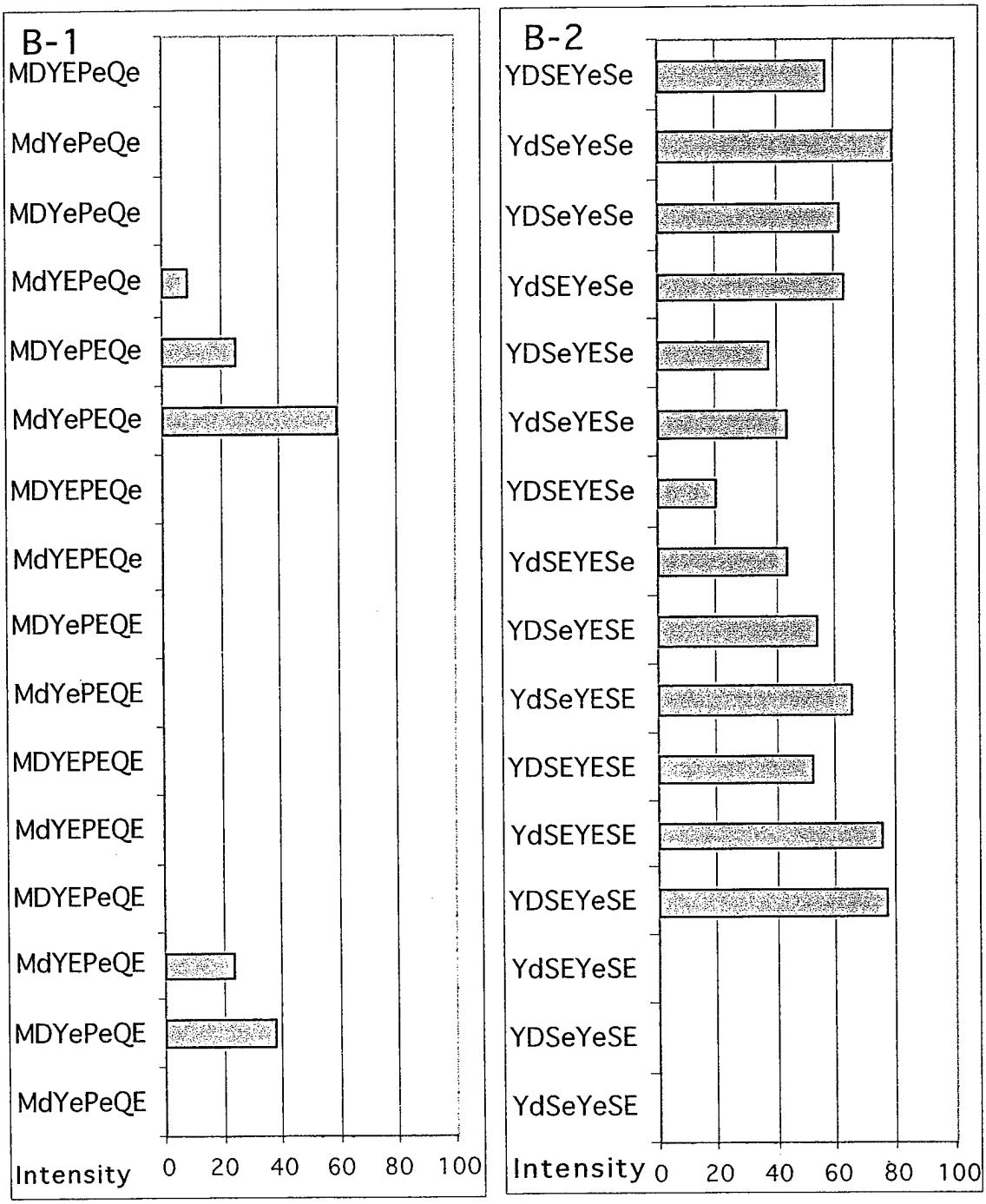
B-1
MDYEPeQe
MdYePeQe
MDYePeQe
MdYEPeQe
MDYePEQe
MdYePEQe
MDYEPEQe
MdYEPEQe
MDYePEQE
MdYePEQE
MDYEPEQE
MdYEPEQE
MDYEPeQE
MdYEPeQE
MDYePeQE
MdYePeQE
Intensity
0 20 40 60 80 100
B-2
YDSEYeSe
YdSeYeSe
YDSeYeSe
YdSEYeSe
YDSeYESe
YdSeYESe
YDSEYESe
YdSEYESe
YDSeYESE
YdSeYESE
YDSEYESE
YdSEYESE
YDSEYeSE
YdSEYeSE
YDSeYeSE
YdSeYeSE
Intensity
0 20 40 60 80 100

Figure 1

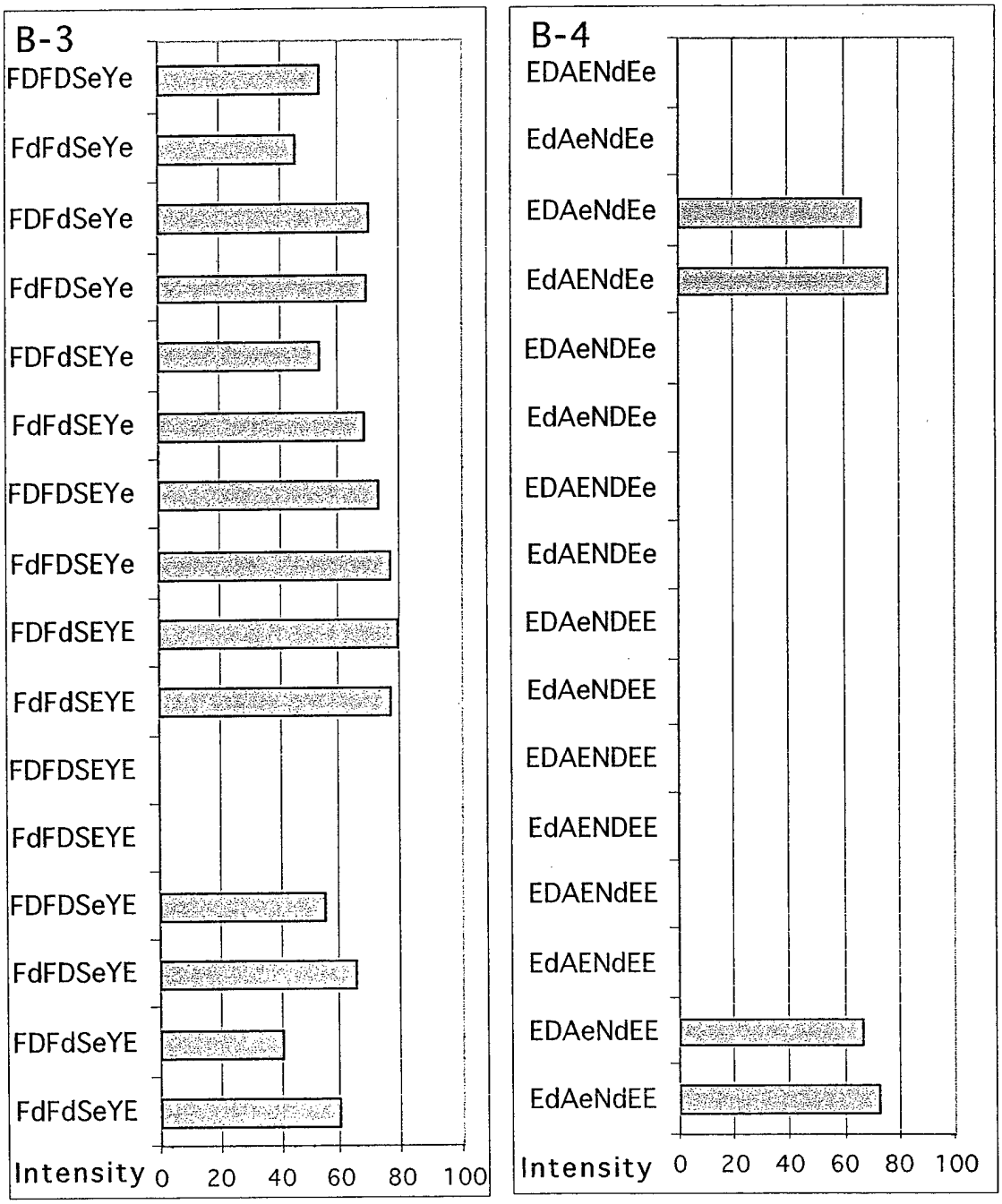

Figure 1
(continued)

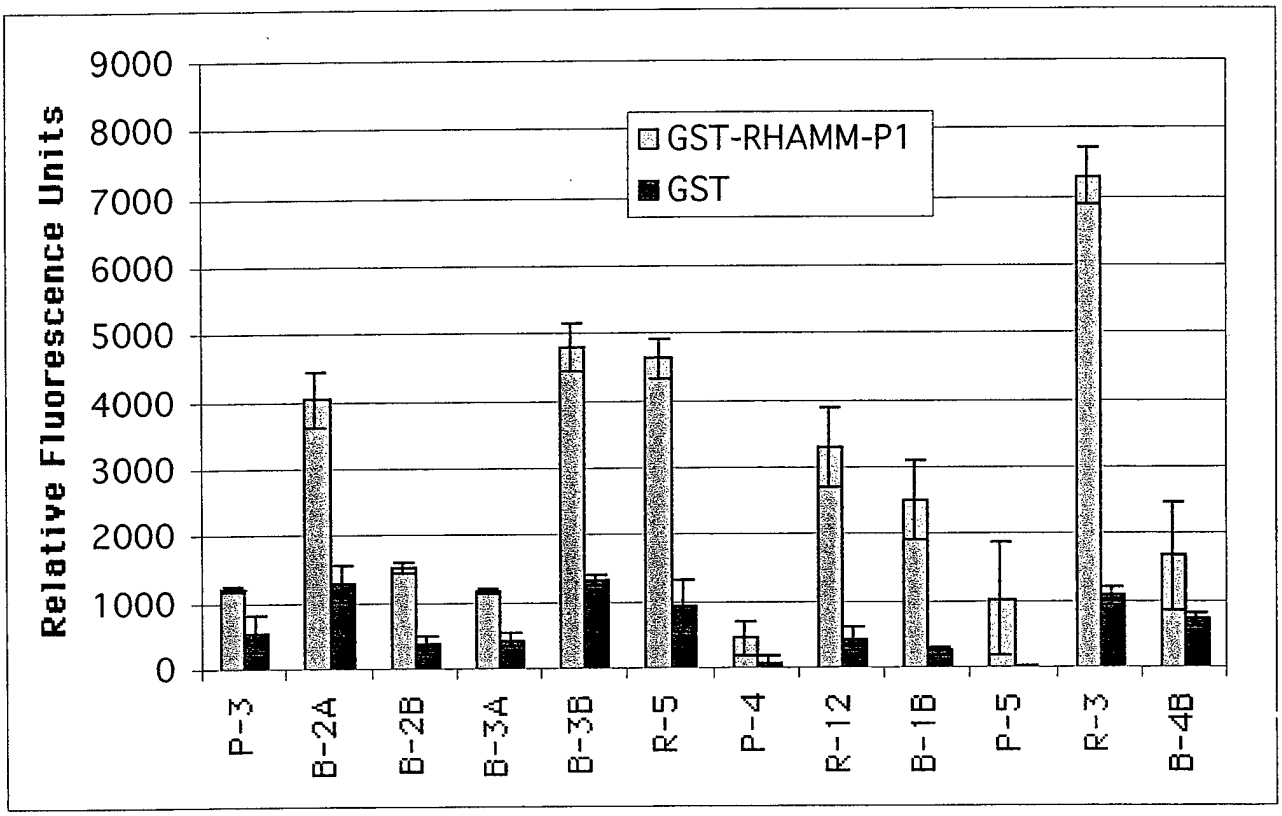
Relative Fluorescence Units
9000
8000
7000
6000
5000
4000
3000
2000
1000
0
GST-RHAMM-P1
GST
P-3
B-2A
B-2B
B-3A
B-3B
R-5
P-4
R-12
B-1B
P-5
R-3
B-4B

Figure 2

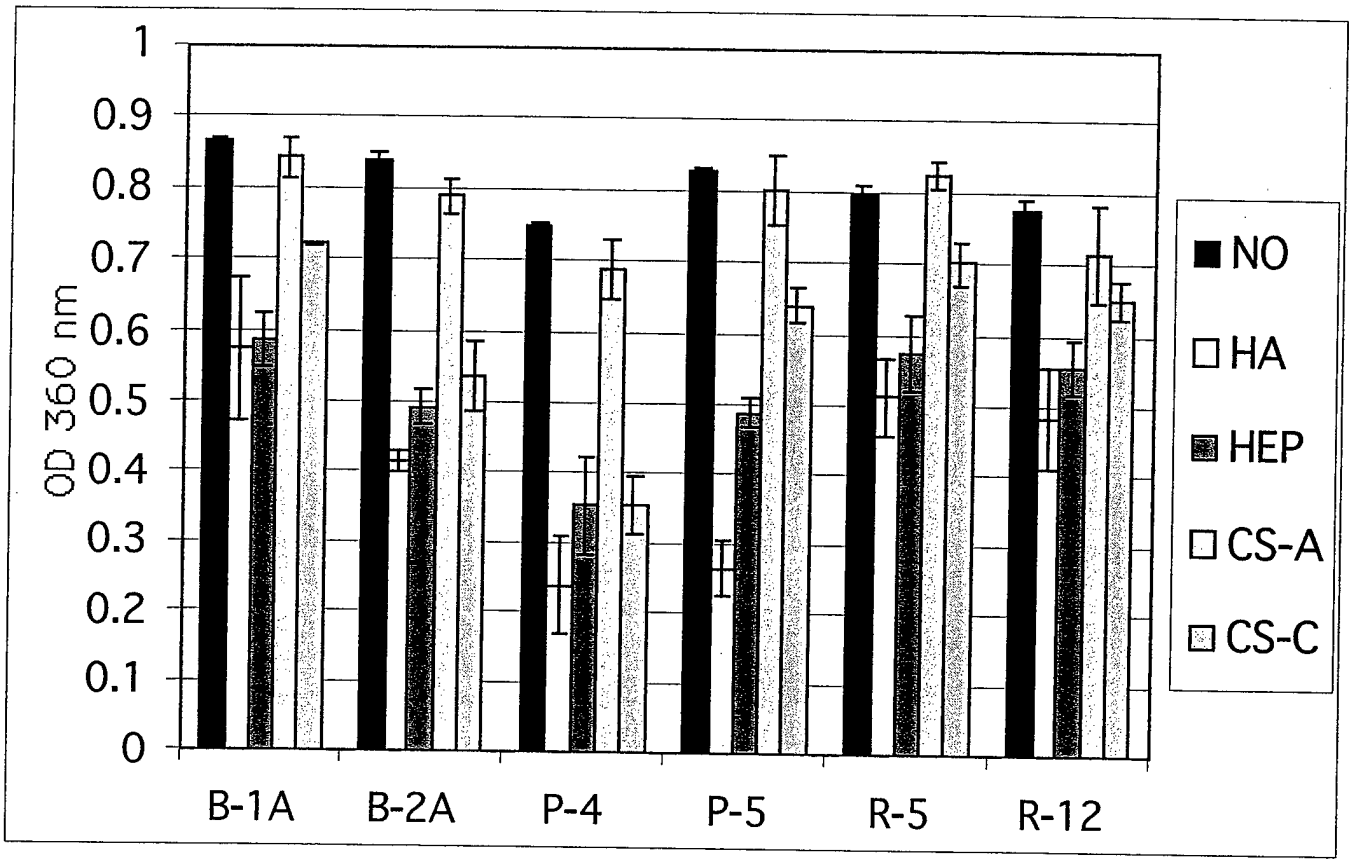
1
0.9
0.8
0.7
0.6
0.5
0.4
0.3
0.2
0.1
0
OD 360 nm
B-1A
B-2A
P-4
P-5
R-5
R-12
NO
HA
HEP
CS-A
CS-C

Figure 3

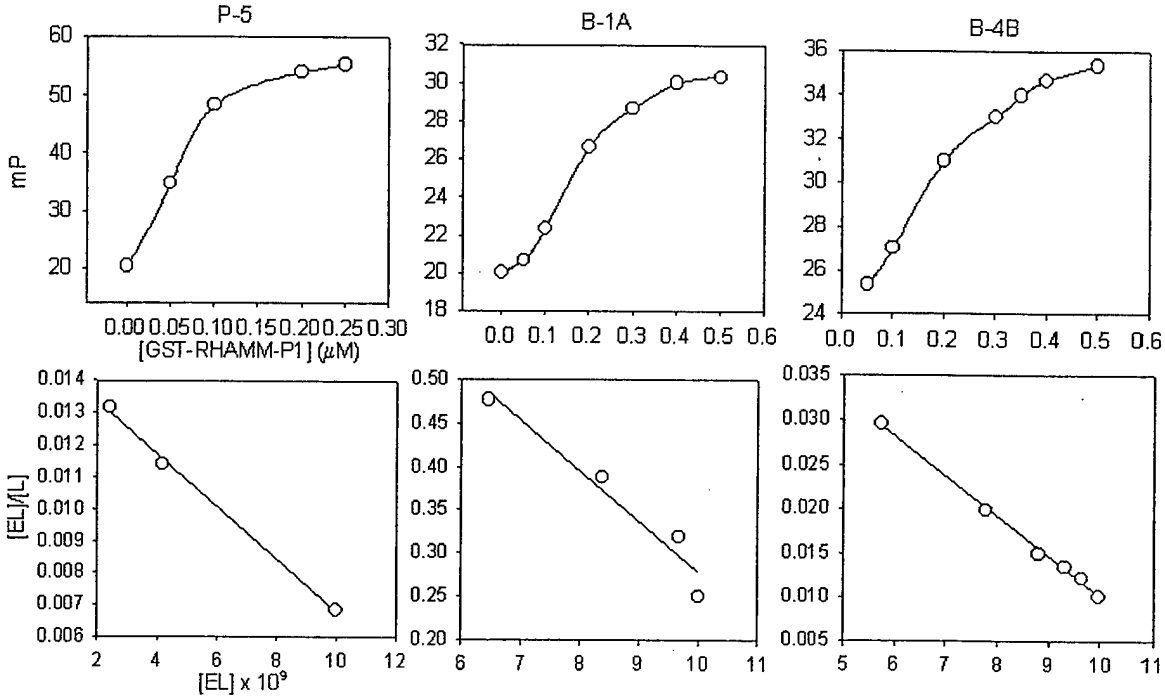

Figure 4

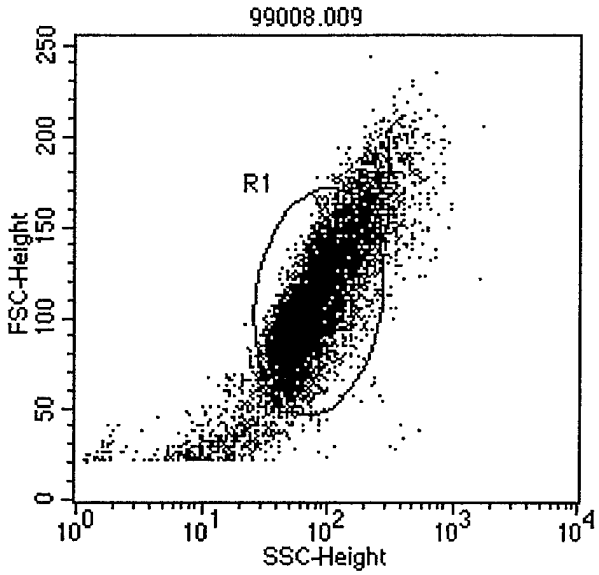
99008.009
R1
FSC-Height
SSC-Height
0
50
100
150
200
250
10^0
10^1
10^2
10^3
10^4

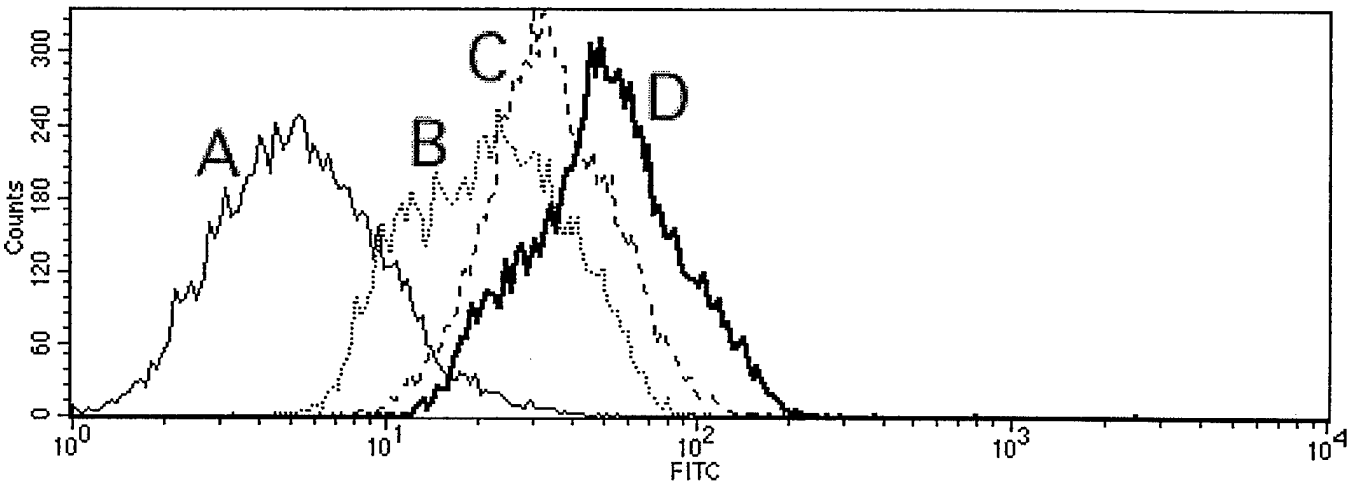
A
B
C
D
Counts
FITC
0
60
120
180
240
300
10^0
10^1
10^2
10^3
10^4

Figure 5

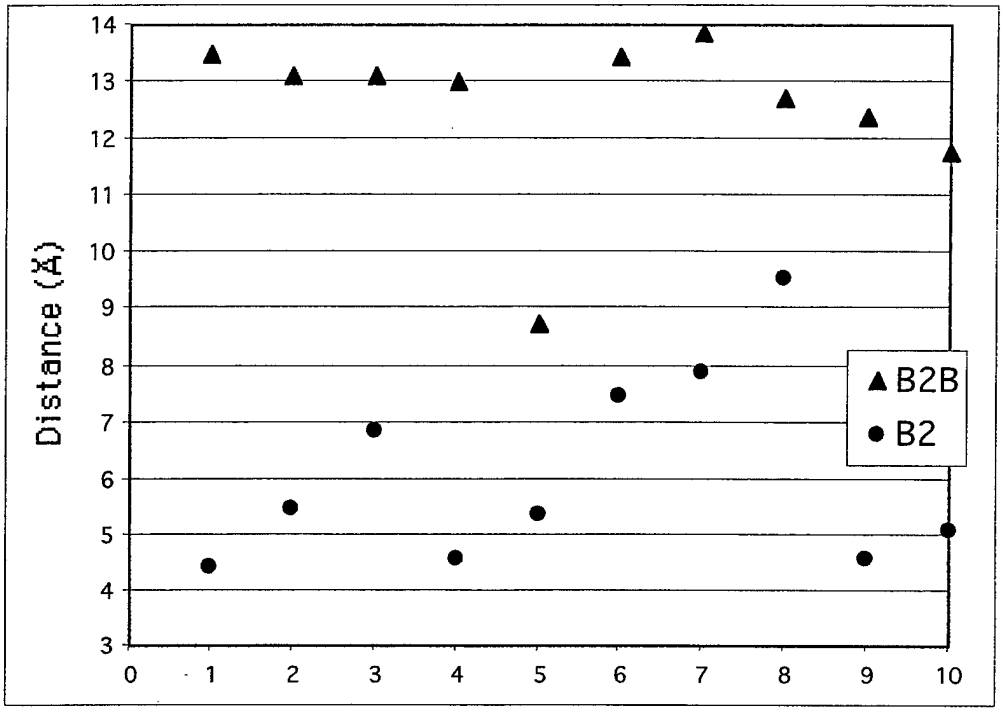
Distance (Å)
14
13
12
11
10
9
8
7
6
5
4
3
0
1
2
3
4
5
6
7
8
9
10
B2B
B2

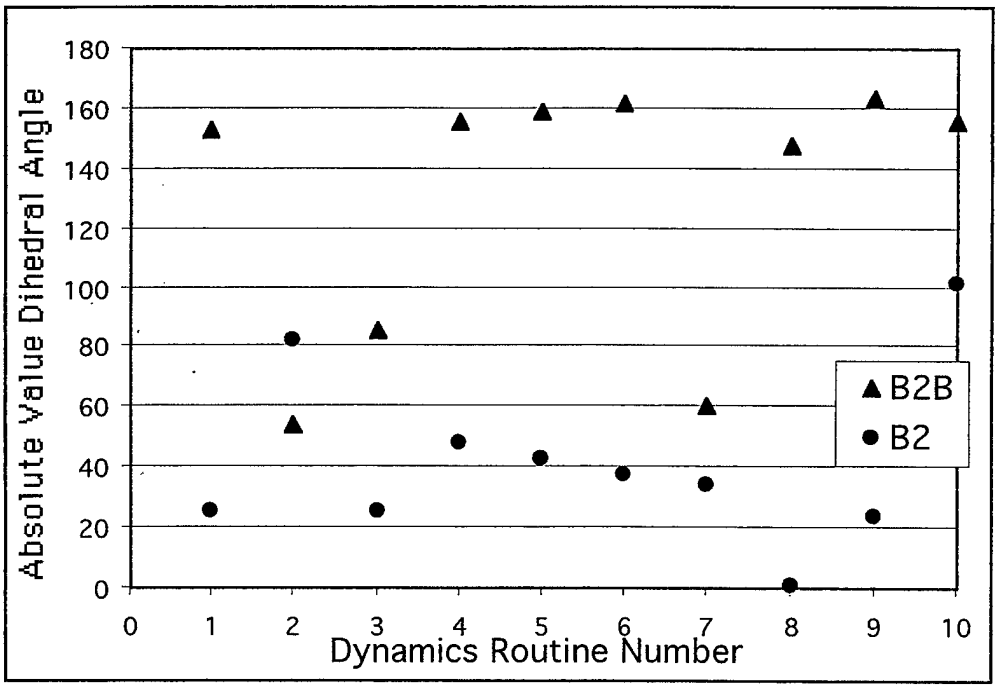
Absolute Value Dihedral Angle
180
160
140
120
100
80
60
40
20
0
0
1
2
3
4
5
6
7
8
9
10
Dynamics Routine Number
B2B
B2

Figure 6

HA

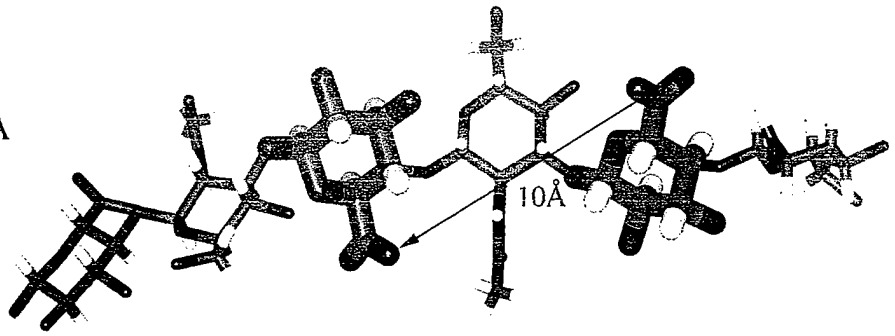

B-2 Peptide (All L)

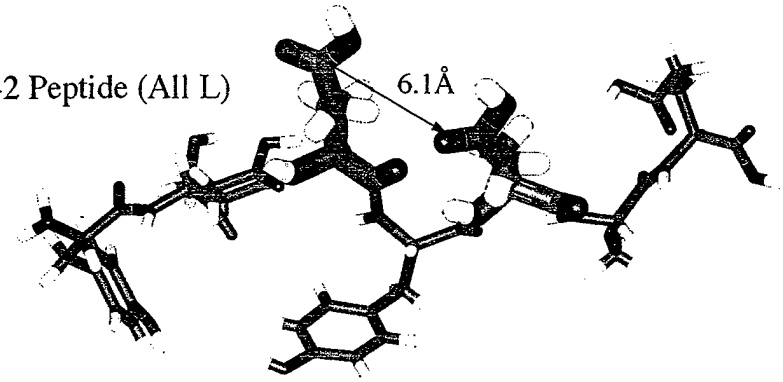

B-2B Peptide (Alternating D and L)

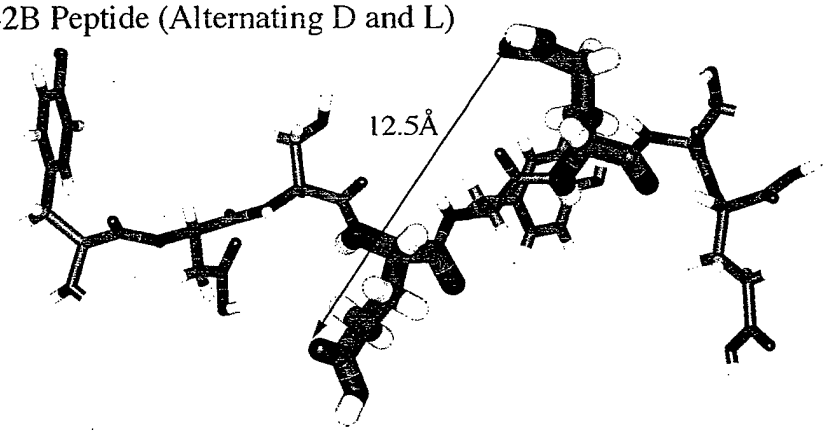

Figure 7

Molec. Cell. Biol., in press (2000).

Intracellular RHAMM is an erk1 Binding Protein and Removal of its N-Terminal Sequence is Required for Activation of erk1

SHIWEN ZHANG,[1] M. ZIEBELL,[2] WING-FAI CHEUNG,[3] JIE LU, [1]
ABRAHAM HADDAD,[1] DAVID LITCHFIELD,[4] NATALIE G. AHN,[5] TONY T. CRUZ,[3]
GLENN D. PRESTWICH,[2] AND EVA A. TURLEY[1]*

[1]Division of Cardiovascular Research, The Hospital for Sick Children, and the Departments of Anatomy/Cell Biology, Laboratory Medicine and Pathology, University of Toronto, Toronto, ON M5G 1X8; [[2]University of Utah, Department of Medicinal Chemistry, Salt Lake City, UT 84112-5820; [3]Samuel Lunenfeld Research Institutre, Mount Sinai Hospital, Toronto, ON M5G 1X5, [4]Department of Biochemistry, University of Western Ontario, London, ON N6A 5C1; [5]Department of Chemistry and Biochemistry, University of Colorado, Boulder, CO 80309-0215

*Corresponding author. The Hospital for Sick Children, Div'n of Cardiovascular Research, 555 University Avenue, Toronto, ON Canada M5G 1X8

Telephone: (416) 813 5918. FAX: (416) 813 7480. e-mail: eturley@sickkids.on.ca

Running title: RHAMM binds to erk1

ABSTRACT

Several molecular weight forms of intracellular RHAMM have been reported to be expressed, a common 95 kDa protein (termed v5) and lesser amounts of 60-73 kDa forms. The latter represent N-terminal truncations of the 95 kDa protein. We show here that ras transformed fibroblasts express 95 and 73 kDa RHAMM forms. The 73 kDa protein corresponds to a RHAMM isoform termed v4, that has previously been shown to be transforming when overexpressed, to co-immunoprecipitate with erk 1 and to be required for activation of erk through ras. *In vitro* binding and competition analyses, as well as *in vivo* analyses of mutant proteins show that both v4 and v5 RHAMM proteins bind directly to erk 1 by two non-contiguous sequences near their COOH-terminus. Both RHAMM proteins associate with MEK1 *in vivo* but do not bind directly to this kinase. This association requires the presence of 20 amino acids present in both proteins and previously shown to be required for the transforming function of RHAMMv4. Overexpression of a cDNA, representing v4, activates erk 1, activates AP-1, enhances expression and release of MMP-9, and transforms fibroblasts. Furthermore, v4 synergizes with mutant active MEK1 to promote activation of erk1 and to strongly enhance transformation of fibroblasts. Deletion of the erk1 binding domains or the domain required for association of MEK1 block the ability of v4 to synergize with mutant active MEK1 and to enhance the expression and release of MMP-9. In contrast, overexpression of v5, which contains additional 163 N terminal amino acids not present in v4, does not affect erk activity and does not transform fibroblasts. Further, v5 only weakly synergizes with mutant active MEK1 to promote activation of erk, and does not enhance the transforming function of the mutant active kinase. These results indicate that intracellular RHAMM forms are erk1 binding proteins that regulate the activation of erk1 at the level of erk1/MEK1 interactions. V5, which is the most common form of intracellular RHAMM, is negatively regulated in this function by its unique N-terminal sequence, while the shorter forms of RHAMM, such as v4, appear to be biologically active . Possible physiological roles for active RHAMM forms are discussed.

Key words: RHAMM, erk1, MEK1, MMP-9, cell transformation

INTRODUCTION

Activating mutations or overexpression of the small GTPase ras are amongst the most common events in human tumors (50). Ras regulates multiple signaling pathways, many of which can lead to tumorigenesis when constitutively activated (5,19,53). Recently, studies using transgenic animal models suggest that amplication of ras and constitutive activation of the erk kinase cascade is a late event associated with tumor progression (23,33,44) consistent with many studies showing activation of this map kinase cascade is required for cell motility, tumor invasion (16,21,22,48,56), the production of several classes of proteases involved in cell motility/invasion (20) and with an ability of transformed cells to metastasize (20,23,53). Delineating the molecular mechanisms controlling erk activation will therefore be highly relevant to understanding the nature of tumor invasion and metastasis.

Identification of yeast Ste-5, a scaffold protein that complexes a map kinase cascade (7,27,38), first suggested that accessory proteins may play key roles in the regulation and compartmentalization of map kinase cascades, a phenomenon that had previously been noted for other signaling cascades (35). The recent identification of a mammalian map kinase accessory protein, MP-1, that enhances activation and association of MEK1 with erk1 (42), as well as of Jip-1 (55), a scaffold protein linking components of the jnk map kinase cascade, and IkAP, a scaffold protein of the Ikappa B lamin complex (8), predict that diverse accessory proteins regulate activation, insulation and targeting of map kinase cascades.

We previously identified a hyaluronan binding protein, RHAMM, as a regulator of ras-controlled cell motility and proliferation (14). This protein occurs both on the cell surface (9,12,14,36,60), despite an apparent lack of signal sequence and transmembrane domain, and intracellularly (3,9,14,17,51). Antibody/peptide mimetic blocking and use of intracellular dominant negative RHAMM mutants, suggest a functional role for both cell surface and intracellular forms of RHAMM in ras-regulated pathways, in particular the erk 1 kinase cascade (9,12,14,36,52,60). We (51) and others (3,17) have noted that the most common murine RHAMM RNA transcript encodes a 95 kDa protein. We have also reported a rare RHAMM

mRNA transcript (v4) that encodes a 73 kDa protein, which lacks 163 N-terminal amino acids found in the longer RHAMM form (10). This shortened RHAMM form associates with erk 1 *in vivo*, is transforming when overexpressed and regulates activation of the erk kinase cascade through ras as determined by use of dominant negative v4 mutants and overexpression of v4 (14,60). Although others (17,24,28) have also noted the presence of both the 95 kDa and 73 kDa proteins in cultured cells, the functional significance of these two RHAMM forms has not previously been determined.

Here, we demonstrate that ras-transformed fibroblasts express both the 95 kDa (termed RHAMMv5) and 73 kDa (termed RHAMMv4) (10) proteins. We note that the v5 mRNA transcript is highly expressed in these cells but a minor v4 transcript, detectable by RT-PCR, is expressed early after cell plating. We confirm that this transcript represents a full length RHAMM mRNA corresponding to the 73 kDa RHAMM protein. Both the v4 and v5 RHAMM proteins directly bind to erk1 and indirectly associate with MEK1. Evidence is presented that the RHAMMv4 protein represents an activated form, resulting from lack of an inhibitory N-terminal domain unique to the longer v5 protein. Thus, only RHAMMv4 is able to activate erk 1, enhance MMP-9 expression and transform fibroblasts. These properties of RHAMMv4 require its erk 1 binding domains and a domain that mediates an indirect association with MEK1. V4 appears to act by enhancing the ability of MEK1 to activate erk1.

MATERIALS AND METHODS

Cell Lines and Cell Culture. The cell lines used were derived from parental murine 10T1/2 or NIH3T3 mutant active fibroblasts. H-*ras*-transfected 10T1/2, CIRAS-3 (C3), RHAMMv4 transfected, RHAMMv5 transfected, 10T1/2 cells expressing RHAMM anti-sense (U21 cells) and parental 10T1/2 cells were grown as described (14). Briefly, cells were maintained at 37°F in 5% CO_2 in DMEM growth medium (GIBCO, Gaithersburg, MD) supplemented with 10% fetal calf serum (Invitrogen). Cells were grown to 70-80% confluence prior to passage. Cell cultures used for analysis were always plated at 50% confluence.

Plasmid Constructs and Protein Purification. For transfection, the RHAMMv4 and v5 cDNA and mutant forms of RHAMM were subcloned into the expression vector phβApr-1-neo as described (14,60). A mutant active MEK1(ΔN3/S218E/S222D) construct was obtained from N. Ahn (Howard Hughes Institute, University of Colorado, Bolder, CO). For transient co-transfection of RHAMMv4 dominant negative with erk1, RHAMMv4 cDNA hyaluronan binding domains were mutated as described (14) and a triple HA tag was placed close to the C-terminus of RHAMMv4 as described (60). A myc-tagged RHAMMv5 was constructed by PCR using primers, 5'-GCCCTCGAGTTGTTGTCTGA GTTGATTTTTC-3' and 5'-GCCCTC GAGCAGAAGCTAATAAGCGAAGAAGACCTCAAC GATGGAAGACTTTAGGAAGCAG. The myc tag sequence (underlined) was inserted between RHAMM #631 and #632 amino acids. Myc-tagged RHAMMv5 cDNA was subcloned into pCDNA3.1 (Invitrogen)with an EcoR I site. A myc-tagged erk1 was generated by polymerase chain reaction using the 5' primer GCGGGAT CCATGGGCGGGGGCGGGGAGCCCAGG and a 3' primer containing myc tag sequence (underlined) ACGGAATTCGTTTAGGTCCTCTTCGCTGATTAGCTTTTGTTCCATGGC CCCTG GCTGGAAGCGGGCTGT. The resulting cDNA was subcloned into expression vector, pCDNA3.1 (Invitrogen) and sequenced.

For recombinant protein purification, the cDNAs of ERK1 and MEK1 were subcloned into the pQE-30 vector (Qiagen). His6-tagged erk1 and MEK1 were expressed and purified on Ni_2 ±NTA agarose and MonoQ (26). To construct fusion protein expression vectors, RHAMMv4 cDNA and mutant cDNAs were subcloned into pGEX-2T plasmids. RHAMMv4 $D5^-$ (mutant hyaluronan binding domains) plasmids were constructed as described (14,57). For the construction of v4 $D4^-$ (repeat sequence) mutant, PCR was used to produce 2 fragments which were inserted into an XhoI site, using four primers. For the N-terminal fragment, two primers, 5'-GCGGGATCCATGAGAGCTCTAAGCCTG-3' and 5'-GCGCTCGAGTGCAATCAAGATG GCTTG-3', were used. For the C-terminal fragment, two primers, 5'-GCCGAATTCTCAGC AGCAGTTTGGGTT and 5'-GCCCTGGAGTATAAGTCATCAACACTTAA-3', were used. The two fragments were ligated with an XhoI site and then subcloned into the pGEX-2T vector with

BamHI and EcoRI sites. To Construct RHAMM4v-D4$^-$ / D5$^-$ mutants, pGEX-v4-D4$^-$ plasmids were digested with BamHI and Bg1 II and then ligated with the released fragment (750 bp) into pGEX-v4-D5$^-$ plasmids, which were digested with BamHI and Bg1 II. Expressed proteins were purified on glutathione beads and cleaved with thrombin (32). All purified proteins were dialyzed against 4 x buffer (15 mM HEPES, 100 mM KCL, 6.25% glycerol, pH 7.3) and concentrated to 1-5 mg/ml with a Microcon 30 concentrator (Amicon, Beverly, MA). Protein was snap frozen in liquid nitrogen and stored, aliquated, at -80°C.

Northern Analysis. mRNA was isolated and analyzed with Northern blots as described by Sambrook et al. (40). Briefly, RNA was prepared from cells harvested at 50-70% confluence, 12-24 hr after cell plating. Cells were lysed in buffer (4m guanidinium thiocyanate, 25 mM EDTA, 0.1 μM21-mercaptoethanal, pH 7.0), and total RNA was extracted using the Guanidine/CsCI method. Poly(A)+ mRNA was purified using an mRNA purification kit (Pharmacia). 10 μg of mRNA were separated by electrophoresis (50% formaldehyde/1.2% agarose), transferred onto nylon nitrocellulose (Amersham) and fixed by U.V. crosslinking, using a U.V. Stratalinker (Stratagene, La Jolla, CA). Membranes were pre-hybridized for 4 hours at 42°C in a solution consisting of 50% formamide, 6X SSPE, 5X Denhardt's solution, 0.5% SDS and denatured salmon sperm DNA. RNA was detected by hybridization with anti-sense ^{32}P-end labeled RHAMM nucleotides (GCTATTTCTTGGATGTATTCTAAGAGTTTTTCTGTTTCACA TTTTTCATCGATCTTTCTTTCTCTATTGAAAC). After hybridization, the membranes were washed with 1X SSPE/0.1% SDS, 0.1X SSPE/0.1% SDS at 42-60°C, and bound label was detected by autoradiography. Equal loading of RNA was confirmed by stripping the filters, then reprobing them with a ^{32}P-labeled GAPDH cDNA. For detecting MMP-9 mRNA expression, 20 μg of denatured RNA was electrophoresed, transferred and hybridized with ^{32}P-labeled cDNAs of mouse MMP-9 (47). The hybridization and washing conditions were the same for detecting mRNA.

RT-PCR. C3 fibroblasts were harvested 8 hr after plating at 50% confluence. Total RNA and mRNA were prepared as described above under Northern analysis. cDNA's were synthesized

using a Clonetech Marathon™ cDNA amplification kit, following manual instructions. For amplification of mouse RHAMMv5 and RHAMMv4, PCR was performed with Advantage Taq polymerase (Clontech) and conditions were as follows: 45 s at 94°C, 40 s at 60°C and 3 minutes at 72°C for 25 cycles. Primer sets for RT-PCR as follows:

Primer 1, 5'-TCAGCAGCAGTTTGGGTTGC-3'

Primer 2, 5'-GAATAGATATCTGAGTTCTTATG-3'

Primer 3, 5'-ATGTCCTTTCCTAAGGCGCC-3'

Primer 4, 5'-CAGGATCTGCATCTCAGCAC-3'

Primer 5, 5'-GAAGCAAAGCTCAATGCAGCA-3'.

Genomic clone. To obtain genomic RHAMM sequence, a portion of a RHAMM cDNA (10) was used to screen a 3T3 mouse fibroblast genomic library. Several clones were isolated, analyzed by restriction mapping and partially sequenced. Clone #1 contained the v4 initiation codon and open reading frame. This clone was completely sequenced to determine whether or not the 5'UTR previously identified by 5'RACE and primer extension of 3T3 cell RNA populations (10) was present in the RHAMM gene.

Stable transfection of fibroblasts. 10T1/2 or NIH 3T3 fibroblast lines were plated at 50% confluence then transfected 12-24 hr after cell plating with 2 μg of the various cDNAs using 25 μg of Lipofectin (GIBCO/BRL). Cells were exposed to these reagents in serum-free medium for 12-16 hours. Serum-free medium was then replaced with DMEM + 10% FBS alone and cells were allowed to recover for an additional 24 hours. Transfected cells were trypsinized and plated onto two 10 mm dishes containing selection medium (DMEM + 10% FBS + 800 μg/ml Geneticin) (Sigma). G418 resistant colonies were cloned by limiting dilution. Clones that overexpressed RHAMM were selected for 2-3 fold enhancement of RHAMM relative to empty-vector transfected cells, using western analyses to detect protein expression (see below).

Transient transfection of 10T1/2 and U21 fibroblasts. 10T1/2 and U21 cells were cultured to 40-50% confluence and transfected with 10 μg of RHAMM wild type or mutant cDNAs in 60 μl superFect reagent. After five hours of incubation, monolayers were washed twice with

PBS and the transfected cells were cultured an additional 48 hours with growth medium supplemental with 10% FBS. The cells were harvested with RIPA buffer and RHAMM expression was detected by western analysis. Only the transfectants which expressed similar level (2-3 fold higher than parental cells) were used for immunoprecipitation assays.

Focus formation. For focus formation assays, cells were grown to 70% confluence (48-72 hr after cell plating) in DMEM supplemented with 10% FBS. Transfections were performed using the Lipofectin reagent. 50 ng of pHβApr-Neo plasmid containing RHAMMv4 and RHAMMv5 cDNA, and/or 50 ng of $PEXV_3$ containing MEK1AN3/S218E/S222D were used for each 100 cm dish. Post-transfected cells were maintained in DMEM supplemented with 10% FBS and 10-15 days later the number of foci were counted after cultures were fixed and stained with methylene blue.

Western Analyses. Cells were plated at 50% confluence and grown for 6-24 hr then monolayers were washed with cold PBS, lysed in RIPA buffer and subjected to SDS-PAGE as described (14). Separated protein was transferred onto nitrocellulose membranes (Bio-Rad) using a transfer buffer of 25 mM Tris-HCI, 192 mM glycine, 20% methanol, pH 8.3. Non-specific binding sites were blocked with 5% defatted milk in Tris buffer (TBST, 10 mM Tris base, 150 mM NaCl, pH 7.4, with 0.1% Tween 20) (57). The blocked membranes were incubated with rabbit anti-RHAMM antibodies (1:1500) overnight at 4°C or for 2 hours at room temperature on a gyratory shaker. RHAMM antibodies (Zymed Laboratories, Inc.) were prepared against the following sequences: antibody 1 (which detects both v4 and v5 forms of RHAMM), peptide sequence: VSIEKEKIDEK. Antibody 2 (which detects only RHAMMv5), peptide sequence: QERGTQDKRIQDME. The anti-HA tag antibody (Boehringer Mannheim) recognizes the peptide sequence, YPYDVPDYA. The anti-c-myc antibody (Santa Cruz) recognizes the peptide sequence AEEQKLISEEDLLRKRREQLKHKLEQLRNSCA. Some blots were incubated with biotinylated hyaluronan for detection of hyaluronan binding capacity of proteins as previously described (14). Membranes were washed 3 times with TBST, then incubated with horseradish peroxidase-conjugated goat anti-rabbit IgG (1:10,000) for 30 minutes at room temperature. Bound antibody

was visualized by chemiluminescence (ECL) (Amersham), according to the manufacturer's instructions. The densitometry was determined with a Multi-Analyst program (Bio-Rad). To determine antibody specificity, anti-RHAMM antibodies were incubated with beads- linked with RHAMM protein (1 μg antibody/20 μl beads for 1 hr at 4°C on a Rotator, then centrifuged for 5 minutes. The supernatant was used to probe membranes.

Zymogram Analysis. Cell culture supernatant medium from subconfluent monolayers was harvested and proteins therein were separated on a 10% SDS-polyacrylamide gel impregnated with 1 mg/ml of gelatin (29). After electrophoresis, SDS was removed from the gel by incubation with 2.5% Triton X-100 for 30 minutes. The gels were then incubated in a buffer containing 50 mM Tris-HC1, 5 mM CaCl2, 0.02% NaN3, pH8.0, at 37°C for overnight. The gels were stained with 0.25% coomassie blue R250 in acetic acid:isopropyl alcohal:water (1:3:6) and destained in water. Proteolytic activity was seen as a clear band against stained blue background. Permanent records were prepared by photography.

Immunoprecipitation and Erk Kinase Assays. Parental 10T1/2 and transfected cell lines were plated at 50% confluence for 6-24 hr and washed two times with cold PBS and lysed in a lysis buffer (25 mM Tris HCl, pH 7.2, 0.1% SDS, 1% triton-X 100, 0.5% sodium deoxycholate, 50 mM NaCl 1 mM EGTA 10 mM $MgCl_2$ and 1mM EDTA) (60) containing the A (1 μg/ml), aprotinin (0.2 TIU/ml), and 3,4-dichloroisocoumarin (200 μM). The lysates were centrifuged and equal amounts of protein (300-400 μg) from each sample were added to 2 μg of anti-RHAMM antibody (R3.2), anti-erk1 (K23), antibody (Santa Cruz) and anti-MEK1 (C18) antibody (Santa Cruz). After 1 hr incubation at 4°C on a Nutator rotator, 50 μl of a 50% solution of protein G Sepharose was added and incubated at 4°C for an additional 1 hr, then washed four times with lysis buffer and once with kinase buffer (25 mM HEPES, pH 7.4, 1 mM dithiothreitol, 10 mM $MgCl_2$, 1 mM EGTA, 3 mM Na3VO4 and 0.3 mg/ml MBP). The protein G antibody-antigen complex was incubated for 20 minutes at 37°C in 15 μl of kinase buffer supplemented with 15 μM ATP and 10 Ci of (γ-32p)ATP (39). 10 μl of each sample was spotted onto P81 filter

paper, washed three times with 75 mM phosphoric acid, and once with 100% acetone. Dried samples were quantified by scintillation counting or developed for autoradiography.

***In vitro* Myelin Basic Protein Kinase Assays.** 1 μg of mutant activate MEK1 His6-fusion protein (MEK1 S/D) (26) was incubated with 2 μg of erk1 with or without RHAMMv4 GST-fusion protein in kinase buffer (25 mM HEPES, pH7.4, 1 mM dithiothreitol, 10 mM $MgCl_2$, 1mM EGTA, 15 μM ATP) using MBP (0.3 mg/ml) as substrate, in the presence of 10 μCi of (γ-^{32}P)ATP for 15 minutes at 30°C (39). Reactions were stopped by the addition of sample loading buffer. Labeled proteins were resolved by polyacrylamide gel electrophoresis and detected by autoradiography.

***In vitro* Binding and Competition Assays.** Purified GST-RHAMM proteins were released from GST with thrombin as described (14) and RHAMM was coupled to Amino Link plus coupling gel (Pierce), following manufacturers instructions. After several washes with PBS, RHAMM-coupled beads were incubated with purified erk1, erk2 or MEK1 His-6-tagged fusion proteins in binding buffer (25 mM HEPES, pH 7.2, 50 mM NaCl 2, 10 mM $MgCl_2$) for 1 hr at 4°C on a Nutator rotator. After several washes with cold binding buffer, the beads were boiled for 2 minutes in loading buffer, then proteins were separated on SDS-PAGE and transferred to nitrocellulose blots for western analyses. Anti-erk1 antibody (K23, Santa Cruz, and anti-MEK1 antibody (C18, Santa Cruz) were used to detect this kinase on western blots. For competition assays, 1 μg purified erk1 His-6 fusion protein was incubated with 10 μg soluble RHAMM protein for 1 hr at 4°C, then incubated with beads-RHAMM for an additional 1 hr. For peptide competition assays, 1 μg of erk1 His-6 fusion protein was incubated with 10 μg of peptides for 1 hr and then incubated with beads-RHAMM for another 1 hr on a Rotator. Three different peptides were used in competition binding assay, D4: QEKYNDTAQSLRDVTAQLESV, D5: KQKIKHVVKLKDENSQLKSEVSKLRSQLVKRK and phage display peptides HA2, GVCNADFCWLPAVVV and HA3, SASPSASKLSLMSTV.

Expression of the RHAMM Hyaluronan Binding Domains (P-1). A C-terminal 70 amino acid GST-RHAMM fusion protein (RHAMM-P1) was expressed which includes the two

amino acid HA binding domains plus additional sequence. This was generated using the sequence specific primers, a 5' primer GCCGGATCCAACCTAAAGCAAAAAATCAAACAT and 3' primer GCCGAATTCGCAGCAGTTTGGGTTGCCTTC and ligated into PGEX-2T. The protein was grown in lubria broth to an OD 1.0, induced with 1 mM IPTG, cells harvested and lysed using standard procedures. The clarified cell lysate was passed over glutathione sepharose, and GST-RHAMM-P1 was eluted using glutathione elution buffer (10 mM Tris, pH 8.0, 50 mM glutathione). The protein was stored in 10% glycerol in -30°C at a stock concentration of 1 mg/mL. To test the above constructs for HA binding, several standard binding assays were used. First a dot blot was performed in which dilutions of the stock protein were placed on PVDF membrane and probed with biotinylated HA (14). After a series of washes, the membranes were incubated with streptavidin horseradish peroxidase (HRP), and binding was detected using TMB (3,3',5'5-Tetramethylbenzidene) substrate.

A low level of HA modification was obtained by using a ratio of EDCI to carboxylic function of 1:10 and a biotin hydrazide ratio of 1:15. The reaction was carried out at pH 4.75 using 50 mM MES, and the product purified using extensive dialysis. The dialysis buffers alternated between 300 mM NaCl, de-ionized water, 20% ethanol, and this cycle was repeated once. Gel permeation chromotography was used to confirm the biotinylated HA was intact and to separate unreacted biotin.

Phage Screening. GST-RHAMM-P1 was either nonspecifically adsorbed onto a 30 mm polystyrene dish, or immobilized on 20 µL of glutathione sepharose in a 1.5 mL microfuge tube. The methods are equivalent but it was noted that more non-specific phage were present using glutathione sepharose. A starting titer of 10^{11} colony forming units (cfu) of fUSE-5 phage hosting random 15 amino acid peptides was diluted 1:1000 in tris buffered saline (20 mM Tris, 130 mM NaCl, pH 7.5) with 0.1% w/v polyvinylpyrolidone and 0.05% Tween 20 (TBS-T/PVP-40). This was applied to the immobilized GST-RHAMM-P1 and incubated at room temperature for one hour. Non-binding phage were washed away in a series of 10 washes, and specifically bound phage were eluted using 1 unit of thrombin incubated at 37°C for 40 minutes. It was anticipated

that RHAMM-P1 would be released using thrombin carrying with it all specifically bound phage, while GST would remain immobilized on the plate or on glutathione sepharose.

The phage were titered by infecting compromised K91-Kan cells and dropping serial dilutions onto LB plates. The phage bound to GST-RHAMM-P1 was propagated in 20 mL cultures overnight, and precipitated from the broth supernatant, after removing cells.

This procedure was repeated a total of four times, each time resulting in retention of fewer phage. In the final screen, phage were eluted with 1 mg/mL hyaluronidase digested HA (MW average 60,000) instead of thrombin. This procedure allowed isolation of phage that bound specifically to the HA binding domains of RHAMM P1. Positive colonies from LB Kan/Tet plates were propagated, the plasmid purified and sequenced.

Positive sequences were then synthesized both as unmodified 15 amino acid sequences and with an N-terminal biotin group. bHA2 and bHA5 were solubilized in 50:50 DMF:water, bHA3 and bHA4 were fully soluble in water to at least 1 mg/mL.

Phage Peptide Binding Assays. To verify that the peptides obtained from phage screening bound to the HA binding domains of RHAMM, a solid phase 96 well plate assay was employed. 50 μL GST-P1 (0.25 mg/mL) in glutathione elution buffer was immobilized in wells of a polystyrene 96 well plate (Greiner). The plate was blocked with 250 μL TBS-PVP-40 BSA (20 mM Tris, pH 7.5, 130 mM NaCl, 0.1% polyvinyl pyrolidone-40, 1% bovine serum albumin) for 2 hours to overnight with shaking. The plate was washed with TBS-PVP-40 (no BSA) and then incubated with excess HA or chondroitin sulfate (CS) for 1 hr prior to the addition of the biotinylated ligand. The biotinylated ligand was incubated for 25 minutes (as determined from an initial time course), washed three times and blocked with TBS-PVP-40-BSA for 1 hr. Streptavidin HRP was added at a dilution 1:10,000 in TBS-PVP-40. HA was added to the streptavidin mix since it is known that streptavidin HRP binds nonspecifically to HA and CS which inherently causes misleading results in the competition experiments. After 40 minutes incubation, the plate was washed and the presence of biotinylated peptide was determined using TMB. Colorimetric development was detected at 590 nm (Perkin Elmer HTS 7000). All measurements are done in

quadruplicate. Eadie Hofstee analysis was performed, assuming that binding can be correlated to the color developed under each condition.

RESULTS

1. Two full length RHAMM mRNA transcripts are detected in ras-transformed 10T1/2 fibroblasts. Two murine RHAMM mRNA transcripts with distinct 5'UTR's have previously been reported (3,10), one initiating at exon 1 (11) and the other downstream at exon 6. The two transcripts encode a 95 kDa protein and a shorter, N-terminally truncated 73 kDa protein, respectively. RHAMM mRNA expression of several oncogene-transfected 10T1/2 fibroblasts was assayed, using Northern blots (Fig. 1A). The presence of a mutant active ras most strongly upregulated RHAMM mRNA, compared to other common oncogenes. The Northern blot suggested the presence of one major but broad mRNA transcript of 3.2 kb (Fig. 1A). RT-PCR analyses were conducted to determine if additional, more minor mRNA transcripts existed. mRNA was harvested 8 hr after cell plating when cells are beginning to locomote, a time previously shown to correspond to maximal expression of a 73 kDa RHAMM protein (41). We first confirmed that the 5'UTR reported to be unique to the v4 transforming mRNA transcript (10), is present in genomic RHAMM sequence upstream of the Kozak consensus sequence predicted to initiate this short transcript. The 5'UTR sequence was found in a genomic clone containing v4 sequence (Fig. 1B), and its sequence contained two in-frame stop codons upstream of the start condon initiating v4 (Fig. 1B). The presence of an intron/exon splice site suggested this putative 5'UTR is not part of exon 6 initiating the v4 open reading frame. The presence of two unique 5'UTR's permits the differential detection of each RHAMM transcript. Using two primer sets shown in Fig. 1C, mRNA inserts corresponding to v4 and v5, as determined by size and sequence, were amplified in RT-PCR (Fig. 1D). To determine whether or not the v4 insert represented partially processed RNA (11), primer sets were designed to assess whether or not a full length v4 mRNA transcript could be amplified (Fig. 1C). Full length v4 mRNA transcript was indeed amplified, as determined by size and

sequence (Fig. 1E). However, it is clearly a minor transcript and present in much smaller amounts than the v5 transcript.

To assess whether v4 can be detected in cell backgrounds other than 10T1/2 fibroblasts, mutant active ras was transiently transfected into an NIH 3T3 cell background. V4 was detected by RT-PCR, as for the ras-transformed 10T1/2 fibroblasts (Fig. 1F). These results suggest that the presence of a mutant active ras permits the expression of a full length mRNA encoding RHAMMv4. An inability to detect this RNA transcript (11) is likely related to its minor expression and the its limited expression, which occurs shortly after cell plating when cell motility is initiated.

2. **Ras-transformed cells express two major RHAMM proteins.** Two polyclonal antibodies were prepared against peptide sequences encoded in RHAMM cDNA (17,51) in order to differentiate between v5 and v4 proteins (see Methods). The first antibody was prepared against sequence encoded in the exon that has been reported to be required by v4 to transform fibroblasts (see Methods) (14). This sequence is encoded in both v5 and v4. The second antibody was prepared against sequence unique to v5 that is present immediately N-terminal to the initiation of a RHAMMv4 protein, as predicted from the v4 mRNA transcript (Fig. 1B) (10). As shown in Fig. 2A, antibody 1 detects both a 95 kDa RHAMM protein, predicted to correspond to v5, and a 73 kDa protein, predicted to correspond to v4. Blocking of these antibodies with either RHAMMv4-GST fusion protein or RHAMM peptide (see Methods) prevented antibody binding to these proteins on western blots (Fig. 2B), confirming the specificity of antibody 1 for RHAMM. In contrast, and as predicted, antibody 2 reacted only with 95 kDa and a minor 90 kDa protein but not with the 73 kDa protein detected with antibody 1 (Fig. 2C). These results indicate that the 73 kDa protein lacks the N-terminal sequence of the 95 kDa protein, consistent with sequence encoded in the v4 mRNA transcript. The specificity of antibody 2 was confirmed by blocking of antibody binding with recombinant RHAMMv5 (Fig. 2D). The size of v4 protein expressed in a 10T1/2 fibroblast background from a transfected, HA-tagged RHAMMv4 cDNA was compared to the RHAMM proteins

expressed in ras transformed cells (Fig. 2E,F). The protein expressed from HA-v4, detected by the HA tag, was identical in MW to the endogenous 73 kDa protein (compare Fig. 2E and 2F), and the tagged RHAMM protein also reacted with Ab 1 but not Ab 2 (Fig. 2E).

These results show that ras transformed fibroblasts express two RHAMM proteins that correspond in size and antibody reactivity to sequence predicted by the v5 and v4 RHAMM mRNA transcripts. The 73 kDa protein corresponding to v4 is most highly expressed at 8 hr after cell plating, consistent with v4 mRNA expression, while the 95 kDa protein is most highly expressed at 24-36 hr after cell plating (Fig. 2A, C). These results suggest the two RHAMM forms may perform different functions.

3. **V4 and v5 bind directly to erk1 and indirectly to MEK1.** The ability of v4, erk1 and MEK1 to co-associate in ras-transformed cells was previously demonstrated by immunoprecipitation assays, using anti-RHAMM antibodies (60). This study had shown that only erk1, but not erk2 or other map kinases, associated with the RHAMM/erk1/MEK complex (60). Here, *in vitro* binding assays using erk1, MEK1 and RHAMM-GST or His-fusion proteins showed that both v4 and v5 RHAMM proteins (Fig. 3A) bound directly to erk1 (v4 shown here, Fig. 3B) but, under our assay conditions, did not bind to MEK1-His-fusion protein, at detectable levels (Fig. 3C). Deletion and mutation analyses of v4 revealed two sites on RHAMM that contributed to erk1 binding (Fig. 3D), a repeated sequence (D4), and D5 domains, the latter previously reported to contain hyaluronan binding motifs (14,57). Peptides mimicking either 21 amino acids of D4 or peptides mimicking D5 significantly reduced binding of erk1 to v4 whereas mixing of both peptides inhibited binding of erk1 to v4 by 90% (Fig. 3D), suggesting these domains likely co-ordinate to act as erk1 binding sites. The use of these domains for associating with erk 1 *in vivo* was then assessed by transient transfection of tagged mutant RHAMM cDNA's into cells that produce little endogenous RHAMM (Fig. 4) (14). RHAMM expressed from v4 and v5 cDNA's co-immunoprecipitated with erk1 when D6 and D5 were intact (Fig. 4A). Interestingly, approximately 3 times more erk1 associated with v4, compared with v5. When the RHAMM D4 and D5- erk1 binding domains were mutated,

erk1 binding to RHAMM was abolished (Fig. 4A). These results confirm that D4 and D5 are sites of RHAMM/erk1 interaction *in vivo*. The key contribution of D5 to erk1 binding *in vivo* provides a molecular rationale for the previously reported ability of RHAMM forms that are mutated in this domain to block both activation of erk and cell transformation by mutant active ras (14,60).

Independent verification of the ability of D5 to interact with protein sequences was confirmed by screening a 15 mer random phage display library using recombinant RHAMM (P1 peptide) containing D5, as bait. Eight peptide sequences were obtained that could be grouped according to shared sequences: A) WPVSLTVCSAV**WCPL**, H**WCLP**LLACDTFARA, GVCNADF**CWLPA**VVV: B) YSVYLSVVHNS**VLPS**, YSVYLSVAHNF**VLPS**, IPP**ILPA**YTLLGHPR: C) PHXRPVV**SASSILPV**; **SASPSAS**KLSMSTV: D) FFAGGLMYRIG**FSS**D and SPSLDCSW**PLVKFSS.** Five of these were confirmed to bind to RHAMM P-1 peptide in ELISA, and binding was quantified with Eadie Hofstee plots (Fig. 5A). Confirmation that these peptides bind to the D5 domain present in the RHAMM P-1 peptide (see Methods), was provided by the ability of hyaluronan to compete with phase peptides for binding to P-1 (Fig. 5B). More importantly, two selected peptides, GVCNADFC**WLPA**VVV and **SASPSAS**KLSLMSTV, competed with erk1 for binding v4 to approximately the same extent as a RHAMM D5 peptide (Fig. 4D).

4. **Interaction of v4 and v5 with MEK1 *in vivo* requires D3.** Deletion of D3 (VSIEKEKIDEKCETEKLLEYIQEIS, Fig. 4A) abolished the co-immunoprecipitation of v4 with MEK1 (Fig. 6A), although this deletion still enabled an interaction with erk1 (Fig. 4A). V5 also co-immunoprecipitated with MEK1, consistent with the presence of D3 sequence in v5 (Fig. 3A), but approximately three-fold less MEK1 associated with this RHAMM protein form (Fig. 6A). Mutation/deletion of either erk1 binding domains also prevented an association of MEK1 with RHAMMv4 (Fig. 6A). *In vitro* kinase assays showed that the presence of GST-RHAMMv4 did not promote activation of His-erk 1, by mutant active His-MEK1 (Fig. 6B)

confirming that other proteins are likely required for the ability of v4 to regulate erk1 activity via MEK1.

5. **Deletion of N-terminal 163 amino acids is required for the transforming function of RHAMM.** V4 overexpression activated erk kinase and was confirmed to transform fibroblasts, as detected by focus formation (Fig. 7A,B). Interestingly, activation of erk kinase by both v4 and mutant active ras required the presence of serum in the 10T1/2 cell background (Fig. 7B). In contrast to v4, overexpression of v5 did not activate erk kinase, and was not transforming in focus forming assays (Fig. 7A). These results indicate that the N-terminal sequence unique to v5 negatively regulates the functions of downstream RHAMM sequence, and that v4, which lacks this sequence, represents the more active form of RHAMM.

The association of RHAMM with MEK1 and the ability of RHAMMv4 overexpression to activate erk 1 suggests RHAMM may modify MEK1 function. The effect of RHAMM overexpression on the ability of mutant active MEK1 to activate erk 1 and to transform fibroblasts (26) was assessed (Fig. 7C,D). V4 strongly synergized with mutant active MEK1 to both activate erk kinase and to enhance transformation of 10T1/2 fibroblasts. This ability to synergize appears to derive from an association of v4 with MEK1 since deletion of D3 blocked this affect (Fig. 7). V4 did not enhance the focus forming ability of oncogenes that it does not associate with such as rac (60, data not shown). Interestingly, v5 slightly enhanced the ability of mutant active MEK1 to activate erk kinase but did not significantly affect the transforming function of mutant active MEK1.

An additional domain, D2, shown in Fig. 3A, is required for the ability of v4 to transform (data not shown) and to enhance the transformation ability of mutant active MEK1. However, deletion of this domain did not affect the association of MEK1 or erk1 with RHAMM (data not shown).

6. **Overexpression of v4 promotes MMP-9 production release and this effect requires the v4 erk1 binding domains.** The effect of v4 and v5 overexpression on gene

expression were compared to begin to address the mechanism(s) by which v4 transforms. Cells stably overexpressing v4 activated AP-1 as determined by gel shift assays, confirming a previous report (Figs. 7, 8) (6). Overexpression of v4 also strongly promoted expression of MMP-9 (Fig. 7), and release of this metalloproteinase, as detected by a zymogram (Fig. 8). Furthermore, overexpression of v4 mutated in its D5 erk1 binding domain blocked release of this metallioproteinase (Fig. 8). In contrast to v4, v5 overexpression had little effect on these parameters.

DISCUSSION

Several forms of intracellular RHAMM have been reported to be encoded by distinct full length mRNA transcripts with the most common form encodes a 95 kDa protein (v5), (10,11,14,51). We (10,28) and others (24,31) have also reported the presence of shorter protein forms, particularly a 73 kDa. The 73 kDa protein is of particular interest since overexpression of a cDNA (v4) encoding a 73 kDa protein that does not contain 163 amino N-terminal amino acids present in v5, is transforming (14), the resulting protein co-immunoprecipitates with erk1 and MEK1 kinases (60) and 73 kDa is required for signaling through mutant active ras (14). The functional properties of the more common v5 form, however, have not been previously reported and the relationship between v4 and v5 has been entirely unclear. We confirm that both v4 and v5 RHAMM forms are expressed in ras transformed cells and show that both are erk1 binding proteins that indirectly associate with MEK1 *in vivo*. Our results clearly show that v4 is a more active form of RHAMM than v5, in terms of its ability to activate erk1 kinase, and to synergize with mutant active MEK1 to enhance its downstream functions. These results indicate that the N-terminal 163 amino acids negatively regulate the ability of RHAMM to function on the erk1 kinase cascade and that RHAMM, like raf and other oncogenes (5), appears to be activated in this function by removal of a regulatory sequence.

The RHAMM N-terminal sequence (D1) that negatively regulates RHAMM-mediated erk activation is characterized by the presence of an SH3 binding site and by multiple putative erk

phosphorylation sites. As a domain, it is an entirely novel sequence (ProDom #75227) and the manner in which it regulates RHAMM-mediated erk activation is not yet clear. Immunoprecipitation data suggest that v5 is less able to interact with erk1 and MEK1 compared to the v4 and this reduced interaction may account, in part, for the restricted ability of v5 to activate erk1. In this regard, D1 may mask key domains such as D3-D5, required for interaction with MEK1 and erk1. However, the presence of an SH3 binding domain and serine/threonine phosphorylation sites raise the possibility that v5 interacts with additional regulatory proteins and/or is targeted to subcellular compartments distinct from v4. Removal of D1 may permit RHAMM to bring erk1/MEK1 complexes close to upstream regulatory proteins and downstream erk1 substrates (5,49). Further studies are required to determine the precise molecular mechanisms by which D1 regulates RHAMM-mediated activation of erk1.

Our results suggest that both v4 and v5 are expressed in sub-confluent ras-transformed fibroblasts. Although both proteins are expressed at this time in ras-transformed cells at equivalent levels, the most common RHAMM mRNA transcript encodes the 95 kDa protein while the mRNA transcript is minor. The role of the full length v4 mRNA in generating this level of v4 protein is therefore not yet clear. It is, of course, possible that the v4 mRNA transcript is more efficiently translated than v5, as has been described for other rare messages (e.g., 61) but v4 may also be generated by other mechanisms. Possibilities include internal start codon usage of the v5 mRNA transcript and/or proteolytic processing of v5 protein. The first possibility is attractive since a number of proteins including myc, p53 and FGF isoforms (2,13,15,25) are generated in this manner. Further, there are several internal conserved consensus Kozak in sequences encoded in v5 that would generate proteins close to 73 kDa in both murine and human cells.

A recent report (11) suggested that v4 represents a partially processed RNA. The presence of the full length v4 transcript in ras-transformed cells is a consistent finding when care is taken to harvest mRNA from subconfluent cultures, to utilize mRNA rather than total RNA and to conduct RT-PCR under conditions reported in this report. The appearance of the full length v4 mRNA

transcript shortly after cell plating (8 hr) and its very minor expression likely contributed to difficulty in detecting this transcript (11).

The potent transforming/MEK1 enhancing function of v4 is related to its ability to promote complexing of MEK1/erk1 with other regulatory accessory proteins and possibly upstream components of this kinase cascade (49). It is relevant that a previously reported MEK1 accessory protein, MEK-1 activating protein (MP-1) (42) has several properties that may place it on the same regulatory pathway as v4. Both v4 (60) and MP-1 (42) specifically activate erk1 and both proteins require the presence of serum supplements in culture medium for this effect to occur *in vivo*. It is also intriguing that MP-1 encodes a six amino acid sequence, VSI/LEKE, that is identical to that present in D3 of RHAMM, which is required both for the association of v4 with MEK1 and its affect on MEK1 function. This domain may serve as a binding site for adapter proteins that link proteins such as MP-1 to v4, permitting activation of erk1 in subcellular sites that v4 is retained in, such as cell lamellae (60). In any case, a consequence of this complex formation is enhanced expression of AP-1 regulated genes such as MMP-9, that have clearly been implicated in the transformation process (37,43,54).

The D5 domains of RHAMM, which mediate binding of the extracellular polysaccharide hyaluronan to a cell surface form of RHAMM (12,14,36), contribute to the binding of erk1 to intracellular RHAMM. Several sequences have been reported to mediate the binding of erk kinases to other erk binding proteins and these include a "D" box, an FXFP motif (18) and a ribosomal 6 kinase sequence, LAQRRVRKL (45). Interestingly, the D5 domains of RHAMM contain a sequence KHVVKL, that is similar to the erk docking site present in ribosomal 6 kinase (45). The sequence in erk1 which is responsible for binding to RHAMM has not yet been defined.

We have previously reported that RHAMMv4 protein is transiently expressed in 3T3 fibroblasts (10) and show here that its maximal expression occurs at culture subconfluence and early after cell plating. However, the physiological role of such a truncated, activated form of RHAMM has not yet been clearly determined *in vivo*. Its location in cell lamellae *in vitro* (60), its ability to promote cell motility (14) and its expression shortly after wounding of cell monolayers

(41) suggest it contributes to initiation of locomotion and possibly progression through cell cycle, following tissue injury. The recent demonstration of high levels of RHAMM in sprouting olfactory nerves *in vivo* (59) and evidence that RHAMM plays a role in the extension of dynamic nor-adrenergic nerve nets such as the lucus coeruleus (31) are consistent with a role for RHAMM in renewal processes that involve lamellae or axonal extension. Finally, the overexpression of several RHAMM protein forms in breast cancer, malignant pancreatic cell lines (1) and aggressive subsets of multiple myeloma cells (9) predict that it also plays a role in neoplastic progression, a process that also involves cell motility. One role for a transiently expressed v4 in these processes may be to irritate expression of AP-1 regulated genes such as MMP-9, resulting from activation of erk1. Enhanced production of metalloproteinases are required for response-to-injury processes (4,29,30,34,46,58) and for neoplastic progression (37,43,54).

In summary, we show that intracellular RHAMM forms are erk1 binding proteins and that the presence of an N-terminal 163 amino acids unique to the commonly expressed RHAMMv5 (95 kDa) suppresses the ability to downstream RHAMM sequence to participate in the activation of erk1. An activated form of RHAMM, corresponding to the previously described v4 (14), is expressed in ras-transformed fibroblasts. The physiological roles of both of these forms of RHAMM is actively under investigation.

ACKNOWLEDGMENTS

This study was funded by an MRC grant, GR-13920 (ET), NCIC grant (ET), MRC studentship (RH), NIH grant GM48521 (NA), U.S. Department of Army Breast Cancer IDEA grant (GDP), and CAN (TC).

REFERENCES

1. **Abetamann, V., H.F. Kern, and H.P. Elsasser.** 1996. Differential expression of the hyaluronan receptors CD44 and RHAMM in human pancreatic cancer cells. Clin. Cancer Res. **2:**1607-1618.
2. **Arnaud, E., C. Touriol, C. Boutonnet, M.C. Gensac, S. Vagner, H. Prats, and A.C. Prats.** 1999. A new 34-kilodalton isoform of human fibroblast growth factor 2 is cap dependently synthesized by using a non-AUG start codon and behaves as a survival factor. Mol. Cell Biol. **19:**505-514.
3. **Assmann, V., J.F. Marshall, C. Fieber, M. Hofmann, and I.R. Hart**. 1998. The human hyaluronan receptor RHAMM is expressed as an intracellular protein in breast cancer cells. J. Cell Sci. **111**:1685-1694.
4. **Bos, T.J., P. Margiotta, L. Bush, and W. Wasilenko.** 1999. Enhanced cell motility and invasion of chicken embryo fibroblasts in response to Jun over-expression. Int. J. Cancer **81:**404-410.
5. **Campbell, S.L., R. Khosravi-Far, K.L. Rossman, G.J. Clark, and C.J. Der**. 1998. Increasing complexity of Ras signaling. Oncogene **17**:1395-1413.
6. **Cheung, W.F., T.F. Cruz, and E.A. Turley.** 1999. Receptor for hyaluronan-mediated motility (RHAMM), a hyaladherin that regulates cell responses to growth factors. Biochem. Soc. Trans. **27:**135-142.
7. **Choi, K.Y., B. Satterberg, D.M. Lyons, and E.A. Elion**. 1994. Ste5 tethers multiple protein kinases in the MAP kinase cascade required for mating in S.cerevisiae. Cell **78**:499-512.
8. **Cohen, L., W.J. Henzel, and P.A. Baeuerle**. 1998. IKAP is scaffold protein of the IkappaB kinase complex. Nature **395**:292-296.
9. **Crainie, M., A.R. Belch, M.J. Mant, and L.M. Pilarksi.** 1999. Overexpression of the receptor for hyaluronan-mediated motility (RHAMM) characterizes the malignant clone

in multiple myeloma: Identification of three distinct RHAMM variants. Blood **93:**1684-1696.

10. **Entwistle, J., S. Zhang, B. Yang, C. Wong, Q. Li, C.L. Hall, J. A, M. Mowat, A.H. Greenberg, and E.A. Turely.** 1995. Characterization of the murine gene encoding the hyaluronan receptor RHAMM. Gene **163**:233-238.
11. **Fieber, C., R. Plug, J. Sleeman, P. Dall, H. Ponta, and M. Hofmann.** 1999. Characterisation of the murine gene encoding the intracellular hyaluronan receptor IHABP (RHAMM). Gene **226:**41-50.
12. **Gares, S.L., N. Giannakopoulos, D. MacNeil, R.J. Faull, and L.M. Pilarski**. 1998. During human thymic development, beta 1 integrins regulate adhesion, motility, and the outcome of RHAMM/hyaluronan engagement. J. Leukoc. Biol. **64**:781-790.
13. **Grunert, S., and R.J. Jackson.** 1994. The immediate downstream codon strongly influences the efficiency of utilization of eukaryotic translation initiation codons. EMBO J. **13:**3618-3630.
14. **Hall, C.L., B. Yang, X. Yang, S. Zhang, M. Turley, S. Samuel, L.A. Lange, C. Wang, G.D. Curpen, and RC Savani**. 1995. Overexpression of the hyaluronan receptor RHAMM is transforming and is also required for H-ras transformation. Cell **82**:19-26.
15. **Hann, S.R.** 1994. Regulation and function of non-AUG-initiated proto-oncogenes. Biochemie **76:**880-886.
16. **Herrera, R**. 1998. Modulation of hepatocyte growth factor-induced scattering of HT29 colon carcinoma cells. Involvement of the MAPK pathway. J. Cell Sci. **111**:1039-1049.
17. **Hofmann, M., C. Fieber, V. Assmann, M. Gottlicher, J. Sleeman, R. Plug, N. Howells, O. von Stein, H. Ponta, and P. Herrlich**. 1998. Identification of IHABP, a 95 kDa intracellular hyaluronate binding protein. J. Cell Sci. **111**:1673-1684.

18. **Jacobs, D., D. Glossip, H. Xing, A.J. Muslin, and K. Kornfeld.** 1999. Multiple docking sites on substrate proteins form a modular system that mediates recognition by ERK MAP kinase. Genes Dev. **13:**163-175.

19. **Janes, P.W., R.J. Daly, A. deFazio, and R.L. Sutherland**. 1994. Activation of the Ras signalling pathway in human breast cancer cells overexpressing erbB-2. Oncogene **9**:3601-3608.

20. **Janulis, M., S. Silberman, A. Ambegaokar, J.S. Gutkind, and R.M. Schultz**. 1999. Role of mitogen-activated protein kinases and c-Jun/AP-1 trans-activating activity in the regulation of protease mRNAs and the malignant phenotype in NIH 3T3 fibroblasts. J. Biol. Chem. **274**:801-813.

21. **Jeffers, M., M. Fiscella, C.P. Webb, M. Anver, S. Koochekpour, and G.F. Vande Woude**. 1998. The mutationally activated Met receptor mediates motility and metastasis. Proc. Natl. Acad. Sci. USA **95**:14417-14422.

22. **Klemke, R.L., S. Cai, A.L. Giannini, P.J. Gallagher, P. de Lanerolle, and D.A. Cheresh**. 1997. Regulation of cell motility by mitogen-activated protein kinase. J. Cell Biol. **137**:481-492.

23. **Liu, M.L., F.C. Von Lintig, M. Liyanage, M.A. Shibata, C.L. Jorcyk, T. Ried, G.R. Boss, and J.E. Green**. 1998. Amplification of Ki-ras and elevationof MAP kinase activity during mammary tumor progression in C3(1)/SV40 Tag transgenic mice. Oncogene **17**:2403-2411.

24. **Lovvorn, H.N.III, D.L. Cass, K.G. Sylvester, E.Y. Yang, T.M. Crombleholme, N.S. Adzick, R.C. Savani.** 1998. Hyaluronan receptor expression increases in fetal excisional skin wounds and correlates with fibroplasia. J. Pediatr. Surg. **33:**1069-1070.

25. **Macejak, D.G., and P. Sarnow.** 1991. Internal initiation of translation mediated by the 5' leader of a cellular mRNA. Nature **353:**90-94.

26. **Mansour, S.J., W.T. Matten, A.S. Hermann, J.M. Candia, S. Rong, K. Fukasawa, G.F. Vande Woude, and N.G. Ahn**. 1994. Transformation of mammalian cells by constitutively active MAP kinase kinase. Science **265**:966-970.

27. **Marcus, S., A. Polverino, M. Barr, and M. Wigler**. 1994. Complexes between STE5 and components of the pheromone-responsive mitogen-activated protein kinase module. Proc. Natl. Acad. Sci. USA **91**:7762-7766.

28. **Masellis-Smith, A., A.R. Belch, M.J. Mant, E.A. Turley, L. M. Pilarksi.** 1996. Hyaluronan-dependent motility of B cell and leukemic plasma cells in blood, but not of bone marrow plasma cells, in multiple myeloma: alternate use of receptor for hyaluronan-mediated motility (RHAMM) and CD44. Blood **87:**1891-1899.

29. **McCawley, L.J., S. Li, E.V. Wattenberg, and L.G. Hudson.** 1999. Sustained activation of the mitogen-activated protein kinase pathway. A mechanism underlying receptor tyrosine kinase specificity for matrix metalloproteinase-9 induction and cell migration. J. Biol. Chem. **274:**4347-4353.

30. **Mira, E., S. Manes, R.A. Lacalle, G. Marguez, and C. Martinez-A.** 1999. Insulin-like growth factor I-triggered cell migration and invasion are mediated by matrix metalloproteinase-9. Endocrinology **140:**1657-1664.

31. **Nagy, J.I., M.L. Price, W.A. Staines, B.D. Lynn, and A.C. Granholm.** 1998. The hyaluronan receptor RHAMM in noradrenergic fibers contributes to axon growth capacity of locus coeruleus neurons in an intraocular transplant model. Neuroscience **86:**241-255.

32. **Ngai, P.K., and J.Y. Chang**. 1991. A novel one-step purification of human alpha-thrombin after direct activation of crude prothrombin enriched from plasma. Biochem. J. **280**:805-808.

33. **Oka, H., Y. Chatani, R. Hoshino, O. Ogawa, Y. Kakehi, T. Terachi, Y. Okada, M. Kawaichi, M. Kohno, and O. Yoshida**. 1995. Constitutive activation of

mitogen-activated protein (MAP) kinases in human renal cell carcinoma. Cancer Res. **55**:4182-4187.

34. **Pacheco, M.M., M. Mourao, E.B. Mantovani, I.N. Nishimoto, and M.M. Brentani.** 1998. Expression of gelatinases A and B, stromelysin-3 and matrilysin genes in breast carcinomas: clinico-pathological correlations. Clin. Exp. Metastasis **16:**577-585.

35. **Pawson, T., and J.D. Scott**. 1997. Signaling through scaffold, anchoring, and adaptor proteins. Science **278**:2075-2080.

36. **Pilarski, L.M., M.J. Mant, and A.R. Belch**. 1999. Drug resistance in multiple myeloma: novel therapeutic targets within the malignant clone. Leuk. Lymphoma **32**:199-210.

37. **Polette, M., and P. Birembaut.** 1998. Membrane-type metalloproteinases in tumor invasion. Int. J. Biochem. Cell Biol. **30:**1195-1202.

38. **Printen, J.A., and G.F. Sprague, Jr**. 1994. Protein-protein interactions in the yeast pheromone response pathway: Ste5p interacts with all members of the MAP kinase cascade. Genetics **138**:609-619.

39. **Robbins, D.J., E. Zhen, H. Owaki, C.A. Vanderbilt, D. Ebert, T.D. Geppert, and M.H. Cobb**. 1993. Regulation and properties of extracellular signal-regulated protein kinases 1 and 2 in vitro. J. Biol. Chem. **268**:5097-5106.

40. **Sambrook, J., E. Fristch, and T. Maniatis**. 1989. Molecular Cloning: a Laboratory Manual, Cold Spring Harbor Laboratory. In: Cold Spring Harbor, NY: 1989: Section 7.2-7.53.

41. **Savani, R.C., C. Wang, B. Yang, S. Zhang, M.G. Kinsella, T.N. Wight, R. Stern, D.M. Nance, and E.A. Turley.** 1995. Migration of bovine aortic smooth muscle cells after wounding injury. The role of hyaluronan and RHAMM. J. Clin. Invest. **95:**1158-1168.

42. **Schaeffer, H.J., A.D. Catling, S.T. Eblen, L.S. Collier, A. Krauss, and M.J. Weber**. 1998. MP1: a MEK binding partner that enhances enzymatic activation of the MAP kinase Cascade. Science **281**:1668-1671.

43. **Shapiro, S.D.** 1998. Matrix metalloproteinase degradation of extracellular matrix: biological consequences. Curr. Opin. CellBiol. **10:**602-608.

44. **Sivaraman, V.S., H. Wang, G.J. Nuovo, and C.C. Malbon**. 1997. Hyperexpression of mitogen-activated protein kinase in human breast cancer. J. Clin. Invest. **99**:1478-1483.

45. **Smith, J.A., C.E. Poteet-Smith, K. Malarkey, and T.W. Sturgill.** 1999. Identification of an extracellular signal-regualted kinase (ERK) docking site in ribosomal S6 kinase, a sequence critical for activation by ERK in vivo. J. Biol. Chem. **274:**2893-2898.

46. **Sympson, C.J., M.J. Bissell, and Z. Werb.** 1995. Mammary gland tumor formation in transgenic mice overexpressing stromelysin-1. Semin. Cancer Biol. **6:**159-163.

47. **Tanaka, H., K. Hojo, H. Yoshida, T. Yoshioka, and K. Sugita.** 1993. Molecular cloning and expression of the mouse 105-kDa gelatinase cDNA. Biochem. Biophys. Res. Commun. **190:**732-740.

48. **Tanimura, S., Y. Chatani, R. Hoshino, M. Sato, S. Wastanabe, T. Kataoaka, T. Nakamura, and M. Kohno**. 1998. Activation of the 41/43 kDa mitogen-activated protein kinase signaling pathway is required for hepatocyte growth factor-induced cell scattering. Oncogene **17**:57-65.

49. **Turley, E., N. Auersperg.** 1989. A hyaluronate binding protein transiently codistributes with p21k-ras in culture cell lines. Exp. Cell Res. **182:**340-348.

50. **Waddick, K.G., and F.M. Uckun**. 1998. Innovative treatment programs against cancer.I.Ras oncoportein as a molecular target. Biochem. Pharmacol. **56**:1411-1426.

51. **Wang, C., J. Entwistle, G. Hou, Q. Li, E. A. Turley.** 1996. The characterization of a human RHAMM cDNA: conservation of the hyaluronan-bonding domains. Gene **174:**299-306.

52. **Wang, C., A.C. Thor, D.H. Moore, Y. Zhao, R. Kerschmann, R. Stern, P.H. Watson, and E.A. Turley**. 1998. The overexpression of RHAMM, a hyaluronan-binding protein that regulates ras signaling, correlates with oversexpression of mitogen-activated protein kinase and is a significant parameter in breast cancer progression. Clin. Cancer Res. **4**:567-576.

53. **Webb, C.P., L.Van Aelst, M.H. Wigler, and G.F. Woude**. 1998. Signaling pathways in Ras-mediated tumorigenicity and metastasis. Proc. Natl. Acad. Sci. USA **95**:8773-8778.

54. **Westermarck, J., and V.M. Kahari.** 1999. Regulation of matrix metalloproteinase expression in tumor invasion. FASEB J. **13:**781-792.

55. **Whitmarsh, A.J., J. Cavanagh, C. Tournier, J. Yasuda, and R.J. Davis**. 1998. A mammalian scaffold complex that selectively mediates MAP kinase activation. Science **281**:1671-1674.

56. **Xie, H., M.A. Pallero, K. Gupta, P. Chang, M.F. Ware, W. Witke, D.J. Kwiatkowski, D.A. Lauffenburger, J.E. Murphy-Ullrich, and A. Wells**. 1998. EGF receptor regulation of cell motility: EGF induces disassembly of focal adhesions independently of the molitity-associated PLCgamma signaling pathway. J. Cell Sci. **111**:615-624.

57. **Yang, B., L. Zhang, and E.A. Turley**. 1993. Identification of two hyaluronan-binding domains in the hyaluronan receptor RHAMM. J. Biol. Chem. **268**:8617-8623.

58. **Yu, Q., and I. Stamenkovic.** 1999. Localization of matrix metalloproteinase 9 to the cell surface provides a mechanism for CD44-mediated tumor invasion. Genes Dev. **13:**35-48.

59. **Zehntner S.P., A. Mackay-Sim, and G.R. Bushell.** 1998. Differentiation in an olfacory cell line. Analysis via differential display. Ann. N.Y. Acad. Sci. **855:**235-239.

60. **Zhang S., M.C. Chang, D. Zylka, S. Turley, R. Harrison, and E.A. Turley.** 1998. The hyaluronan receptor RHAMM regulates extracellular-regulated kinase. J. Biol. Chem. **273:**11342-11348.

61. **Zhou, B., and M. Rabinovitch.** 1998. Microtubule involvement in translational regulation of fibronectin expression by light chain 3 of microtubule-associated protein 1 in vascular smooth muscle cells. Circ. Res. **83:**481-489.

LEGENDS

FIG. 1. Ras-transformed cells express two RHAMM mRNA transcripts. A) Northern blot analysis of mRNA from oncogene-transfected 10T1/2 fibroblasts. Mutant active H-ras most strongly upregulated a RHAMM mRNA transcript of 3.2 kb. GAPDH was used as a control for loading RNA. B) The 5'UTR previously described for a v4 mRNA transcript (10) is confirmed to be present immediately upstream of the exon initiating the v4 open reading frame. This UTR encodes 2 in-frame stop codons upstream of the initiating ATG. C) Primers used for RT-PCR analysis of RHAMM mRNA populations. P3 +(P1 or P4) were used for detecting v5 while P2 +(P1 or P4) were used to detect v4. D) Primers used to detect partial mRNA transcripts confirm a previous study (10) showing an insert of the size expected for v4 and v5 in ras-transformed 10T1/2 fibroblasts. V5 is the major transcript, consistent with Northern Blot analysis. E) Primers used to detect full length mRNA transcript confirm the presence of a minor but full length v4 mRNA and a full length v5 transcript. Again, the v5 transcript is the major RHAMM mRNA. F) RT-PCR was used to detect v4 and v5 transcripts in ras-transformed NIH3T3 fibroblasts.

FIG. 2. Ras-transformed cells express two major RHAMM proteins. A) antibody 1, which detects sequence common to both v5 and v4 forms, reacts with two proteins of 95 and 73 kDa. B) Blocking of antibody with v4 GST-fusion protein abolishes reactivity with the 95 and 73 kDa proteins but not the non-specific protein bands C) antibody 2 was prepared against sequence immediately upstream of v4 and detects v5 and a 90 kDa RHAMM protein but not the 73 kDa protein. D) blocking of antibody with v5 GST-fusion protein abolishes reactivity with the 95 and 90 kDa proteins but not the non-specific protein bands. E) antibody 1 was used to detect v4 and v5 in ras transformed, parental 10T1/2 cells and in 10T1/2 cells transfected with an HA-tagged v4. Note that ras-transformed fibroblasts express more of both v5 and v4 protein than parental 10T1/2 cells, as predicted by Northern blot shown in Fig. 1A. F) The HA tag antibody detects only a 73 kDa RHAMM protein expressed from the v4 cDNA in transfected cells. This protein reacts with

antibody 1 and has an identical MW to the 73 kDa protein expressed in ras transformed cells. A non-specific band is also seen with the HA tag antibody.

FIG. 3. RHAMM proteins are erk1 binding proteins. A) Diagram of the v5 and v4 proteins noting the domains previously shown to be important in cell motility and transformation (14). B) Recombinant v4 and mutant v4 proteins were linked to agarose beads and incubated with His-erk1 fusion protein and bound erk1 protein was separated on SDS-PAGE then identified in western analyses. The ability of unbound v4 protein to compete with erk for v4-agarose beads confirms the specificity of binding. C) In similar assays, His-MEK1 fusion protein did not bind to v4 protein, suggesting that previously noted association of MEK1 with v4 (60) is indirect. D) Identification of D4 and D5 as sites to which erk1 binds. Mutant proteins that contained deletions/mutations of D4-D5, previously implicated in v4 signaling (14, 60) were used for *in vitro* binding assays as described in B above. V4 proteins mutated in D4 and, particularly in D5, showed reduced binding to erk1. Furthermore, peptides mimicking sequence within D4 or D5 also reduced binding of erk1 to v4 in competition assays. The presence of mutations in both D4 and D5 or, in competition assays the presence of both D4 and D5 peptides, reduced erk1 binding to v4 by 90% providing evidence that both domains are involved in this interaction.

FIG. 4. D4 and D5 mediate the association of RHAMM with erk1 *in vivo* A) Mutant v4 proteins were transfected into 10T1/2 cells that express little RHAMM (14). Transfected RHAMM was immunoprecipitated with antibody 3.2 which detects sequence between D4 and D5. Both v4 and v5 RHAMM forms associate *in vivo* with erk1 although v4 appears to bind more erk1 than v5. Deletion of D3, previously shown to be involved in activation of erk1 reduced but did not abolish the interaction of v4 with erk1. Expression of only the D4 and D5 domains (14) permitted binding of erk1 to this RHAMM fragment but binding was reduced compared to intact v4. Deletion or mutation of either D4 or D5 reduced binding of v4 to erk1 beyond detection capability of the assay. B) erk1 expression of cells used in A) to show that erk1 levels were equivalent.

FIG. 5. Confirmation that D5 interacts with peptide sequences. The D5 domain was expressed as a GST-fusion protein and used as bait to screen a random peptide phage display library. The ability of four of these peptides to bind to D5 in ELISA assays is shown in A). To confirm that phage peptides are binding to sequences within the hyaluronan binding motifs, hyaluronan was shown to compete with the phage peptides.

FIG. 6. D3 of RHAMM mediates association with MEK1 *in vivo*. A) RHAMM variants and mutants/deletions were transfected into cells and RHAMM was immunoprecipitated with antibody 3.2. MEK1 was detected in western analyses. Both v5 and v4 associated with MEK1, although more MEK1 associated with v4. Deletion of either the erk1 binding domains, D4 and D5, or D3, required for activating erk1 *in vivo* (60), abolished the association of MEK1 with RHAMM. B). *In vitro* kinase assay using mutant active MEK1 to activate erk1. The addition of v4 did not enhance the ability of erk1 to phosphorylate MBP in this *in vitro* assay.

FIG. 7. Overexpression of v5 does not enhance erk kinase activity *in vivo* or transform fibroblasts. A) focus formation assay shows that transfection of v5 (c) does not enhance focus formation above vector only controls (a) while transfection of either v4 (b) or mutant active ras (d) promote focus formation. B) Stable overexpression of v5 (or v5 protein levels 3.2 fold above vector controls) did not promote activation of erk kinase *in vivo*, as detected by erk kinase assays using immunoprecipitated erk1 and myelin basic protein as a substrate. In contrast, stable overexpression of v4 (v4 protein levels, 3.0 fold above vector controls) activated erk kinase to a similar level as mutant active ras, using identical kinase assays. As previously reported (42), the ability of ras to activate erk kinase required serum supplements in the cell growth medium, as did v4-mediated erk1 activation. C) V4 synergized with mutant active MEK1 to enhance erk kinase activity, detected by erk kinase assays described in (B) and this required the presence of D3. V5 synergized weakly with mutant active MEK1. D) V4 enhanced the ability of mutant active MEK1 to transform fibroblasts and this required D3. Both v4 and mutant active MEK1 transformed

fibroblasts, detected by focus formation, to a similar extent. Co-transfection of both v4 and mutant active MEK1 enhanced transformation by 6 fold. V5, which is not itself transforming, also did not significantly enhance transformation by mutant active MEK1.

FIG. 8. V4 activates AP-1 and enhances expression and release of metalloproteinase MMP-9: This requires the erk1 binding domains of v4. Stable overexpression of v4 enhanced AP-1 activation to a greater extent than a similar level of v5 overexpression. V4 transfected cells expressed increased levels of MMP-9, detected in a Northern blot using GAPDH as RNA loading control. Supernatant medium collected from v4-transfected cells showed a high activity of MMP-9 using a zymogram assay while v5-transfected cells did not. Overexpression of a v4 mutated in its D5 (erk1 binding) domain reduced activity of MMP-9 to the level of v5-transfected cells.

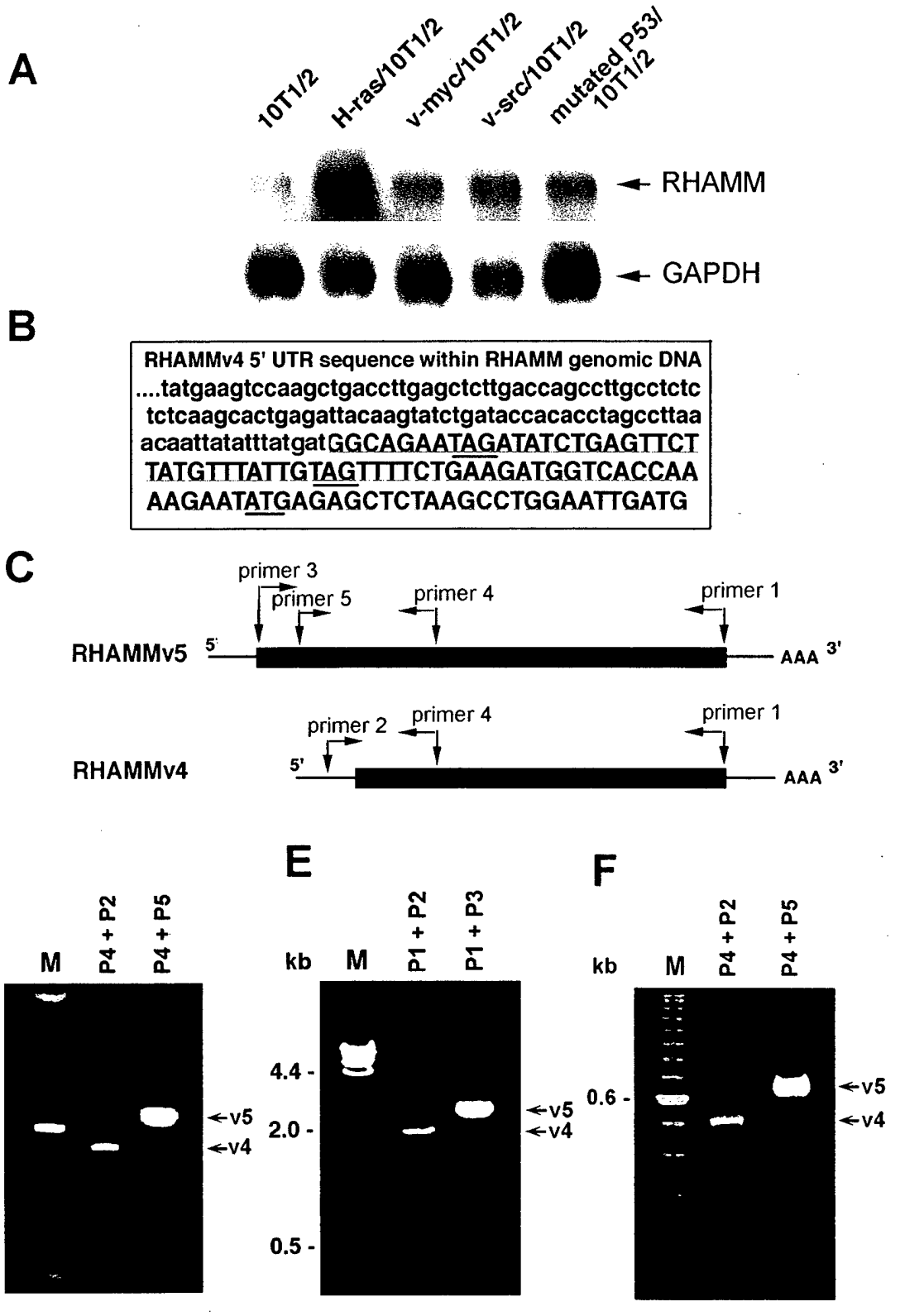
A
10T1/2
H-ras/10T1/2
v-myc/10T1/2
v-src/10T1/2
mutated P53/ 10T1/2
RHAMM
GAPDH
B
RHAMMv4 5' UTR sequence within RHAMM genomic DNA
....tatgaagtccaagctgaccttgagctcttgaccagccttgcctctc
tctcaagcactgagattacaagtatctgataccacacctagccttaa
acaattatatttatgatGGCAGAATAGATATCTGAGTTCT
TATGTTTATTGTAGTTTTCTGAAGATGGTCACCAA
AAGAATATGAGAGCTCTAAGCCTGGAATTGATG
C
primer 3
primer 5
primer 4
primer 1
RHAMMv5
5'
AAA 3'
primer 2
primer 4
primer 1
RHAMMv4
5'
AAA 3'
D
kb
M
P4 + P2
P4 + P5
0.6 -
v5
v4
E
kb
M
P1 + P2
P1 + P3
4.4 -
2.0 -
0.5 -
v5
v4
F
kb
M
P4 + P2
P4 + P5
0.6 -
v5
v4

Figure 1

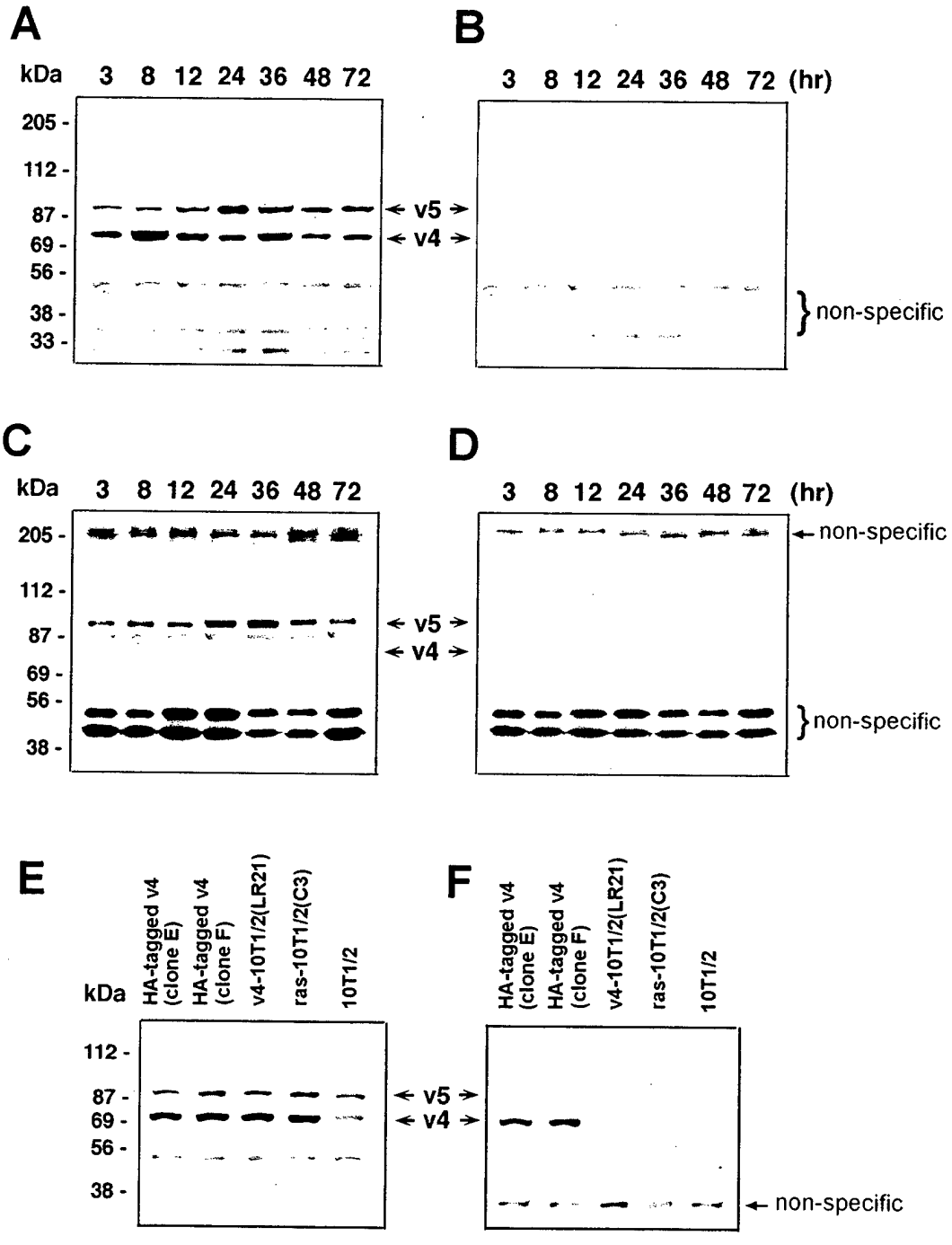
A
B
kDa
3 8 12 24 36 48 72
3 8 12 24 36 48 72 (hr)
205 -
112 -
87 -
69 -
56 -
38 -
33 -
v5
v4
non-specific
C
D
kDa
3 8 12 24 36 48 72
3 8 12 24 36 48 72 (hr)
205 -
112 -
87 -
69 -
56 -
38 -
v5
v4
non-specific
non-specific
E
F
kDa
HA-tagged v4 (clone E)
HA-tagged v4 (clone F)
v4-10T1/2(LR21)
ras-10T1/2(C3)
10T1/2
112 -
87 -
69 -
56 -
38 -
v5
v4
non-specific

Figure 2

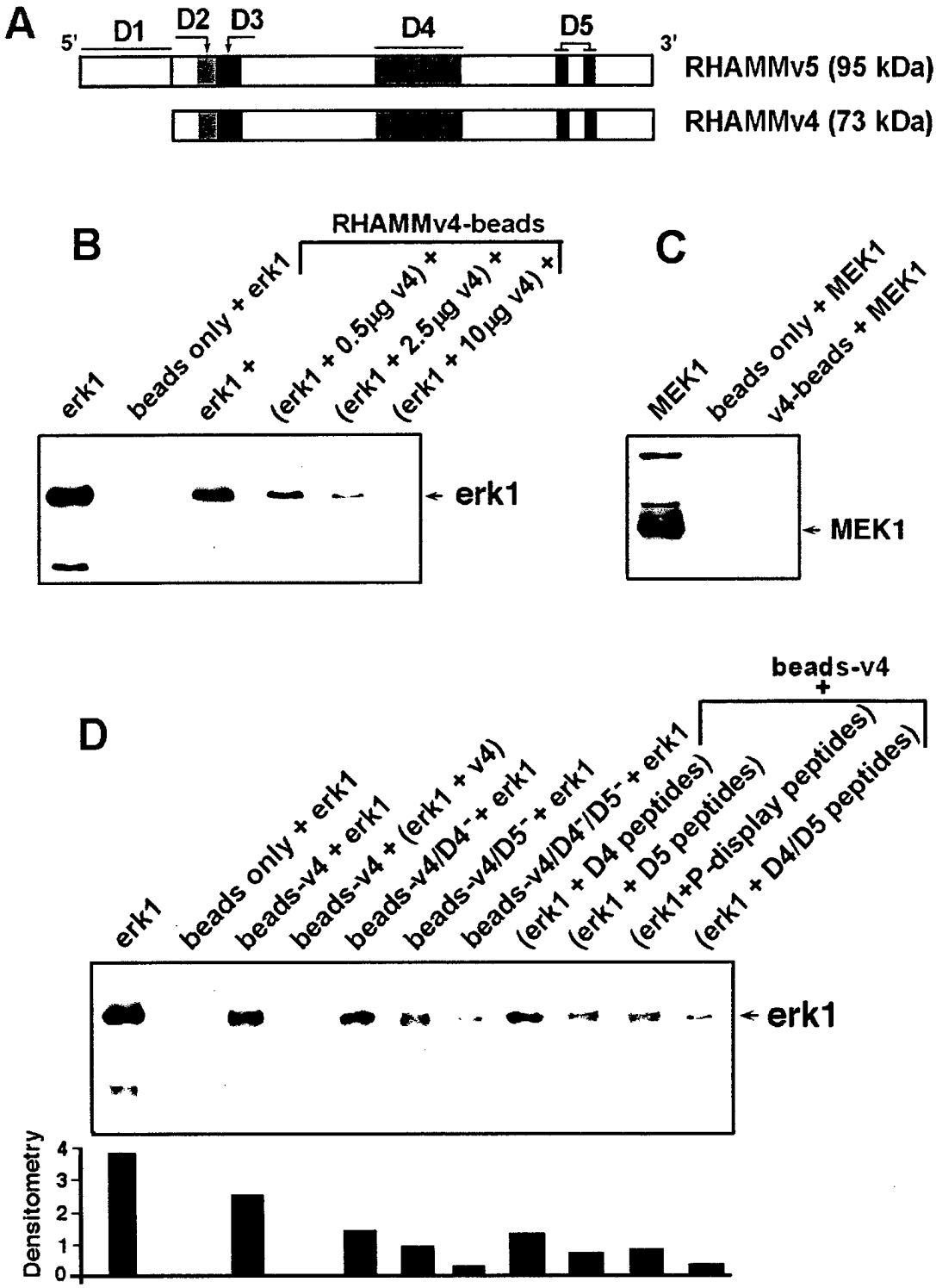
A
5'
D1
D2
D3
D4
D5
3'
RHAMMv5 (95 kDa)
RHAMMv4 (73 kDa)
B
RHAMMv4-beads
erk1
beads only + erk1
erk1 +
(erk1 + 0.5µg v4) +
(erk1 + 2.5µg v4) +
(erk1 + 10µg v4) +
erk1
C
MEK1
beads only + MEK1
v4-beads + MEK1
MEK1
D
beads-v4
+
erk1
beads only + erk1
beads-v4 + erk1
beads-v4 + (erk1 + v4)
beads-v4/D4- + erk1
beads-v4/D5- + erk1
beads-v4/D4-/D5- + erk1
(erk1 + D4 peptides)
(erk1 + D5 peptides)
(erk1+P-display peptides)
(erk1 + D4/D5 peptides)
erk1
Densitometry
4
3
2
1
0

Figure 3

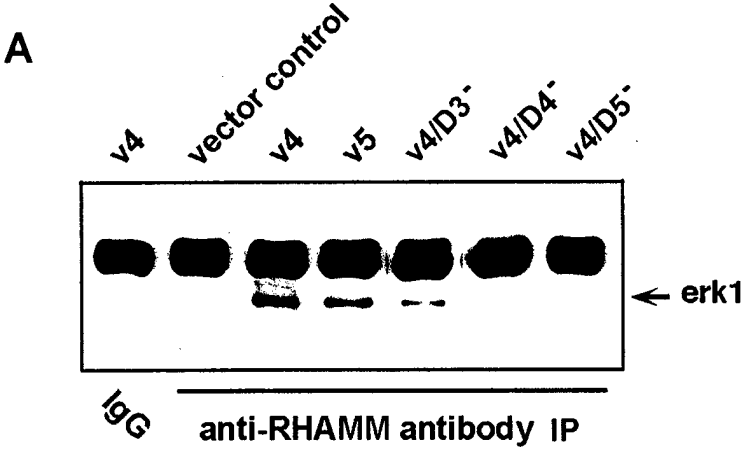

Figure 4

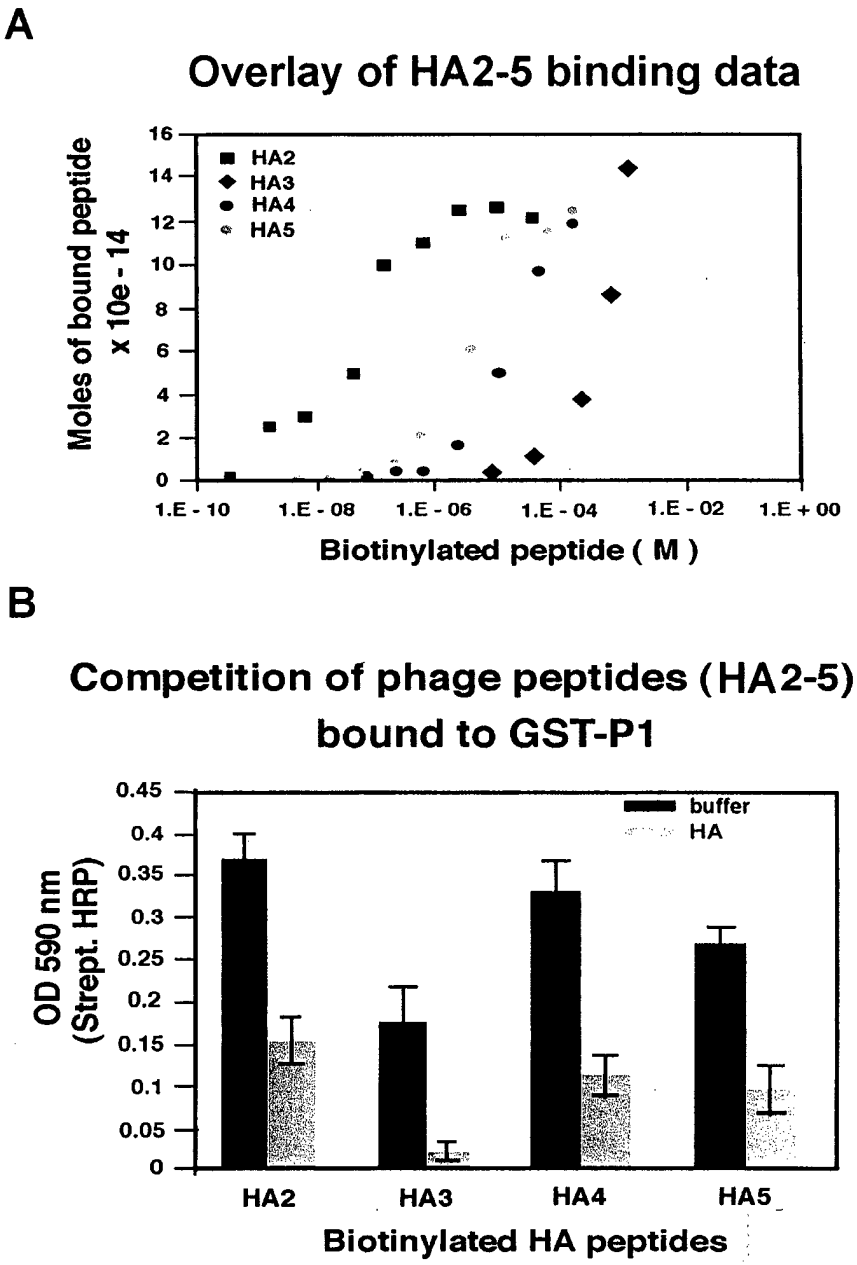

Figure 5

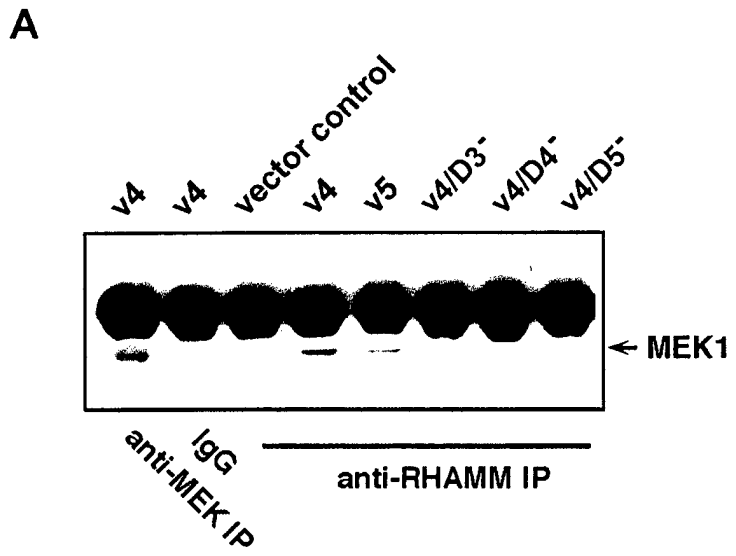

Figure 6

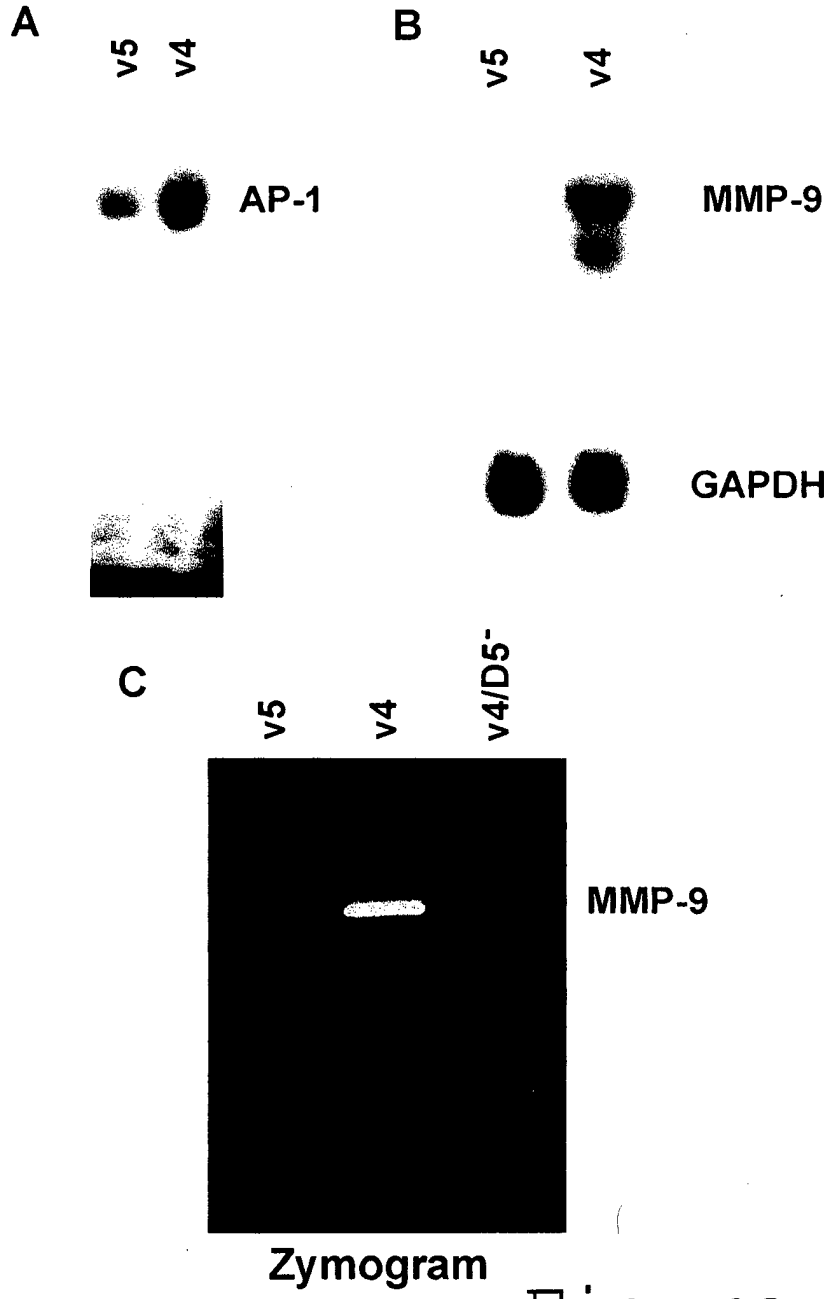

Figure 8

A
a
b
c
d
B
MAP kinase activity
(cpm x 1000)
10% FBS
Serum starvation
10T1/2
v4/10T1/2
v5/10T1/2
H-ras/10T1/2
C
MEK1*
+
vector control
v4/D3-
v5
v4
MEK1*
v5
v4
v4/D3-
MBP
D
Number of foci

Figure 7